UNIVERSITY OF BATH

PHD

Polymeric prodrugs for selective delivery to prostate tumours and heterocyclic isoform-selective inhibitors of nitric oxide synthase

Suaifan, Ghadeer A. R. Y.

Award date:
2004

Awarding institution:
University of Bath

[Link to publication](#)

Alternative formats

If you require this document in an alternative format, please contact:
openaccess@bath.ac.uk

Download date: 11. May. 2021

Polymeric prodrugs for selective delivery to prostate tumours and heterocyclic isoform-selective inhibitors of nitric oxide synthase

submitted by

Ghadeer A. R. Y. Suaifan

for the degree of PhD

of the University of Bath

2004

The research work in this thesis has been carried out in the Department of Pharmacy and Pharmacology under the supervision of Dr Michael D. Threadgill.

.....*Ghadeer Suaifan*..........

8-09-2004

UMI Number: U181068

UMI

Dissertation Publishing

ProQuest

Abstract

In prostate cancer, chronic administration of cytotoxins leads to systemic cytotoxicity. A new prostate-selective delivery system has been designed. Polymeric prodrugs are selectively retained in solid tumours by the enhanced permeability and retention effect but intracellular drug release is slow. In the designed prodrug, the drug would be released by the action of prostate specific antigen (PSA) that is active extracellularly in the tumour site only. Tumour–selectivity would be binary. PSA selectively cleaves the peptide sequence HSSKLQ.

The PSA-activated prodrug comprises a tripartite system, including a PSA-cleavable linker, a molecular clip and a model drug. A model drug (2-(4-nitrophenyl)ethylamine) was attached through an amide to the dipeptide molecular clip Xaa-2,2-dimethylthiazolidine. A 5,5-dimethylthiaproline (Me_2Thiazolidine) forces peptides into the *cis* conformation, enhancing cyclisation, diketopiperazine (DKP) formation and drug liberation. Targets with different L-amino-acids (H, CH_3, $CH(CH_3)_2$, CH_2Ph, $CH_2CH(CH_3)_2$) were coupled with R and S Me_2Thiazolidines. Cyclisation was faster in the L,S compounds. In the L,R series, increasing the side-chain bulkiness slows cyclisation; in the L,S compounds, bulky groups speed cyclisation. The initial ring-closure is rate-determining.

The structures of the DKPs *cyclo*-L-Ala-*R*-dimethylthiazolidine and *cyclo*-L-Val-*R*-dimethylthiazolidine were established by X-ray crystallography and by ^{1}H NMR. The DKP ring was in the boat conformation, with the thiazolidine in a half-chair. The geminal 2,2-dimethyl groups are equatorial and axial; the Me and isopropyl side chains are *pseudo*-equatorial, remote in space from the dimethyl. In both DKPs, the solution-phase conformation was similar. The DKP rings in *cyclo*-L-Val-*S*-dimethylthiazolidine and *cyclo*-L-Leu-*S*-dimethylthiazolidine were almost planar.

PSA-sensitive prodrugs CbzSKLQVOMe, CbzSSKLQV-Me_2ThProNPEA and CbzSKLQVMe_2ThProNPEA was synthesised using orthogonally protected amino-acid active esters in solution-phase coupling. Incubation of the prodrugs with PSA revealed cleavage L↓Q, rather than the predicted Q↓V.

A short series of disubstituted thiophenes, carrying thiourea head groups, was synthesised and evaluated for inhibition of isoforms of nitric oxide synthase.

Acknowledgments

In the Name of Allah, the Most Gracious, the Most Merciful

Contents

List of Figures, Schemes and Tables

Figures

Contents

Chapter 2   Aim and objectives

Chapter 3   Discussion

List of Figures, Schemes and Tables

Figures

Schemes

Tables

Abbreviations

AcOH	Acetic acid
ADEPT	Antibody-directed enzyme prodrug therapy
AMC	7-amino-4-methylcoumarin
Aq	Aqueous
BH_4	Tetrahydrobioterin
BNH	Benign nodular hyperplasia
Boc	1,1-Dimethylethoxycarbonyl
CaM	Calmodulin
Cbz	Phenylmethoxycarbonyl
CD	Cytosine deaminase
cNOS	Constitutive nitric oxide synthase
COSY	Correlation spectroscopy
DAST	Diethylaminosulfur trifluoride
DCC	Dicyclohexylcarbodiimide
DEAD	Diethyl azodicarboxylate
DKP	Diketopiperazine / piperazine-2,5-dione
DMAP	4-(Dimethylamino)pyridine
DMF	Dimethylformamide
DMP	Dimethoxypropane
$DMSOd_6$	Bis(trideuteriomethyl)sulfoxide
DNA	Deoxyribonucleic acid
DNR	Daunomycin
Dox	Doxorubicin
DSB	DNA double strand break
DSC	Differential scanning calorimeter
EEDQ	2-Ethoxy-1-(ethoxycarbonyl)-1,2-dihydroquinoline
eNOS	Endothelial nitric oxide synthase
EPR	Enhanced permeability and retention
Eq	Equivalent
Et_3N	Triethylamine
Et_2NH	Diethylamine

EtOAc	Ethyl acetate
Et$_2$O	Diethyl ether
FAB	Fast atom bombardment
FAD	Flavin adenine dinucleotide
5-FC	5-Fluorocytosine
FMN	Flavin mononucleotide
Fmoc	Fluoren-9-ylmethoxy carbonyl
FSH	Follicle-stimulating hormone
GDEPT	Gene-directed enzyme prodrug therapy
GnRH	Gonadotropin-releasing hormone
HOBt	1-Hydroxybenzotriazole
HPLC	High pressure Liquid Chromatography
HPMA	($\pm$)-N-(2-hydroxypropyl)-methacrylamide
iNOS	Inducible nitric oxide synthase
IR	Infra-red
KOBu^t	Potassium *tert*-butoxide
LH	Luteinising hormone
LHRH	Luteinising hormone-releasing hormone
L-NIO	N$^\gamma$-iminoethyl-L-ornithine
MeCN	Acetonitrile
MeOH	Methanol
Me$_2$ThPro	2,2-Dimethyl-4-thiaproline
MMC	Mitomycin C
MoAbs	Monoclonal antibodies
mp	Melting point
MW	Molecular weight
NADPH	Nicotinamide adenine diphosphate (reduced form)
NBS	N-Bromosuccinimide
nNOS	Neuronal nitric oxide synthase
NOESY	Nuclear Overhauser enhancement spectroscopy
NOS	Nitric oxide synthase
NPEA	2-(4-Nitrophenyl)ethylamine
NSu	Succinimide
PFPOH	Pentafluorophenol

Pr^{i}₂NEt	Diisopropylethylamine	
PSA	Prostate specific antigen	
RES	Reticuloendothelial system	
RNA	Ribonucleic acid	
p.p.m.	Part per million	
PSMA	Prostate-specific membrane antigen	
Rt	Ambient temperature	
PTSA	Toluene-4-sulfonic acid	
Sg	Semenogelin	
SPPS	Solid phase peptide synthesis	
TFA	Trifluoroacetic acid	
TFAOPFP	Pentafluorophenyl trifluoroacetate	
THF	Tetrahydrofuran	
TLC	Thin layer chromatography	
TS	Thymidylate synthase	
UV	Ultraviolet	
VDEPT	Virally directed enzyme prodrug therapy	

Amino Acids

Ala	Alanine	A
Arg	Arginine	R
Asn	Asparagine	N
Chg	Cyclohexylglycine	
Cys	Cystiene	C
Gln	Glutamine	Q
Gly	Glycine	G
His	Histidine	H
Hyp	*trans*-4-Hydroxyproline	
Ile	Isoleucine	I
Leu	Leucine	L
Lys	Lysine	K
Phe	Phenylalanine	F
Pro	Proline	P
Pyg	Pyroglutamine	

Ser	Serine	S
Thr	Threonine	T
Tyr	Tyrosine	Y
Val	Valine	V
Glu	Glutamic acid	E
Asp	Aspartic acid	D
Trp	Tryptophan	W
Met	Methionine	M

Acknowledgments

In the Name of Allah, the Most Gracious, the Most Merciful

Contents

Chapter 2   **Aim and objectives**

Chapter 3   **Discussion**

List of Figures, Schemes and Tables

Figures

Schemes

Tables

Abbreviations

AcOH	Acetic acid
ADEPT	Antibody-directed enzyme prodrug therapy
AMC	7-amino-4-methylcoumarin
Aq	Aqueous
BH_4	Tetrahydrobioterin
BNH	Benign nodular hyperplasia
Boc	1,1-Dimethylethoxycarbonyl
CaM	Calmodulin
Cbz	Phenylmethoxycarbonyl
CD	Cytosine deaminase
cNOS	Constitutive nitric oxide synthase
COSY	Correlation spectroscopy
DAST	Diethylaminosulfur trifluoride
DCC	Dicyclohexylcarbodiimide
DEAD	Diethyl azodicarboxylate
DKP	Diketopiperazine / piperazine-2,5-dione
DMAP	4-(Dimethylamino)pyridine
DMF	Dimethylformamide
DMP	Dimethoxypropane
$DMSOd_6$	Bis(trideuteriomethyl)sulfoxide
DNA	Deoxyribonucleic acid
DNR	Daunomycin
Dox	Doxorubicin
DSB	DNA double strand break
DSC	Differential scanning calorimeter
EEDQ	2-Ethoxy-1-(ethoxycarbonyl)-1,2-dihydroquinoline
eNOS	Endothelial nitric oxide synthase
EPR	Enhanced permeability and retention
Eq	Equivalent
Et_3N	Triethylamine
Et_2NH	Diethylamine

EtOAc	Ethyl acetate
Et$_2$O	Diethyl ether
FAB	Fast atom bombardment
FAD	Flavin adenine dinucleotide
5-FC	5-Fluorocytosine
FMN	Flavin mononucleotide
Fmoc	Fluoren-9-ylmethoxy carbonyl
FSH	Follicle-stimulating hormone
GDEPT	Gene-directed enzyme prodrug therapy
GnRH	Gonadotropin-releasing hormone
HOBt	1-Hydroxybenzotriazole
HPLC	High pressure Liquid Chromatography
HPMA	($\pm$)-N-(2-hydroxypropyl)-methacrylamide
iNOS	Inducible nitric oxide synthase
IR	Infra-red
KOBu^t	Potassium *tert*-butoxide
LH	Luteinising hormone
LHRH	Luteinising hormone-releasing hormone
L-NIO	N$^\gamma$-iminoethyl-L-ornithine
MeCN	Acetonitrile
MeOH	Methanol
Me$_2$ThPro	2,2-Dimethyl-4-thiaproline
MMC	Mitomycin C
MoAbs	Monoclonal antibodies
mp	Melting point
MW	Molecular weight
NADPH	Nicotinamide adenine diphosphate (reduced form)
NBS	N-Bromosuccinimide
nNOS	Neuronal nitric oxide synthase
NOESY	Nuclear Overhauser enhancement spectroscopy
NOS	Nitric oxide synthase
NPEA	2-(4-Nitrophenyl)ethylamine
NSu	Succinimide
PFPOH	Pentafluorophenol

Pr$^i_2$NEt	Diisopropylethylamine	
PSA	Prostate specific antigen	
RES	Reticuloendothelial system	
RNA	Ribonucleic acid	
p.p.m.	Part per million	
PSMA	Prostate-specific membrane antigen	
Rt	Ambient temperature	
PTSA	Toluene-4-sulfonic acid	
Sg	Semenogelin	
SPPS	Solid phase peptide synthesis	
TFA	Trifluoroacetic acid	
TFAOPFP	Pentafluorophenyl trifluoroacetate	
THF	Tetrahydrofuran	
TLC	Thin layer chromatography	
TS	Thymidylate synthase	
UV	Ultraviolet	
VDEPT	Virally directed enzyme prodrug therapy	

Amino Acids

Ala	Alanine	A
Arg	Arginine	R
Asn	Asparagine	N
Chg	Cyclohexylglycine	
Cys	Cystiene	C
Gln	Glutamine	Q
Gly	Glycine	G
His	Histidine	H
Hyp	*trans*-4-Hydroxyproline	
Ile	Isoleucine	I
Leu	Leucine	L
Lys	Lysine	K
Phe	Phenylalanine	F
Pro	Proline	P
Pyg	Pyroglutamine	

Ser	Serine	S
Thr	Threonine	T
Tyr	Tyrosine	Y
Val	Valine	V
Glu	Glutamic acid	E
Asp	Aspartic acid	D
Trp	Tryptophan	W
Met	Methionine	M

Introduction

1.1 Male reproductive system

The male reproductive system is essential to the perpetuation of life. It is the means by which we propagate and ensure our continued existence. Individual life is possible without it but human existence as a whole is not.
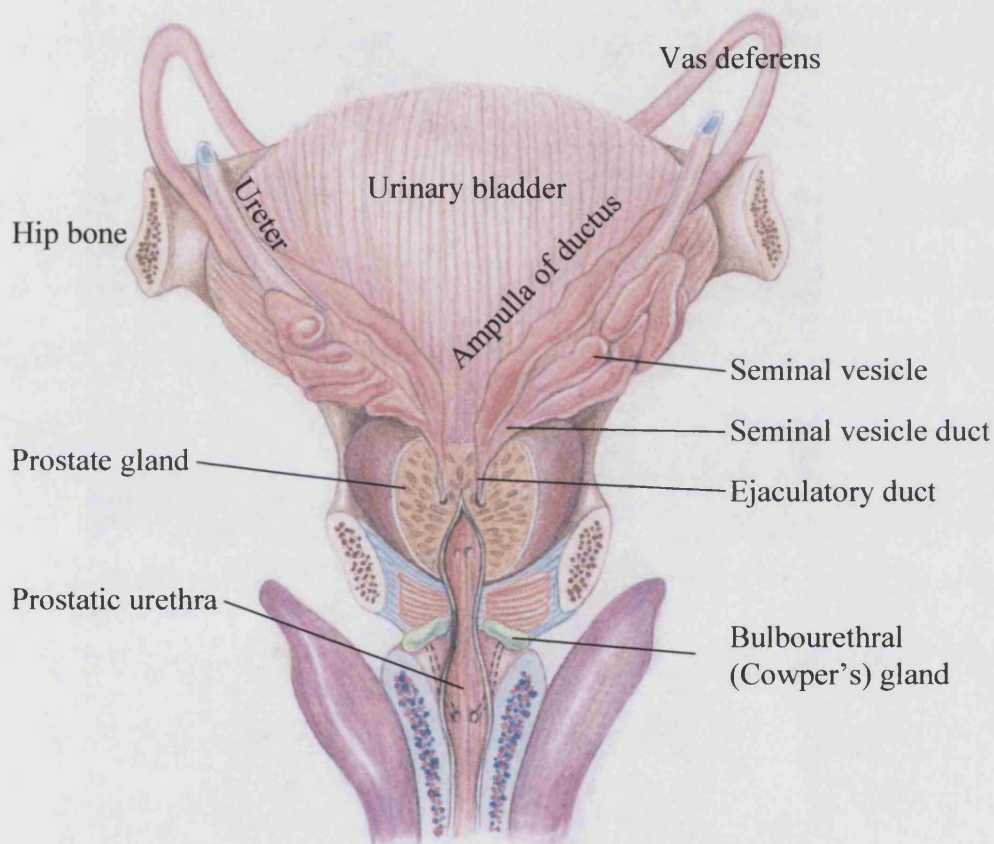
Figure 1.1 *Posterior view of the male accessory organs of reproduction.*

The male reproductive system **(Figure 1.1)** is composed of essential and accessory organs. The essential organs (*gonads, testes*) produce gametes. The accessory organs include genital ducts, glands and supporting structures. The *genital* ducts serve to convey sperm to the outside of the body and include a pair of epididymides, a pair of vasa deferentia, a pair of ejaculatory ducts and the urethra. The accessory *glands*, which include a pair of seminal vesicles, one prostate and a pair of bulbourethral (Cowper's) glands produce secretions that

serve to nourish, transport and mature sperm. The *supporting structures* include the scrotum, the penis and a pair of spermatic cords.[1]

1.1.1 Testes

The male reproductive system normally contains two testes. They are small ovoid glands, measure about 4 or 5 cm in length and weigh 10 to 15 g. The left testis is generally located about 1 cm lower in the scrotal sac than the right. Each testis is composed of up to 900 coiled *seminiferous tubules*, in which spermatogenesis occurs.[1,2] The formed sperm would then empty into the *epididymis*, another coiled tube about 6 m long. The epididymis then leads into the *vas deferens*, which enlarges into the *ampulla of the vas deferens* immediately before entering the body of the prostate gland.[3] The testes secrete several male hormones, which are collectively called androgens. All androgens are steroid compounds, as shown by the formulae for testosterone **(1)** and dihydrotestosterone **(2)** **(Figure 1.2)**. They play a critical role in spermatogenesis, prostate cell growth and are responsible for many male features such as lower voice, male hair patterns and the male libido or sexual drive.[3]
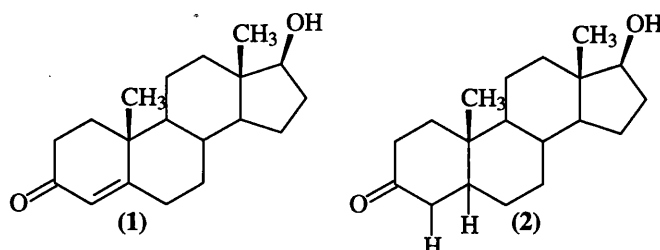
Figure 1.2   *Chemical structures of testosterone (1) and dihydrotestosterone (2).*

1.1.2 Seminal vesicles

There are two seminal vesicles. Each is a tortuous, loculated tube lined with a secretary epithelium and secrets a mucoid material containing an abundance of fructose and citric acid, as well as large quantities of prostaglandins and fibrinogen. They are located on each side of the prostate. During emission, each vesicle, together with the ampulla, empties its contents into the *ejaculatory duct*, leading through the body of the prostate gland and then emptying into the *internal urethra*.[3]

1.1.3 Prostate gland

The prostate is a single, muscular, walnut-sized gland, located beneath the urinary bladder and in front of the rectum.[2] The normal gland weighs about 20 g and it is enclosed in a fibrous capsule.[4] The gland increases slowly in size from birth to puberty and then expands rapidly. However, the size attained by age 30 typically remains stable until about age 45, when further enlargement may occur.[2]

Within the prostate, there are three groups of glands arranged concentrically around the urethra: an inner peri-urethral group, the submucosal glands and the external group or main prostatic glands. From all three groups, ducts converge and open into the prostatic urethra.[3] The prostate gland secretes a thin, milky fluid that constitutes about 31% of the seminal fluid volume.[1] This fluid contains several substances, such as citric acid, which is used by sperm for ATP production *via* the Krebs cycle, several proteolytic enzymes, such as prostate specific antigen (PSA), pepsinogen, lysozyme, amylase, and hyaluronidase which break down the clotting protein from the seminal vesicles, in addition to an acid phosphatase whose function is unknown.[2]

During emission, the capsule of the prostate gland contracts simultaneously with the contractions of the vas deferens. Consequently, the prostate gland fluid is added to the bulk of the semen.[3] For successful fertilization of the ovum, the prostatic fluid should have a slight alkaline pH to protect the sperm from the acidic environment in the male urethra and female vagina (pH 3.5-4.0).[1,3]

1.1.4 Bulbourethral glands (Cowper's glands)

The paired glands resemble peas in size and shape. They are located below the prostate on either side. A duct approximately 2.5 cm long connects them with the penile portion of the urethra. During sexual arousal, the glands would secrete an alkaline fluid into the urethra. This, consequently, protects the passing sperm by neutralising acids resulting from urine in the urethra. Also, they secrete mucus which lubricates the end of the penis and the lining of the urethra, thus decreasing the number of sperm damaged during ejaculation.[1,2]

1.2 Male Sex Hormone

The sexual function of male is controlled by the release of *gonadotropin-releasing hormone (GnRH)* secreted by the hypothalamus. This hormone, in turn, stimulates the gonadotropes cells in the anterior pituitary gland to secrete two other hormones:

1-*Luteinising hormone (LH)* which is the primary stimulus for the secretion of testosterone by the testes Leydig cells which constitute about 20% of the mass of the adult testes.

2-*Follicle-stimulating hormone (FSH)* which mainly stimulates spermatogenesis.[3]

So, in the absence of GnRH, the gonadotropes cells secrete almost no LH or FSH. Furthermore, testosterone secreted has a reciprocal effect of inhibiting anterior pituitary secretion of LH and FSH. This inhibition results from the direct effect of testosterone on the hypothalamus to decrease the secretion of GnRH. Consequently, there is a corresponding decrease in the secretion of both LH and FSH. This, in turn, decreases the secretion of testosterone. Thus, whenever secretion of testosterone is too high, an automatic negative feedback effect will decrease the testosterone secretion back toward the required operating level.[3]

In the prostate gland, the testosterone hormone enters the prostatic cells very quickly (usually within a few minutes) after secretion; then it will be converted to dihydrotestosterone by the intracellular enzyme 5α-reductase. Dihydrotestosterone, in turn, binds with a cytoplasmic receptor protein. This combination then migrates to the cell nucleus, where it binds with the nuclear protein and induces DNA-RNA transcription. Within 30 min, RNA polymerase becomes activated and the concentration of RNA increases in the prostatic cell, followed by a progressive increase in cellular protein. After a couple of days, the quantity of DNA increases in the prostate with a simultaneous increase in the number of prostatic cells.[3]

1.3 Incidence of prostate disease

Diseases of the prostate are common causes of urinary problems in men, the incidence of which increases with age, especially beyond 60 years.[4] The most common types of prostate diseases are:

1.3.1 Benign nodular hyperplasia (BNH)

BNH is a non-neoplastic enlargement of the prostate gland (benign neoplasm).[4] It is very common and the incidence increases after the age of 50. The cause is obscure but it is thought to be related to a hormonal imbalance, although the exact mechanism is uncertain. The enlargement of the prostate inside its capsule results in the blockage of the urethra and consequently may develop slowness or dribbling in the urinary stream, hesitancy or difficulty in starting urination, feeling of urgency to urinate, even when the bladder is empty, and frequent urination, especially at night.[4,5]

1.3.2 Prostatitis

Prostatitis is an infection and / or inflammation of the prostate gland which can be caused by bacteria **(Figure 1.3)**. Prostatitis may be subdivided into:

Normal Urethra   **Narrowed Urethra**
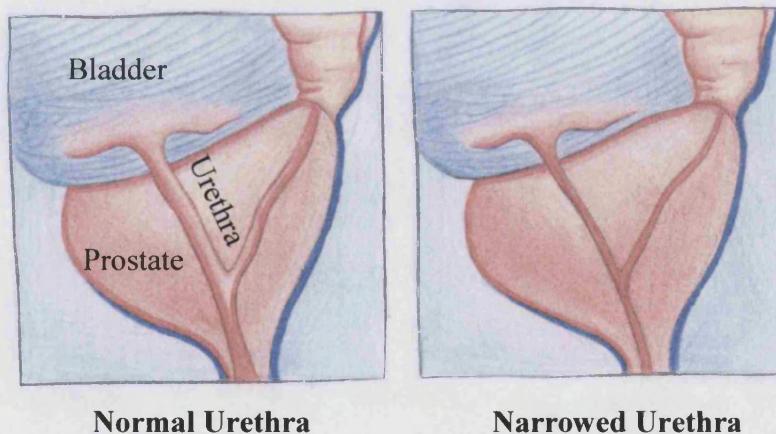
Figure 1.3   *Drawing of the normal urethra and the narrowed urethra in prostatitis.*

A   *Acute Prostatitis*

It is a bacterial infection, characterised by an acute inflammation of the prostate, which usually follows an acute infection in the bladder or urethra.[6] It is particularly common following urethral catheterisation or endoscopy.[4] The common causative micro-organism is

E. coli. Furthermore; sexually transmitted diseases, particularly *gonococcus* and *chlamydia* (a cause of non-gonococcal urethritis) may cause prostatitis.[4,6]

B   *Chronic Prostatitis*

It is also associated with lower urinary tract infection, results from inadequately treated acute prostatitis due to resistance, relapse and short-course therapy.[6] The prostate gland shows increased stromal fibrosis, with an infiltrate of lymphocytes and plasma cells, associated with acinar atrophy.[4]

C   *Granulomatous Prostatitis*

It is a heterogeneous group of lesions, all of which may cause enlargement of the gland and urethral obstruction. The inflammatory component and the associated fibrosis produce a firm, indurated gland, which, upon rectal examination, mimics the neoplasm clinically. Consequently, it is very important to diagnose this type of Prostatitis correctly.[4]

1.3.3   Prostatic carcinoma

Prostate cancer is among the most common malignant disease for which health-care intervention is sought worldwide.[7] It is the most common non-cutaneous cancer in most developed countries and could become the commonest male cancer worldwide. In term of male cancer deaths, it is the second cause of death after lung cancer.[8,9] Prostate cancer is diagnosed in a very few people aged younger than 50 years (<0.1% of all patients).[10] However, the peak incidence is between 60-85 years.[4]

1.3.3.1 Aetiology

The aetiology of the disease is unknown, although it is probable that hormonal changes, which occur with increasing age, are involved. With advancing age, there would be a decrease in the circulating androgen levels. This decrease is associated with involution of the outer zone of the prostate where most tumours arise.[4] However, although common lesions prostatic carcinoma and BNH frequently coexist coincidentally in the same gland,

there is virtually no evidence that BNH is causally related to the development of malignancy. Therefore, BNH is not considered a pre-neoplastic lesion.[4,5]

1.3.3.2 Epidemiology

⊙ Incidence of the disease varies widely between ethnic populations and countries. The lowest rate is usually in Asia and the highest rates are in North America and Scandinavia. This difference is attributed to a combination of other underlying differences, such as genetic susceptibility, exposure to unknown risk factors, or artifactual reasons, such as cancer registration and difference in health care.[10] Other factors may also attribute and include:

A   Genetic factors

Genetic factors are the cause behind prostate cancer clustering in families. About 10-15 % of patients have at least one relative who is also affected. Furthermore, the risk of developing the disease in relatives increases with an increase in the number of affected individuals in the family.[10]

B   Dietary factors

Epidemiological studies suggested that prostate cancer is associated with Western lifestyle and in particular, diet that includes a high intake of fat, meat, and dairy products.[11]

C   Hormones and other risk factors

Andogens play an important role in the development of healthy prostate and in the treatment of the cancer. That is, the hormones influence on the growth of normal prostate cells is maintained in malignancy. Withdrawal of these hormones, by surgical or medical castration, results in the arrest of prostatic cell multiplication.[10] Different ways can be used to remove androgens from the body. These methods include the removal of man's testes (called an orchiectomy), drugs that block the production of androgens (called Luteinizing Hormone-Releasing Hormone (LHRH) agonists), drugs that block androgen receptors (called anti-androgens and oestrogens).[9]

1.3.3.3 Clinicopathology

Two clinicopathological types of prostatic carcinoma are recognised:

A   Clinical (symptomatic) carcinoma

The tumour spread within the gland and may cause urethral obstruction. However, most active tumours arise in the posterior lobe of the gland, mainly in the subcapsular area. As a result, retropubic prostatectomy for BNH dose not remove the posterior zone; this explains why carcinoma sometime may develop following such a prostatectomy.[4]

The large majority of prostatic carcinomas are adenocarcinomas, usually well differentiated, forming acini, tubules or a cribriform pattern. The convoluted outline of the glands is lost and neoplastic acini are formed.[4,5] Also, it has been found that the tumour may metastasize to adjacent tissue widely and silently. This spread may be; (A)-lymphatic, initially to presacral, iliac and para-aortic lymph nodes, but often extending widely; (B) retrograde venous, to the lumber spine; (C) by the blood stream causing widespread metastases, with a marked predilection for the skeleton.[4,5]

B   Latent (incidental) carcinoma

Microscopic foci of carcinoma are found incidentally on histological examination of prostatectomy specimens or in the prostate at autopsy. The incidence of these foci depends largely on the age of the patient. In addition, such foci are found in about 30% of prostate glands over the age of 50 and about 80% of the glands over the age of 75. It is, therefore, much commoner than the clinically symptomatic form of the disease.[4,5]

Latent tumours are adenocarcinomas (like symptomatic lesion). The concept of this tumour has been questioned, with the recognition that some of them eventually progress and metastasise. The disease progression occurs in about 30% of the patients after 10 years. However, the majority probably remain as latent or dormant lesions and, in practical terms, the presence of minute tumour foci in the prostatectomy specimen is not an indication for immediate hormonal therapy.[4]

Unfortunately, to date, there are no laboratory techniques available to identify which of these microscopic tumour foci will progress, so that, most surgeons will choose to follow up the patient without any initial therapy.[4]

1.3.3.4 Clinical features

The clinical features of prostatic carcinoma include:

-Urinary outflow obstructive symptoms such as difficulty or increased frequency of nicturition and urinary retention.

-Digital rectal examination would reveal hard craggy prostate.

-Bone metastases often present as localised bone pain, pathological fracture and anaemia.

-Lymph node metastases due to metastatic prostate carcinoma.[4]

1.3.3.5 Gleason grading system

After prostate cancer diagnosis, determination of the stage of the cancer is important for planning the appropriate treatment. Staging indicates the size and location of the cancer and if the cancer has been metastasised beyond the prostate.

The gleason grading system is the most frequently used system **(Figure 1.4)**.[12] In this system, the prognosis of the cancer is considered to be the intermediate between the grade of the most predominant pattern of cancer seen in microscopic sample and the grade of the second most predominant pattern. Each of these patterns are identified and graded separately from 1 (almost normal) to 5 (very abnormal). The two grades are then added together.[13]

Data from the Veterans Administration Cooperative Urological Research Group study indicate that clinical staging and histological grading can be combined to provide increased discrimination in predicting the biological malignancy of prostatic carcinoma. Therefore, prostatic carcinoma was classified according to gleason grading system into: **(A)** Gleason grade 2-4 in which prostatic tumour tend to grow slowly and takes long time to become clinically significant. The time required for the tumour to be doubled in size is measured in terms of years; **(B)** Gleason grade of 5 or 6 in which prostatic tumours are clinically significant if they occur in younger men below the age of 70-75. Over the age of 80, the

patient is more likely to die of other causes than prostate cancer; **(C)** Gleason grades 8, 9, or 10, which is very aggressive and the time required for the tumour to be doubled in size is measured in terms of weeks or months; **(D)** Gleason Grade 7 in which cancers act in between the moderate and high grade cancers and must be considered significant but not incurable.[13,14]
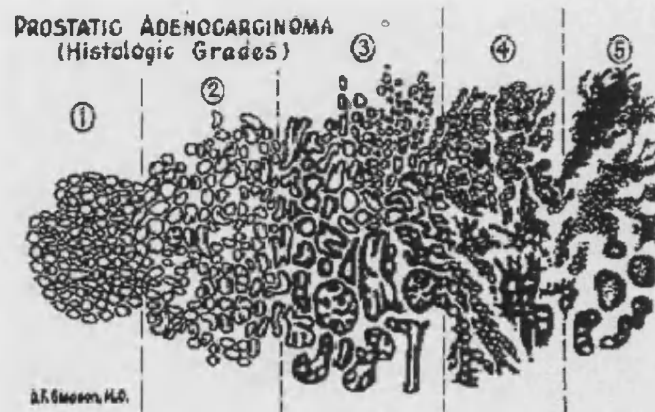
Figure 1.4 *Prostatic carcinoma grades. This illustration shows Dr. Gleason's own simplified drawing of the five Gleason grades of prostate cancer. Grade 1 appears on the far left and grade 5 on the far right.*[12]

1.3.3.6 Diagnosis

Useful diagnostic investigations include diagnostic imaging such as ultrasound, cytoscopy such as transurethral resection and chemical pathology which include the presence of high levels of serum acid phosphatase in patients with associated bone metastases,[3] high level of serum alkaline phosphate n patient with osteosclerotic bone metastases as a result of osteoblast proliferation[15] and high level of prostate specific antigen present in malignant prostatic epithelium.[16] Other diagnostic investigations include haematology, such as leukoerythroblastic anaemia, which develops upon widespread carcinomatous infiltration of the bone marrow and evinced by the presence of primitive red and white cell precursors in the peripheral blood[3] and biopsy.

1.4 Treatment

1.4.1 Surgery

In surgery, the concept of treatment is simple. If the cancer is localised within the prostate gland and the gland is removed, the cancer is cured. The most common known surgical procedure is radical prostatectomy.[17] Radical prostatectomy can be divided into *retropubic* and *perineal*. In radical retropubic prostatectomy, the lymph node can be dissected and the prostate is removed in a single incision, whereas, in radical perineal prostatectomy, a separate incision is required for lymph-node dissection and for prostatectomy.[7] It is noteworthy that prostatectomy, in the early stages of the cancer when it is localised, helps 85% -90% of the patient to survive for up to 15 year after operation.

Following prostatectomy, PSA is expected to be undetectable. However, any rise will be a suspicious sign for local recurrence. As a result, patients with a local recurrence after prostatectomy require an adjuvant radiation therapy.[18]

Unfortunately, urinary incontinence will develop after radical prostatectomy. Urinary incontinence definition ranging from the occurrence of urinary dribbling during stressful activity to the requirement of urinary pads.[19] The incidence of incontinence is quite high, immediately after surgery, but decreases with time. About 2 – 5% of patients suffer from severe incontinence 6 months after surgery.[20] Additionally, potency could be diminished after surgery. This is because the neurovascular bundles are manipulated or severed. However, to date, new surgical approaches which spare the neurovascular bundle through unilateral or bilateral nerve-sparing techniques have reduced impotence rates.[21]

1.4.2 Radiation

External-beam radiotherapy has undergone a technological revolution. It is virtuous in the treatment of localised prostate cancer and has the following advantages; (A) unlike surgery, no anaesthetic is required. As a result, it is used in a wide spectrum of patients; (B) accompanied urinary toxic effects can be managed with α-adrenergic blockers; (C) potency preservation rates are higher compared to patients who have undergone

11

prostatectomy.[7] On the other hand, rectal complications usually result from the uncontrolled delivery of radiation to the prostate.[22]

Brachytherapy is the direct placement of the radioactive beam into the region of interest. It is used for the treatment of early-stage prostate cancer. Unlike external-beam radiotherapy, the incidence of rectal complications is lower due to the localised dose distribution. Also, it offers better potency preservation in comparison with radical prostatectomy. On the other hand, the trauma of needle placement into the prostate can result in prostate oedema and cause urinary toxic effects. These effects are usually treated with α-adrenergic blockers and corticosteroids.[23]

Generally, it has been found that 10-year disease-specific death after radiotherapy ranged from 4% to 54%, for well- and poorly-differentiated local disease, respectively.[17]

1.4.3 Hormones

The prostate is a hormone-responsive organ.[7] In the early stages; prostate cancer growth is enhanced by androgens. In the majority of the advanced stages, this disease remains sensitive to hormone manipulation. The role of hormones on the growth of normal prostate cells is maintained in malignancy. The growth of these cells is stimulated by testosterone and other androgens produced by the testis and the adrenal glands. Withdrawal of these hormones results in the control of prostatic cell proliferation in 75 – 80% of patients with advanced prostate cancer.[10,24] Consequently, androgen ablation is the mainstay of primary therapy.

Previously androgen-ablation therapy was accomplished surgically by orchiectomy. Presently, this has been replaced with medical castration.[7] Many hormonal agents work at different points in the hormone biosynthesis cascade. They either inhibit testosterone production or block its action. These include; **(A)** steroidal anti-androgens, such as the progestogens (megestrol acetate) and the imidazole derivative Ketoconazole. The progestogen agent suppress Luteinising hormone (LH) release at the level of the hypothalamic-pituitary axis and then reduce testosterone levels, block conversion of testosterone to dihydrotestosterone and prevent binding of androgens to receptors. Imidazole derivatives are adrenal enzyme synthesis inhibitors, block the function of

cytochrome P-450 and suppress the synthesis of both testicular and adrenal androgens; (B) nonsteroidal anti-androgens, such as flutamide, block androgen action at the cellular target level, do not alter LH secretion and have the advantage of preserving libido; (C) gonadotropin-releasing hormone (GnRH) agonists, down regulate pituitary receptors resulting in the loss of normal pituitary secretion and in castration of serum androgen level. (D) oestrogens, such as diethylstilboestrol, suppress the hypothalamic secretion of GnRH and, consequently, LH secretion.[17,25]

The relative value of these various methods of achieving androgen ablation does not show any preference of one over the other, except with regards to different cost.[26] About 70% to 80% of patients initially respond to hormonal manipulation. However, the overall survivals range between 24 to 36 months. So, early stage hormone therapy refines the quality of patients` life but does not lengthen their survival.[27]

Unfortunately, disseminated prostate cancer will eventually escape the primary monotherapy (first-line hormonal therapy) and requires a second line of treatment modalities. As an example, the addition of non-steriodal anti-androgen to orchiectomy will result in total androgen blockade and consequently increase the survival rate in patients.[24] In addition; combination of hormones with radiotherapy improves survival.[7]

Hormonal therapies have common side effects which include, hot flushes, loss of libido or erectile function, weight gain, gynaecomastia, liver inflammation and osteoporosis. Although these side effects are usually mild in case of short-course treatment, they should be balanced against the benefit.[28] As a conclusion, hormonal ablation therapy is the main choice for the treatment of localised and disseminated prostate cancer but, unfortunately, after a brief period, prostate cancer commonly recurs and the patients relapse with androgen-independent tumours.[29]

MacNeal has identified premalignant changes in prostate cancer.[30] One of the early changes which lead to malignancy is the lack of senescence. This means that prostate cancerous cells do not die as normal cells. This lack of cell death results in a greater number of cancerous cells. These cells, which do not age normally, can escape the normal control mechanisms of hormones.[30] Coffey and Isaacs, have identified three different mechanisms for the development of hormone-independent cells;[31] (A) the direct mutation

of DNA; **(B)** the ability of the cells to adapt to environment changes; in other words, as androgens are withdrawn by hormonal therapy, the cells learn to live in a low-androgen environment; **(C)** the hormone independent cells are present since the beginning of the growth, albeit in comparatively small numbers, which become obvious after tumour treatment with hormone manipulation or other therapeutic modalities.[31]

Finally, when the tumour is metastatic, the treatment of hormone-refractory prostate cells may be accomplished by chemotherapeutics.

1.4.5 Chemotherapy

In 1941, the idea of using chemotherapy in the treatment of malignant disease was born. In the following year,[32] Gilman and others started clinical studies on the nitrogen mustards and discovered that mechlorethamine was effective against Hodgkins disease and lymphosarcoma.[33] In the next decade, antimetabolites such as methotrexate **(3)** (1949), 6-mercaptopurine **(4)** (1952) and 5-fluorouracil **(5)** (1957) were discovered. Also, alkylating agents, such as melphalan **(6)** and cyclophosphamide **(7)** were developed. In addition, natural products, such as mitomycin C **(8)** and alkaloids were discovered in this period. During the 1960s, progress continued in all these areas with the discovery of doxorubicin **(9)**.[34] It is noteworthy that there are many other chemotherapeutic agents present but I will discuss the most principle ones.

1.4.5.1 Alkylating agents

Melphalan (6)   **Cyclophosphamide (7)**
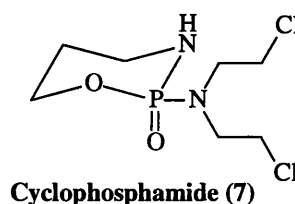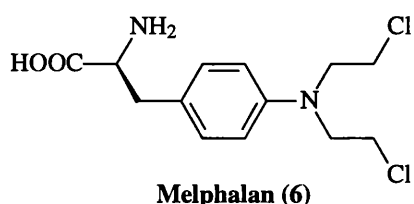
They are highly reactive agents; form covalent links with biomolecules containing –SH, NH_2 and OH nucleophiles, such as nucleic acids and proteins. The alkylation of nucleic acids involves a substitution reaction in which a nucleophilic atom (Nu) of the biopolymer displaces a leaving group from the alkylating agent.[34]

$$\text{Nu-H} + \text{Alkyl-Y} \longrightarrow \text{Alkyl-Nu} + \text{H}^+ + \text{Y}^-$$
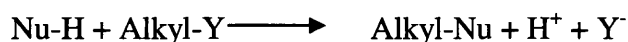
Alkylating agents cause different types of damage to DNA, which include; **(A)** single alkylation of a base leading to errors in DNA function; **(B)** alkylation of two bases to cross-link them, either within the same or different strands; **(C)** single or double strand breaks. A consequent physiological repair process will take place. However, it is not efficient in highly alkylated and cross-linked regions. So, DNA damage will give rise to a chain breaks and faulty transcription of the information in the DNA.[35]

It is noteworthy that mitomycin C **(8)** is commonly listed among the antibiotics although its mechanism of action is reductive-activated alkylation and strand breakage of treated DNA.[35]

Mitomycin C (8)
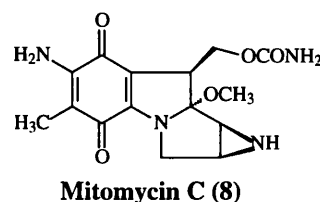
1.4.5.2 Antimetabolites

Antimetabolites are compounds that prevent the biosynthesis of cellular metabolites by acting as enzyme inhibitors or by preventing their utilisation by acting as analogues. For example:

Methotrexate (3) stops DNA synthesis by acting as a potent inhibitor of the enzyme dihydrofolate reductase, which is essential in the synthesis of tetrahydrofolate needed for the biosynthesis of both thymidylate and purine. There are two processes by which this drug enters the cell, active transport and passive diffusion. The former

Methotrexate (3)

process is very limited; as a result, high doses of drug are required. The resulting high plasma level will increase the rate of passive diffusion process and, consequently elevate intracellular concentrations, resulting in sustained inhibition of DNA synthesis. However, such high level results in highly toxic side effects.[34,35]
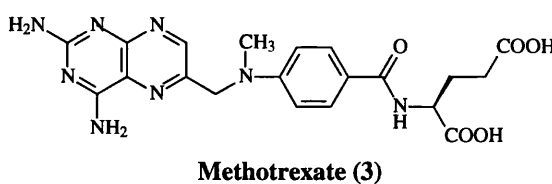
6-Mercaptopurine (4) is a purine analogue, converted into its ribonucleotide by the enzyme hypoxanthine-guanine phosphoribosyltransferase. This nucleotide inhibits the first step in the pathway of purine biosynthesis, the formation of 5-phosphoribosylamine, as well as later steps in the interconversion of various purine nucleotides. Neoplasms that lack this enzyme are resistant to the drug. Toxicity takes the form of bone marrow depression, with a delayed leukopenia and evidence of liver damage.[34,35]
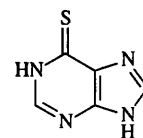
6-Mercaptopurine (4)

5-Fluorouracil (5) in the form of 5-fluoro-2-deoxyuridylic acid is a powerful competitive inhibitor of thymidylate synthetase, the enzyme required for the formation of thymidylate. Bone marrow depression is the major toxic side effects. Other side effects include diarrhoea, stomatitis, ulceration of the gastrointestinal tract, hair loss, dermatitis, cerebullar damage as dizziness and ataxia.[34,35]
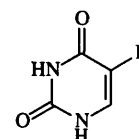
5-Fluorouracil (5)

1.4.5.3 Antibiotics

Different antibiotics have been established in clinical anticancer therapy. These compounds were originally rejected as antibacterial agents because of their cytotoxicity. Later on, it has been found that this toxicity could turn into an advantage in cancer chemotherapy. There are two major mechanisms for these drugs to deform DNA structure and so terminate its biological function; **(A)** intercalation into the double helix DNA strand. This in turn creates local unwinding in DNA helix; **(B)** Inhibition of the enzyme topoisomerase II. This enzyme is fundamental for the regulation of DNA topology in all living organisms. It prevents DNA tangling during replication, cleaves DNA strands reversibly to create a DNA "gate", allow the second, nearby double helix to pass through this break and then reseal the break and dissociates from the DNA. However, this enzyme requires appropriate orientation and separation of DNA strands for their activity.[34,36]

Anthracycline antibiotics, such as doxorubicin (9) and its derivatives, inhibit cell growth and lead to cell death. They dissociate DNA double helix by intercalation resulting in the formation of anthracyclin-DNA complex, inhibit topoisomerase II enzyme by forming stable DNA-enzyme-drug complexes thus, hindering the regulation of DNA strand by the enzyme and resulting in irreversible DNA break which then lead to cell death.[24,37]
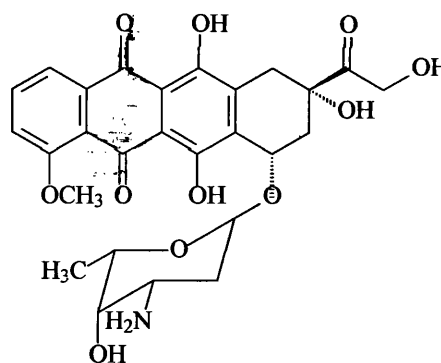
Doxorubicin (9)

Doxorubicin (9) is among the most effective chemotherapeutic agents for the treatment of advanced hormone-refractory prostate cancer. However, the high incidence of cardiac toxicity persuades many clinicians not to use it in old patients or to use low doses which unfortunately, would lower drug efficacy.[24,38]

1.5   Structure-activity relationships of anthracycline antibiotics

The complete structure of anthracyclines is a glycoside (sugar + aglycone).[34] Recent studies indicate the crucial role of the sugar moiety and cyclohexene ring (A) in their action.[39,40] These studies examined different analogues, with different substituents at the 3' and 4' site of the sugar moiety and / or the removal of the methoxy group at position 4, with respect to their stimulation of DNA fragmentation at an equitoxic drug concentration (**Figure 1.5**). It has been found that compound (12) stimulate the largest number of DNA strand break (DSB), compounds (13) and (14) stimulate intermediate amounts of DSB, while the lowest level of DSB was seen with compounds (9), (10), (11), and (15). However, the results corresponding to compound (14) were surprising, because previous studies of the cytotoxic potency of these compounds showed that it is less potent than (9) (**Figure 1.5**), nevertheless, it stimulates larger amount of DNA strand breakage. So, there would be another factor affecting the cytotoxic potency of anthracyclines.

17
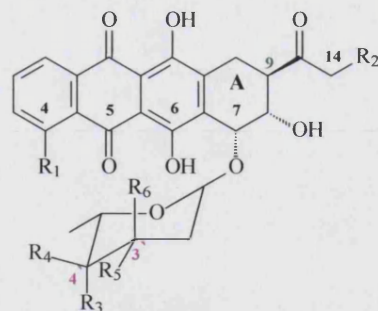
	Compound	R_1	R_2	R_3	R_4	R_5	R_6	Cytotoxicity IC_{50}, μM
(9)	Doxorubicin	OCH_3	OH	OH	H	NH_2	H	0.80
(10)	**Daunorubicin**	OCH_3	H	OH	H	NH_2	H	0.20
(11)	**Idarubicin**	H	H	OH	H	NH_2	H	0.02
(12)	**4-demethoxy-3'-deamino-3'-hydroxy-4'-epi-doxorubicin**	H	OH	H	OH	OH	H	0.17
(13)	**3'-deamino-4'-deoxy-4'-epi-amino-idarubicin**	H	H	H	NH_2	H	H	0.05
(14)	**3'-epi-daunorubicin**	OCH_3	H	OH	H	H	NH_2	**1.37**
(15)	**3'-deamino-3'-epi-hydroxy-4'-deoxy-4'-amino-daunorubicin**	OCH_3	H	NH_2	H	H	OH	2.60

Figure 1.5 *The chemical structures of anthracycline derivatives. IC_{50} values were determined from the dose-response curves of three independent experiments. The cytotoxic activity was determined on human HL60 leukemic cells using a cell growth inhibition assay after 1 h at 37° drug exposure.*[39]

Previous studies of anthracyclines which stimulate topoisomerase II-mediated DNA cleavage, in a DNA sequence-specific manner, have shown that compound **(14)** has a markedly different sequence-specificity, as compared to the parent drug **(9)**. Compound **(9)** requires an adenine and a thymine at positions -1 and -2, respectively, corresponding to the two nucleotides at the 3'-terminus of a strand cut, whereas compound **(14)** prefers guanine.

This change in the sequence-specificity is due to the configuration of the amino group of the sugar moiety. This amino group interacts strongly with the phosphate backbone of nucleic acid. In addition, it is speculated that the OH at C-9 of the ring A is involved in its interactions with the enzyme.[40]

Generally speaking, three distinct functional domains of the anthracycline molecule may be defined in the ternary complex (DNA-drug-enzyme): the planar ring system, the sugar moiety, and the cyclohexane ring (A). The first two domains are likely to interact with the DNA, whereas the A ring and its substituents at the C-9 may be closer to the enzyme.[40] **(Figure 1.6)**.
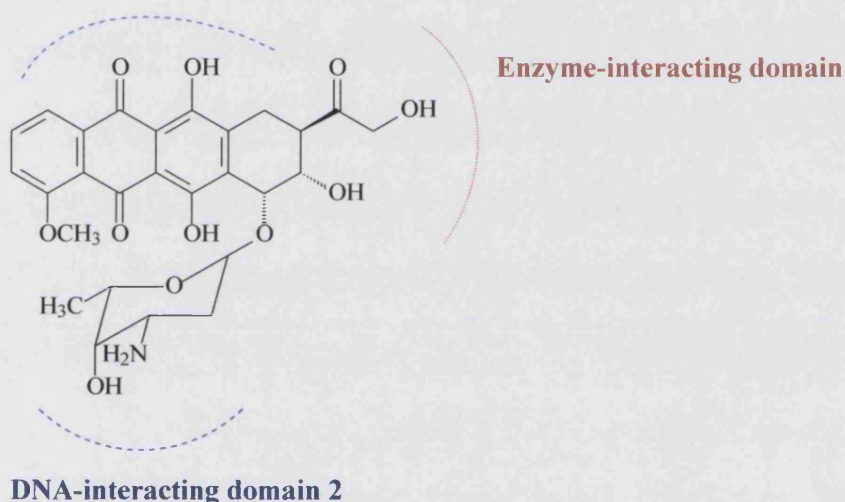
Figure 1.6   *Putative functional domains of the anthracyclines molecule.*

1.6   Drug targeting

Conventional therapies such as surgery, radiotherapy, hormone-ablation and chemotherapy, used to eradicate prostate cancer, have resulted in prolonged survival and cure in a few patients. However, relapse and metastases occur in most of the cases and, in general, are unresponsive to these treatments any more in the conventional doses. So, to overcome this resistance, an aggressive treatment was required, which includes a combination of chemotherapeutic agents. This, unfortunately, results in severe side-effects and is rarely curative. Therefore, conventional doses of the drug should be delivered to the

targeted area, so as to decrease the toxic side-effects. This could be achieved by the invention of site-specific drug delivery systems.

The degree of specificity achieved by drug targeting is classified according to the level of selectivity of the delivery system into; **(A)** first-order (organ targeting) refers to targeting of individual organs or tissue; **(B)** second-order (cellular targeting) refers to targeting of a specific cell type(s) within a tissue; **(C)** third-order (subcellular targeting) refers to targeting of selected intracellular compartment in the target cells. Various delivery systems could attain each of these levels but not all the three together. The majority of cytotoxic agents act at a variety of subcellular sites, so, a third order level of targeting may be necessary to ensure maximum therapeutic efficiency.[41]

1.6.1 Mode of drug targeting

The systems available for achieving site-specific drug delivery range from direct chemical modification of the drug molecule, such as prodrug design,[42] to the use of carriers, such as macromolecules.[43] In general, site-specific drug delivery systems are classified according to the methods by which they achieve the target site. They are distinguished into "passive" and "active" drug targeting.

1.6.1.1 Passive targeting

Passive drug targeting refers to the natural distribution pattern of the drug *in vivo*. The fate of drug distribution depends largely on the physicochemical properties of the drug particles, such as the number, size, shape, surface characteristics and surface charges. Therefore, these properties have been exploited to increase targeting efficiency.[43] For example:

A   *Passive lung targeting*

Passive lung targeting of anticancer agents depends on the entrapment of large particles (>7 µm) in the capillary bed of the lung.

B   Passive reticuloendothelial system (RES)

RES system is a collective name for a group of highly phagocytic cells derived from the bone marrow.[44] These cells are present either at fixed sites or free in the circulation throughout the body. They are found in large concentration in the liver (fixed macrophages called Kupffer cells), spleen and bone marrow. RES-mediated clearance is considered to be a major factor in determining biodistribution.[41]

Macrophages are important part of the host defence mechanism against tumour cells. They are activated by lymphokines, such as macrophage activating factors, or synthetic compounds, such as muramyl dipeptide. Upon activation, they are capable of killing tumour cells *via* an immunologically non-specific mechanism. However, macrophage-mediated destruction of large tumour burdens is not feasible. So, this approach is either used to eradicate micrometastases or to remove any residual tumour cells remaining after surgery or chemotherapy.[41,45]

C   Passive intra-arterial targeting

In general, intra-arterial injection of large drug particles results in entrapment by the first capillary bed encountered. This entrapment would be useful upon injection of antitumour agents into the arteries supplying a tumour site. This will result in drug accumulation in the tumour site before RES clearance takes effect. For example, starch microspheres, co-injected with cytotoxic agents, result in the blockage of tumour arterioles and, consequently, induce localised hypoxia and high concentration of drug. However, this approach is of little or even no value in the treatment of disseminated tumours or metastases. It is only useful in case of well-localised solid tumours.[41,46,47]

1.6.1.2 Active targeting

Active targeting refers to the deliberate modification of the natural distribution pattern of the drug, in order to direct it to a specific organ tissues or cells. Modifications, such as prodrug design with the trigger-linker-effecter concept, constitute a potential strategy to overcome the limitations of chemotherapeutic agents. Prodrugs are comprised of two major domains; a "trigger" unit, which is the substrate for the activating enzyme or system, and

an "effecter" unit (the active drug), which is activated or released by a metabolic process; these are sometimes joined by a definable linker.[48] **(Figure 1.7)**. Prodrugs are often divided into two groups:

Trigger	Linker	Effector
Selective metabolism	Deactivate effector	Potent & diffusible cytotoxic
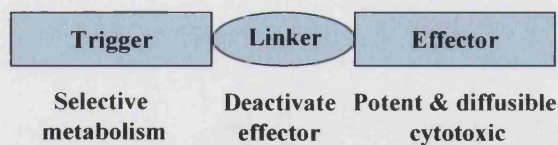
Figure 1.7   *Trigger-linker-effecter concept for prodrug design.*

1.6.1.2.1 Prodrugs designed to increase the bioavailability to improve the pharmacokinetics of antitumour agents

These prodrugs would overcome the problem associated with numerous antitumour drugs that possess a limited bioavailability due to low chemical stability, limited oral absorption or rapid breakdown *in vivo*. The activation process of the prodrugs is preferred to be relatively slow in the blood or liver, thus preventing acute toxic effects due to high peak concentration of the active drug. After activation, the drug has to be transported *via* the blood stream to the tumour site where it can exert its antitumour action.[49]

It is noteworthy that the bioavailability of rapidly metabolised antitumour drugs could be improved by altering the metabolism system itself, without altering drug design. For example, the blockage of RES (especially the Kupffer cells), by the use of RES depressant agents, such as dextran sulfate 500, will protect the drug from being captured by these cells. Illum *et al.*[47] have used dextran sulfate to block the RES of rabbits. Upon subsequent injection of radiolabelled polystyrene particles, 30% of the injected dose accumulates in the liver and spleen, compared with 90% in the unblocked RES animals. The drawback of this approach results from the possibility of dose overload upon subsequent dosing. So, the use of this technique in clinical trial is doubtful.[47]

1.6.1.2.2 Prodrugs designed to increase the local delivery of antitumour drugs

The concept of this design is referred to as targeting, organ-specific and tumour-specific prodrug activation. In organ-specific targeting approach, prodrug activation is achieved by an enzyme selectively presented in the targeted organ, whereas, in the tumour-specific targeting approach, the enzyme responsible for prodrug activation should be uniquely

active in the tumour.[50] Another method for tumour-specific targeting is by making use of the hypoxic environments present in solid tumours by the synthesis of bioreductively activated prodrugs.[51] In organ-specific and tumour-specific targeting methods, enzymes of high catalytic efficiencies are beneficial, enabling a rapid activation of the prodrug. A drawback associated with the tumour-specific targeting approach is that, unlike bacteria and viruses, cancer cells do not contain molecular targets which are completely foreign to the host.[52] Examples of the most common alternative strategies encountered in targeting include:

1.6.1.2.2.1 Bioreductive prodrug targeting

In the 1950s, Tomlinson and Gray observed that the diffusion limitation of O_2 led to the presence of hypoxic cells in tumours. This hypoxic condition has been purported to be an important biological factor in the failure of radiotherapy to achieve local control.[53] On the other hand, it is beneficial in the development of site-specific drug delivery systems. This hypoxic condition has been exploited for the development of bioreductively activated drug targeting systems. The idea starts with the development of inactive prodrugs, which are stable in normoxic tissue and are activated upon bioreduction under the hypoxic condition to release the active drug. It is noteworthy that the hypoxic condition is also associated with a number of other pathological diseases, such as rheumatoid arthritis, diabetes, renal disease and some cardiovascular diseases. As a result, hypoxia-based therapeutic strategies become more important day-by-day.[54]

Hypoxia has been shown to control enzyme expression, *via* hypoxia-inducible factors, which results in the regulation of reductase enzymes required for the activation of inactive prodrugs. So, hypoxia has a dual advantage; (A) increase the levels of reductase and so enhance activation of inactive prodrug; (B) reduce the concentration of oxygen and so facilitate the reduction process.[54] Several classes of compounds have been considered for the development of hypoxia-selective cytotoxins. For example:

A   *Nitroheterocycles*

In the development of bioreductive delivery systems, nitroheterocycles have a number of advantages; (A) they by themselves are used as anti-microbial agents and, in many cases,

have a limited side-effect profile; (**B**) they vary greatly in their one-electron reduction potentials, thus enhances adaptation for targeting drugs to mammalian tissues; (**C**) in many models of drug conjugation; they have been shown to release the active drug, despite having a relatively stable linker bond.[55,56]

B *Indolequinones*

The introduction of indolequinones in bioreductive delivery system grew from the research done on the use of mitomycin C (**8**) as an anticancer agent. Their one-electron reduction potentials made them suitable for bioreductive targeting to hypoxic tissue. A number of structural modification analogues of the base indolequinone have been synthesised and used in conjugation with a variety of drugs, such as anti-inflammatory agents[57] and anti-cancer agents.[58]

C *Self-alkylating bioreductives*

In many diseases, it was essential to use an inert delivery system. In this system, it was essential to avoid the deleterious adduct formation with macromolecules such as DNA after drug release following bioreduction. The self-alkylating delivery concept was designed to incorporate a nucleophile within the bioreductive prodrug. The nucleophile will preferentially react with the bioreduced remnant, through an intramolecular cyclisation process, during or after drug release, thus assisting drug release, stabilising the bioreductive remnant and preventing DNA adduct formation.[54]

1.6.1.2.2.2   Antibody-drug conjugates targeting

This strategy involves the conjugation of a number of antitumour drugs, such as anthracyclines with antibodies. Antibodies are proteins of the immune system, capable of differentiating malignant cells from their normal counterparts. In 1975 a new method to produce large quantities of monoclonal antibodies (MoAbs), or antibodies to any antigen has been published and showed preferential specificity for tumour cells.[59]

The most commonly used anthracycline chemotherapeutics in constructing drug-MoAb conjugate are daunorubicin and doxorubicin. Both are the best recommended drugs to be

used in the treatment of advanced stage prostate cancer.[59] A number of conjugates prepared have shown respectable activity against human tumour xenografts implanted into nude mice. However, the few which have undergone clinical evaluation have been disappointing in their activity. This could be attributed to the decrease in the potency of doxorubicin (9) and daunorubicin (10) as a result of the conjugation with MoAbs, even in the case of the most releasable constructs. Furthermore, the amount of MoAb-drug conjugate localised within the tumours in a clinical trial is 3 to 4 times lower than in experimental mice, as determined by studying radiolabelled MoAbs.[59]

1.6.1.2.2.3   Antibody-directed enzyme prodrug therapy

The method of ADEPT has been designed in an attempt to improve the outcome of the drug-MoAb approach. In this approach, an enzyme is conjugated to MoAb instead of the drug. This enzyme-MoAb conjugate is then localised into tumour and, after clearance of conjugate from the circulation, anthracycline prodrug would be injected. This prodrug is inactive alone but becomes active by the effect of the enzyme.[60] (Figure 1.8). An example of this approach can be seen in the conjugate between alkaline phosphatase and MoAb. The 14-phosphate derivative of doxorubicin was used as a prodrug because it is incapable of penetrating cell membranes. Good antitumour activity has been detected, whereas each of them alone was inactive under the same conditions.[61]
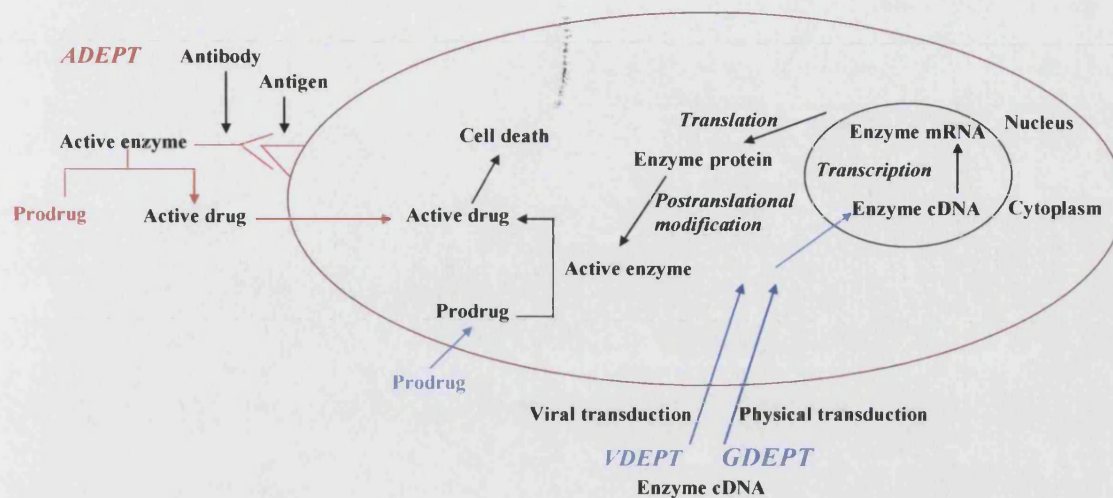
Figure 1.8 *General outlines of the delivery methods for an enzyme/prodrug cancer strategy; divided into two major classes: GDEPT and VDEPT, which refers to the delivery of genes that encode prodrug-activating enzymes into tumour tissues; and ADEPT, which deliver active enzymes onto tumour tissue.*

1.6.1.2.2.4   Gene-directed enzyme prodrug therapy

Gene therapy is a genetic technology of modifying cells for therapeutic gain. Genetic modification is possible on both malignant and non-malignant cells. There are two suicide gene approaches. The first approach is termed toxin gene therapy and aims to deliver toxic genes to the malignant cells where the protein produced will direct tumour cell killing. The second approach is termed gene-directed enzyme prodrug therapy (GDEPT) or virally directed enzyme prodrug therapy (VDEPT), where foreign enzymes (non-human) are expressed in target cells and activate subsequently administered non-toxic, inactive prodrugs into active drugs.[62,63] **(Figure 1.8)**

For successful GDEPT, a number of factors must be accomplished, which include; **(A)** gene, which express an exogenous enzyme or an endogenous enzyme that is poorly expressed in tumours and is able to activate a prodrug; **(B)** a means by which gene would be delivered to the target cells; **(C)** a prodrug.[62] The gene should be expressed mainly in tumour cells or with relatively high ratio compared to normal cells. The enzyme should be able to catalyse different types of reactions, such as scission reactions or redox reactions; different from endogenous circulating enzyme, accessible to the prodrug and expressed in

26

high amount in the targeted tumour cells. <u>The prodrug</u> should be an efficient and selective substrate for the expressed enzyme and diffuse through tumour cell membranes efficiently to permit its intracellular activation by the enzyme. <u>The active drug</u> should be an effective cytotoxin and have good bystander effects (an ability to diffuse to and kill neighbouring tumour cells).[62,48]

A number of prodrugs have been explored in GDEPT, such as 5-fluorocytosine (5-FC)/*E. coli* cytosine deaminase (CD) therapy. CD is an *E. coli* enzyme,[62] similar to human cytidine deaminase but with different substrate specificity. It converts the inactive, non-toxic 5-FC to 5-fluorouracil, which is a powerful competitive inhibitor of thymidylate synthase (TS), a key enzyme in DNA biosynthesis, thus causing cell death. CD/5-FC therapy has been tested *in vivo* and *in vitro* and has been used for the treatment of colorectal carcinoma. It has been found that CD expression increases the sensitivity of tumour cells to 5-FC in vitro, by ~1000 fold (from $IC_{50} = 26$ mM to 27 μM).[64] However, in mice bearing xenografts expressing CD, 5-FU generated after 5-FC administration could be detected in the environment surrounding the tumour and contributed to the bystander effect.[65]

The most significant problem in gene chemotherapy is the prediction of a way to deliver therapeutic genes to the tumour. In all currently performed clinical trials, direct intratumour injection of the vector is the method. This method has certain limitations because it fails to address the problem of delivery to the sites of metastatic spread where tumour cells are too numerous and inaccessible with direct injection. Many efforts have been made to overcome this problem.[66]

1.6.1.2.2.5   Enzymatic prodrug delivery targeting

The concept of this approach is not far from what had previously been seen in sections **1.6.1.2.2.1** and **1.6.1.2.2.4**. In the aforementioned, the prodrugs are converted to their active analogue by direct reduction, whereas in the second the prodrugs are activated by exogenous enzymes expressed in tumour cells by the action of the delivered genes. In this section the prodrugs are activated by endogenous enzymes expressed selectively in tumour cell.

A = Bipartite Prodrug

B = Tripartite Prodrug
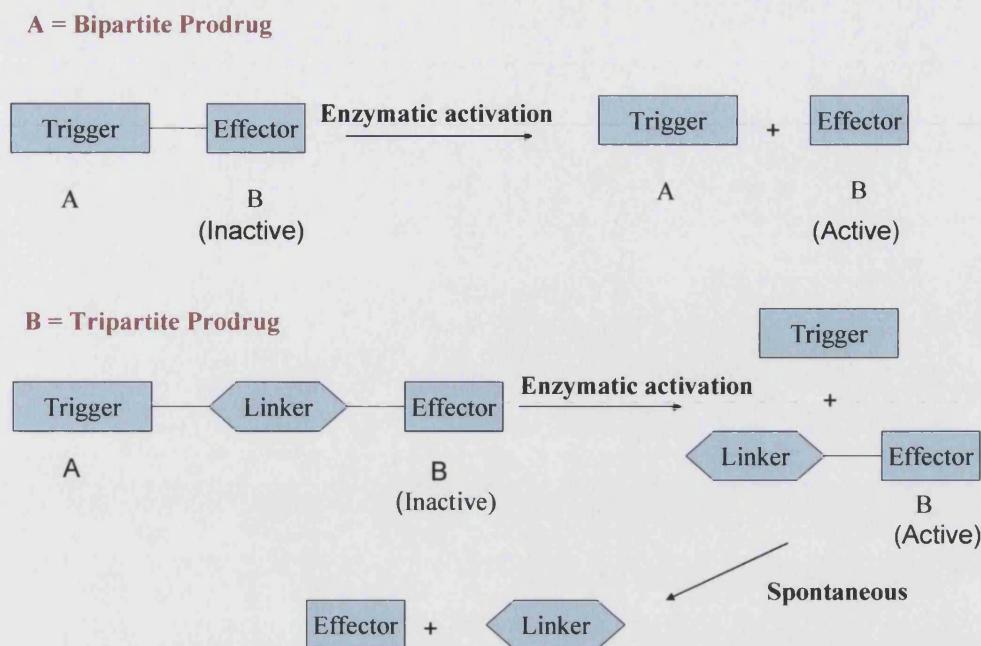
Figure 1.9 *Representative schemes of enzymatic bipartite and tripartite prodrugs targeting approaches.*

Prodrugs are agents that undergo chemical or enzymatic transformation to the parent drug following delivery, so that the parent drug (metabolic product) can subsequently exert its therapeutic effect.[67] They are divided into Bipartite or Tripartite systems **(Figure 1.9)**; The bipartite prodrug system consist of a trigger (carrier) moiety **A** and a effector (drug) moiety **B**. Moiety **A** is the means by which, prodrug would be delivered to a specific site and, become a specific substrate for a particular enzyme. Enzymatic hydrolysis of the bond between **A** and **B** releases effector (active drug) **B** in the body. In certain cases this basic prodrug tactic fails. It is possible that the linker bond between **A** and **B** is unstable due to its inherent nature or the prodrug **A-B** is quite stable but the electronic and steric features of **B** hinder the hydrolysis of the linker bond by the target enzyme.

As an example, the enzymatic hydrolysis of peptide-doxorubicin conjugates results in the release of a doxorubicin-amino acid conjugate, which had lower activity than the parent drug.[68] So, to overcome the previous difficulty, a tripartite prodrug tactic (three-component system) is designed, where the trigger and the effector are linked together by a special type of connecter group **(Figure 1.9)**. Consequently, the enzymatic hydrolysis will occur in the **A**-linker bond rather than the **A-B** bond. Then linker-B bond would hydrolyze spontaneously, under the physiological conditions, to release the active, parent drug **B**.[67]

28

Several models gave promising results in studies *in vitro*.[67] This leads to its application in site specific prodrug delivery of cytotoxic agents' such as doxorubicin and vinblastine **(Scheme 1.2)** and **(Scheme 1.3)** respectively. [69,70]

In the following model **(Scheme 1.1)**, The N^{α}-Boc-Lys **(17)** is the trigger moiety, the *p*-aminobenzyloxycarbonyl is the linker moiety and *p*-nitroaniline **(22)** is the effector. In the presence of trypsin, the tripartite prodrug undergoes rapid hydrolysis and consequently releases *p*-nitroaniline **(22)** ($t_{1/2}$ ~11 min at 25°C). This rapid release presumably works through a 1,6-elimination process, which gives an unstable carbamic acid that is unstable and rapidly loses CO_2 to produce *p*-nitroaniline **(22)**.[6]
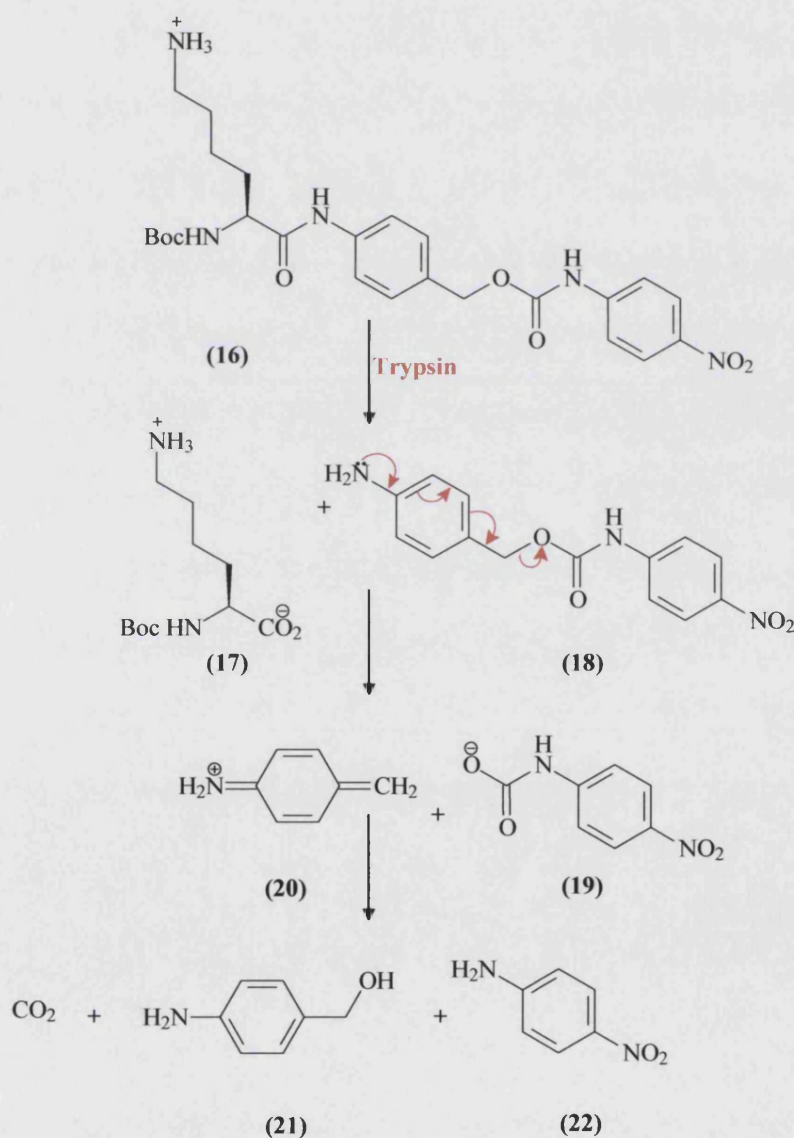
Scheme 1.1   *Enzymatically activated tripartite prodrug model for 4-nitroaniline.*

In the following model **(Scheme 1.2)**, the Cbz-Phe-Lys is the trigger moiety, the *4-aminobenzyloxycarbonyl* is the linker moiety and doxorubicin **(9)** is the effector. In the presence of cathepsin B, the tripartite prodrug undergoes rapid hydrolysis and consequently releases doxorubicin (t$_½$ ~8 min at 25°C).[69]
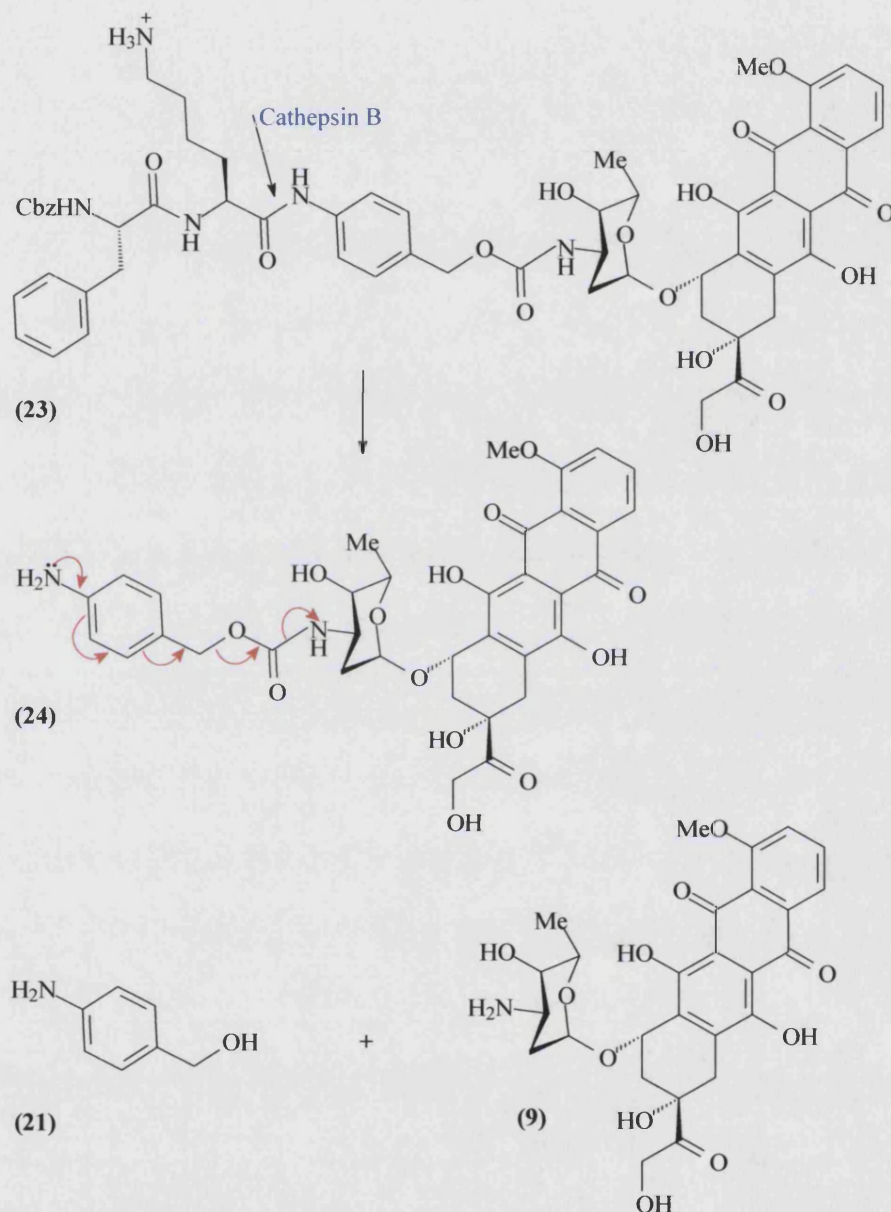
Scheme 1.2 *Enzymatically activated tripartite prodrug model for doxorubicin (9).*

In the following model **(Scheme 1.3)**, the Ac-Hyp-Ser-Ser-Chg-Gln-Ser-Ser is the trigger moiety, the proline amino acid is the linker moiety and vinblastine **(28)** is the effector. In the presence of prostate specific antigen (PSA), the tripartite prodrug undergoes rapid

cleavage and consequently intramolecular cyclisation to release the drug ($t_{\frac{1}{2}}$ ~12 min at 37°C).[70]
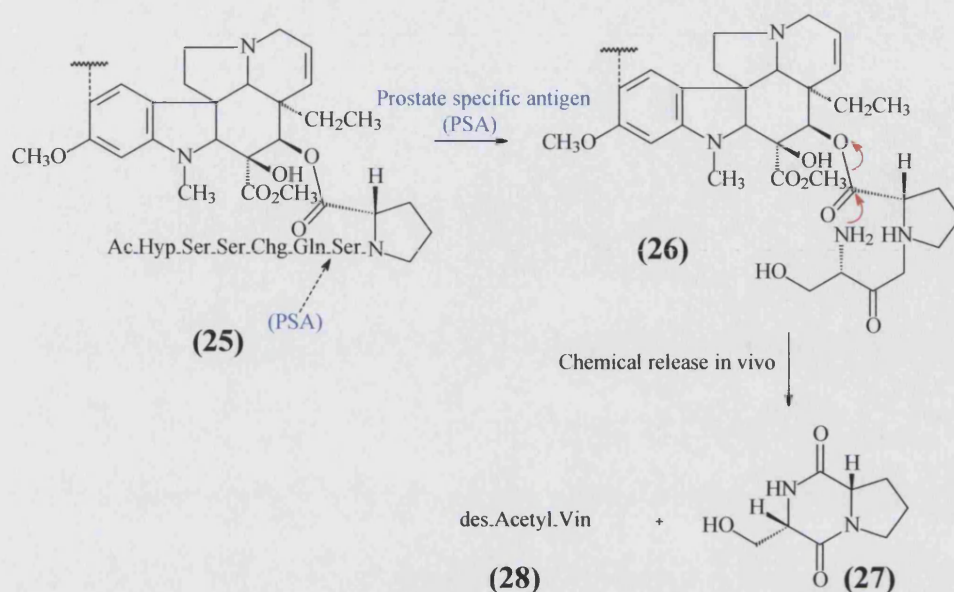
Scheme 1.3 *PSA-activated tripartite prodrug for vinblastine.*

1.6.1.2.2.6 Water-soluble polymeric prodrug targeting

1.6.1.2.2.6.1 Classification of macromolecular drugs

Kálal *et al.*[71] classified macromlecular drugs into: **(A)** drugs of polymeric nature, in which the therapeutic benefit is solely dependent on their macromolecular properties, such as plasma expanders; **(B)** polymer-bound drugs, in which drugs could exert their therapeutic effect without being detached from the polymer. In this prodrug system, the main polymeric chain is biologically inert and the therapeutically active group constitutes part of that chain; **(C)** polymer-carried drugs, in which drugs are bound to the polymer and must be detached to exert their therapeutic effect.[71,72]

1.6.1.2.2.6.2 Rationale for the concept of macromolecule-drug conjugates

In chemotherapy, the main objective is to optimise the therapeutic effect of the drugs and to reduce or even overcome the toxic side-effects. This could be attained by successful site-specific drug delivery and by accumulation of drug into tumour sites. Macromolecular

31

prodrugs are of increasing interest in cancer chemotherapy because they manage to fulfil the targeting and controlled-release criteria.

In general, most pharmacologically active agents are low molecular weight compounds, which penetrate readily into the cells by diffusion and are excreted rapidly from the body. Consequently, repeated doses must be given, in order to maintain the therapeutic effects, but this will also increase their cytotoxicity.[73] A number of sophisticated approaches managed to sort out the targetability point. However, we are still looking toward increasing the duration of action, either by the retention of drugs in the tumour site or by decreasing their biodegradability.

1.6.1.2.2.6.3 Tumouritropic principles of macromolecular drugs

In cancer, the vasculature characteristics of tumour tissues differ fundamentally from their normal counterparts. These include **(A)** tumour angiogenesis *i.e* the process by which tumours enhance ingrowths of new capillaries resulting in hypervasulature **(B)** hyperpermeability **(C)** hypoplastic or minimally effective lymphatic system producing minimal tumour drainage.[43,74]

It has been reported that a large number of solid tumours possess blood vessels that are relatively permeable to macromolecules. This has been loosely attributed to be related to the morphological features of permeability, such as the presence of enlarged interendothelial cell junctions in a minority of tumours. Later on, Dvorak *et al.*[75] have established the factors underlying tumour-enhanced permeability of macromolecules. They have found that extravasation of large macromolecules was restricted to mature veins at the interface of the tumour with normal tissue. The blood capillaries responsible appeared morphologically normal, without any sign of a presence of obviously enlarged interendothelial cell spaces. So, they have suggested that the phenomenon of increased permeability might be mediated by enhanced vesicular transport, rather than simple leakage from interendothelial cell junctions.[43,75] This phenomenon is widely spread in solid tumours.[76]

Hypoplasticity is another phenomenon characteristic of solid tumours but not normal tissues. Hypoplastic or minimally effective lymphatic systems produce minimal tumour

drainage.[43,74] In normal tissue, fluid and small solutes which diffuse from the bloodstream into tissue can drain back *via* postcapillary venules, while macromolecules will drain back *via* the lymphatic system. However, in tumours, fluid and small molecules could either feedback into the postcapillary venules or pass through the tumour interstitium while macromolecule can only pass through the tumour interstitium (the dead end).[74] **(Figure 1.10)**. Thus, the enhanced permeability and retention (EPR) phenomenon of macromolecules in solid tumour is considered the focus of interest in developing new tactics in cancer-targeting chemotherapy.[43,77,78]
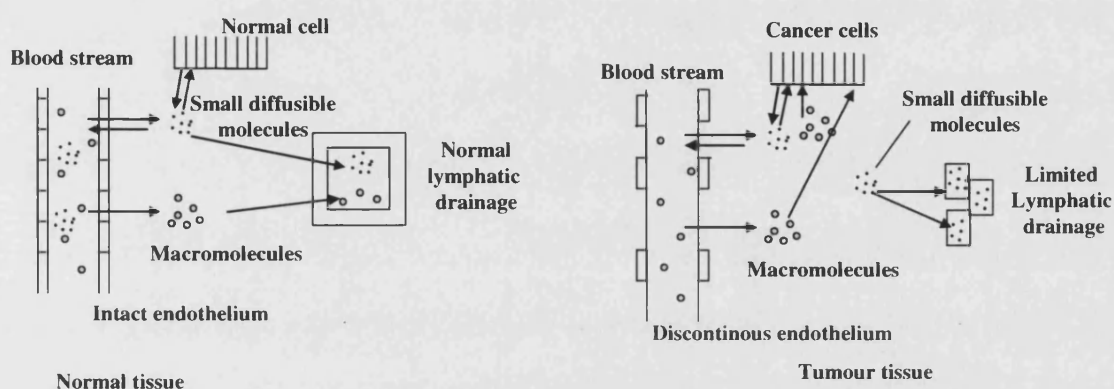
Figure 1.10 *Diagrammatic representation of the enhanced permeability and retention effect (EPR).*

The drawback associated with polymer drug conjugates arises from the process of their cellular uptake. Unlike low molecular weight drugs, in which cellular uptake is limited by diffusion, polymer drug conjugate (molecular size above 50,000 Da) uptake is limited by endocytosis. Endocytosis can be considered of two types; pinocytosis and phagocytosis.[77] Soluble macromolecules are taken up by pinocytosis and not phagocytosis. However, pinocytosis is a relatively slow process and the pinocytised materials will be transferred to the lysosomal compartment of the cell *via* endosomes (receptosomes). Thus, binding of the drug to a water soluble-macromolecule will render them lysosomotropic.[79]

A sophisticated way to overcome the pinocytotic and lysosomotropic processes would be by designing a polymeric prodrug system from which the active drug could be released by the action of an endogenous enzyme that is catalytically active only in the tumour and is located either on the outer surface of the cell or in the extracellular space. The tumour-

selectivity of the polymeric prodrug delivery system would then be binary, involving; **(A)** the EPR effect; **(B)** tumour-localisation of the enzyme.

1.6.1.2.2.6.4   Models for macromolecule-drug conjugate

A general scheme of the model is represented in **(Figure 1.11)**. The polymer backbone, which is generally biodegradable but sometimes biostable, is modified by three functional moieties. One part is used to fix the therapeutic agents *via* a covalent bond. This bond could be permanent or transient depending upon the nature of the drug, whether it is active while it is part of the polymer, or it should be released from the polymer to be active. The second part is a linker, necessary to provide physical separation between the drug and the polymer and so, facilitate their conjugation and the third part is a device to control the physico-chemical properties of the conjugate system.[72]
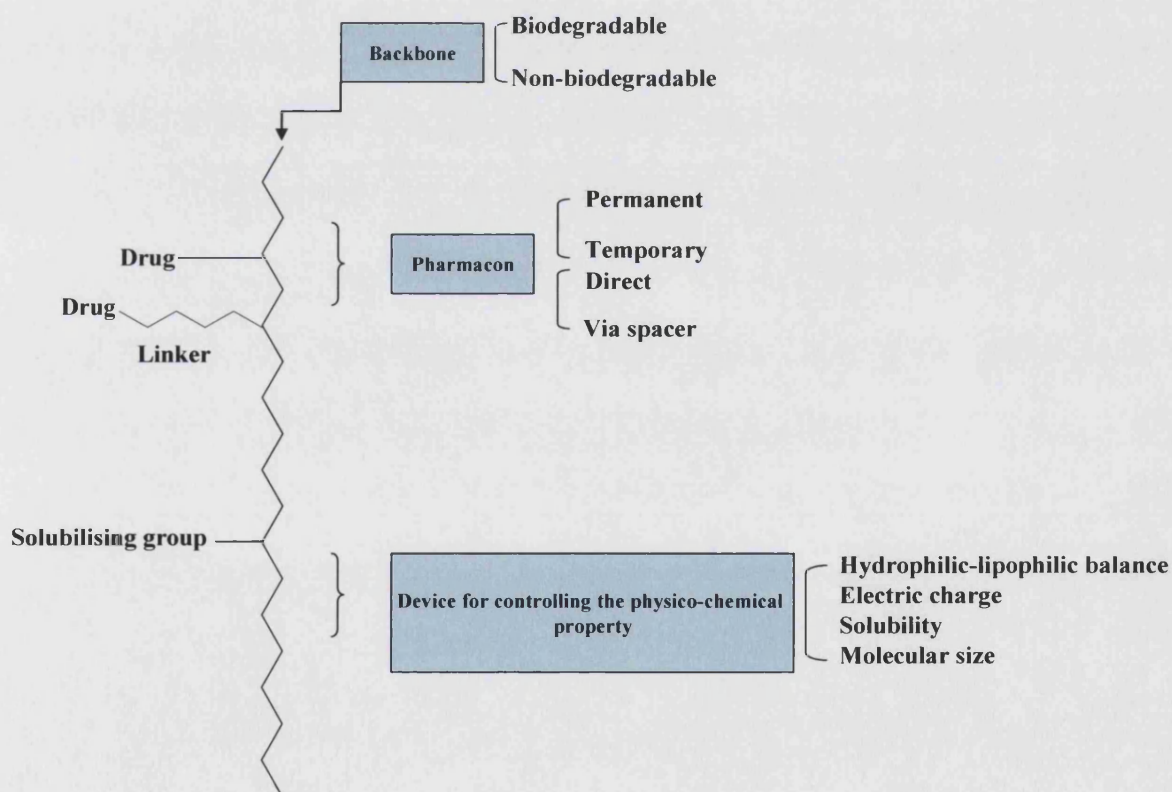
Figure 1.11   *Model of macromolecule-drug conjugate.*

1.6.1.2.2.6.5 Macromolecular carriers

In macromolecule-drug conjugates, the macromolecular carrier is the major determinant unit of the pharmacokinetic properties *in vivo*. Ideal carriers should be easily synthesised, accessible to chemical modification, water-soluble, biodegradable, non-toxic and non-immunogenic.[80] However, at present, no carrier has been found to fulfil all these criteria.[77] A number of naturally occurring and synthetic soluble macromolecular carriers are presented in **(Figure 1.12)**.
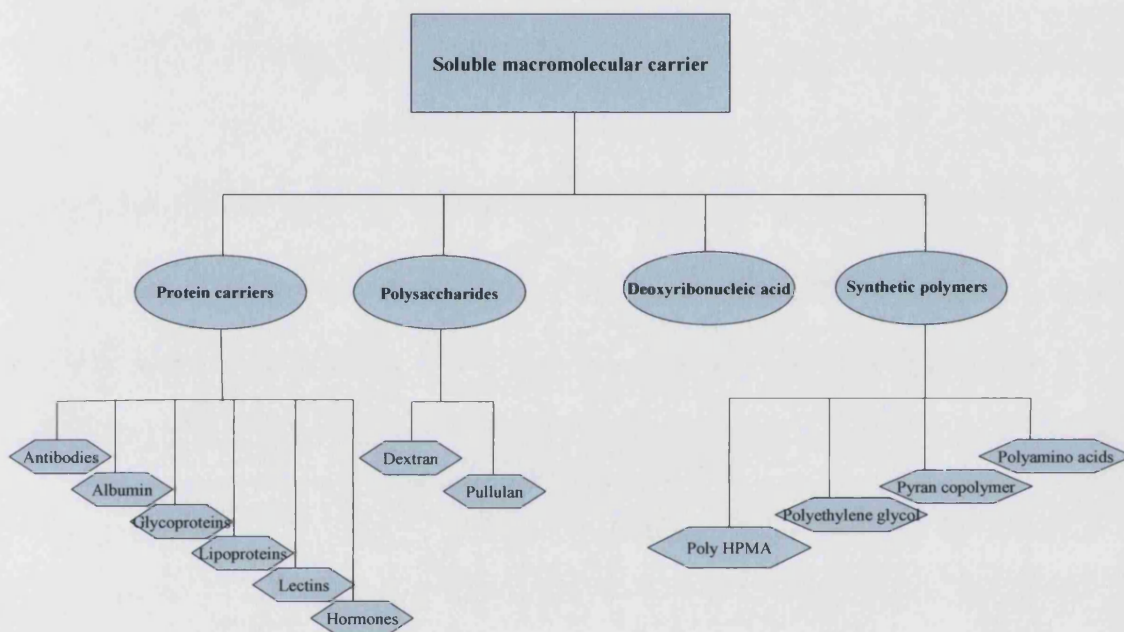
Figure 1.12   *Classification of soluble macromolecular carriers.*

1.6.1.2.2.6.6 Clinically active polymeric prodrugs

Examples of some polymeric prodrugs models, which showed activity in clinical trials include:

A   *Mitomycin C polymeric prodrug*

The general structure of mitomycin C (MMC)-dextran conjugates is represented in **(Figure 1.13)**. The drug is attached to the carrier by linkage through the aziridine nitrogen. The linker used was 6-aminohexanoic. The choice of the linker is important because of its influence on the rate of conjugate cleavage. The studies have shown that MMC-dextran

conjugate **(29)** of MW 70 KDa, based on this linker, exert higher antitumour activity when compared with free MMC against certain murine model tumours (*e.g.* Ehrlich ascites) *in vivo*.[43] The activity of the conjugate is thought to be mediated by extracellular hydrolytic release of the drug.[81]
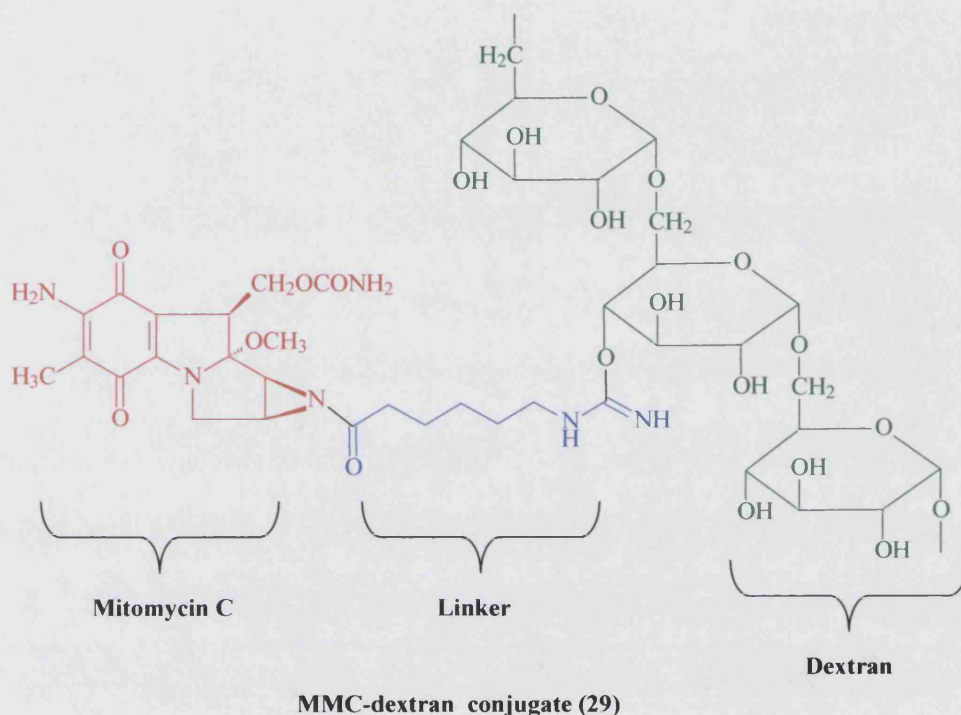
Figure 1.13   *General structure of mitomycin C (MMC)-dextran conjugates.*

B   *5-Fluorouracil polymeric prodrug*

Several molecular prodrugs of 5-FU have been developed. In most cases, the antitumour activity results from the non-specific chemical hydrolysis of the ester,[82] carbamate,[83] carbamoyl[82] or amide bond[82] between the active drug and the polymer backbone.

A pro-prodrug polymer conjugate system (multi-prodrug, cascade system) has been designed.[84] This system will provide a tumour-specific release of 5-FU under the environmental conditions of the tumour cells. The free drug would be released by a step-wise enzymatic and chemical cleavage of several chemical bonds. The first bond will be between the polymer backbone and the prodrug, whereas the second bond is inside the prodrug system. This system will control the rate and time of the drug release.[85]

36

Nichifor et al.[86] have synthesised a pro-prodrug polymer conjugate of 5-FU by attaching oligopeptide chains, having a 2-(5-fluorouracil-1-yl)glycine ethyl ester residue at the C-terminus to dextran. This conjugate displayed high cytotoxicity in vitro against murine C26 cells. In addition, intraparental administration to murine C26 tumour-bearing mice caused no acute toxicity and increased the life-span of the treated animals.

C   Doxorubicin polymeric prodrug

Doxorubicin is the mainstay in clinical treatment of a variety of malignant diseases, notably in metastatic prostate cancer.[24] However, chronic administration of high doses leads to severe systemic toxicity. Thus, new studies have been oriented toward the use of the soluble macromolecules as a method of selective targeting of doxorubicin.

Doxorubicin (9) is an amphipathic molecule, containing a hydrophobic anthraquinone structure and a hydrophilic amino-sugar (daunosamine); thus it is freely soluble in aqueous and organic solutions and can readily penetrate the cell membrane. It has been conjugated with a range of soluble macromolecules, such as proteins, DNA, dextran, poly(aminoacids) and methacrylamide-based copolymers. The chemistry of its derivatisation with the carriers has been elucidated carefully and a range of different modes of attachment have been used. In considering the reduction of cardiotoxicity, similar results have been obtained as with particulate formulations of the drug. However, in term of specific therapeutic activity, it has been increased. As a result, the increase in specific activity of a polymer-doxorubicin conjugate is independent of the decrease in toxicity, which permits the administration of higher drug doses.[43]

The first observation of increased drug-specific activity has been seen with a dextran-daunomycin (DNR) conjugate. This conjugate showed improved therapeutic activity, when compared with same dose of free drug.[87] Later, DNA-anthracycline and protein-anthracycline conjugates (lysosomotropic) have been synthesised. The former conjugate was designed to release the drug intracellularly[88] but they were poorly stable in plasma.[89] Nevertheless, DOX-DNA and DNR-DNA conjugates showed improved therapeutic activity against the model L1210 tumor system.[90]

A water-soluble polymer, PK1 [HPMA (±)-N-(2-hydroxypropyl)methacrylamide] was conjugated with doxorubicin through a tetrapeptide (GFLG) linker. This polymer-drug conjugate was designed to be cleaved intracellularly by cathepsins B, H and L.[43,91,92] The molecular weight (MW) threshold permitting renal excretion of HPMA homopolymer was found to be approximately 45,000 Da.[93] Thus, the developed conjugates were designed to use a copolymer backbone of a MW about 20,000 Da. This conjugate system displays increased specific drug efficacy, compared with the same dose of the free drug.[43]

However, this approach is limited by two factors; **(A)** the sole basis of tumour-selectivity of delivery is concentration of the prodrug by the EPR effect. Cells in normal tissue are also capable of cleaving the GFLG sequence, thus releasing doxorubicin; **(B)** the enzyme that cleaves the GFLG peptide is lysosomal and thus the whole release mechanism is essentially intracellular.

The problem with polymeric prodrugs is associated with the pinocytosis process by which they access the cells. Pinocytosis is a relatively slow throughput process. Thus, the release of active drug is limited. Much more attractive would be a polymeric prodrug system from which the active drug is released by the action of an endogenous enzyme that is catalytically active in tumour site only and is located either on the outer surface of the cells or on the extracellular space. The tumour-selectivity of drug delivery would then be binary (EPR effect and tumour-localisation of the enzyme) and the rate of site-selective drug release would be much greater. Prostate specific antigen (PSA) fulfils excellently both criteria for an activating enzyme.

1.7   Tumour markers for adenocarcinoma of the prostate

1.7.1   Acid phosphatase

During the past years, acid phosphatase enzyme has been considered the standard marker for adenocarcinoma of the prostate. It has been used by urologists in the diagnosis and staging of the disease, as well as in monitoring patients' response to therapy. However, unfortunately, the inability of this marker to report the serum concentration of the

isoenzyme produced by prostatic tissue without interference from other isoenzymes generated by other body organs, constitutes the major difficulty in its usage.[94,95]

1.7.2 Prostate specific proteins

Among several prostate-specific proteins, prostate-specific membrane antigen (PSMA) and prostate-specific antigen (PSA) are sensitive markers for diagnosis of prostate cancer.[96]

1.7.2.1 Prostate specific membrane antigen (PSMA)

PSMA is a glutamate carboxypeptidase, membrane-bound glycoprotein, highly restricted to prostatic epithelial cells and over-expressed in hormone-refractory disease. The PSMA gene encodes PSMA, which is exclusively expressed in metastatic prostate carcinoma.[97] PSMA cleaves the terminal γ-linked glutamate residue from poly-γ-glutamated folates by its carboxypeptidase activity. This process is essential for γ-glutamate transport into cells.[98] Thus, an approach to target prostate cells that over-express PSMA is by designing a prodrug containing H-3 toxin. H-3 is a 25-amino-acid toxin capable of penetrating into the lipid bilayers by forming a pore, through which cell macromolecules or electrolyte leak resulting in cell death.[99] H-3 was inactivated by the addition of two glutamate residues. Selective activation of the prodrug would result from the cleavage of the terminal glutamates by PSMA. This model prodrug was demonstrated *in vitro*.[100] However, it is noteworthy, that PSMA is also expressed in normal brain and salivary gland tissue, *i.e* it is not completely prostate-specific. As a result, it is unclear whether or not it can be used for targeting therapy *in vivo*.[101]

1.7.2.2 Prostate specific antigen

Recently, prostate specific antigen (PSA) has been identified, characterised and found to be produced exclusively by the prostatic tissue. In fact, it is the most meaningful and useful tumour marker in prostate cancer.[102]

1.7.2.2.1   Discovery of PSA

In 1971, Hara *et al.*[103] discovered PSA in seminal plasma. At that time, PSA has been referred to as *gamma*-seminoprotein. Two years later, Li and Beling[104] were able to isolate this protein from the seminal plasma, identify its molecular weight (31,000 Da) and described it as E_1 antigen. In 1978, Sensabaugh[105] truly characterised this "semen-specific protein". He identified that this protein was highly immunogenic, had several sugar moieties, with a molecular weight of 33,000 Da and he referred to it as p30 because of its molecular weight. Interestingly, Grave *et al.*[106] suggested that p30 would be an excellent marker for semen identification and so could be used in identification of rape victims. In 1979 Wang *et al.*[107] identified this antigen to be specific to all types of prostatic tissue (normal, benign hyperplasia and malignant) and so it could not be found anywhere else in human tissue. As a result, this antigen is termed prostate specific antigen. Finally, Papsidero *et al.*[108] identified PSA in human serum and verified that this molecule was identical to the one seen in prostatic tissue.

1.7.2.2.2 Biomolecular characteristics

PSA is a member of the human kallikrein family that exhibits serine protease activity.[16] It is a single-chain glycoprotein with a MW 33,000-34,000 Da, comprising 240 amino acid residues (93% w/w) with four carbohydrate side-chains (7% w/w). Subsequent studies have shown that one carbohydrate side-chain exists at the N-side-chain of amino-acid 45 (asparagine) while the other three exist at the O-side-chain of the amino acids 69 (serine), 70 (threonine) and 71 (serine). The N-terminal amino-acid of the sequence is isoleucine and the C-terminal residue is proline.[15]

1.7.2.2.3 Function

PSA is produced by the epithelial cells lining the acini and ducts of the prostate gland. It is secreted at 0.5-2.0 g L^{-1} into the seminal plasma. Most PSA passes into the gland lumen, where it is involved directly in the liquefaction of the seminal gel-forming proteins, semenogelin(Sg) I and II, during ejaculation. Usually, a tiny proportion is absorbed into the bloodstream where levels should be <4 ng ml^{-1}. In normal men, the prostate capsule creates a barrier which will prevent the escape of PSA into the peripheral circulation. However,

barrier disruption by disease allows PSA into the peripheral circulation. Thus, PSA is used as a diagnostic tool for the detection and monitoring of prostate cancer and clinically it is the best known serological marker for the presence of prostate cancer.[16,109]

1.7.2.2.4 PSA in the staging of prostate cancer

The serum PSA concentration correlates well with the number of malignant prostate cells. This is because it is synthesised and secreted in large amounts by malignant prostatic epithelial cells and, at a lower level, by corresponding normal cells in the prostate.[110] The concentration of PSA in the extracellular fluid of normal human prostate and primary human prostate cancer is 1600-2100 nM; 80-90 % of this PSA is enzymatically active. In contrast, none of the PSA present in serum is enzymatically active.[111] This is because it forms a complex with the serum inhibitory proteins α1-antichymotrypsin and α2-macroglobulin, resulting in a predominant inactive form of PSA in the serum.[112] Thus, it is proteolytically active exclusively in the prostate, the target tissue for anti-prostate cancer therapy, and is an ideal enzyme for the release of drugs from polymeric prodrugs.

1.7.2.2.5 Substrate-specificity of PSA

On the basis of the PSA cleavage maps for Sg I and II, small peptides were synthesised containing the amino-acid sequence proximal to the PSA proteolytic sites[113] Coombs *et al.*[91] studies have converged on the amino-acid sequence SS(Y/F) Y↓S(G/S) as a preferred subsite occupancy for PSA **(Figure 1.14)**. However, this sequence has been found to be cleaved efficiently by chymotrypsin.
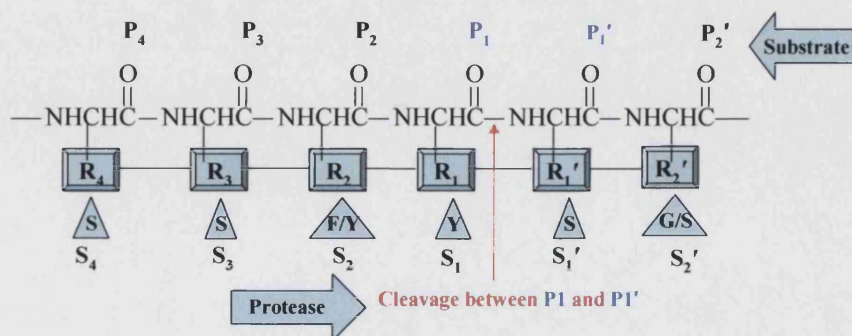
Figure 1.14 *Peptide sequences efficiently cleaved by PSA.*

Substrate group	Peptide sequence[b]	pmol of substrate hydrolyzed/min/100 pmol of indicated protease						
		PSA	Chymotrypsin	Elastase	Trypsin	Plasmin	hK1	hK2
1	KGISSQY	510	4290	3068	658	ND	ND	UD[c]
	SRKSQQY	234	3630	2788	260	0.4	2.0	UD[c]
	GQKGQHY	49.6	4274	922	122	UD	ND	UD[c]
2	EHSSKLQ	31.6	UD	UD	UD	UD	UD	UD[c]
	QNKISYQ	16.8	9.0	9.0	UD	UD	ND	UD[c]
	ENKISYQ	14.4	3.6	2.6	1.8	0.6	UD	ND
	ATKSKQH	16.0	38.8	UD	UD	UD	UD	ND
	HSSKLQ	62.7	UD	UD	UD	UD	UD	UD
	SKLQ	29.6	UD	UD	UD	UD	UD	ND
	KLQ	UD	10.6	0.4	UD	ND	UD	ND
	LQ	UD	UD	UD	UD	UD	ND	ND
	Q	UD	UD	0.7	UD	UD	ND	ND
3	KGLSSQC	13.6	12.2	950	UD	UD	UD	ND
	LGGSQQL	6.0	314	94.0	UD	UD	ND	ND
4	QNKGHYQ	1.8	0.2	0.6	UD	UD	UD	ND
	TEERQLH	1.2	48.8	1.0	UD	3.8	UD	UD[c]
	GSFSIQH	UD	3.6	0.4	0.4	0.2	ND	ND

Table 1.1   *Peptide substrates for assaying PSA activity (UD, undetectable <0.1 pmol of substrate hydrolysis/min/100 pmol of protease; ND, not done; hk1, human plasma kallikrein; hk2, human glandular kallikrein). [b]Substrate at 0.2 mM concentration in PSA assay buffer.[114]*

Denmeade *el al.*[114] identified four groups of seven amino-acid substrates based on PSA activity and specificity. The first group (KGISSQY, SRKSSQY and GQKGHY) were cleaved most efficiently by PSA, but were even better substrates for chymotrypsin and elastase. The second group (EHSSKLQ, QNKISYQ, ENKISYQ and ATKSKOH) were moderately cleavaged by PSA but with greater specificity. The third group (KGLSSQC and LGGSQQL) were also cleaved by PSA but with lower specificity than the second group. The fourth group (QNKQHYQ, TEERQLH and GSFSIQH) had little susceptibility to all proteases tested. So, it has been noticed that all substrates lacking Tyr at the cleavage site had no detectable activity with serum proteases and high activity with PSA, chymotrysin, trypsin, elastase enzymes *i.e.* they are not specific to cleavage by PSA. Therefore, a follow-up research on the second group indicated that substrates such as

(HSSKLQ and SKLQ) are extremely specific to cleavage by PSA irrespective of their low rate of cleavage. (Table 1.1)

Also, Denmeade *el al*.[114] have identified that the length of the amino acid sequence plays a role in the ability of PSA to cleave the peptide, with at least a tetrapeptide sequence required for activity. In a small-molecule study, the arylamine 7-amino-4-methylcoumarin (AMC) was attached *via* an amide bond to the C-terminal carboxy group of Gln in the peptide sequence HSSKLQ. The HSSKLQ------AMC construct was not hydrolysed by a panel of purified extracellular proteases except PSA. Thus, HSSKLQ can be used as a carrier to target prodrugs for activation within sites of metastatic prostate cancer producing enzymatically active PSA.[114]

A doxorubicin-peptide construct has been built and examined *in vitro* for its behaviour as a targeted prodrug for PSA-secreting tumour cells. Unfortunately, PSA was unable to hydrolyze the amide bond between glutamine and Dox. However, a previously described doxorubicin derivative consisting of the amino acid L-leucine linked to the primary amine of doxorubicin (Leu-Dox) was demonstrated to have activity against cancer cell lines in animal models.[115] This result has turned the view toward additional incorporation of an amino acid. The whole construct is now HSSKLQL-----Dox. PSA then released L-Dox, rather than the parent drug. As a conclusion, PSA is only capable of hydrolysing amide bond adjacent to an aromatic ring or to an aminoacyl group.[109,68]

1.7.2.2.6 PSA-activated prodrugs

The site-specific release of a high concentration of Leu-Dox in the environment surrounding prostate cancer cells by the proteolytic activity of PSA led to the search for other cytotoxic agents that might be conjugated to the hydrolysed peptide. For example:

Thapsigargin is a potent inhibitor of the Ca^{2+} dependent ATPase pump. This inhibition will elevate Ca^{2+} concentration and cause cell death.[116,117] Thapsigargin's cytotoxicity is, however, unlikely to be prostate-(or cell-type-) specific, given its mechanism of action; therefore, it cannot be administered systemically as a therapeutic agent without encoding host toxicity. Ten years ago, a prodrug approach for thapsigargin was based on direct coupling of a primary amine-containing thapsigargin analogue to a peptide carrier. The

resulting water-soluble compound was then delivered systemically.[117] However, this prodrug was inactive because the carrier peptide prevents it from invading the cell until the thapsigargin analogue is liberated from the carrier peptide by proteolytic degradation.

Therefore, a meaningful strategy was required for the selective targeting of thapsigargin to prostate cancer cells only, without harming normal cells. Gaining advantage from the existence of PSA, specifically in prostate cancer cells, a new prodrug was designed by coupling amine-containing thapsigargin analogue 12ADP to the HSSKLQ peptide sequence which is selectively cleaved by PSA. **(Scheme 1.4)**. This prodrug was efficiently hydrolysed by PSA and was thus selectively toxic to PSA-producing prostate cancer cells *in vitro;* it was also stable in human plasma. Furthermore, continuous subcutaneous administration of the prodrug in mice causes complete growth inhibition of established PSA-producing prostate cancer xenograft tumours and had no effect on renal carcinoma xenograft tumours which do not produce PSA. As a conclusion, the development of PSA-activated thapsigargin prodrugs as a therapy for metastatic prostate cancer is warranted.[118,119]

| Mu | His | Ser | Ser | Lys | Leu | Gln | 8-*O*-(12-[L-leucinoylamino]dodecanoyl])-8-*O*-debutanoylthapsigargin (Leu-12ADT) |
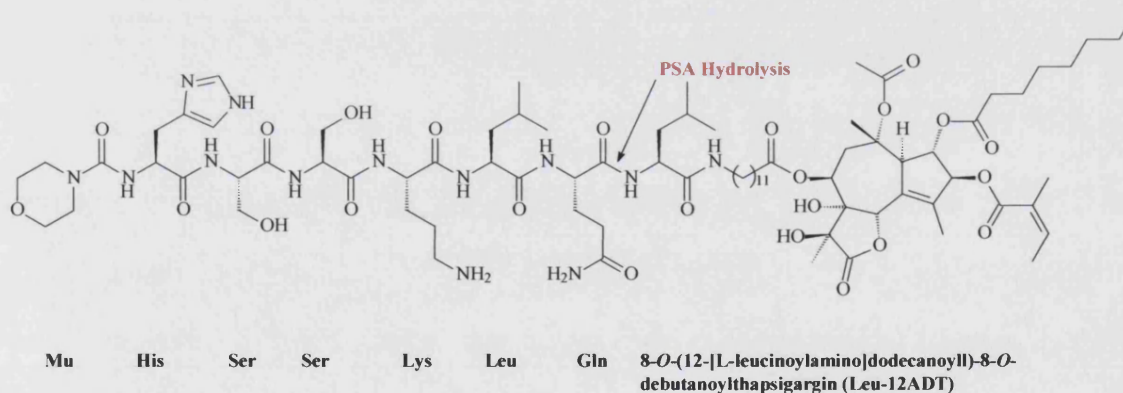
(30)

Scheme 1.4 *Chemical structure of MuHSSKLQ//L12ADT. The arrow indicates the site of prostate-specific antigen (PSA) hydrolysis.*

As a single agent, doxorubicin has been one of the best chemotoxins against metastatic prostate cancer.[24] Advances in the knowledge of the mechanism of action of doxorubicin highlight the enzyme DNA topoisomerase II as its primary cellular target. This enzyme is fundamental for the regulation of DNA topoplogy in all living organisms.[34,36,37]
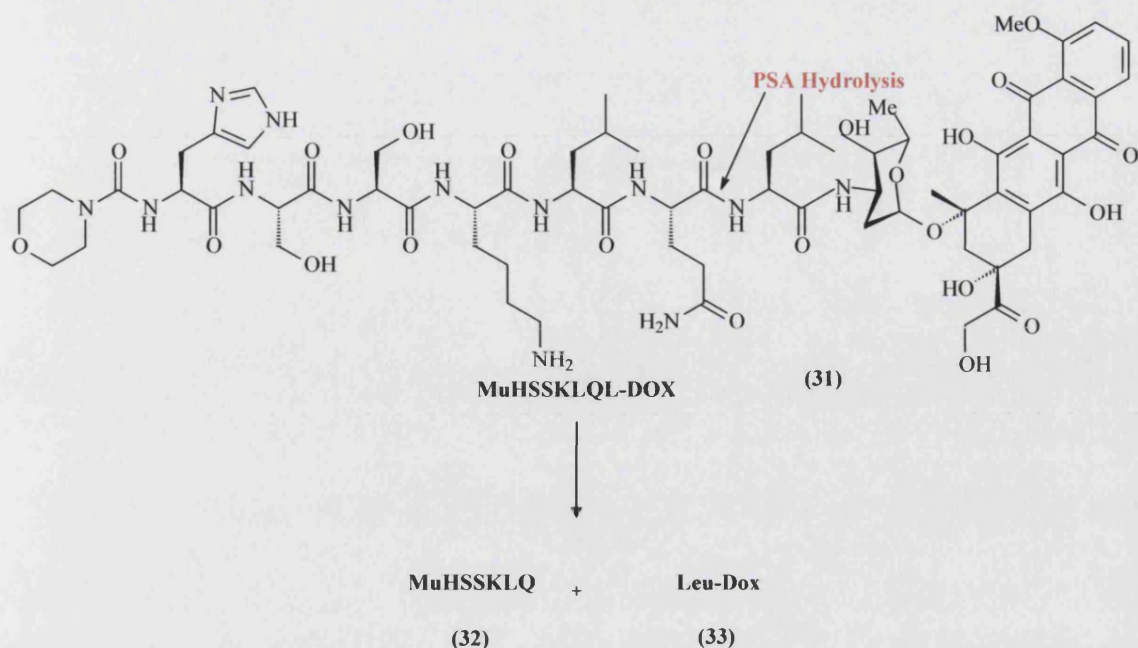
Scheme 1.5 *PSA-triggered release of doxorubicin from a tripartite prodrug system.*

Unfortunately, chronic administration of high doses is usually not possible because of the dose-limiting systemic toxicities. Therefore, new strategies, which deliver doxorubicin specifically to sites of metastatic prostate cancer while avoiding systemic toxicity, were crucial. Doxorubicin targeting by means of a specific antitumour monoclonal antibody has been investigated as a means to mitigate toxicity against normal tissue. However, this method has some limitations with regards to the effective dose of drug that can be delivered per antibody molecule.[59] Denmeade *et al.*[68] have designed a good inactive prodrug of doxorubicin. This prodrug was synthesised by coupling the primary amine of doxorubicin to the carboxyl terminal of the HSSKQL peptide carrier. The linker amide bond was documented to be hydrolysed specifically by PSA to liberate the active cytotoxin Leu-Dox **(33) (Scheme 1.5).**

The specificity of the cytotoxic response to the prodrug was recognized when 70 nM of the prodrug killed 50% of the PSA-producing LNCaP cells, whereas no cytotoxic effect on PSA-nonproducing TSU human prostate cancer cells *in vitro* was seen. Currently, the Mu-HSSKLQL-Dox **(31)** prodrug is in studies *in vivo* in LNCaP and PC-82 tumour-bearing mice.[119]

A method for Dox drug targeting to the sites of metastatic prostate cancer by the use of the polymeric prodrug concept would be useful with the aim of lowering the cardiotoxicity and improving the therapeutic index. In this thesis, part of this targeting polymeric prodrug design will be addressed. The designed prodrug will ensure the release of the active drug without any interfering pendant amino acids. The prodrug was synthesised by coupling of a model drug to a PSA-peptide *via* a self immolative molelecular clip linker to produce CbzSSKLQV-2,2-dimethyl-4-thiazolidine-model drug and CbzSKLQV-2,2-dimethyl-4-thiazolidine-model drug. These prodrugs serves as a substrate for PSA. This approach permitted efficient conversion of the inactive prodrug back to the active form by the enzymatic activity of PSA which is highly expressed in prostate cells, thus improving the specific therapeutic acitivty.

Aims and objective

2.1 Aim of the research

The aim of this research is to design a novel prodrug that will release doxorubicin selectively in prostate tumours through an innovative system. This polymeric prodrug system could also deliver other cytotoxins selectively.

2.2 Research proposal

2.2.1 Design of a PSA-activated polymeric prodrug system

The general features of the design for a prostate-specific PSA activated polymeric prodrug are shown in figure **2.1**.
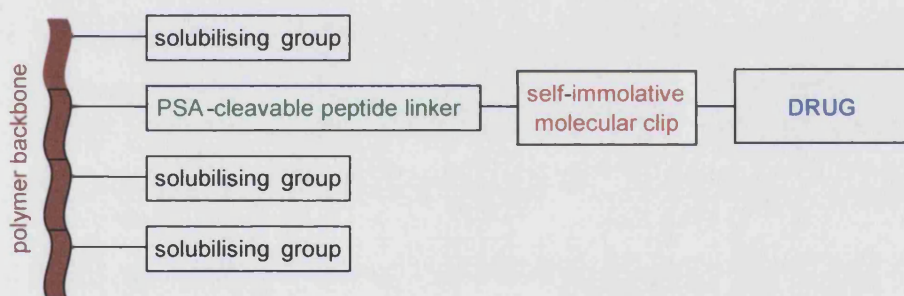
Figure 2.1 *General structure of the proposed polymeric prodrug for prostate-specific drug release.*

The first key feature in the polymeric prodrug is the polymeric backbone, which will be polyacrylate similar to that of the poly(HPMA), PK1 [HPMA = (±)-N-(2-hydroxypropyl)-methaacrylamide]. As in PK1, simple solubilising groups will occupy many of the sites. The homopolymer (poly(HPMA) and PK1 have been demonstrated to be non-immunogenic.[43]

The second key feature is the PSA-cleavable peptide linker. However, based on previous work carried out by Denmeade *et al.*[68] on small-molecule prodrug study, a model drug

(containing amine) will be attached to a PSA-cleavable peptide linker. This linkage substantially inhibits the non-specific toxicity of the drug. Denmeade and coworkers have reported that arylamine 7-amino-4-methylcoumarin (AMC) is released from the peptide construct HSSKLQ—AMC. However, HSSKLQ—doxorubicin is not cleaved by PSA. To achieve cleavage, the construct HSSKLQL—Dox was used; PSA then released L-Dox, rather than parent drug (Dox).

These data strongly indicate the need for the development of a tripartite prodrug system, where the peptide sequence and the drug are linked by a "*self-immolative molecular clip*". Enzymatic hydrolysis of the peptide—clip bond will liberate the clip—drug moiety, the clip is designed to become detached from the drug spontaneously, through an intramolecular cyclisation process, resulting in the release of *free drug* without any interfering pendant amino acids or short peptide fragments. The self-immolative molecular clip is a major point in the construction of this polymeric prodrug system. The drug for the study is doxorubicin, but this innovative design could be applied to other drugs that contain amines (e.g. doxazosin, a very recent drug of interest in prostate cancer).[29] However, alternatively, 2-(4-Nitrophenyl)ethylamine (NPEA) is used as a drug model with a primary aliphatic amine. Firstly, it is a lot less toxic to deal with; secondly, it is less expensive and, thirdly, it has a good UV chromophore, thus facilitating its release detection in HPLC studies that would be carried out later on.

Thus, as a means to test the rationale of the proposed prodrug, putative self- immolative molecular clip has to be designed and optimised. The designed work is initially divided into two parts:

A   Development of self-immolative aminoacyl-dimethylthiazolidine molecular clip.

The clip must be peptide-like in structure, to encourage binding to the PSA active site but expel the drug rapidly after enzymatic release of the clip-drug moiety. Prodrug strategies based on intramolecular cyclisation reactions have been reviewed.[120] Several effective examples are known but none use cyclisation of modified dipeptides; thus the proposed design is novel.
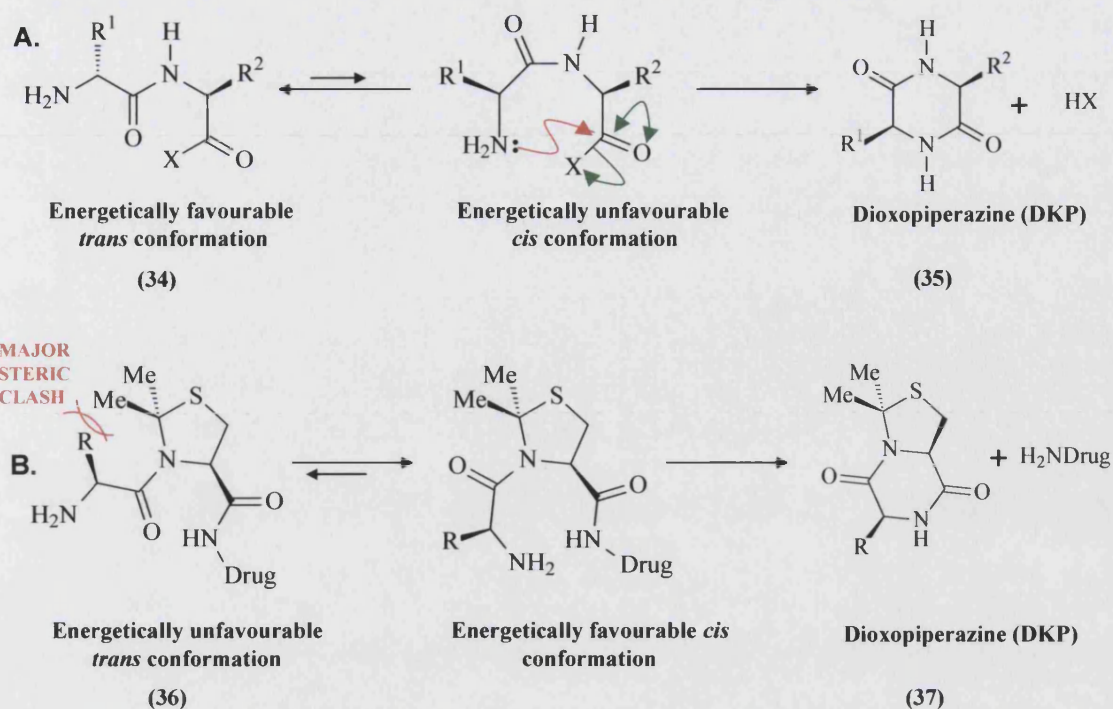
Scheme 2.1 *A. DKP formation from peptides. **B.** Design of aminoacyl-dimethylthiaproline molecular clip.*

In peptides with free N-terminal amines, the N-terminal amino acid pair cyclise to give a dioxopiperazine (diketopiperazine, DKP); the remainder of the peptide is expelled **(Scheme 2.1 A)**. The rate of DKP formation depends on the proportion of the dipeptide in the reactive *cis* conformation.[121] However, most peptide sequences adopt only the *trans* conformation, because it is energetically favourable. The presence of proline at the penultimate position greatly enhances the rate of DKP formation and expulsion of the amine leaving group, owing to the greater propensity to adopt a *cis*-amide conformation (AlaPro is 13% cis[121,122]). Interestingly, replacement of Pro with 2,2-dimethyl-4-thiazolidine (Me$_2$ThPro) forces peptides into 100% *cis* conformation,[122] owing to the major steric clash between the side-chain R of the terminal amino acid and the geminal dimethyl groups **(Scheme 2.1 B)**. DKP formation and expulsion of the leaving group (the drug) should then be rapid.

Therefore, an aminoacyl-Me$_2$Thiazolidine unit will be used as a molecular clip between the PSA-cleavable peptide linker and the model drug. Exposure of the amine by the PSA-mediated cleavage should initiate rapid DKP formation and expulsion of the drug.

Scheme 2.2 *Optimisation of aminoacyl dimethylthiazolidine molecular clip. (R = H, Me, Pr^i, CH$_2$Ph, CH$_2$Pr^i).*
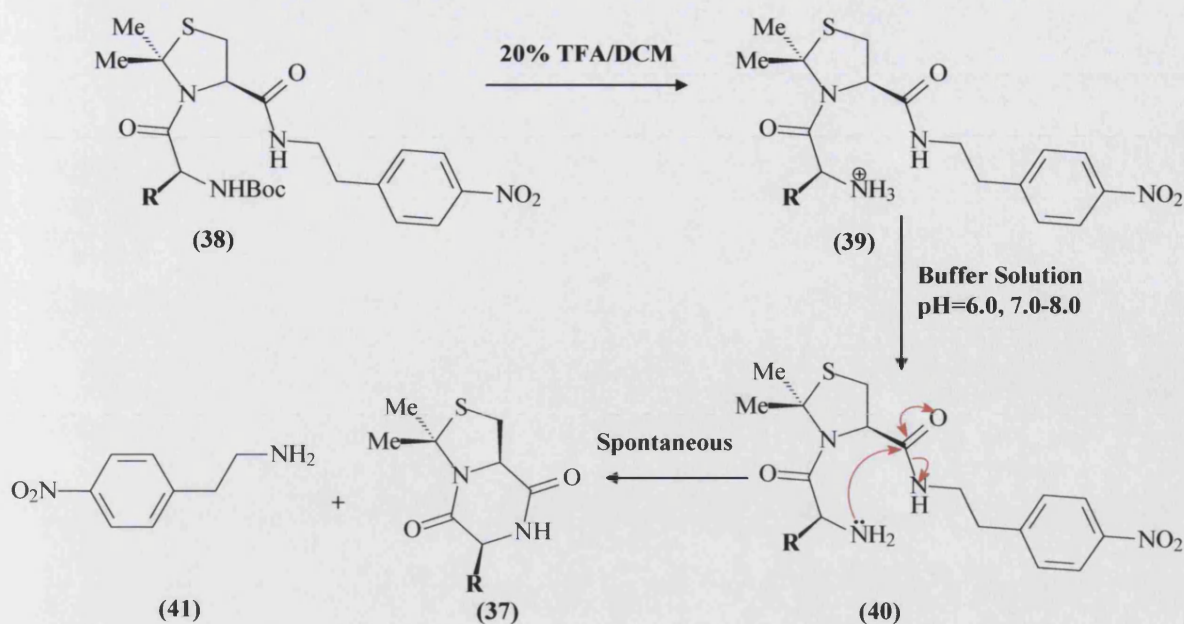
Optimisation of the function of this molecular clip is the next step forward **(Scheme 2.2)**. Aminoacyl-Me$_2$Thiazolidine-NPEA potential clips with different R groups **(38)** will be synthesised; all are protected by *t*-butoxycarbonyl (Boc) at the N-terminal. The *R* and *S*-Me$_2$Thiazolidine stereoisomers will be prepared by cyclocondensation of L-Cys and D-Cys respectively.[123] Selective deprotection with acid will give the N-protonated species **(39)**. These species will then be placed in a buffer solution of different pH values 6.0, 7.0 and 8.0 at 37°C, mimicking physiological media to give the free amine species **(40)**; the rate of formation of DKP **(37)** and liberation of the model drug NPEA **(41)** will be then monitored by HPLC analysis. Different R substituents are necessary to study the importance of the size of the side-chain in forcing the clip into the reactive *cis* conformation. Hence, the function of the molecular clip will thus be optimised to be used in the subsequent step.

B   Synthesis and evaluation of a monomeric model for PSA triggered release of NPEA.

A complete monomeric prodrug model will be constructed **(42) (Scheme 2.3)** for the study of PSA-triggered release of NPEA. In this model, the benzyloxycarbonyl moiety will be linked to the N-terminus of the PSA-sensitive peptide sequence to provide a chromophoric tag. Constructs containing two peptide sequences SSKLQ and SKLQ, will be synthesised and examined. Actually, Denmeade *et al.*[68] used HSSKLQ in his monomeric prodrug model but an earlier study of PSA substrate-specificity showed that histidine is probably

unnecessary.[114] The aminoacyl-Me$_2$Thiazolidine molecular clip optimized in the previous study will then be used. The constructed models CbzSSKLQXMe$_2$ThProNPEA and CbzSKLQXMe$_2$ThProNPEA will then be evaluated for cleavage by PSA, liberating XMe$_2$ThPro-NPEA and, hence, NPEA. HPLC analysis of the incubation mixtures will be facilitated by the chromophoric tag of the benzyoxycarbonyl moiety attached to the cleaved peptide **(43)**.
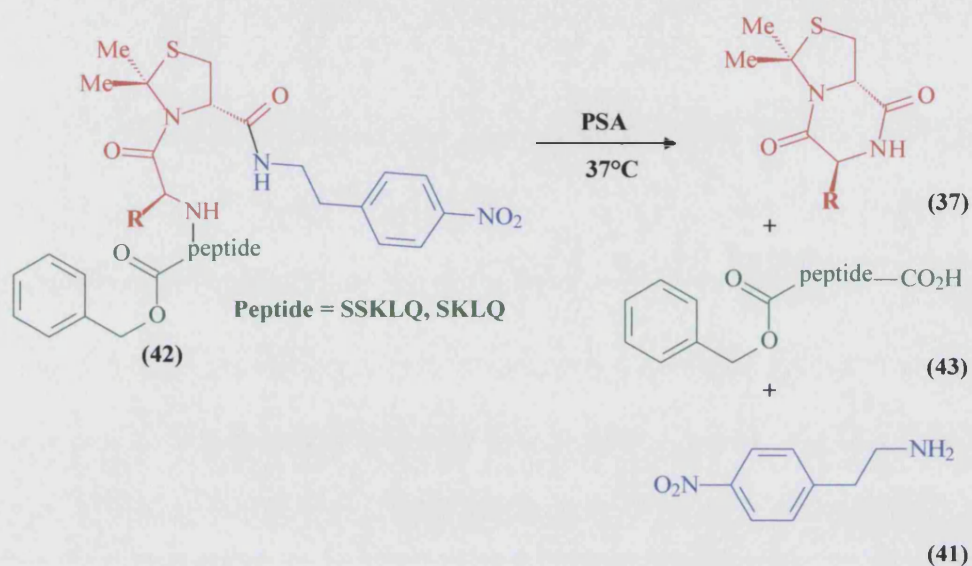
Scheme 2.3   Proposed PSA-triggered release of NPEA from the monomeric model.

51

Discussion

3.1 Development and optimisation of self-immolative molecular clip

Since the advent of solid phase peptide synthesis (SPPS),[124] many efforts have been devoted to achieve successful peptide assembly. However, problems such as poor solvation of the growing peptide chain during solid phase synthesis, as well as limited solubility of the fully protected peptide fragments in the solution approach resulting from intermolecular hydrophobic peptide aggregation, self-association, and β-sheet structure formation, often leads to incomplete coupling steps. Reported attempts to overcome these undesirable physicochemical problems during aminoacylation reactions were made through "external factors". For example, solvent composition,[125] elevated temperature[126] and solubilising protecting groups have been used,[127] all of which shown to have variable efficiencies.

In proteins, the planar peptide bond (C-N) is known to occur predominantly in the *trans* configuration, often resulting in β-sheet structure formation. In addition, the low occurrence of *cis* amide bonds is due to the steric conflicts between adjacent α-carbon substituents. Therefore, it is noteworthy that the undesirable physicochemical problems are attributed to the existence of peptide amino acids in the *trans* conformation. Interestingly, proline residue plays a peculiar role in peptide synthesis. It is the only naturally occurring cyclic amino acid. Unlike other peptide amino acids, which predominantly adopt the *trans*-amide bond conformation, the imidic bond formed with preceding residue (Xaa-Pro) is readily subject to cis/trans isomerisation. The *cis* and *trans* states are of similar energies, with about a 20 Kcal mol^{-1} barrier for their interconversion.[128,129,130]

Proline analogues can be tailor made to fit with the required cis/trans conformation ratio. For example: (a) 5-Oxoproline (44) exhibits an exclusive *trans*-amide isomer which is stabilised by both steric and electronic effects due to the replacement of the tertiary amide bond by an imide structure;[131] (b) 5,5-Dimethylproline (45) was shown to exist solely in the *cis*-conformation in the tripeptide Ac–Tyr-5-Me$_2$Pro–Asn (**Figure 3.1**).[128]
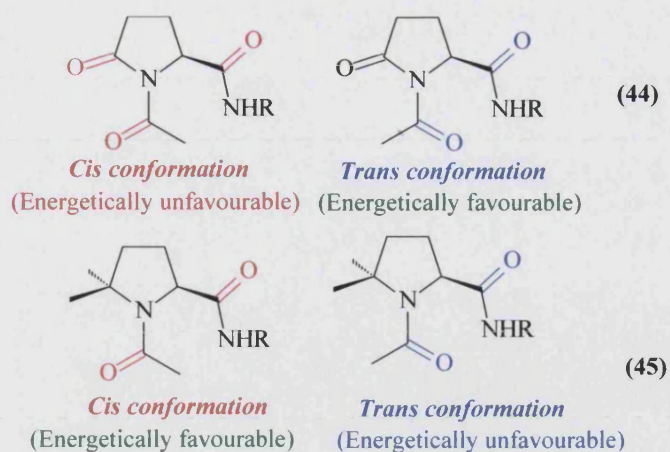
Figure 3.1 *The cis/trans amide conformations of 5-oxoproline (44) and 5,5-dimethylproline (45).*

Recently, Ser/Thr-derived oxazolidine and Cys-derived thiazolidine derivatives (*pseudo*-prolines, ψPro) have been reported to induce a "kink" conformation in the peptide backbone, originating in the preference for *cis*-amide bond conformation. Consequently, ψPro prevents the intermolecular hydrophobic peptide aggregation, self-association, and β-sheet structure formation, thus improving solvation and coupling processes. Such building blocks are readily accessible by cyclocondensation of Ser, Thr, or Cys with aldehyde or ketones **(Scheme 3.1)**, providing a useful protecting tactic for the parent amino acids. Furthermore, different substituents R_1 and R_2 at position 2 affect the ring stability and result in different ψPro units with different chemical stability. Actually, these substituents provide an efficient synthetic tool to tailor the cis/trans ratio of the amide bond in peptide synthesis.[132, 133]

H^+

R_1

$O=$

R_2

Fmoc-Xxx-OPfp

R

R_1

X

R_2

N　CO$_2$H

Fmoc-Xxx-Xaa-OH

R = Xaa(ψ^{R_1, R_2} pro)

Fmoc-Xxx-F
(or-NCA)

H^+

R_1

$O=$

R_2

Fmoc-Xxx-Xaa(ψ^{R_1, R_2}Pro)-OH

Incorporation into peptides
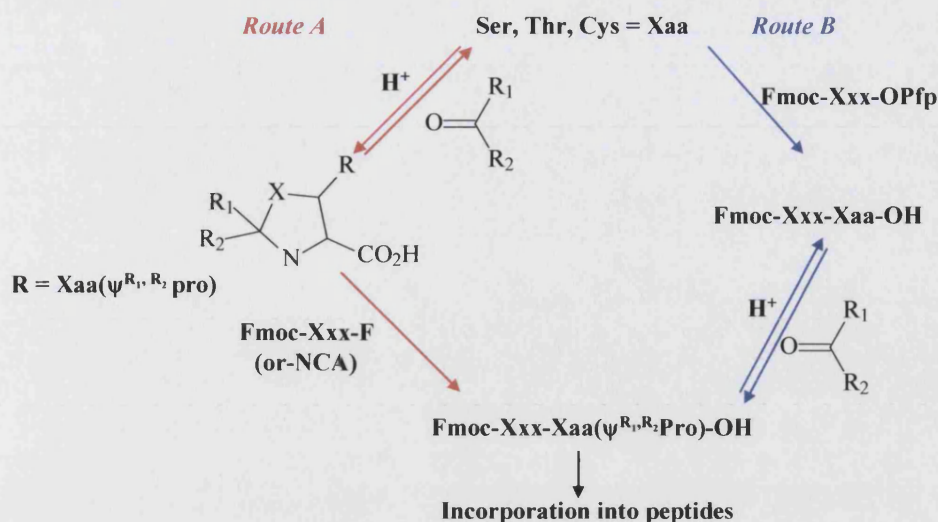
Scheme 3.1　*Pseudo-proline units and overview of the ψPro building block synthesis according to routes A and B.　Route A proceeds firstly by acid-catalysed cyclocondensation, followed by amino acid fluoride coupling. However, route B proceeds firstly by amino acid PFP coupling, followed by the acid-catalyzed cyclocondensation. Both routes produce L-serine (X = O, R = H) and L-threonine (X = O, R = methyl) derived 4-oxazolidinecarboxylic acid (Ser($\psi^{R1, R2}$ pro); Thr ($\psi^{R1, R2}$ pro)); L-cysteine (X = S, R = H) derived 4-thiazolidinecarboxylic (Cys(($^{\psi R1, R2}$ pro)); R_1 and / or R_2 = alkyl, aryl].*

Synthetic analysis **(Scheme 3.2)** suggested that Me$_2$Thiazolidine **(47)** would be prepared by cyclocondensation of L-cysteine **(46)** with acetone in the presence of 2,2-dimethoxypropane (DMP) which serve as a reactant and a dehydrating agent.[123] This condensation process usually proceeds in the presence of an acid catalyst. However, L-Cys was used in the hydrochloride salt form. Thus, no acid addition is required in this reaction. The designed strategy was then to protect the N-terminal by *tert*-butoxycarbonyl (Boc). The electron withdrawing effect of the carbamate group will decrease the nucleophilic activity of the nitrogen.
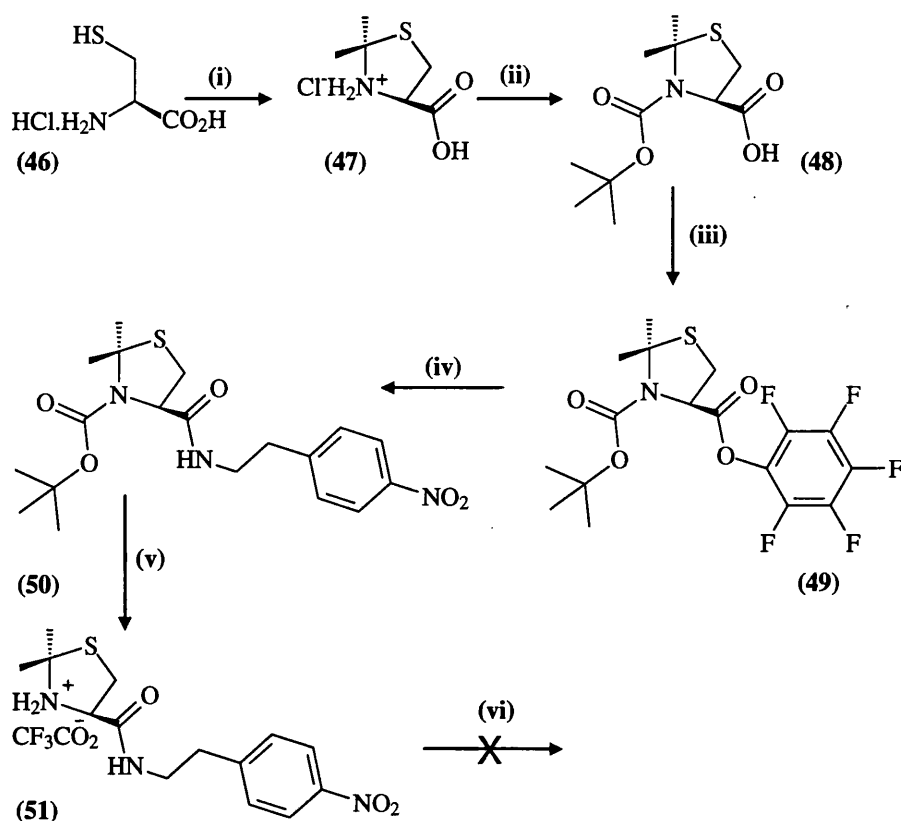
Scheme 3.2 *Synthetic steps toward the formation of (51). (i) (CH₃)₂CO, DMP; (ii) di-t-butyl dicarbonate, Pr^{i}₂NEt, MeCN; (iii) PFPOH, DCC, EtOAc; (iv) 4-Nitrophenylethylamine hydrochloride, Et₃N, CH₂Cl₂; (v) 20% CF₃CO₂H / CH₂Cl₂; (vi) Boc-Gly-OPFP or Boc-Ala-OPFP, Pr^{i}₂NEt, DMF.*

The Boc-thiazolidinecarboxylic acid **(48)** was previously synthesised by Woodward *et al.*[134] by the reaction of **(47)** with the highly unstable *tert*-butyloxycarbonyl chloride. Designing a more facile preparation using commercially available di-tert-butyl dicarbonate presents two difficulties. Firstly, the nitrogen in **(47)** is much hindered, being bonded to a quaternary carbon and a tertiary carbon with a bulky electron-withdrawing carboxylate. Secondly, C-2 substituted thiazolidines are very susceptible to alkaline hydrolysis and methods of Boc introduction using strong base or even excesses of non-nucleophilic tertiary amines led to very low yields (<10%) of intractable mixtures containing both Boc-cysteine and Boc-thiazolidinecarboxylic acid **(48)**. However, in contrast to the literature report,[135] treatment of **(47)** with di-*tert*-butyl dicarbonate in acetonitrile containing equivalents of triethylamine gave only 11% yield of **(48)**. Repeated attempts using other solvents and bases did not show any valuable improved yields.

The ^{1}H NMR spectrum of (48) showed two conformations due to restricted rotation about the Boc carbonyl-N bond (*cis* and *trans* conformations); this is particularly evident in the broad doublet and double doublet signals of the 4-H of the thiazolidine (**Figure 3.2**). A variable temperature study of the NMR spectra of (48) in DMSOd$_6$ at 20°C and 80°C has been done. At 20°C, the rate of interconversion of the two conformations is slow and so the conformers give separate signals. Raising the temperature to 80°C causes the rate of exchange to increase and the separate signals for 4-H coalesces and appears as a single double doublet. (**Figure 3.2**)

A

The proton NMR spectrum
of compound (48) at 20°C in CDCl$_3$

Chemical shift (ppm)

B

20°C, (CD$_3$)$_2$SO   δ (4.74)   δ (4.67)

80°C, (CD$_3$)$_2$SO

δ (4.72)

Temperature dependence of the two conformation of (48)
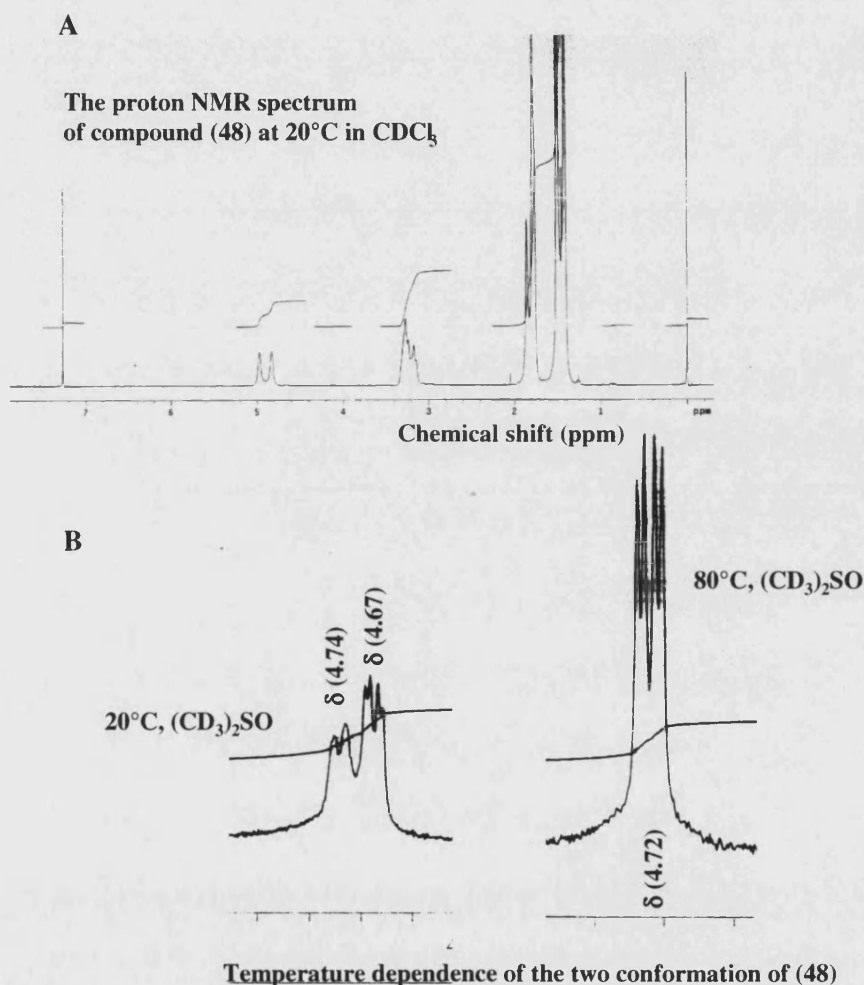
Figure 3.2 *A The full ^{1}H NMR spectrum of compound (48) at 20°C in CDCl$_3$. B selected fragment from a ^{1}H NMR spectrum of a variable-temperature study of (69) at 20°C and 80°C in (CD$_3$)$_2$SO.*

The carboxylic acid compound (48) was converted to its pentafluorophenyl active ester (49) by coupling with pentafluorophenol (PFPOH)[135] using dicyclohexylcarbodiimide

(DCC) in ethyl acetate at 0°C. Reaction of (49) with 2-(4-nitrophenyl)ethylamine (41) afforded the amide (50) in 93% yield (Scheme 3.2).

Boc protecting groups are easily and rapidly removed on treatment with acid. The most common method involves the use of trifluoroacetic acid. This acts as the solvent and reagent, yielding the unprotected peptide as the trifluoroacetate salt. Therefore, deprotection of (50) was carried out with 20% trifluoroacetic acid in dichloromethane, affording the trifluoroacetate salt (51) in a quantitative yield. This ratio of solvents and reagent is very important to prevent ring-opening, since the thiazolidine ring is acid-sensitive. Unfortunately, attempted couplings of (51) with the pentafluorophenyl esters of Boc-glycine and Boc-alanine were unsuccessful; the ^{1}H NMR spectra of the crude products indicated that the thiazolidine ring had opened (absence of the characteristic 2,2-dimethyl peaks).

A convenient synthesis pathway was to follow *route A*[132] in (Scheme 3.1). The design now is firstly to couple the amino acids with compound (47) and, later on, attach the nitrophenylethylamine (NPEA) moiety (Scheme 3.3).

The presence of an electron-withdrawing carboxylate in position 4 of the ring system will reduce the nucleophilic character of the nitrogen atom in position 3, usually resulting in poor acylation yields at the N-terminus. Consequently, rapid-acting acylating agents must be used in an attempt to improve the coupling yield. In the literature, direct N-acylation of (47) with N$^\alpha$-Fmoc-protected amino acid fluorides (Route A, Scheme 3.1) afforded the corresponding product in a yield ranging from 60 to 95%.[132] This is relatively high when compared with the yield obtained upon acylation of (47) with di-*tert*-butyl dicarbonate (<30%).

ClˉH₂N⁺ ... S ... O OH (47)

+

R BocHN ... F O (52) R=H (52) R=CH₃ (53) R=CH(CH₃)₂ (54) R=CH₂Ph (55)

(i) →

O=...N ... S ... O OH Rʹ NH Boc

R=H (56) R=CH₃ (57) R=CH(CH₃)₂ (58) R=CH₂Ph (59)

(ii) →

O=...N ... S ... O O F F F F F Rʹ NH Boc

R=H (60) R=CH₃ (61) R=CH(CH₃)₂ (62) R=CH₂Ph (63)

(iii) ↓

O=...N ... S ... O HN NO₂ Rʹ NH Boc

R=H (64) R=CH₃ (65) R=CH(CH₃)₂ (66) R=CH₂Ph (67)

(iv) ←

O=...N ... S ... O HN NO₂ Rʹ ⁺NH₃ CF₃CO₂⁻

R=H (68) R=CH₃ (69) R=CH(CH₃)₂ (70) R=CH₂Ph (71)
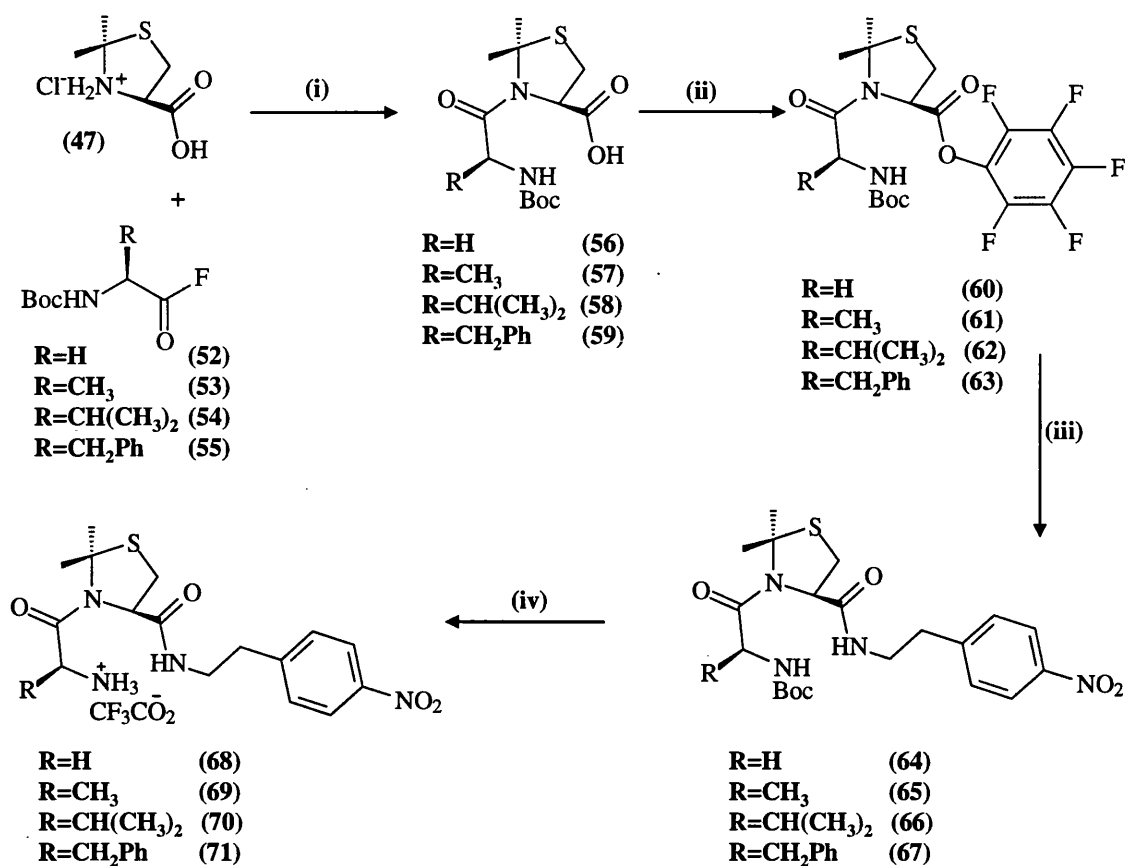
Scheme 3.3   *Chemical synthesis of the* L,R *configuration self-immolative molecular clips (68), (69), (70) and (71). (i) Prⁱ₂NEt, DMF; (ii) PFPOH, DCC, EtOAc; (iii) 4-nitro-phenylethylamine hydrochloride, Et₃N, CH₂Cl₂; (iv) 20% CF₃CO₂H / CH₂Cl₂.*

As a result, the next step forward is to synthesise a series of rapid-acting acylating agents. Acyl fluorides are versatile functional groups in organic chemistry due to the unique nature of the carbonyl-fluorine bond. They possess greater stability than the corresponding acid chlorides and are of high reactivity toward amines.[136] Generally speaking, they are stable, rapid-acting acylating reagents for peptide bond formation. Furthermore, no significant loss of optical purity was observed during the conversion of acid fluorides to amides.[137] A variety of techniques are available for the generation of these acyl fluorides, including halogen exchange from the corresponding acyl chloride with potassium fluoride, potassium hydrogen fluoride and many other reagents.[138] However, there are disadvantages associated with those methods, such as poor yields, dangerous or toxic chemicals, forcing reaction conditions and costly reagents. An alternative method was the use of diethyaminosulfur trifluoride (DAST)[139] or cyanuric fluoride.[136,138] Cyanuric fluoride is a very mild reagent,

very reactive and convenient. Interestingly, a new method using [bis(2-methoxyethyl)amino]sulfur trifluoride was recently published.[140] The acid fluorides of Boc-protected glycine (52), L-alanine (53), L-valine (54) and L-phenylalanine (55) were prepared by the treatment of the corresponding Boc-protected amino acid with cyanuric fluoride.[136] Pyridine was found to promote the fluorination reaction, which proceeds by nucleophilic displacement of fluoride from the cyanuric fluoride by the carboxylate anion, followed by attack of the liberated fluoride at the activated carbonyl.

These crude acid fluorides were used directly in the next coupling reactions with (47), without any purification attempts, to avoid any possible racemisation. Coupling proceeds in the presence of two equivalents of base (diisopropylethylamine). The resulting Boc-aminoacylthiazolidinecarboxylic acids (56), (57), (58) and (59) were purified *via* chromatography which required the use of small quantities of glacial acetic acid in the eluant to maintain the product carboxylic acids in the electrically neutral form. Unfortunately, the best yield obtained was 35%. The rationale for this is the presence of the acid-labile protecting group (Boc), unlike the Fmoc protecting group,[132] could be cleaved easily during work-up or purification. Compounds (56), (57), (58) and (59) were obtained in moderate yields, 35%, 30%, 27% and 30% respectively. Coupling of (56), (57), (58) and (59) with pentafluorophenol and DCC in ethyl acetate at 0°C afforded the active acylating agents (60), (61), (62) and (63) in 92%, 89% 93% and 92% yields, respectively. Consequent reaction of these compounds with 2-(4-nitrophenyl)ethylamine (41) afforded the required amides (64), (65), (66) and (67) in 76%, 75%, 73% and 95% yields, respectively. Deprotection of (64), (65), (66) and (67) with 20% trifluoroacetic acid in dichloromethane for 45 min afforded the trifluoroacetate salts (68), (69), (70) and (71) in quantitative yields.

As for **(48)**, the ^{1}H NMR spectra of BocGly(dimethylthiazolidine)CONHCH$_2$CH$_2$PhNO$_2$ **(64)** showed evidence of restricted rotation about the carbonyl-thiazolidine amide bond. CMe$_3$ group were separate in the spectrum run at 20°C; singlets were observed at δ 1.32 and at δ 1.38 in the approximate ratio of 1:11. To investigate this phenomenon, a variable temperature ^{1}H NMR study in (CD$_3$)$_2$SO was carried out, with spectra being recorded at 20, 30, 40, 50, 60, 70, 80 and 100°C. At 30°C, the signals broaden and at 40°C coalesce to a single peak.
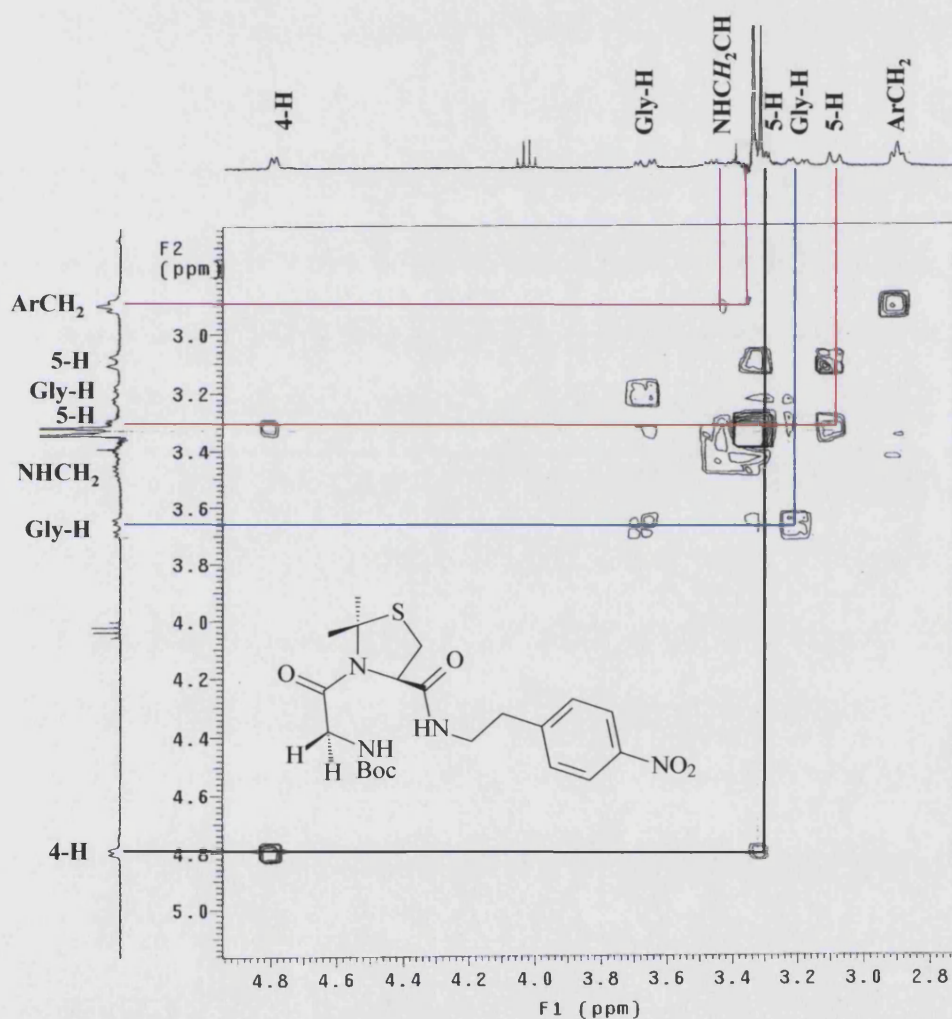
Figure 3.3   *^{1}H-^{1}H COSY NMR spectrum of compound **(64)** at 20°C in (CD$_3$)$_2$SO.*

Assignment of the signals in the ^{1}H NMR spectrum of **(64)** was confirmed with a ^{1}H-^{1}H COSY spectrum **(Figure 3.3)**. A cross-peak between signals at δ 2.91 (ArCH$_2$) and δ 3.39,

δ 3.47 (NHCH$_2$CH), a cross-peak between signals at δ 3.20 (Gly-H) and δ 3.67 (Gly-H) and a cross-peak between signals at δ 3.10 (5-H), δ 3.31 (5-H) was identified. Interestingly, a cross-peak between δ 3.31 (only one 5-H) and δ 4.79 (4-H) is identified but there was no cross-peak between the signals at δ 3.10 and δ 4.79, corresponding to the very low coupling (<0.2 Hz) between these protons arising from a dihedral angle close to 90°. Furthermore, a NOESY spectrum **(Figure 3.4)** was studied in an attempt to determine the conformation of the major rotamer **(Figure 3.5)**. The spectrum showed NOE connectivities between signals at δ 3.31 (5-Hα) and δ 4.79 (4-H) and between signals at δ 3.67 (Gly-Hα) and δ 4.79 (4-H). No cross-peak was seen for 4-H to 5-Hβ, confirming the assignment of the 5-protons. Cross-peaks for 4-H to Gly-Hβ and from the thiazolidine 2,2-dimethyl protons to Gly-H were also absent. These data confirm that the major rotamer of **(64)** has the required Z (*cis*) amide conformation.
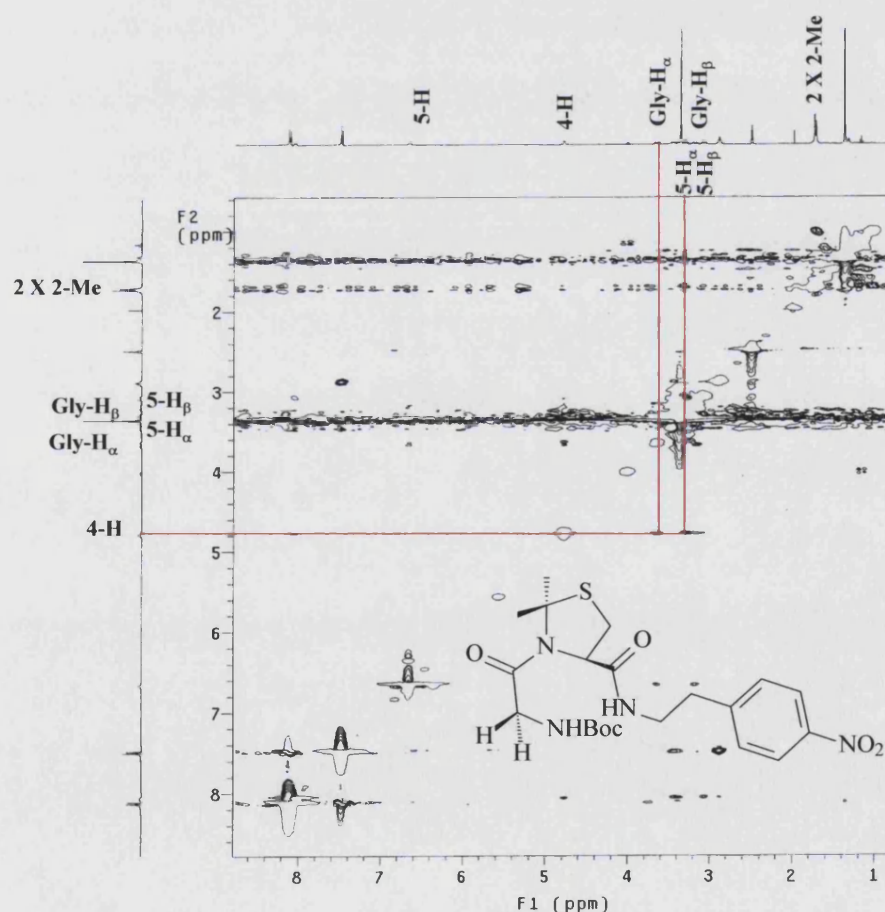
Figure 3.4 ^1H-^1H *NOESY NMR spectrum of compound* **(64)** *at 20°C in* (CD$_3$)$_2$SO.

61

(64)
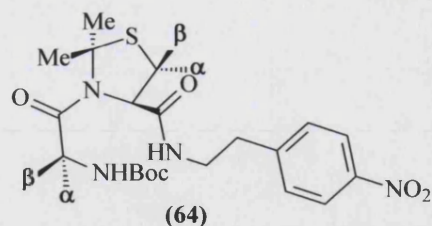
Figure 3.5   *The Z (cis) amide conformation of the major rotamer of compound (64).*

Studies were also carried out on the conformations of the pentafluorophenyl esters **(61)** and **(62)**, containing L-Ala and L-Val, respectively. On the bases of their ^{1}H NMR and ^{19}F spectra, two distinct populations were observed for each in the ratio of 7:3. Again, the acyl-thiazolidine tertiary amide bond shows restricted rotation. Presumably, the major conformations of these synthetic intermediates still have the *Z* (*cis*) amide but NOESY experiments have not been carried out to confirm this. The shifts in the rotamer populations may be driven by the steric bulk of the pentafluorophenyl ester which could compete with the geminal dimethyl unit and the R group for steric repulsion **(Figure 3.6)**. In contrast, the PFP esters derived from the Gly and Phe compounds **(60)** and **(63)** showed only one conformation. Interestingly, removing the bulky Boc group drives back the mixture to one conformation (*vide infra*).

Z   E
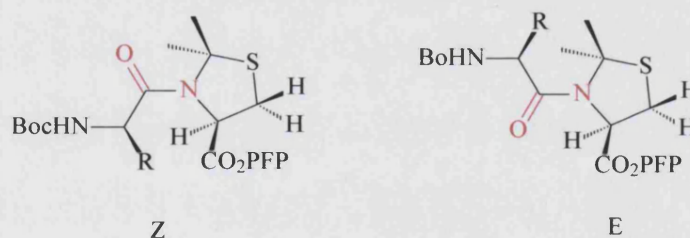
Figure 3.6   *The Z and E conformations of Boc-Xaa-(Me$_2$Thiazolidine)PFP esters.*

However, since this compound was a synthetic intermediate in the overall process and the effect of PFP moiety will be temporary, a decision was taken to proceed into the next coupling step to generate the nitrophenylethyl amides.

Whereas the Gly compound **(64)** showed an 11:1 mixture of conformers, L-Ala compound **(65)**, L-Val compound **(66)** and L-Phe compound **(67)** were identified as being in only one conformation by ^{1}H NMR. NOESY analysis of **(65)** has been done to assign the conformation *E* or *Z*. The spectrum showed expected NOE connectivities between signals

at δ 1.12 (Ala β-H$_3$) and δ 7.06 (Ala-NH) and between δ 2.95 (ArCH$_2$) and δ 7.49 (Ar 2,6-H$_2$). More informatively, an NOE connectivity was seen between δ 3.84 (Ala α-H) and δ 4.73 (4-H). Enticingly, no through-space correlations were seen between any of the methyl groups at position 2 and Ala β-H$_3$ or Ala α-H. These data confirm that compound (65) exists in the required Z (cis) amide conformation (Figure 3.7).
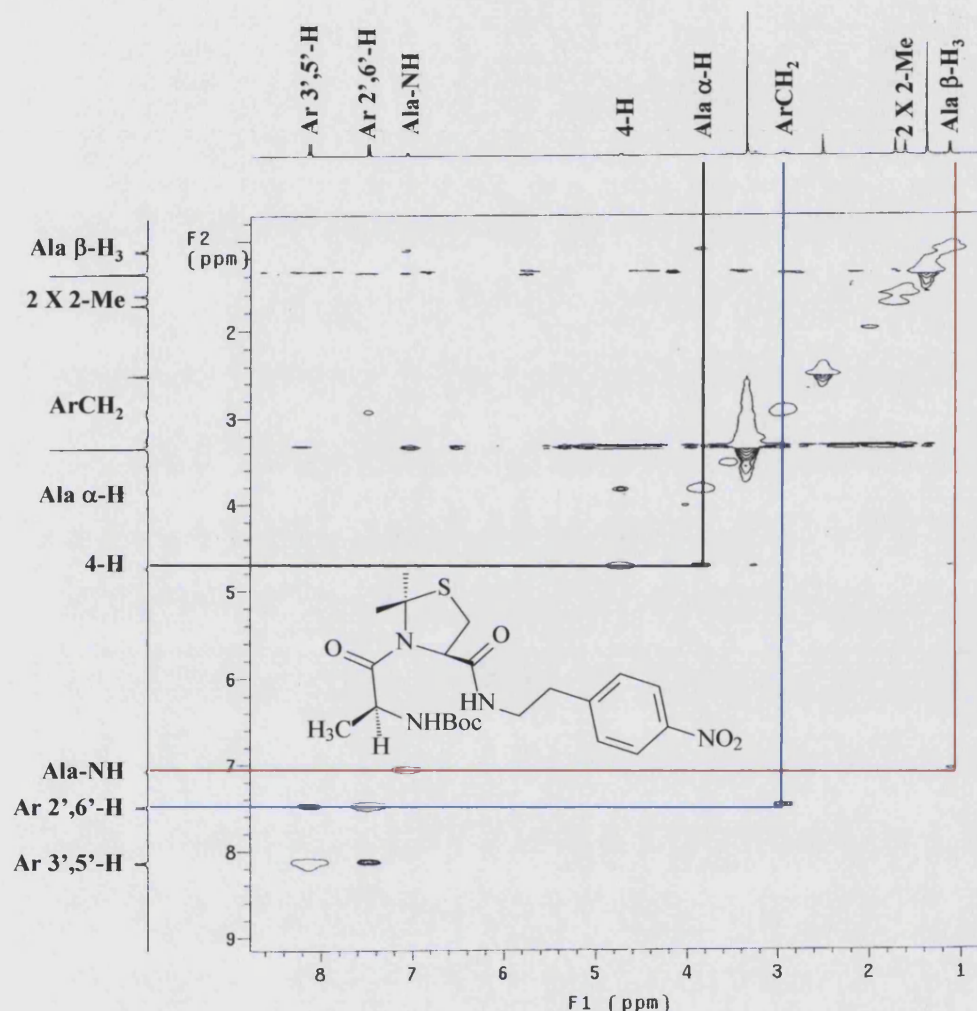
Figure 3.7 ^{1}H-^{1}H NOESY NMR spectrum of compound (65) at 20°C in (CD$_3$)$_2$SO.

The ^{1}H-^{1}H COSY spectrum of (66) helped in the assignment of the H-H coupling relationships (Figure 3.8). The similarity of the spectra of (66) to those of (65) suggests that (66) also exists in the Z (cis) amide conformation. The sole conformation of (67) is also taken to be Z (cis). Although these are the N-Boc protected compounds, it is very encouraging to note that they all exist (almost) completely in the conformation that would be required for cyclisation of the deprotected derivatives.
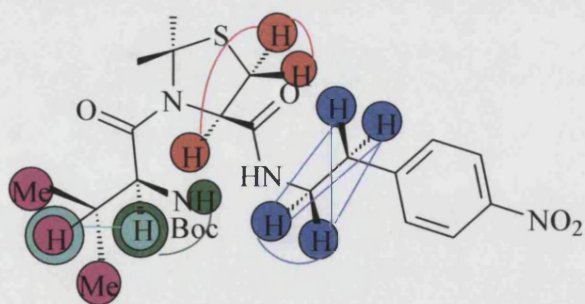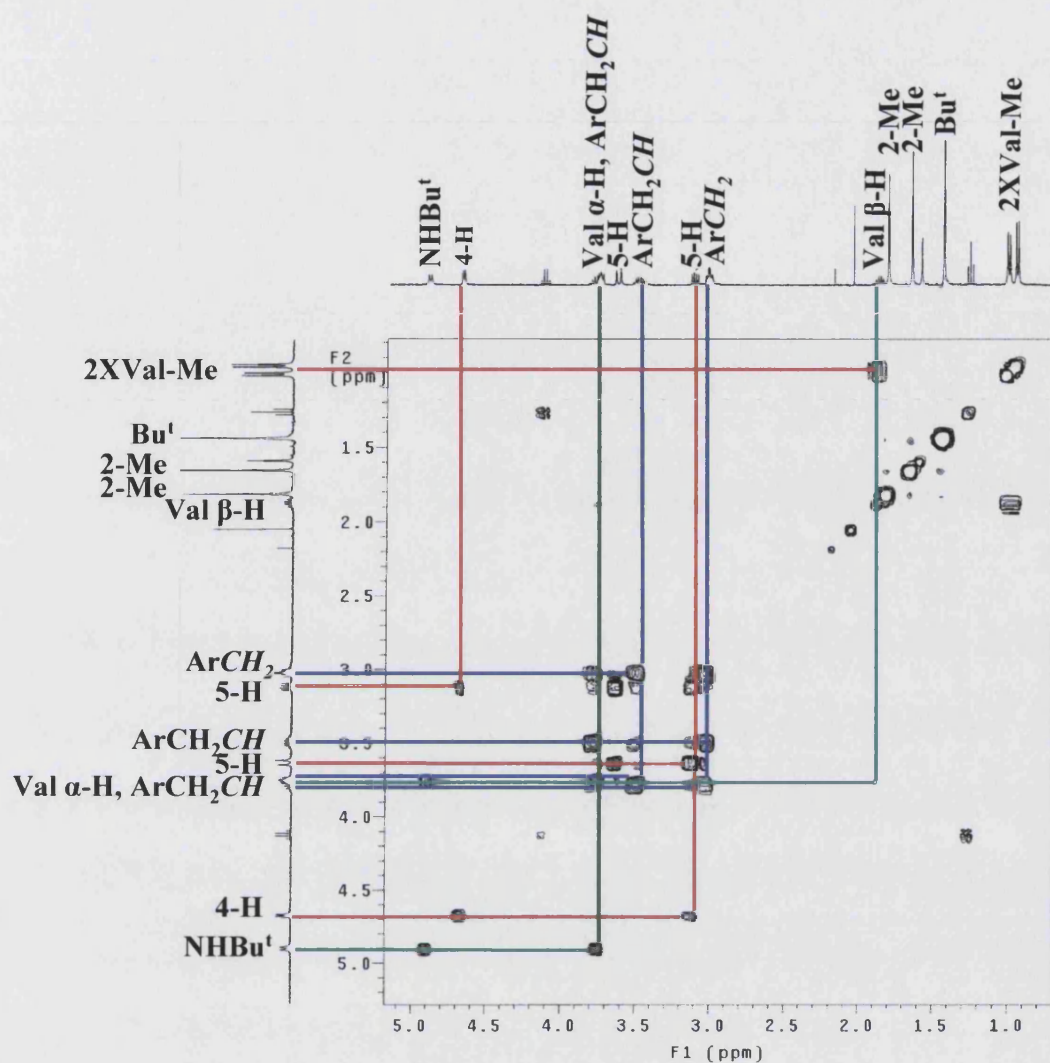
Figure 3.8 *¹H-¹H COSY NMR spectrum of compound **(66)** at 20°C in CDCl₃.*

The deprotected compounds **(69)** and **(70)** were identified as being in only one conformation by ¹H NMR. ¹H-¹H COSY spectra of **(69)** and **(70)** helped in the assignment of the H-H coupling relationships **(Figure 3.9)** and **(Figure 3.10)** respectively.
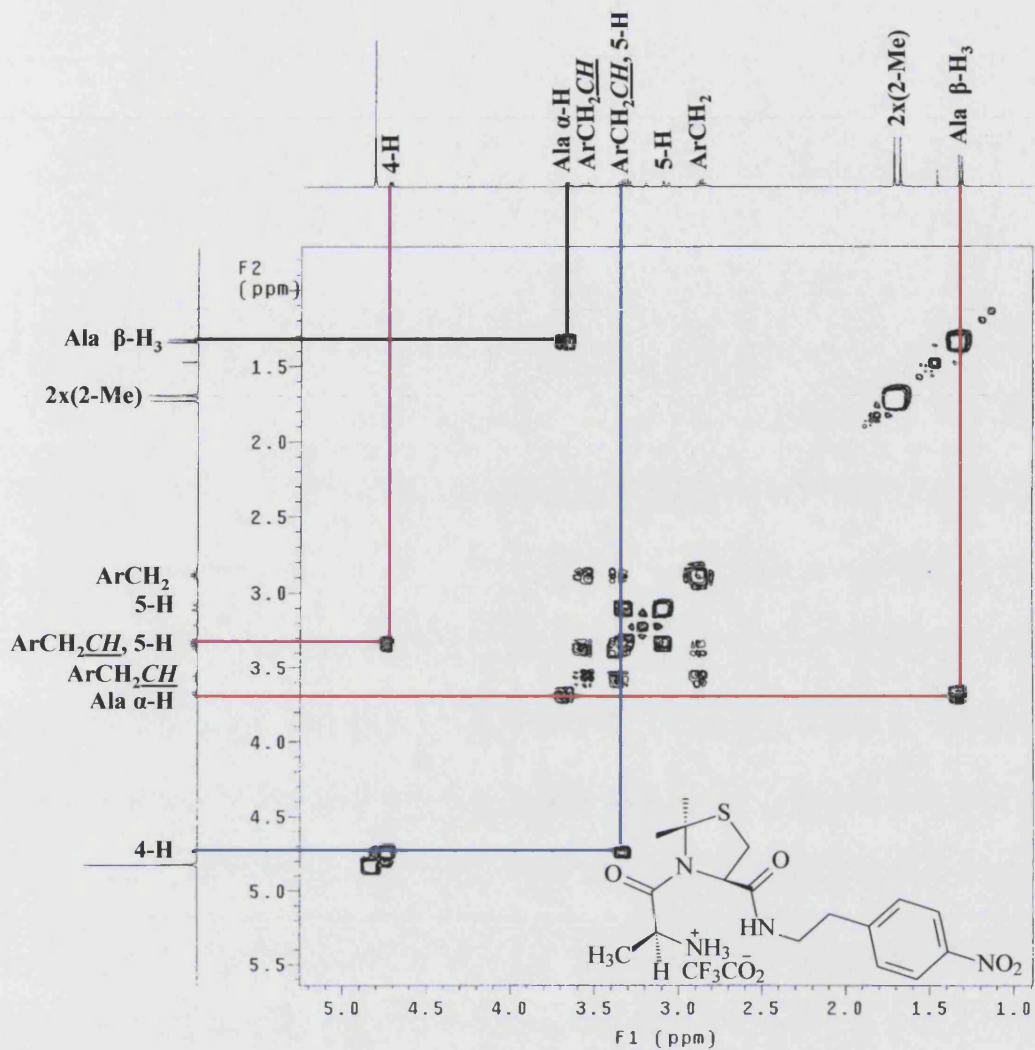
Figure 3.9 $^1H-^1H$ COSY NMR spectrum of compound **(69)** at 20°C in $(CD_3)_2SO$.

65
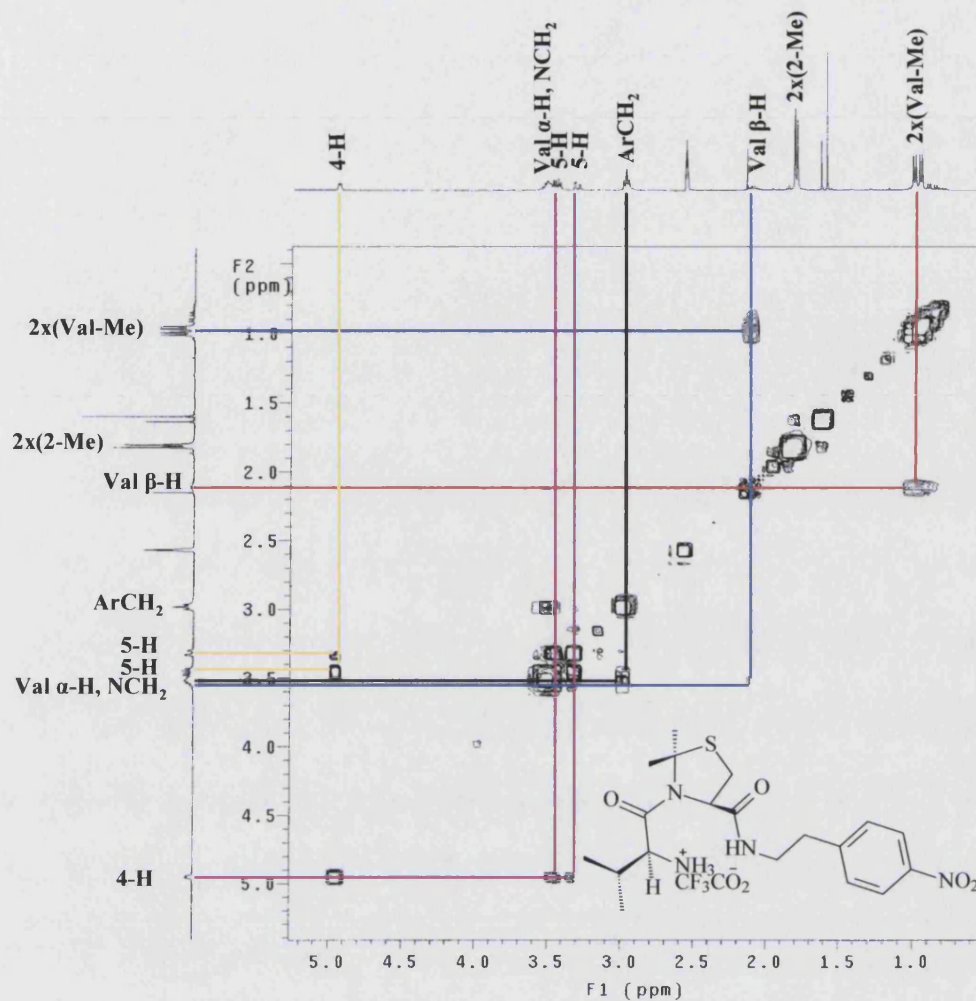
Figure 3.10 *^1H-^1H COSY NMR spectrum of compound (70) at 20°C in (CD$_3$)$_2$SO.*

At this point, a series of experiments was conducted to ensure that the apparent mixtures of conformers were indeed a mixture of conformers and not mixtures of diastereoisomers. Similarly, a check on the stereochemical integrity of the coupling reactions was required; *i.e.* a check that no racemisation had occurred during the various couplings reactions.

A fingerprint experiment with a tailor-made mixture of D-Ala and L-Ala amino acid fluorides **(72)** in a ratio of 3:2 was performed **(Scheme 3.4)**. The rationale of this experimental mixture was to follow the consistency of the ratio through the synthetic pathway and to find out if any racemisation has occurred.

66
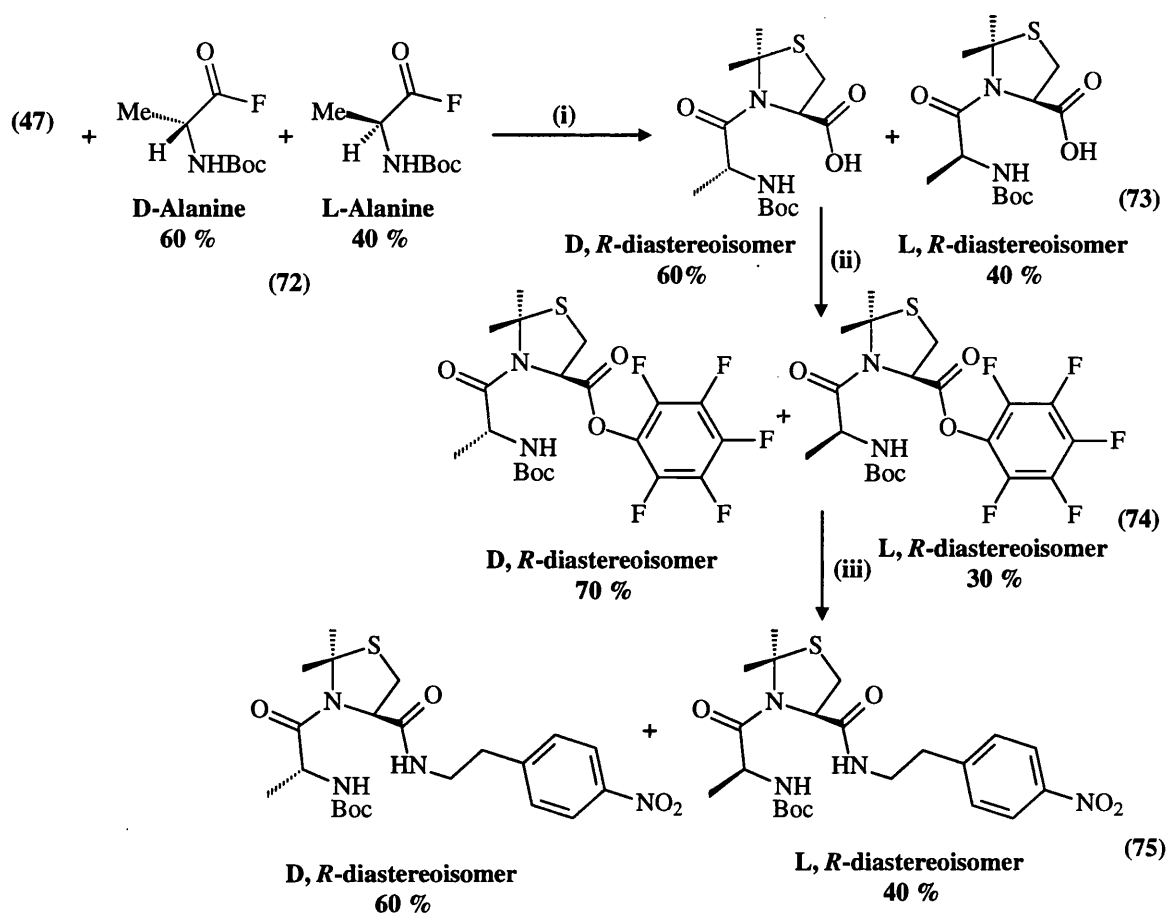
Scheme 3.4 Chemical synthesis of D,R and L R- diastereoisomers (75) (i) Pr$^i_2$NEt, DMF; (ii) PFPOH, DCC, EtOAc; (iii) 4-nitrophenylethylamine hydrochloride, Et$_3$N, CH$_2$Cl$_2$.

The acid fluorides of the mixture consisting of 60% Boc-protected D-alanine and 40%Boc-protected alanine (D and L) (72) were prepared by the method used previously.[136] Coupling of the crude mixture with (47) afforded the mixture (73) in 36% yield as a mixture of two diastereoisomers *before purification* in a ratio of 3:2 for the D,R-diastereoisomer and L,R-diastereoisomer, respectively. The ^{1}H-^{1}H COSY spectrum of (73) highlighted the separate signals of the two diastereoisomers (**Figure 3.11**). The comparison of compounds (57) and (73) spectra confirmed that (57) was indeed the L,R stereoisomer only. Furthermore, the similarity of the ratio of products to the ratio of acid fluorides confirms that there is little or no diastereoselectivity in the coupling reaction. Coupling of the mixture (73) with pentafluorophenol under the usual conditions afforded the active acylating agent mixture (74) in 80% yield. The ^{19}F NMR spectrum of (74) was complex and indicated the presence of two conformers for each of the two diastereoisomers.
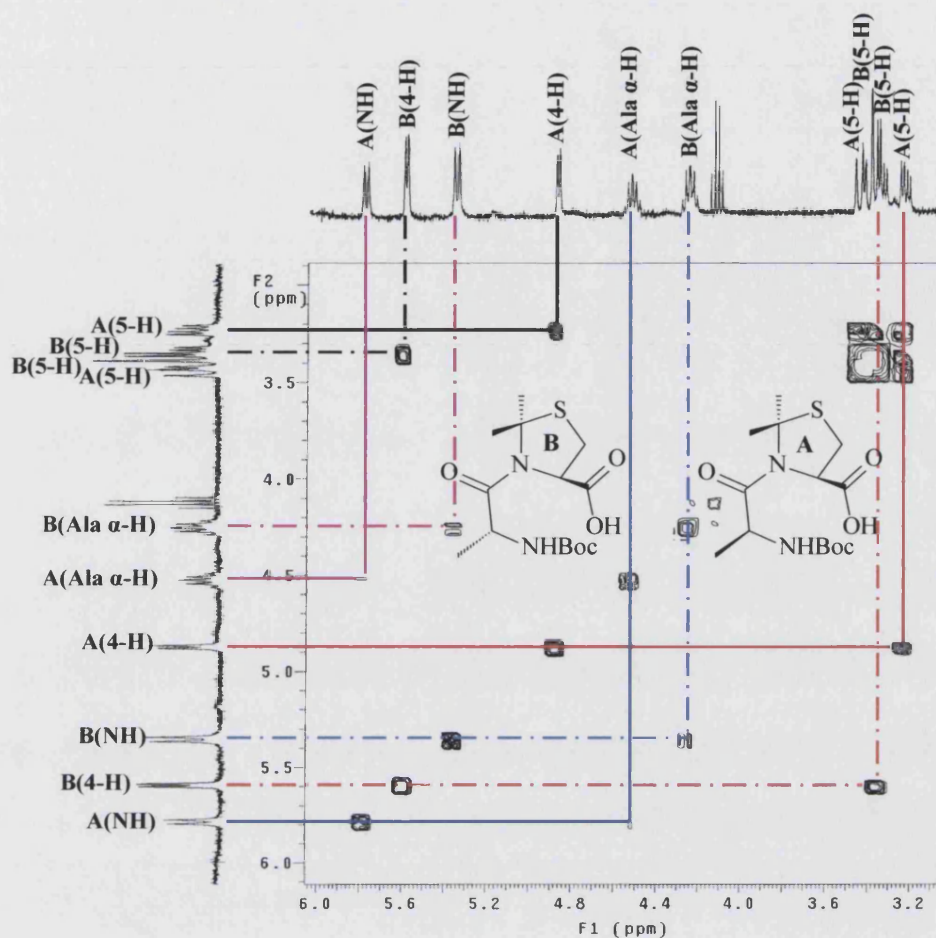
Figure 3.11 ^1H-^1H *COSY NMR spectrum of compound* **(73)** *in CDCl₃. **A** corresponds to the L,R-diastereoisomer;* **B** *corresponds to the D,R-diastereoisomer.*

Two distinct diastereoisomers in a ratio of 6:4 for the D, *R*-diastereoisomer and L, *R*-diastereoisomer respectively was seen in ^1H NMR and ^{19}F spectra. From these data, it is clear that the two populations of **(61)** are not diastereoisomers but are conformers.

Coupling of the diastereomeric mixture **(74)** with 2-(4-nitrophenyl)ethylamine afforded mixture **(75)** in 76% yield. Interestingly, two diastereoisomers in the initial ratio 3:2 was identified for the (D,*R*-diastereoisomer) and (L,*R*-diastereoisomer) respectively. The wide range melting point 69-80°C of **(75)** is attributed to the presence of these diastereoisomers. Clearly, the identification of two diastereoisomers in the spectra of the mixture **(75)** will highlight the fact that no racemisation occurred in the synthesis of the target compounds **(64)**, **(65)**, **(66)**, and **(67)**.

68

Diastereoisomers differ in their physical and chemical properties. On this basis, it was important to study their effect on the rate of intramolecular cyclisation of the self-immolative molecular clip and, in consequence, the drug release. Thus a pure diastereoisomer of one of the previously studied molecular clips was needed for this study. The diastereoisomer of compound (66) was taken as an example. This diastereoisomer could either be (D,R) or (L,S), which are enantiomers and should have identical chemical properties under achiral conditions. The synthesis of these diastereoisomers could be attained by two pathways (Scheme 3.5). Applying these two pathways in the synthesis will add to the body of knowledge valuable information about the ease of the synthesis in both pathways. Initially, since D-Cys.HCl is much more expensive than D-Val, pathway A was investigated. It will be interesting to compare the final output products of the two enantiomers.

On the basis of **pathway A (Scheme 3.5)**, the Boc-protected D-valine acid fluoride (76) was prepared by the treatment of Boc-protected D-valine with cyanuric fluoride, as previously. The crude product was coupled directly with (47) in the presence of tertiary amine base. Purification *via* chromatography afforded compound (77) in 50% yield. It is noteworthy that this yield was relatively high upon comparison with the yield obtained for the L,R-diastereoisomer (58) and may suggest some diastereoselectivity in the coupling with Val, in contrast to the lack of selectivity with Ala (*vide supra*).

On the basis of **pathway B (Scheme 3.5)**, compound (81) was prepared by cyclo-condensation of D-Cys.HCl.H$_2$O (80) with acetone[123] in the presence of 2,2-dimethoxypropane (DMP) which serves as a reactant. The crude Boc-protected L-valine acid fluoride (54) was coupled directly with (81). Purification *via* chromatography afforded crude compound (82) in 35% yield.
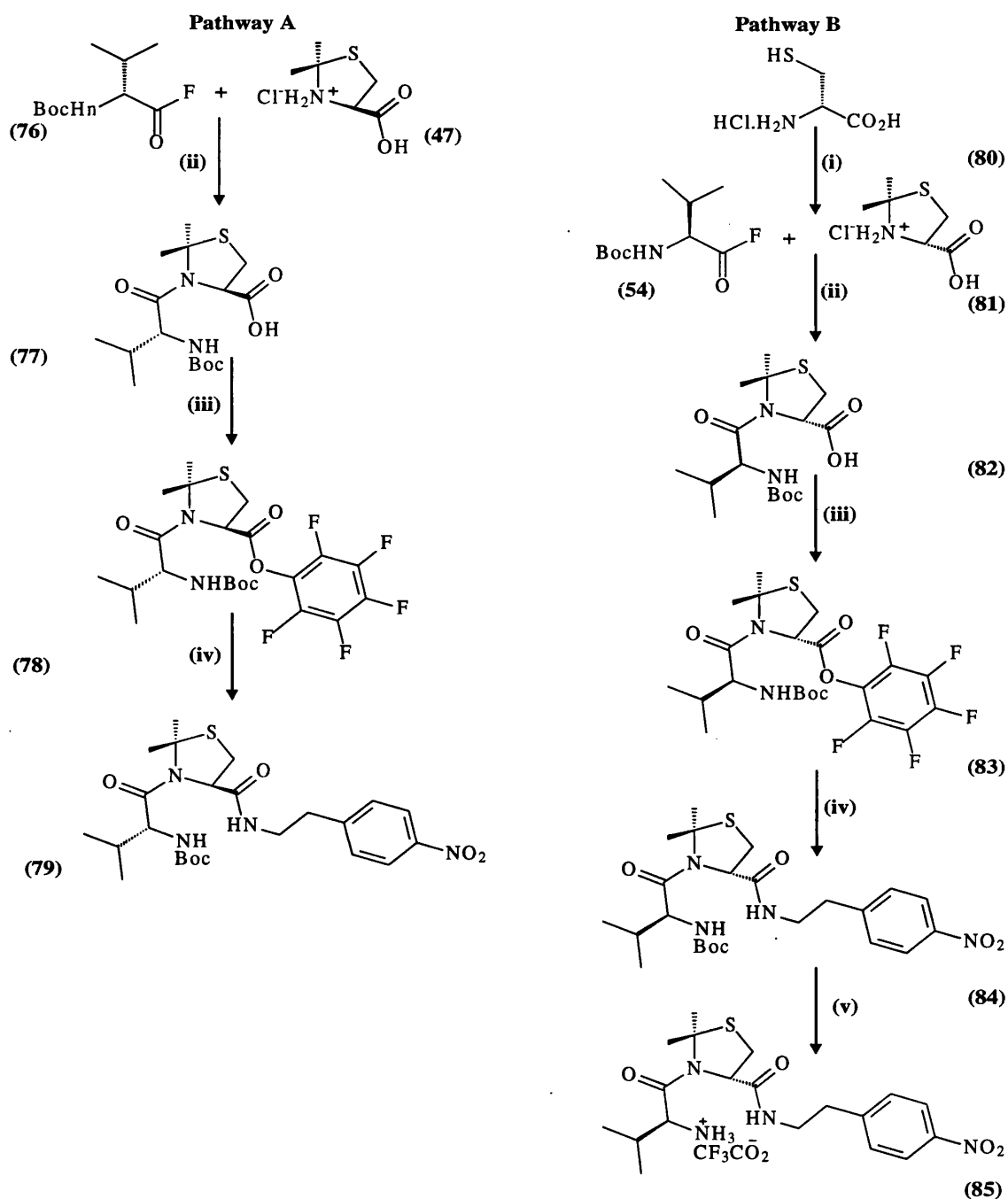
Scheme 3.5 *Chemical synthesis of the enantiomeric self-immolative molecular clips (79) and (85), according to pathways A and B, respectively. (i) (CH₃)₂CO, DMP; (ii) Prⁱ₂NEt, DMF; (iii) PFPOH, DCC, EtOAc; (iv) 4-nitrophenylethylamine hydrochloride, Et₃N, CH₂Cl₂; (v) 20% CF₃CO₂H / CH₂Cl₂.*

The ^{1}H NMR spectra of **(77)** and **(82)** were essentially identical, as is required for enantiomers. However, significant differences were seen between the spectra of the diastereoisomers. The most marked differences were for the Val α-H (δ 3.86 for **(77)** and δ 4.50 for **(58)**) and 4-H (δ 5.66 for **(77)** and δ 5.02 for **(58)**), with smaller differences being observed for other signals.
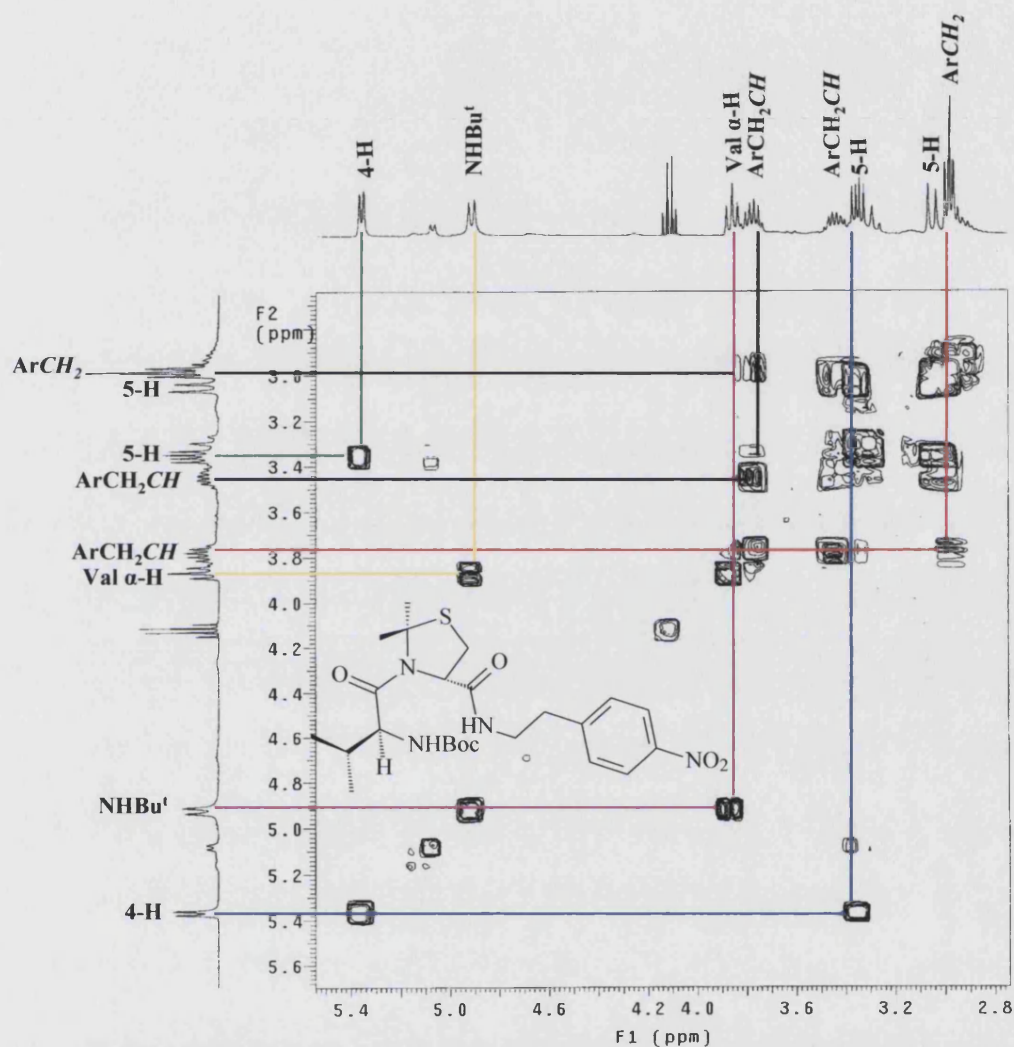
Figure 3.12 ^{1}H-^{1}H COSY NMR spectrum of compound **(84)** at 20°C in CDCl₃.

Activation of **(77)** and **(82)** by coupling with pentafluorophenol in the presence of DCC afforded crude **(78)** and **(83)**. Subsequent coupling with 2-(4-nitrophenyl)ethylamine **(41)** granted the amides **(79)** and **(84)** as gummy oils in 17% and 49% yields, respectively. The ^{1}H-^{1}H COSY spectrum of **(84)** helped in the assignment of the ^{1}H-^{1}H coupling relationship **(Figure 3.12)**. Deprotection of compound **(84)** afforded the trifluoroacetate salt **(85)** in a quantitative yield.

For compounds (79) and (84), two distinct sets of signals were observed in the ^{1}H NMR spectra with relative populations of 80% and 20% at 20°C in CDCl$_3$, indicating that two (Z and E) amide conformations are present. These compounds (79) and (84) are enantiomers and both are diastereoisomeric to compound (66) (**Figure 3.8**). The identification of the two sets of signals in the spectra of (79) and (84) as arising from the conformers, rather than any racemisation, was confirmed by the fact that neither set corresponded to the signals from the diastereoisomer (66). Comparison of the spectra of (84) in (CD$_3$)$_2$SO at 20°C and 80°C have showed line-broadening and movement towards coalescence for the 4-H signal at the higher temperature. However, since coalescence was not complete at 80°C, the energy barrier to rotation must be relatively high. The ^{1}H NMR spectra of compounds (79) and (84) were identical; this confirms that they are enantiomers (**Figure 3.13**).

A

B

C
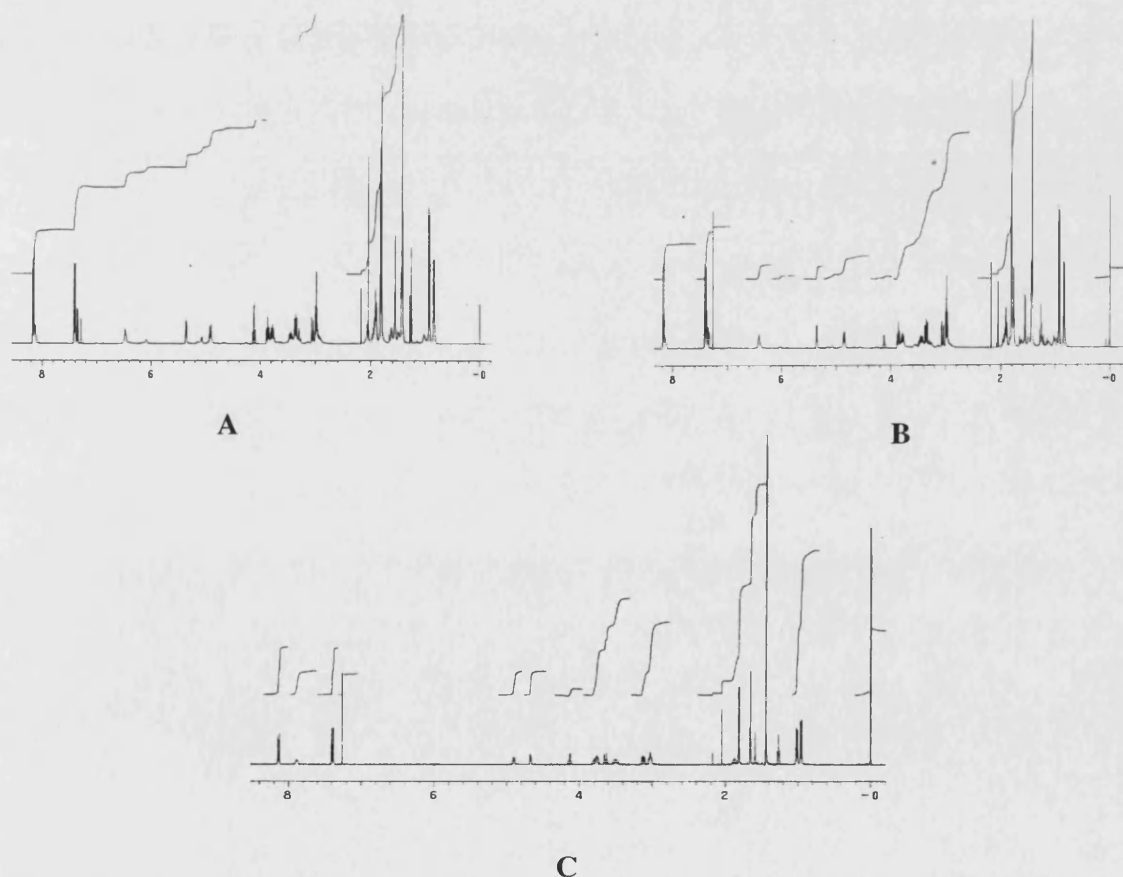
Figure 3.13   *A and B are ^{1}H NMR spectra of the enantiomeric compounds (79) and (84) respectively in CDCl$_3$, while C is the ^{1}H NMR spectrum of the diastereoisomeric compound (66) in CDCl$_3$.*

As a conclusion, the results of the tailor-made enantiomeric D/L-Ala mixture experiment, together with the synthesis of the Val-containing stereoisomers by two pathways, confirms that no loss of stereochemical integrity had taken place during any of the coupling reactions.

However, in order to increase the body of knowledge, another experiment was performed by substituting the amino-acid L-valine with L-leucine (Scheme 3.7) in the L,S diastereoisomer. The rationale for this experiment is to highlight the role of the size of the side-chain in forcing the clip into the reactive cis (Z) amide conformation and as a consequence, the rate of intramolecular cyclisation of the self-immolative molecular clip.

Previously, the acid fluorides were used for coupling with the $Me_2Thiazolidine$ moiety. Experiments (vide supra) to attempt to use pentafluorophenyl active esters with the dimethylthiazolidine nitrophenylethyl amide (51) resulted in opening of the thiazolidine ring (Scheme 3.2). Nevertheless, Fmoc-L-ValOPFP (87) ester[141,142] coupled very effectively with the S-dimethylthiazolidinecarboxylic acid (81) (Scheme 3.6).

FmocHN CO_2H FmocHN   OPFP
        (86)   O   (87)
                          +

$Cl^-H_2N^+$ ... O   (ii)
        (81)   OH   OH
                               NHFmoc
                        (88)
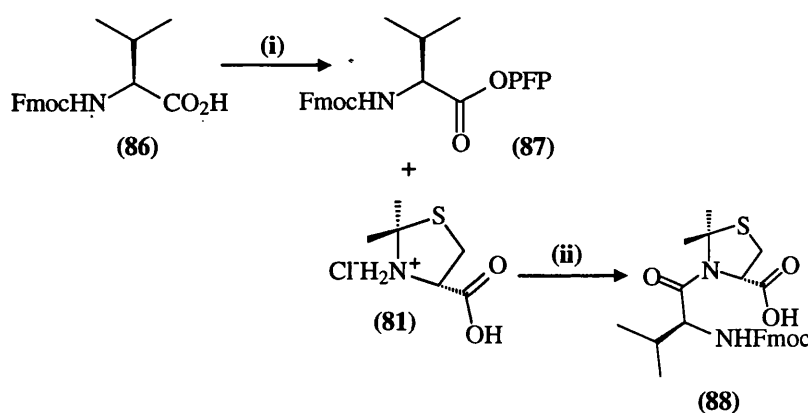
Scheme 3.6 Chemical approach for the synthesis of (88). (i) PFPOH, DCC, EtOAc; (ii) Pr^i_2NEt, DMF.

However, unlike Boc protecting group, Fmoc moiety is not acid-labile and has an excellent chromophore, which facilitates detection via UV. It is also not removed by the acetic acid which is necessary for the chromatographic purification. Unfortunately, in the synthesis pathway of the clip, Fmoc-protected amino-acids cannot be used in the coupling process due to the cyclisation that would follow Fmoc deprotection under alkaline conditions. However, this experiment gives valuable information about successful coupling of PFP and acid fluorides with the $Me_2thiazolidine$ moiety.

Using the success of the previous model (**Scheme 3.6**), Boc-L-Leu was converted to its pentafluorophenyl ester (**90**)[143] with DCC by the usual methodology (**Scheme 3.7**). Consequent coupling with (**81**) afforded (**91**). After simple work-up procedures, the preliminary ^{1}H NMR spectrum indicated that this compound is 90% pure and the impurities were identified to be related to DCU. On the basis of ^{1}H NMR spectroscopy, compound (**91**) exists solely as one diastereoisomer and one conformer. ^{1}H-^{1}H COSY analysis of (**91**) helps in the assignment of the H-H coupling relationship. Conversion of (**91**) to the pentafluorophenyl active ester (**92**) was followed by coupling with the appropriate amine to give the nitrophenylethyl amide (**93**) in 58% yield. ^{1}H and ^{19}F NMR spectroscopy indicates the presence of mainly one conformer of (**92**). The ^{1}H NMR spectrum of (**93**) showed the presence of two rotamers in the ratio 4:1, similar to the ratio seen for the corresponding Val dipeptide. Deprotection of (**93**) afforded the trifluoroacetate salt (**94**) in a quantitative yield.
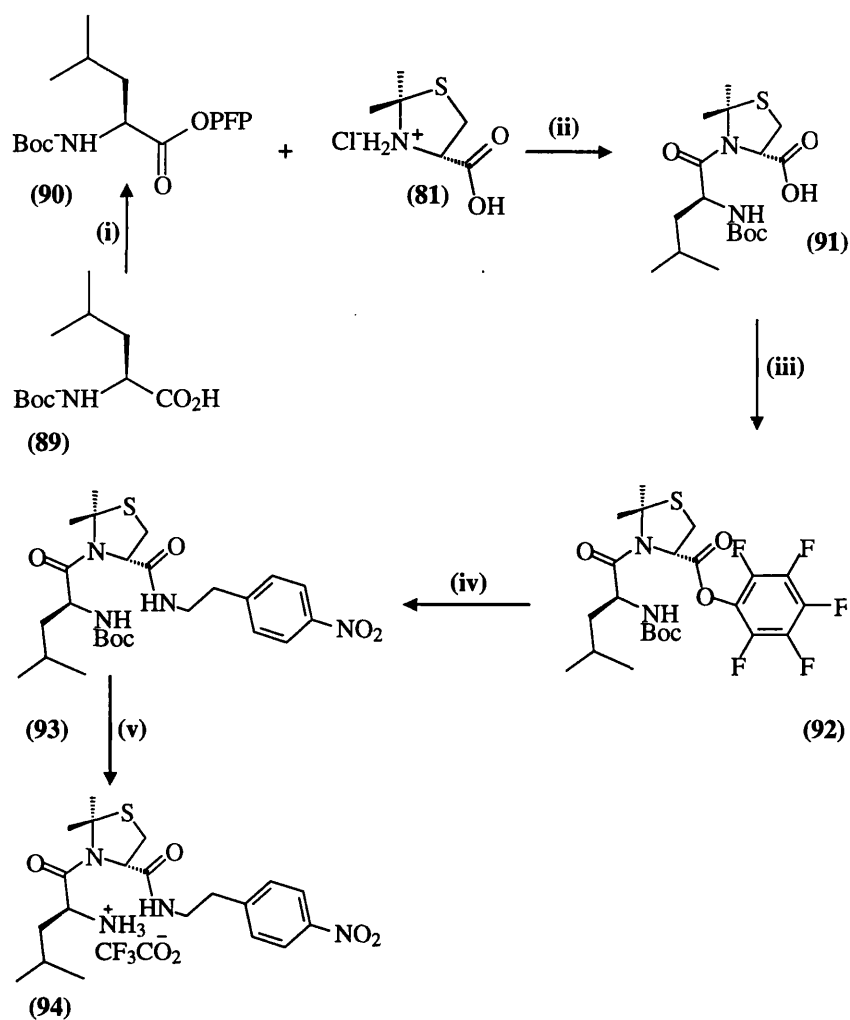
Scheme 3.7 *Chemical synthesis of the L,S-diastereoisomer (94). (i) PFPOH, DCC, EtOAc; (ii) Pr$^i_2$NEt, DMF; (iii) PFPOH, DCC, EtOAc;(iv) 4-nitrophenylethylamine hydrochloride, Et$_3$N, CH$_2$Cl$_2$; (v) 20% CF$_3$CO$_2$H / CH$_2$Cl$_2$.*

3.2 Synthesis of diketopiperazines (DKPs)

In the course of solid-phase synthesis of the peptide sequence D-Pro-D-Val-L-Pro, it has been found that a carboxylic acid-catalysed intramolecular aminolysis of the ester bond to the resin occurs at the dipeptide stage. This result accounts for the considerable loss of the dipeptide from the resin, which amounted for 70% during the step of coupling with Boc-D-Proline and DCC. However, this cyclisation was repressed by adding the carbodiimide reagent prior to the carboxyl component. The resulting diketopiperazine of D-valyl-L-proline was isolated and characterized.[144] Generally speaking, DKP formation occurs as a disturbing reaction in the synthesis and long-term storage of peptides.[121] However, DKP formation is known to occur easily for dipeptide esters because of the presence of alkoxy good leaving groups. In addition, peptides with alternating chirality form DKPs more easily because of the higher stability of the resulting DKPs.[121] DKPs are conformationally constrained scaffolds with side chains that are oriented in a spatially defined manner. As an example, in the D/L DKPs, the amino acid side chains will lie on opposite sides of the plane of the cycle. It is noteworthy, as in compound (36) (Scheme 2.1 B), that the peptide bonds must be in the *cis* conformation; the cyclisation reaction is usually promoted by an N-alkylated residue in the first position, because of their high propensity to form a *cis* peptide bond with the preceding residue.[145]

In general, rates of cyclisation vary markedly with ring size;[146] five and six-membered rings cyclize rapidly, however, four and seven-membered rings are very much slower. The classical explanation is usually attributed to the unfavourable strain energy, which hinders the formation of small rings, while this strain becomes negligible in five and six-membered rings. Another factor is the presence of alkyl substituents, which usually causes a large enhancement of the rate of cyclisation; this is the "gem-dialkyl" effect.[147]

Recently, an efficient novel route for the synthesis of DKPs on a solid-phase system has been described.[148] Also solution-phase synthesis has been reported.[144] The strategy now is to synthesise the DKPs corresponding to the self-immolative molecular clips previously synthesised, in order to identify the side-product (DKPs) of the intramolecular cyclisation process during the HPLC analysis. Retrosynthetic analysis exploits the general recognised propensity for dipeptide esters to form diketopiperazines, where the unprotonated nitrogen

atom of the N-terminal amino acid can attack the carbonyl carbon atom of the ester of the second cyclic residue causing the formation of a six-membered ring DKPs in a good rate. The route of DKP synthesis will start with the pentafluorophenyl active esters of the L,R dipeptides **(60)**, **(61)**, **(62)** and **(63)** **(Scheme 3.8)**.

R = H   (60)
R = CH$_3$ (61)
R = CH(CH$_3$)$_2$ (62)
R = CH$_2$Ph   (63)

R = H   (95)
R = CH$_3$ (96)
R = CH(CH$_3$)$_2$ (97)
R = CH$_2$Ph   (98)

(i)

(ii)

R = CH$_3$ (99)
R = CH(CH$_3$)$_2$ (100)
R = CH$_2$Ph   (101)
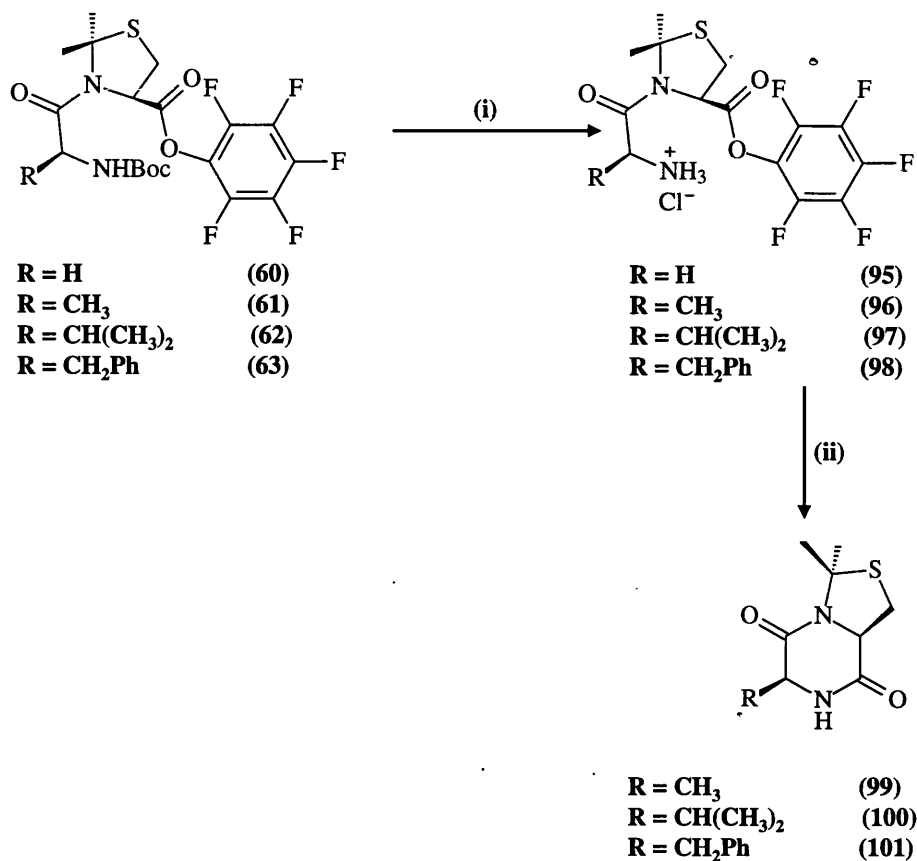
Scheme 3.8   *Chemical synthesis of the authentic diketopiperazines (99), (100) and (101). (i) HCl / CH$_2$Cl$_2$; (ii) Et$_3$N / CH$_2$Cl$_2$.*

Removal of the Boc protecting group was achieved rapidly by passing hydrogen chloride through **(60)**, **(61)**, **(62)** and **(63)** in dichloromethane to afford **(95)**, **(96)**, **(97)** and **(98)** in quantitative yields. Enticingly, on the basis of ^{1}H NMR spectral analysis, these intermediate deprotected compounds were identified; however, by the time that the ^{19}F NMR spectrum and mass spectroscopy were conducted, a hydronium ion-catalyzed cyclisation reaction **(Scheme 3.9)** had occurred, resulting in the formation of the corresponding DKPs. The ^{1}H-^{1}H COSY spectrum of **(97)** helped in the assignment of the H-H coupling relationship. The NOESY spectrum showed the usual through-space

connectivity between 4-H and only one 5-H but did not reveal which conformer was present **(Figure 3.14)**.
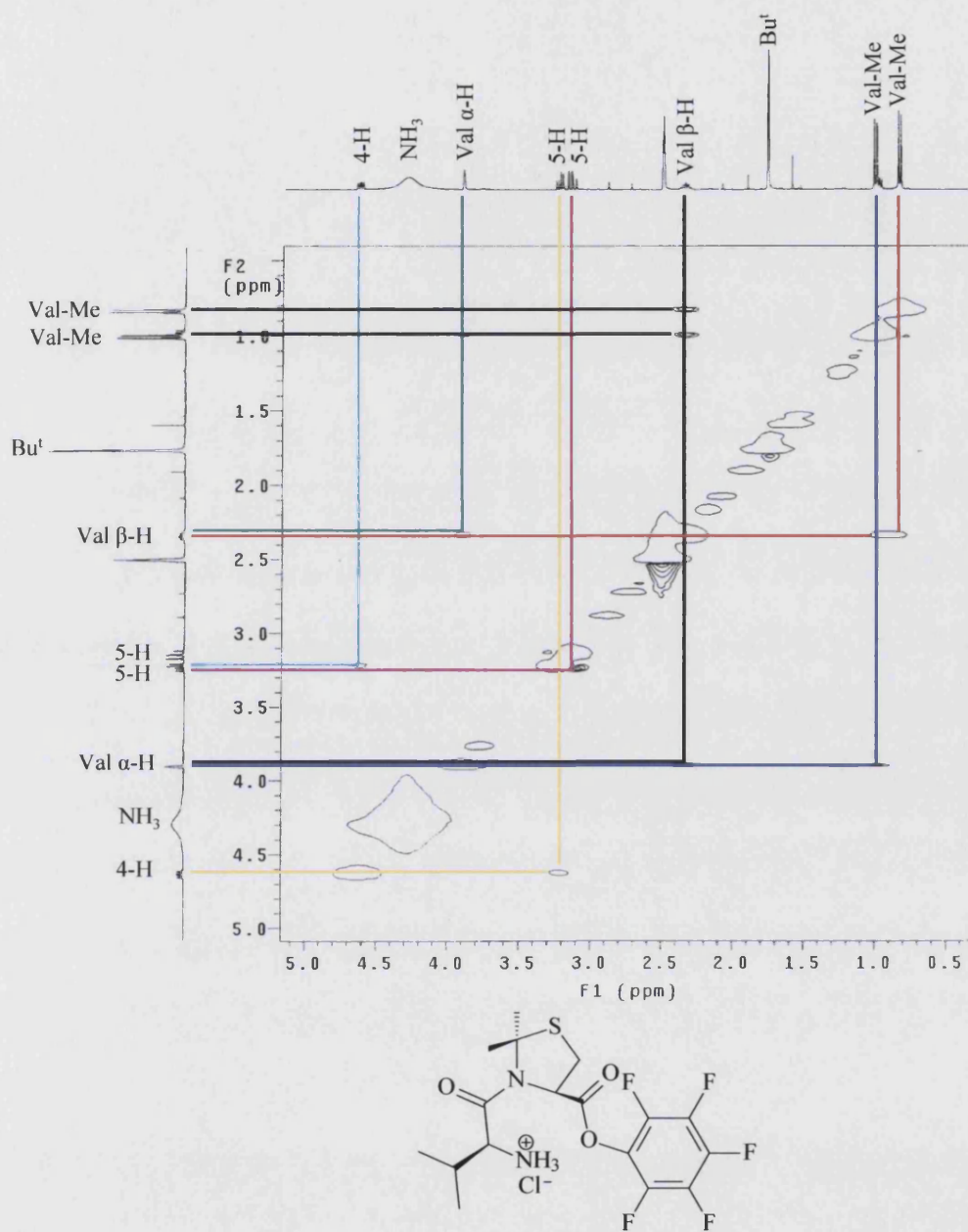
Figure 3.14 ^1H-^1H *NOESY NMR spectrum of compound* **(97)** *at 20°C in* $(CD_3)_2SO$.

The NOESY spectrum of **(98)** is shown **(Figure 3.15)**. Notably, there is NOE connectivity between the upfield 2-CH$_3$ (δ 1.87) and the ortho protons of the phenyl group. There is also connectivity between the downfield 2-CH$_3$ (δ 1.92) and the Phe α-H (δ 4.24). These data allow assignment of the individual singlets for the 2-methyl groups. Similarly the individual protons of the 5-CH$_2$ can be assigned because the signal for one of them (δ 3.26) has an NOE correlation with the 4-H (δ 4.53). Other NOE correlations were seen between the NH and Phe α-H, between NH and the phenyl protons and between NH and the Phe β-H$_2$.
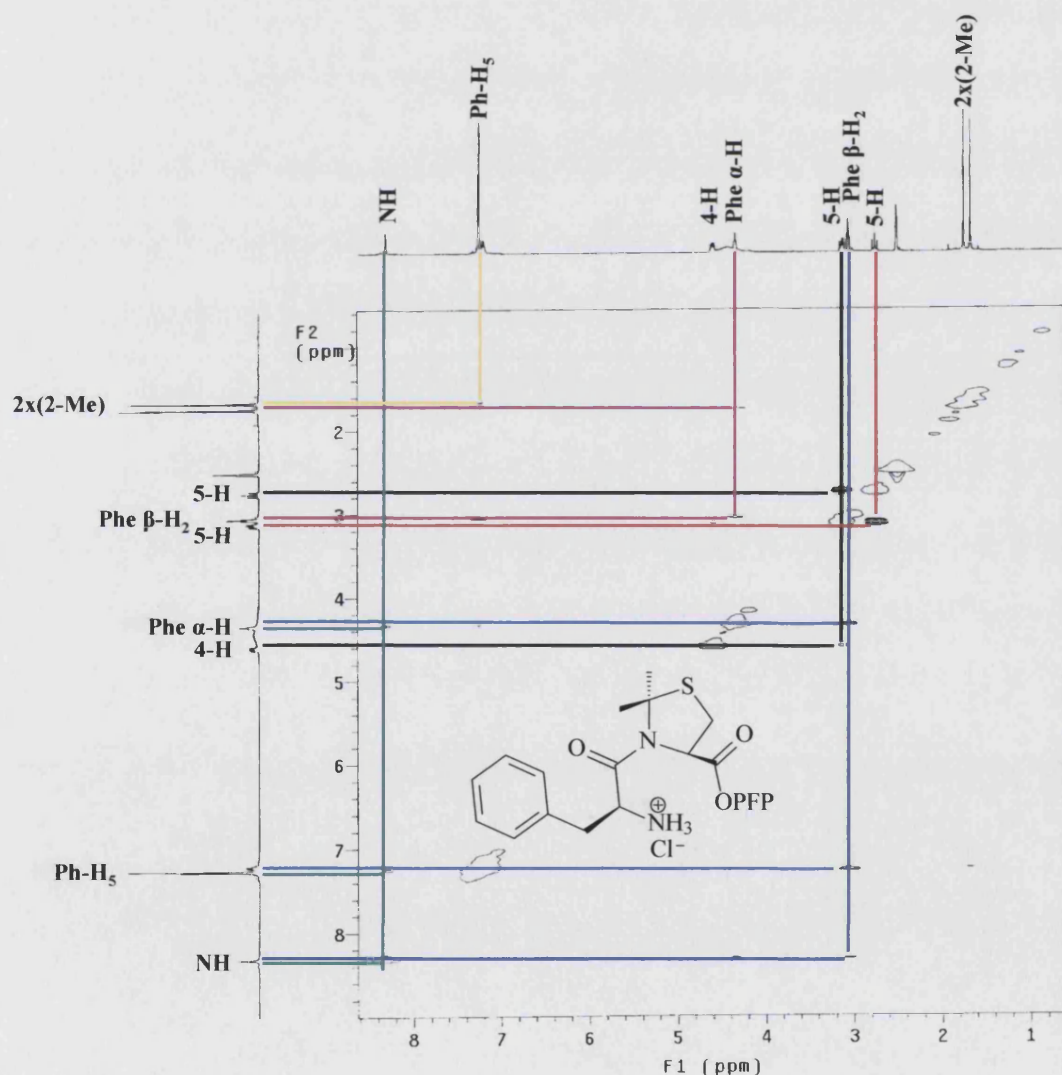
Figure 3.15 ^1H-^1H NOESY NMR spectrum of compound **(98)** at 20°C in (CD$_3$)$_2$SO.

79

Acid-catalysed DKP formation is due to the protonation of the carbonyl oxygen atom, which lowers the activation energy of the nucleophilic addition on the carbonyl carbon atom **(102)**, resulting in direct formation of a cationic tetrahedral intermediate **(103)**. This is the expected route for DKP formation **(105)** at low pH. On the other hand, base-catalysed formation of the DKPs **(99)**, **(100)** and **(101)** proceeded swiftly upon stirring with a non-nucleophilic base (triethylamine). The unprotonated N-terminal amino group undergoes the ring-closure reaction very quickly.
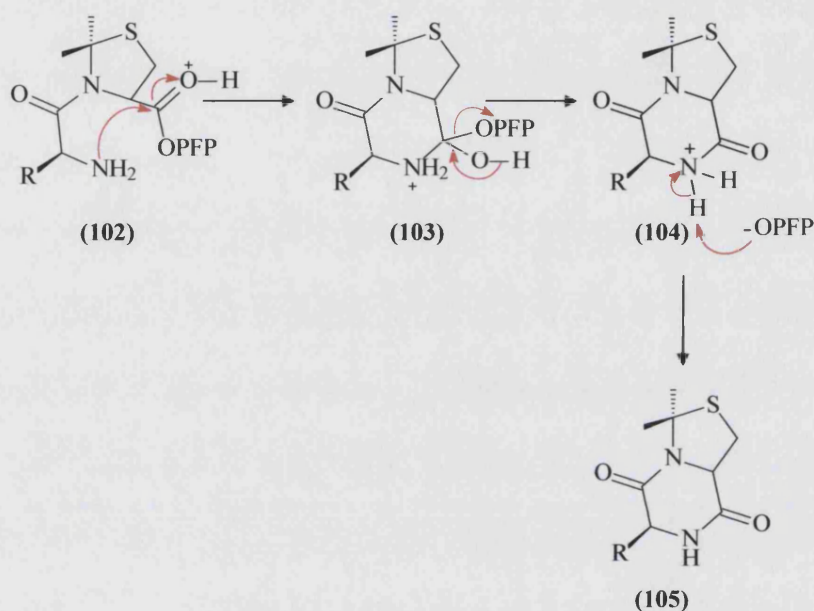
Scheme 3.9 *Proposed mechanism of acid-catalysed formation of diketopiperazines (105).*

The structures of the DKPs **(99)**, **(100)** and **(101)** were confirmed by ^{1}H NMR; the assignments of the signals were aided by the ^{1}H-^{1}H COSY spectra **(Figure 3.16)**, **(Figure 3.17)** and **(Figure 3.18)**, respectively. It should be noted that the numbering system of the DKPs is different to that of the parent dipeptides; the bicycle is numbered with sulfur at position 2, the gem-dimethyl at position 3 and carbonyls at positions 5 and 8.
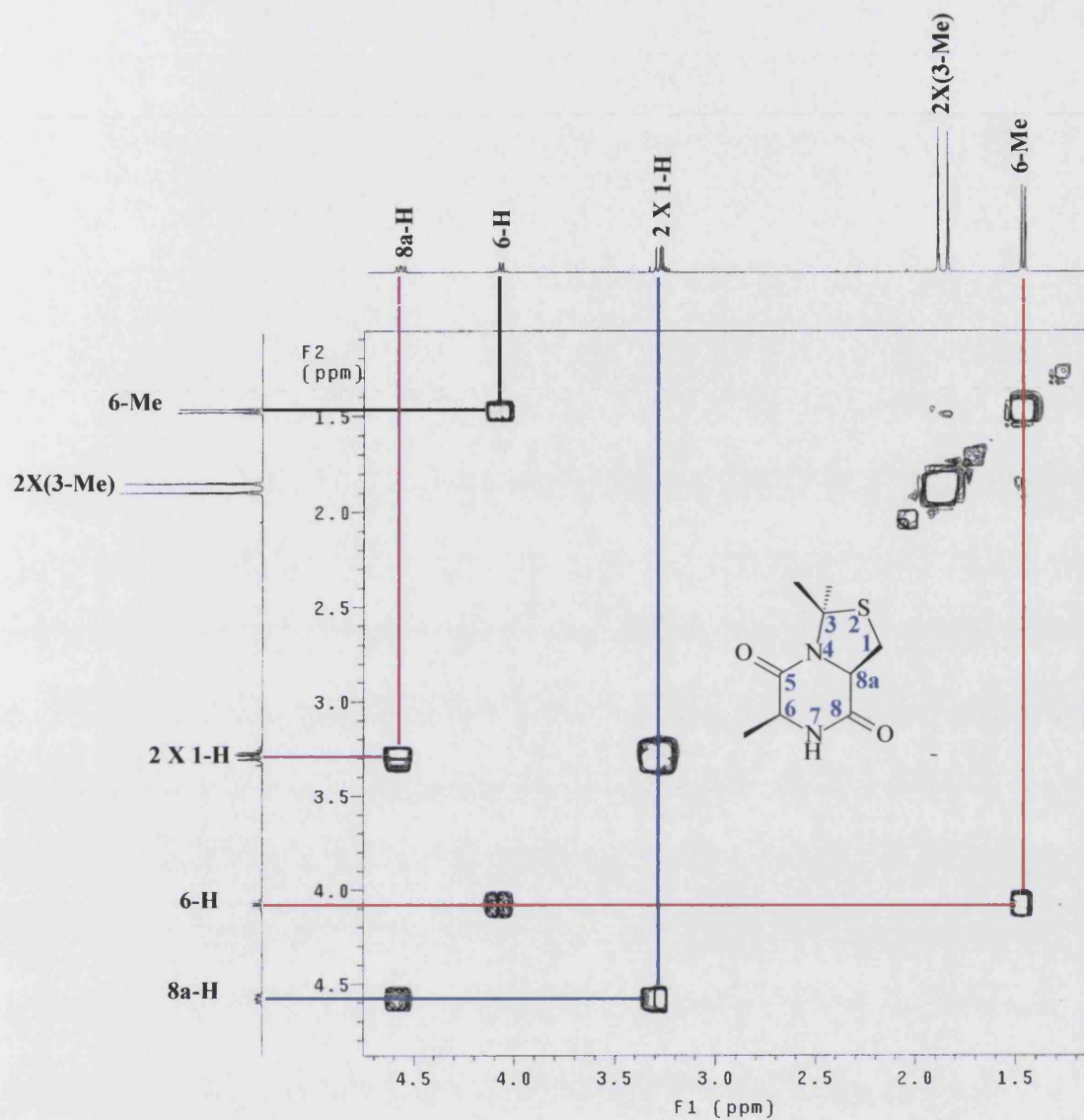
Figure 3.16 *^{1}H-^{1}H COSY NMR spectrum of compound (99) at 20°C in (CD$_3$)$_2$SO.*
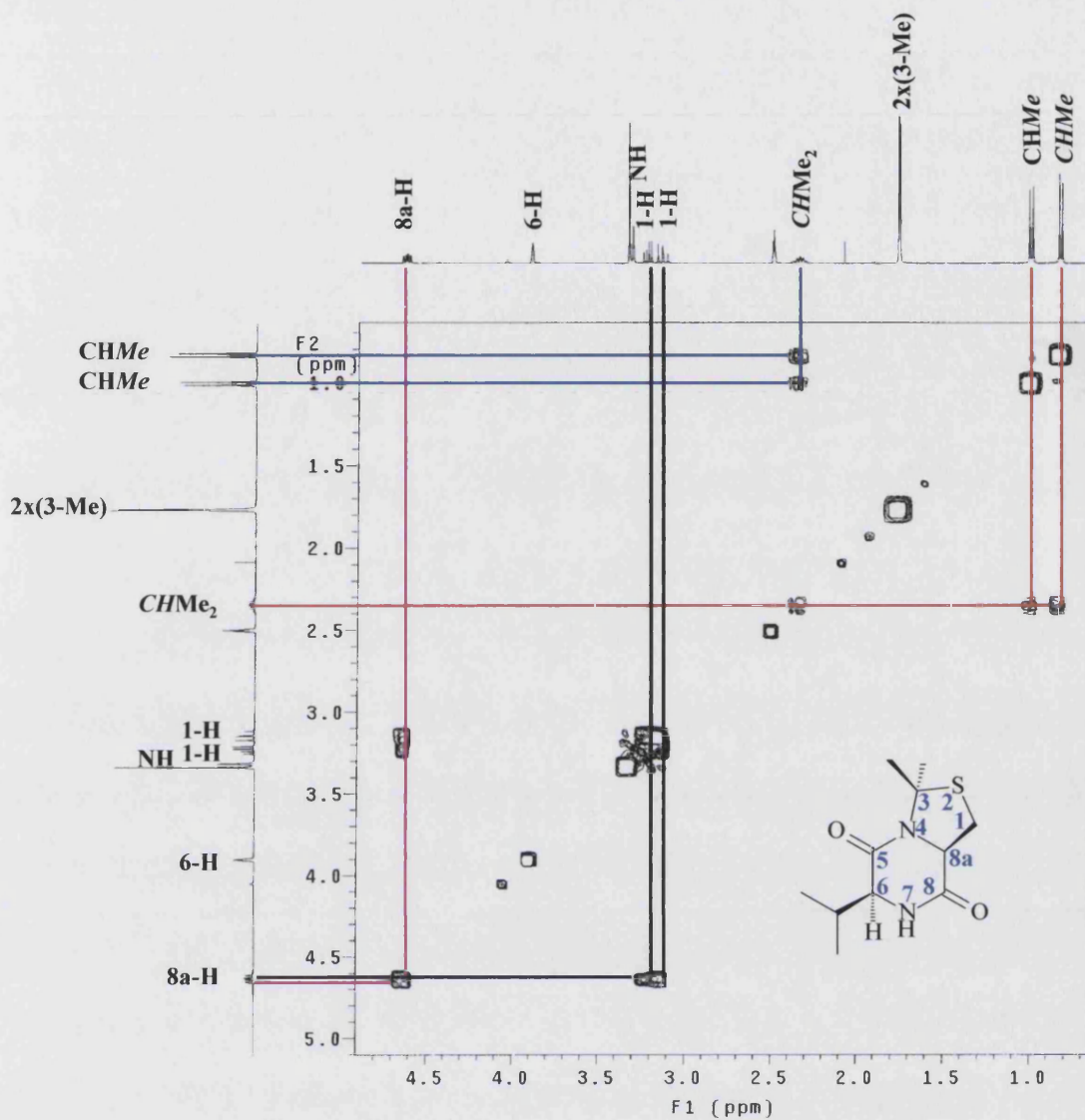
Figure 3.17 ^1H-^1H COSY NMR spectrum of compound **(100)** at 20°C in $(CD_3)_2SO$.
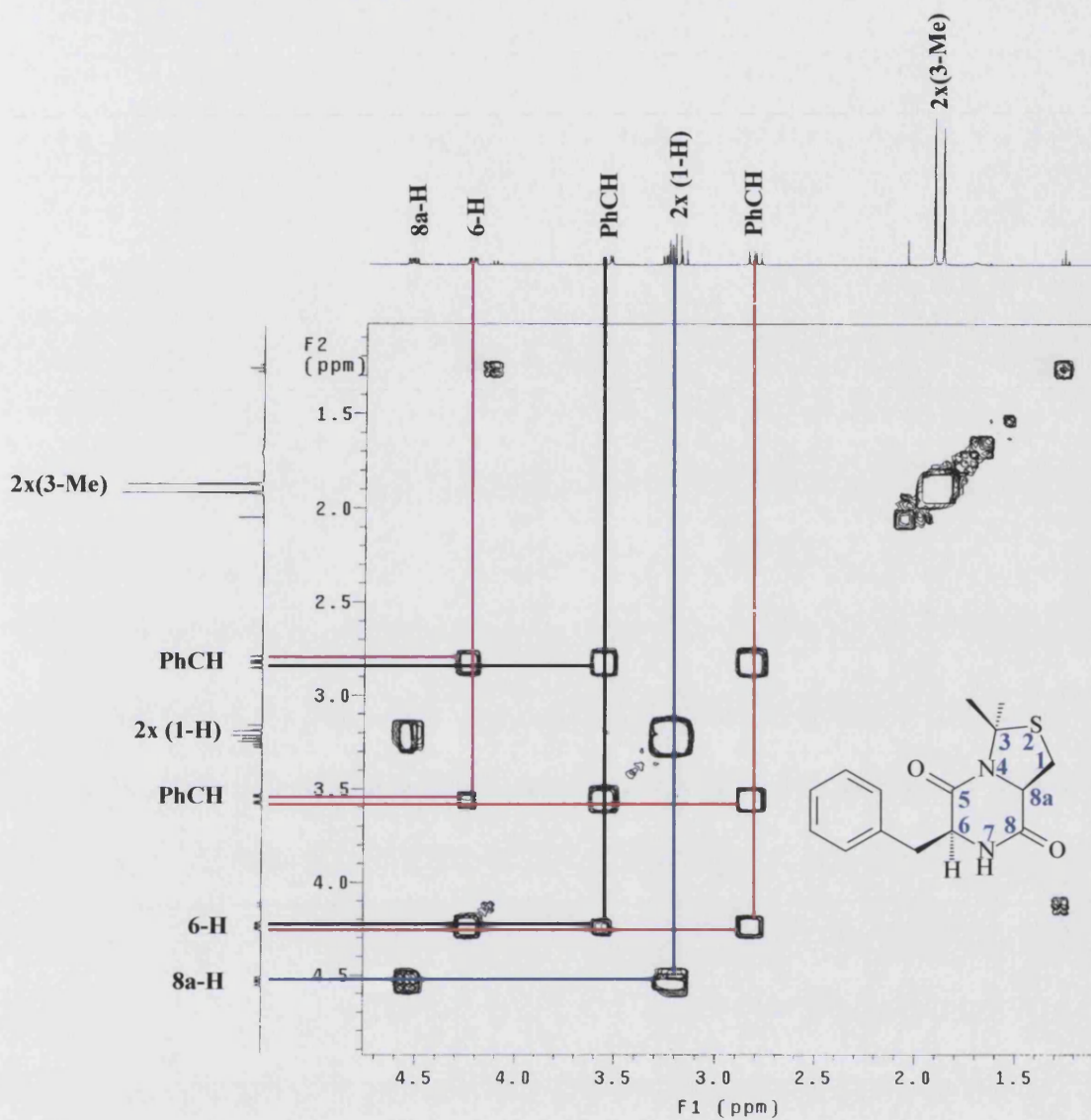
Figure 3.18 *¹H-¹H COSY NMR spectrum of compound (101) at 20°C in CDCl₃.*

83
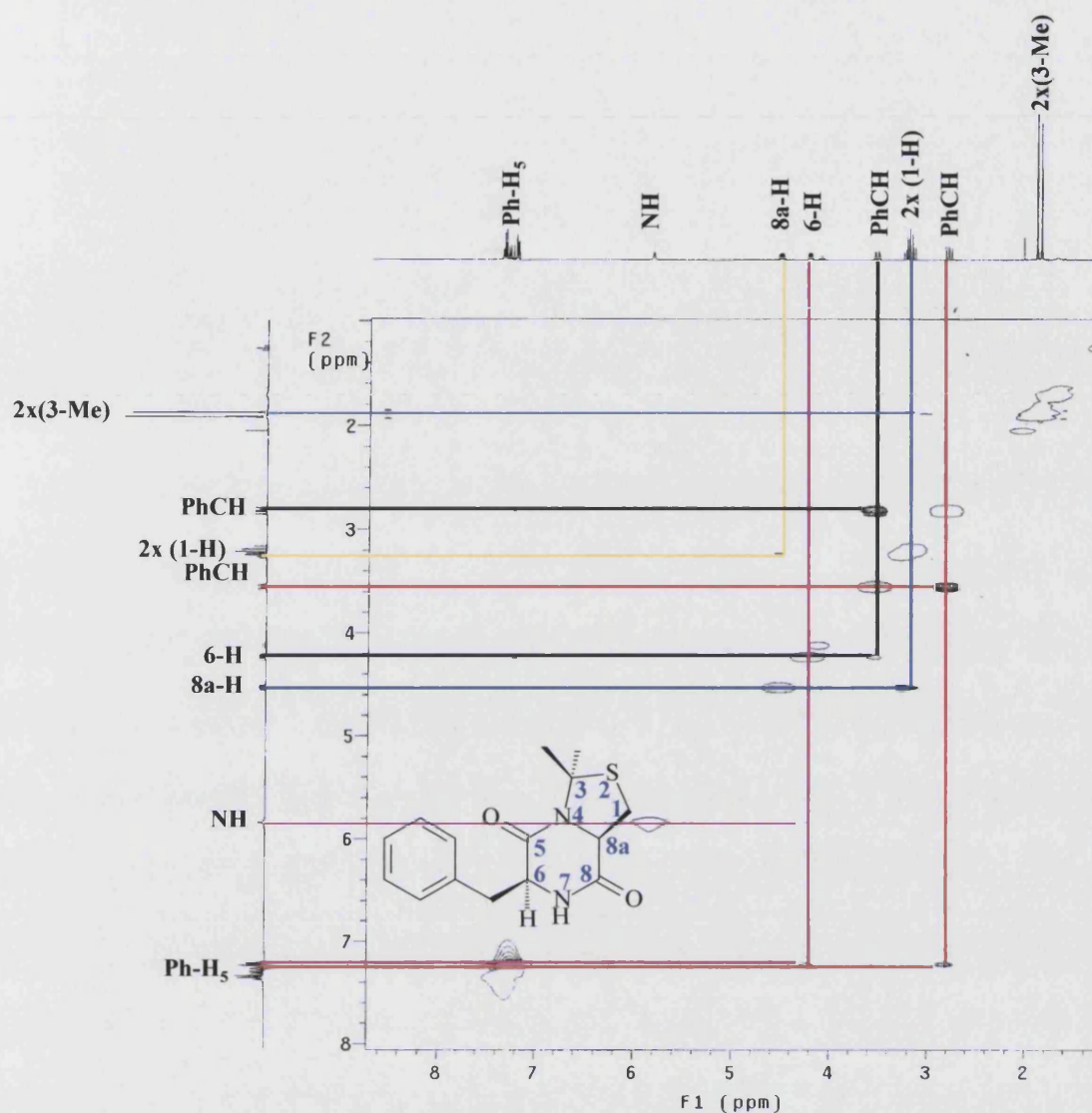
Figure 3.19 ^1H-^1H *NOESY NMR spectrum of compound* **(101)** *at 20°C in CDCl3.*

The detailed conformations of the DKPs were needed to understand the relative rates of ring-closure. The DKPs **(99)** and **(100)**, derived from L-Ala and L-Val, respectively, form good crystals and X-ray crystal structure determinations were carried out (*vide infra*). However, the L-Phe-derived DKP **(101)** was a gum. The NOESY spectrum of **(101)** **(Figure 3.19)** showed expected NOE connectivity between 1-H (δ 3.20) and 8a-H (δ 4.53) and between 6-H (δ 4.24) and NH (δ 5.82). Another NOE connectivity was seen between the ortho protons of the phenyl group (δ 7.21) and the 6-H (δ 4.24) and both PhCH (δ 2.82 and δ 3.56). Notably, an NOE connectivity was seen between the upfield 3-CH$_3$ (δ 1.87) and the other 1-H protons.

In the other diastereomeric series, the DKPs **(108)** and **(109)** derived from the L,*S*-Val (Me₂thiazolidine) and L,*S*-Leu (Me₂thiazolidine) diastereoisomers were also synthesised **(Scheme 3.10)**.

R = CH(CH₃)₂   (83)
R = CHCH₂(CH₃)₂   (92)

R = CH(CH₃)₂   (106)
R = CHCH₂(CH₃)₂   (107)

R = CH(CH₃)₂   (108)
R = CHCH₂(CH₃)₂   (109)
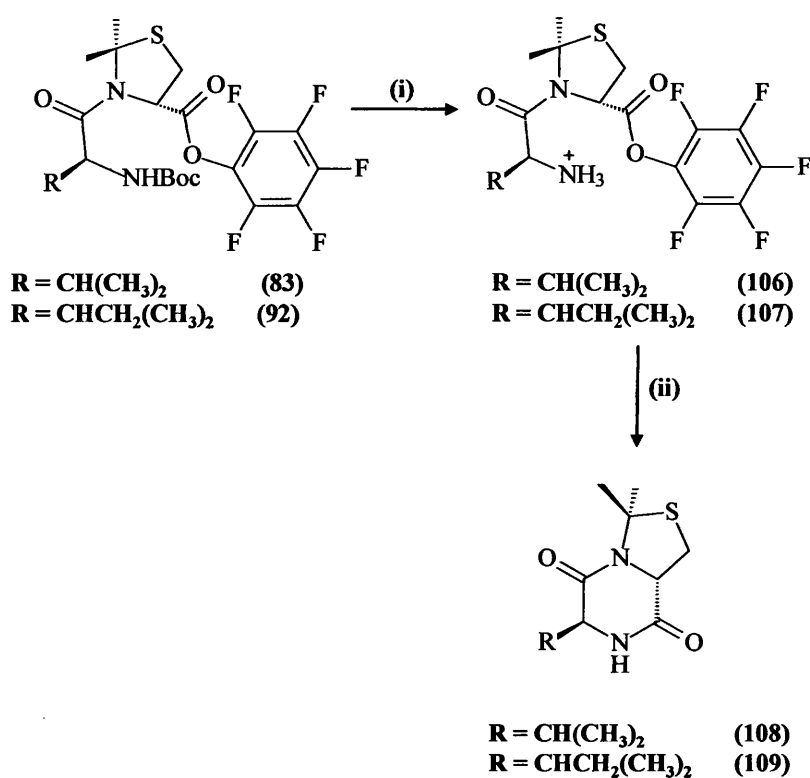
Scheme 3.10 *Chemical synthesis of the authentic diketopiperazines* **(108)** *and* **(109)**. *(i) HCl / CH₂Cl₂ or 20% CF₃CO₂H / CH₂Cl₂; (ii) Et₃N / CH₂Cl₂.*

The synthesis route follows the same methodology used previously. Hydrogen chloride-catalysed deprotection of compound **(83)** afforded **(106)** quantatively, whereas deprotection of **(92)** was successfully achieved by treatment with a mixture of 20% trifluoroacetic acid in dichloromethane and afforded **(107)** quantitavely. Subseqently, base-catalysed formation of the DKPs **(108)** and **(109)** proceeded swiftly upon treatment with triethylamine in dichloromethane.
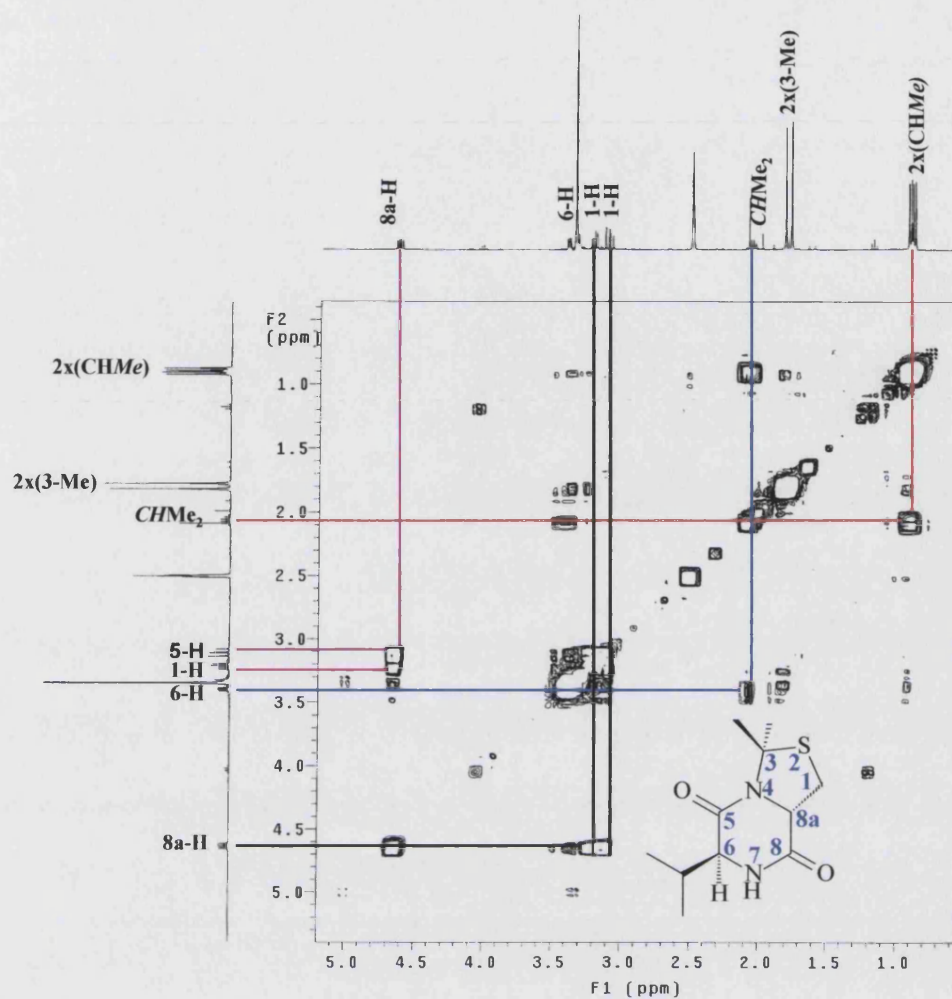
Figure 3.20 *^1H-^1H COSY NMR spectrum of compound (108) at 20°C in (CD₃)₂SO.*

The ^1H-^1H COSY NMR spectrum of **(108)** helped in the assignment of the H-H coupling relationships **(Figure 3.20)**.

3.3 Conformational studies on the DKPs derived from the molecular clips

The structures of the DKPs (99), (100), (101), (108) and (109), derived from L-Ala-*R*-dimethylthiazolidinecarboxylic acid, L-Val-*R*-dimethylthiazolidinecarboxylic acid, L-Phe-*R*-dimethylthiazolidinecarboxylic acid, L-Val-*S*-dimethylthiazolidinecarboxylic acid and L-Leu-*S*-dimethylthiazolidinecarboxylic acid, respectively, were established by the conventional spectroscopic methods (*vide supra*). Part of the study on the rates of formation of the DKPs and liberation of the model drug from the clips was to investigate the effect of the size of the amino-acid side-chain. The bulk of the side-chains may influence the cyclisation / drug release in several ways. Firstly, it may influence the *cis/trans* amide conformer ratio. Secondly, steric clashes may occur during the ring-closure reaction steps. Since it was not clear whether having a bulky side-chain would increase or decrease the rate of cyclisation and drug release, the conformations of the product DKPs were studied to assess the extent of steric crowding.

X-ray crystallography, performed by Dr. Mary F. Mahon, Department of Chemistry, University of Bath, provided the solid-state conformations for (99) and (100). Crystals suitable for the diffraction studies have not yet been grown for (101), (108) and (109).

3.3.1 Intermolecular hydrogen-bonding

The structures of compounds (99) (Figure 3.21) and (100) (Figure 3.22) each contain one hydrogen-bond donor and two acceptors. Each shows intermolecular hydrogen-bonding of the N–H⋯O=C type in the crystal. Only the secondary amide carbonyl is involved in this bonding. However, the pattern of the hydrogen bonding differs between the two molecules. In (99), the N–H and C=O of one molecule bond to different adjacent molecules, resulting in a chain of hydrogen-bonded molecules, as shown in (Figure 3.21). However, in (100), the N–H and C=O of the secondary amide of one molecule form two hydrogen-bonds with the C=O and N–H of the secondary amide of one adjacent molecule, resulting in the formation of a hydrogen-bonded dimer (Figure 3.22).
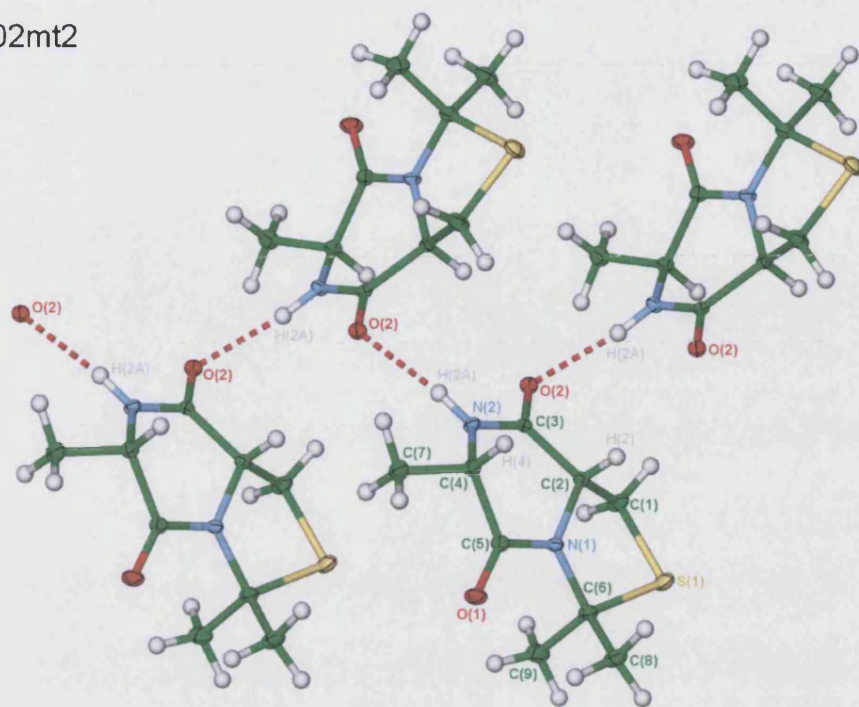
Figure 3.21 *X-ray crystallographic structure of compound **(99)**, showing the intermolecular hydrogen-bonding interactions.*
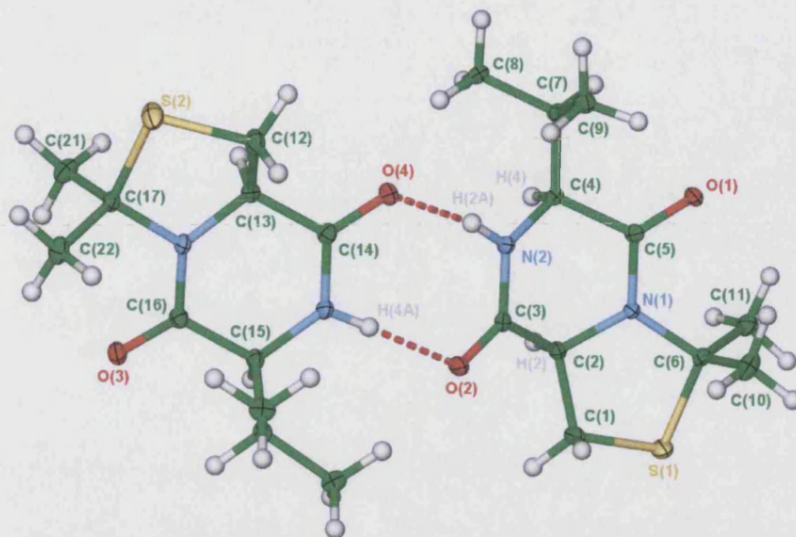
Figure 3.22 *X-ray crystallographic structure of compound **(100)**, showing the intermolecular hydrogen-bonding interactions.*

3.3.2 Conformational analysis of the DKPs

A previously reported X-ray analysis of the symmetrical unsubstituted DKP, cyclo-GlyGly, indicated it adopts a planar conformation.[149] In cyclo-L-Ala-L-Ala, which carries two methyl groups on the same face of the ring, the DKP ring is puckered and has been described as a twist boat.[150] On the other hand, the opposite diastereoisomer cyclo-D-Ala-L-Ala, with the methyls on opposite sides, is nearly planar.[150] When one of the amino-acids is Pro, the conformations adopted by the DKPs deviate from planarity, owing to the restriction imposed by the fused pyrrolidine ring. The two amides individually remain planar but they do not both lie in the same plane. Thus cyclo-L-Pro-L-Leu and cyclo-L-Pro-L-Phe adopt boat conformations.[151,152] Crystal structures of DKPs containing thiazolidines, in place of the pyrrolidine of Pro, have not been reported.

89
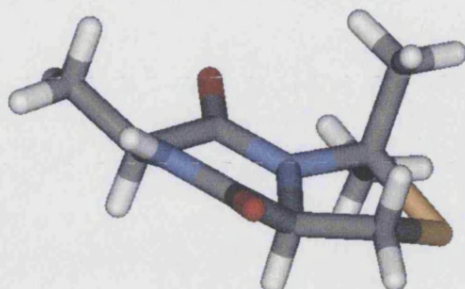
Figure 3.23 *X-ray crystallographic view of the structure of compound **(99)**. The red color refers to oxygen atom, the yellow refers to sulfur, the blue refers to nitrogen and the gray refers to the carbon atom.*

Figure 3.23 shows a view of the structure of **(99)**. The DKP ring is in a flattened boat conformation, with the thiazolidine in a half-chair. This ring conformation places the geminal methyl groups at position-3 in equatorial and axial positions; the 6-methyl occupies a *pseudo*-equatorial position. Notably, this 6-methyl group is remote in space from the geminal dimethyl unit and, indeed, from other sterically bulky groups.

A similar conformation is also likely to be adopted in solution in chloroform, since it is consistent with several NMR observations. The ^3J coupling constants between the axial 8a-H and the 1-H protons are 10.2 Hz and 6.6 Hz. These are consistent with dihedral angles (8a-H)-(8a-C)-(1-C)-(1β-H) of 166° and (8a-H)-(8a-C)-(1-C)-(1α-H) of 44°, according to the Karplus relationship. The axial 6-H couples with the adjacent N-H by $^3J = 1.0$ Hz, which corresponds with the dihedral angle of 97°. Longer-range couplings are also observed. A four-bond coupling $^4J = 1.6$ Hz is seen between 8a-H and the NH; the coupling path between these atoms contains four atoms in one plane and one terminal atom out of that plane, thus the **W**-arrangement is almost adopted. Excitingly, a five-bond coupling $^5J = 0.8$ Hz was observed between the axial 8a-H and the axial 6-H. Maes *et al.*[153] observed a similar coupling in ditryptophenaline, a natural product from *Aspergillus flavus* var. *columnaris*; this molecule contains a

90

cyclo-L-Phe-L-Pro unit fused to a heterocycle through the Pro side-chain loop. They use this long-range coupling to confirm that the DKP is in a boat conformation in solution where the corresponding protons are axial and *cis*. This then confirms that the solution conformation of **(99)** has these protons axial and *cis* and thus the solution conformation is similar to the solid-state conformation shown in **(Figure 3.23)**.
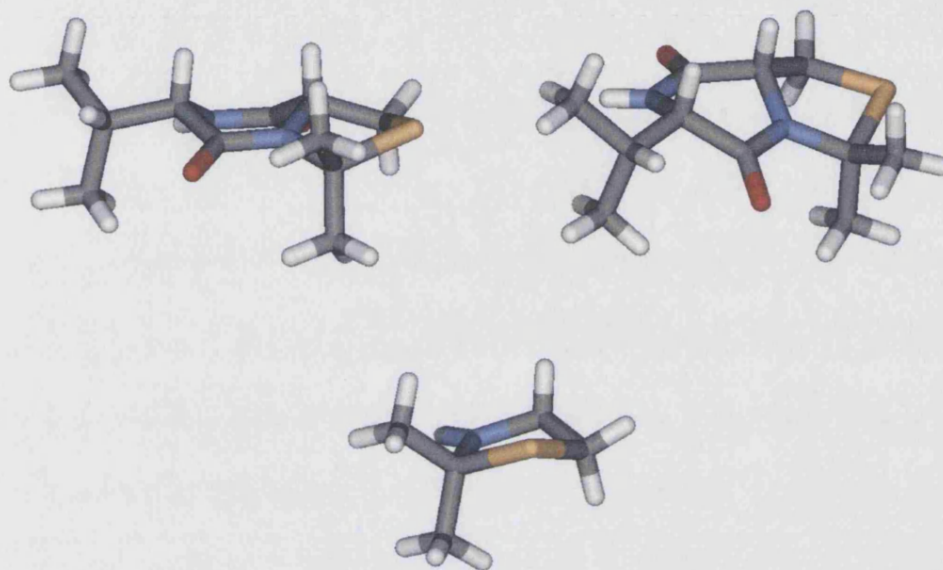
Figure 3.24 *Three views of the X-ray crystallographic structure of **(100)**. In the lower view, parts of the molecule have been omitted for clarity.*

The X-ray crystallographic study on the DKP **(100)** derived from L-Val-*R*-dimethyl-thiazolidinecarboxylic acid showed this molecule to adopt a conformation similar to that of **(99)**. **Figure 3.24** shows three views of the structure of **(100)**. Again, the DKP ring is in a boat conformation, with the thiazolidine in a half-chair. The geminal methyl groups at position-3 are in equatorial and axial positions; the 6-isopropyl occupies a *pseudo*-equatorial position. Notably, this 6-isopropyl group is remote in space from the geminal dimethyl unit.

The solution conformation of **(100)** in $(CD_3)_2SO$ is similar, as shown by the ^1H NMR spectra. The ^3J coupling constants between the axial 8a-H and the 1-H protons are 11.7 Hz and 5.9 Hz. These are consistent with dihedral angles (8a-H)-(8a-C)-(1-C)-(1β-H) of 169° and (8a-H)-(8a-C)-(1-C)-(1α-H) of 41°. In this case, the coupling

between axial 6-H and the adjacent N-H is too small to be resolved; the dihedral angle in the crystal structure is 98°. The five-bond coupling $^5J = 1.2$ Hz was observed between the axial 8a-H and the axial 6-H, which again confirms the boat conformation in solution.[153] Looking at the conformation of the side-chain, a $^3J = 2.3$ Hz coupling is seen between 6-H and the adjacent Me$_2$CH. In the solid state, the corresponding dihedral angle is 70°.

The DKP (101) derived from L-Phe-R-dimethylthiazolidinecarboxylic acid was a gum and a crystal structure could not be determined. However, the ^{1}H NMR spectra in chloroform do give useful conformational information. The boat conformation of the DKP ring was confirmed by the presence of the five-bond coupling $^5J = 0.8$ Hz between the axial 8a-H and the axial 6-H.[153] Therefore, the PhCH$_2$ side-chain is in an equatorial position and is far from the geminal dimethyl unit. The thiazolidine is probably in the half-chair conformation, with a three-bond trans-diaxial coupling $^3J = 11.3$ Hz between 8a-H and one of the 1-H protons. The corresponding three-bond axial-equatorial coupling between 8a-H and the other 1-H is $^3J = 5.9$ Hz. A four-bond coupling $^4J = 1.6$ Hz is observed between 8a-H and NH; an identical coupling was seen for (99). The three-bond coupling constants from the Ph-CH$_2$ protons to the 6-H are $^3J = 10.2$ Hz and $^3J = 3.9$ Hz; thus the Ph cannot be antiperiplanar to the 6-H, as a coupling constant of 10.2 Hz is only consistent with antiperiplanar H—C—C—H. The phenyl is either orientated towards the nitrogen or towards the carbonyl oxygen. These data contrast with those for ditryptophenaline (vide supra), in which the two corresponding coupling constants between Ph-CH$_2$ and 6-H are $^3J = 4.4$ Hz and $^3J = 3.1$ Hz; these values are used to support a conformation with Ph located over the DKP ring.[153] However, the data for (101) are consistent with the X-ray structure-derived conformation reported for cyclo-L-Phe-L-Pro, in which the DKP is boat, CH$_2$Ph is equatorial and the phenyl is antiperiplanar to the carbonyl.[152]

No X-ray crystal structures were available for the other diasereoisomeric DKPs (108) and (109) but certain inferences can be drawn from NMR data. Most notable is the coupling of 6-H with the adjacent NH, with $^3J = 3.5$ Hz for (108) and with $^3J = 5$ Hz for (109). In the crystal structure of L,R diastereoisomer (100), the dihedral angle (7-H)-(7-N)-(6-C)-(CHMe$_2$) is 13°. Simple exchange of the hydrogen and isopropyl

groups at C-6 would give the new diastereoisomer. However, this would place the isopropyl *pseudo*-axial and the hydrogen *pseudo*-equatorial and give the (7-H)-(7-N)-(6-C)-(CHMe$_2$) dihedral angle as 13°; this is inconsistent with the coupling constant of 3.5 Hz. Consequently, the conformation of the DKP is unlikely to be boat but may be almost planar. Such planarity would relieve steric compression between the isopropyl groups and 8a-H. The flattening effect is less in (109) where the CH$_2$CHMe$_2$ group is less sterically demanding than the CHMe$_2$ of (108). With this flattening of the DKP, the side-chain is moved away from the geminal dimethyl unit.

3.4 Study on the rates of cyclisation of candidate molecular clips

The prodrug system comprises the polymer, the PSA-cleavable peptide, the molecular clip and the drug. Each of these components needs to be tested and optimised for efficiency independently (with the exception of the drug). In this section, the optimisation of the molecular clip will be discussed. Analysis has been conducted to evaluate the efficiency of cyclisation of the putative self-immolative molecular clips **(68)**, **(69)**, **(70)**, **(71)**, **(85)** and **(94)** to liberate the model drug **(Scheme 3.11)**. For each clip, the Boc protecting group of the precursor was removed with trifluoroacetic acid, giving the clip-drug units as their trifluoroacetate salts. In these salts, the amine nitrogen is protonated, preventing premature cyclisation. The salts were placed in aqueous buffers at three different pH values, generating the free amines. The rates of cyclisation and liberation of the model drug (2-(4-nitrophenyl)ethylamine) were determined by HPLC analysis.
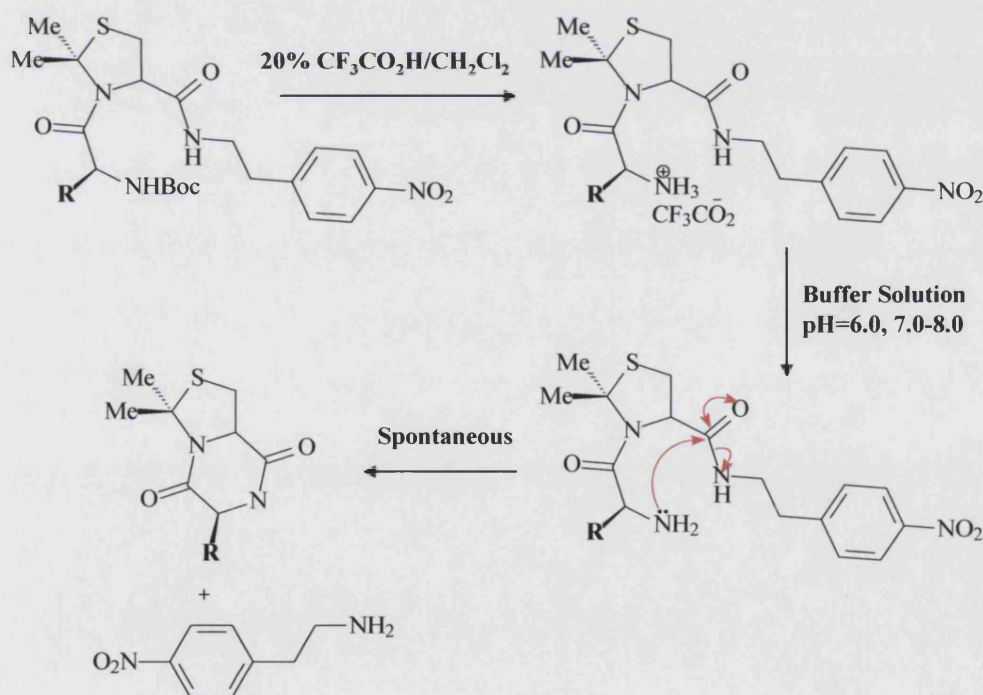
Scheme 3.11   Optimisation of aminoacyl dimethylthiazolidine molecular clip. (R = H (68), Me (69), Pr^i (70 and 85), CH$_2$Ph (71), CH$_2$Pr^i (94)).

3.4.1 Quantitation of the percentage of model drug (NPEA) released

The percentage was determined by calculating the ratio of the peak area of NH_2XMe_2Thiazolidine-NPEA at each defined time of the analysis with respect to the initial area at zero time. Representative graphs are provided to show the consistent decrease in the area of H_2NXaa-Me_2Thiazolidine-NPEA and increase in the area of DKPs and the model drug (NPEA). Results are reported as the time required for 50% of the drug to be released (half-life).

3.4.2 Results and discussion

The first fundamental step in the release study will be the analysis of the authentic diketopiperazines **(99)**, **(100)**, **(101)**, **(108)**, **(109)** and the model drug NPEA. The corresponding retention times (Rt) are shown in **(Table 3.1)**.
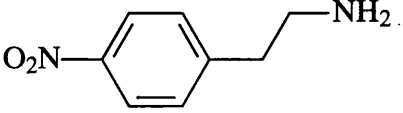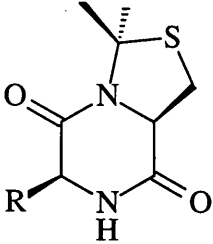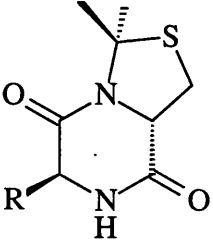
Standards	Derivatives (R)	Ret. Time (min), 37°C		
		pH 6.0	pH 7.0	pH 8.0
O_2N—⟨benzene⟩—CH₂CH₂—NH₂	(41)	3.7	3.9	4.2
[bicyclic thiazolidine-diketopiperazine structure with O, N, S, R', NH, O]	CH_3 (99)	4.9	4.9	4.9
	$CH(CH_3)_2$ (100)	7.8	7.6	7.9
	CH_2Ph (101)	12.3	12.9	12.5
[bicyclic thiazolidine-diketopiperazine structure with O, N, S, R', NH, O]	$CH(CH_3)_2$ (108)	6.9	6.7	7.0
	$CH_2CH(CH_3)_2$ (109)	10.9	10.9	11.1

Table 3.1 *HPLC analysis (monitored at 225 nm) at 37°C of the authentic diketopepirazines (97), (98), (99), (108) and (109) at pH 6.0, pH 7.0 and pH 8.0.*

As noted in **(Table 3.1)**, the retention times of all the authentic standards appear consistent. All DKPs have retention times which are independent of the pH (as expected for amides) and the NPEA has a slightly shorter retention time at low pH due to protonation. Further, the retention times of the $H_2NXaa-Me_2Thiazolidine-NPEA$ derivatives **(68)**, **(69)**, **(70)**, **(71)**, **(85)** and **(94)** were also measured **(Table 3.2)** These derivatives have a lower retention time at lower pH because of protonation. Interestingly, each of these derivatives has a retention time, which is different from the retention time of the analytes (DKPs and NPEA) of the cyclisation process.
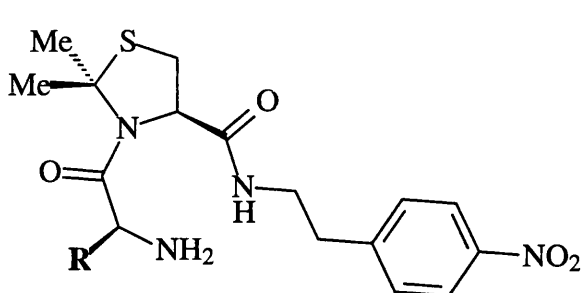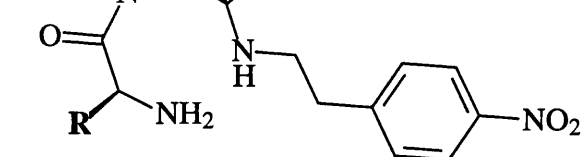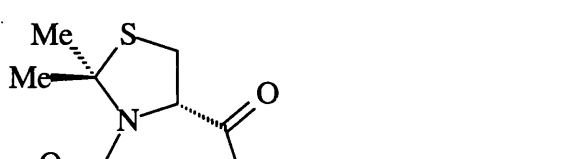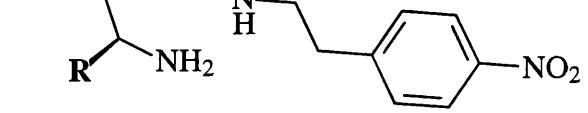
Aminoacyldimethylthiazolidine molecular clips	Derivatives (R)	Ret. Time (min), 37°C		
		pH 6.0	pH 7.0	pH 8.0
	H (68)	ND	7.2	7.5
	CH$_3$ (69)	ND	6.5	9.0
	CH(CH$_3$)$_2$ (70)	ND	13	17.5
	CH$_2$Ph (71)	ND	29.5	30.3
	CH(CH$_3$)$_2$ (85)	8.2	11.8	15.9
	CH$_2$CH(CH$_3$)$_2$ (94)	ND	17	22

Table 3.2   *HPLC analysis (monitored at 225 nm) at 37°C of the aminoacyl dimethylthiazolidinemolecular clips (68), (69), (70), (71), (85) and (94) at various pHs. ND (Not done).*

The rate of cyclisation and subsequent drug release was studied at three different pHs:

A   Release studies at pH 8.0

In this first set of experiments, the chemical cyclisation of compounds **(68)**, **(69)**, **(70)**, **(71)**, **(85)** and **(94)** was studied at pH 8.0 (37°C) where the release rate is predicted to be maximal, as the proportion of unprotonated nucleophilic amine should be higher at this pH than at the lower pH values. The progress of the cyclisations was monitored by decreases in the peaks corresponding to the starting materials and increases in the peaks corresponding to the DKP and NPEA products. In all cases, the formations of the products corresponded to the consumption of the starting material since no by-products or intermediates were detected. It is noteworthy that each experiment has been repeated twice and the chromatograms were monitored at 225 nm and 275 nm in order to follow the DKPs and NPEA, respectively. The results are presented in the following figures.
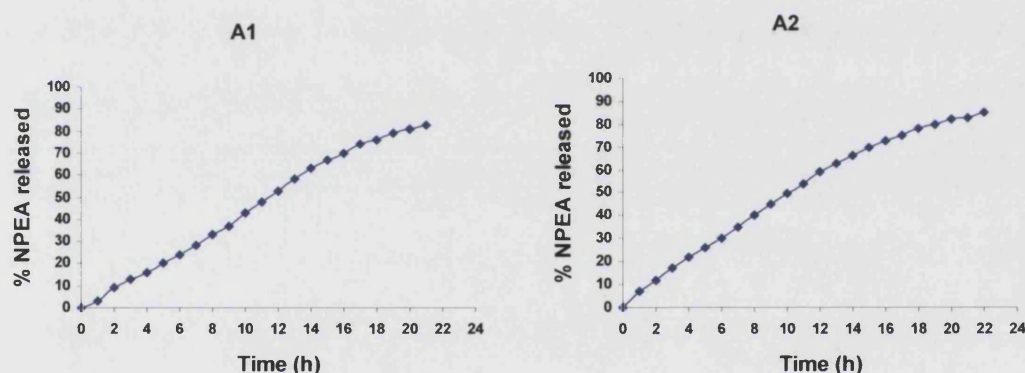
Figure 3.25   *Time courses of chemical cyclisation of compound (68) at pH 8.0 (37°C) of the two trials, as monitored by consumption of the starting material.*

98

A2
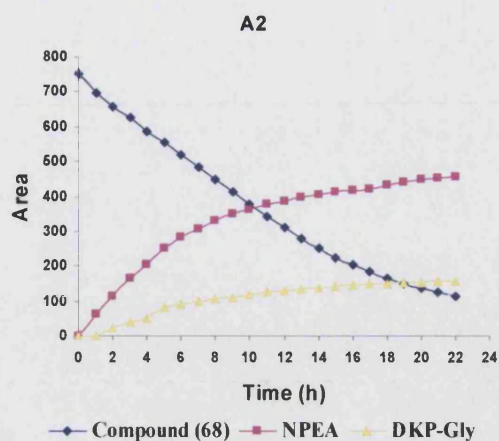
Figure 3.26 *A plot of the time versus area of compound (68) and the analytes L-Gly-derived DKP and the model drug NPEA (41) at pH 8.0 (37°C) of trial A₂.*

B1   **B2**
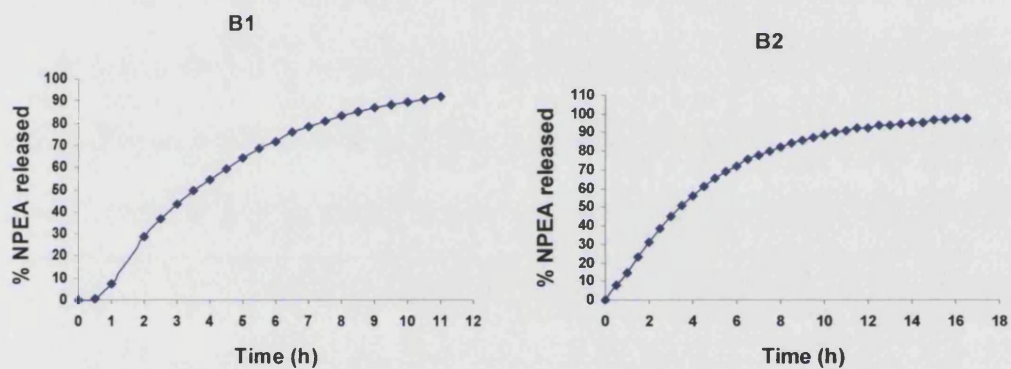
Figure 3.27 *Time courses of chemical cyclisation of compound (69) at pH 8.0 (37°C) of the two trials, as monitored by consumption of the starting material.*

B1   **B2**
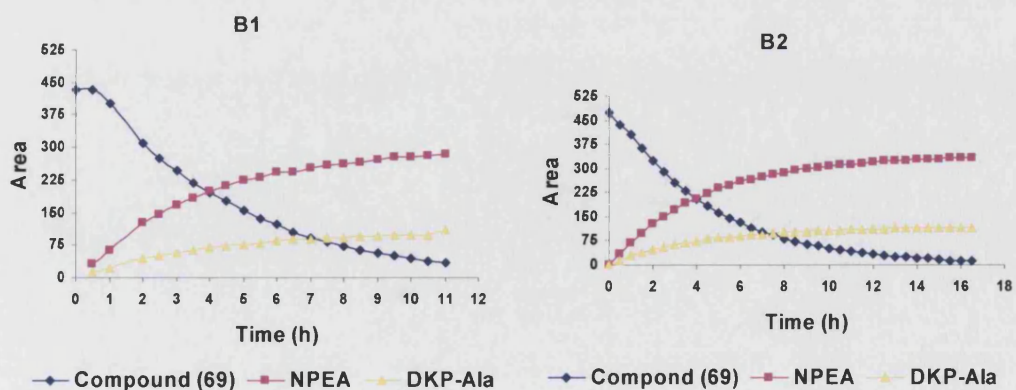
Figure 3.28 *A plot of the time versus area of compound (69) and the analytes L-Gly-derived DKP and the model drug NPEA (41) at pH 8.0 (37°C) of trial B₁and B₂.*
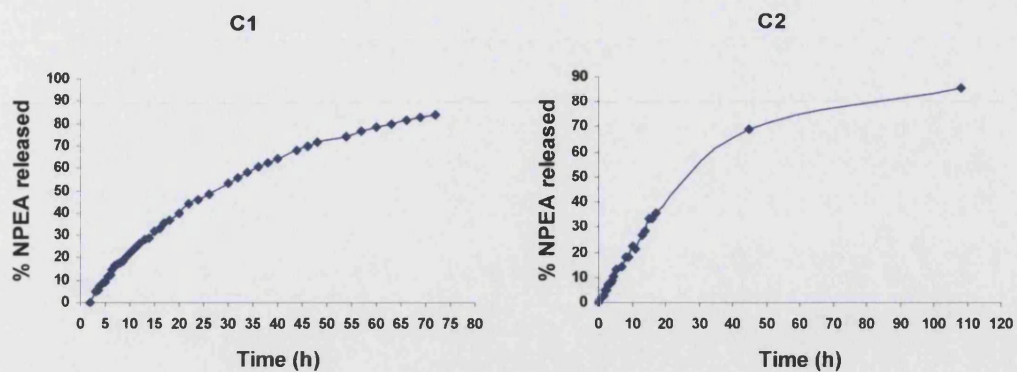
Figure 3.29 *Time courses of chemical cyclisation of compound (70) at pH 8.0 (37°C) of the two trials, as monitored by consumption of the starting material.*
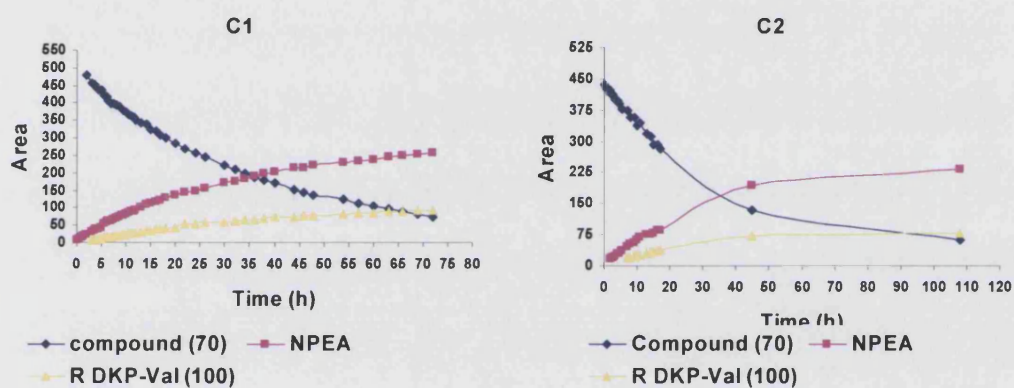
Figure 3.30 *A plot of the time versus area of compound (70) and the analytes L-Val-derived R DKP (100) and the model drug NPEA (41) at pH 8.0 (37°C) of trial C_1 and C_2.*
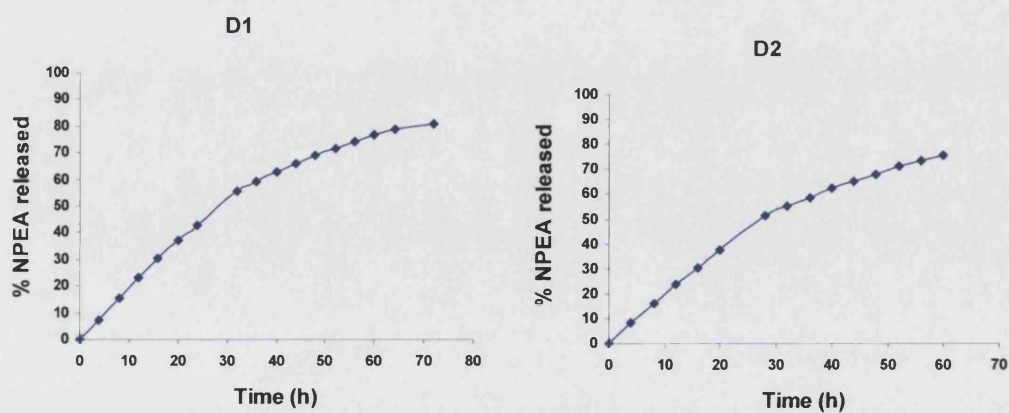
Figure 3.31 *Time courses of chemical cyclisation of compound (71) at pH 8.0 (37°C) of the two trials, as monitored by consumption of the starting material.*

100
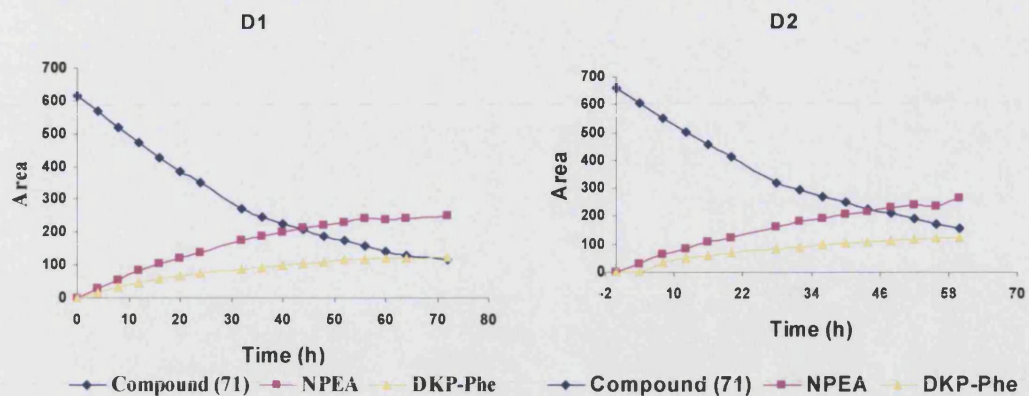
Figure 3.32 *A plot of the time versus area of compound **(71)** and the analytes L-Phe-derived DKP **(101)** and the model drug NPEA **(41)** at pH 8.0 (37°C) of trial D₁ and D₂.*
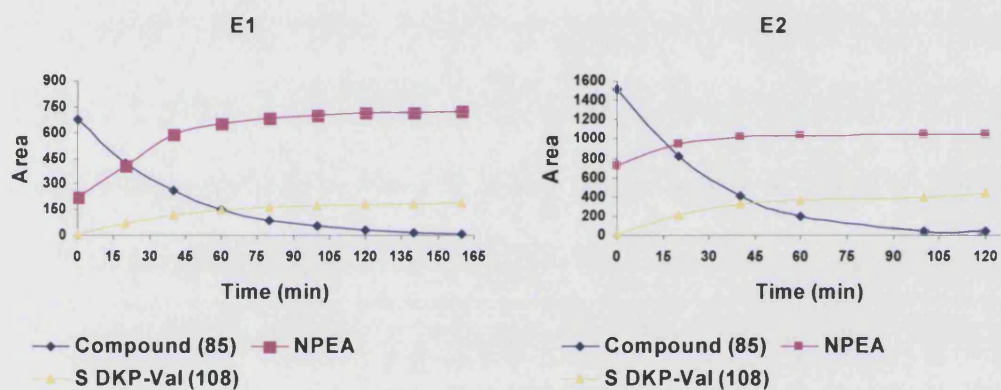
Figure 3.33 *A plot of the time versus area of compound **(85)** and the analytes L-Val-derived S DKP **(108)** and the model drug NPEA **(42)** at pH 8.0 (37°C) of trial E₁ and E₂.*
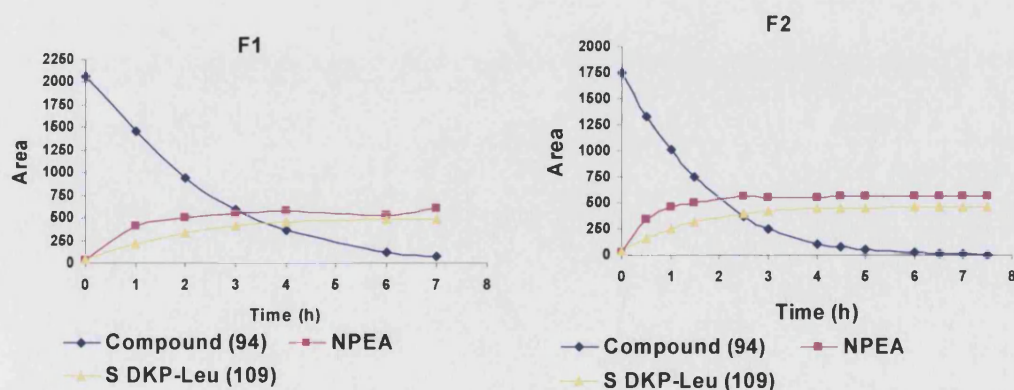
Figure 3.34 *A plot of the time versus area of compound **(94)** and the analytes L-Leu-derived DKP **(109)** and the model drug NPEA **(41)** at pH 8.0 (37°C) of trial F₁ and F₂.*

101

Since the reactions of compounds **(85)** and **(94)** are fast, some drug release has already occurred at the time required for the assay of the sample injected at "zero time". However, estimation can be done. The corresponding $t_{1/2}$ of all **NH₂XaaMe₂Thiazolidine-NPEA** derivatives at pH 8.0 will be summarised in **(Table 3.3)**.

B   *Release studies at pH 7.0*

In this second set of experiments, the chemical intramolecular cyclisation of compounds **(68)**, **(69)**, **(70)**, **(71)**, **(85)** and **(94)** was studied at pH 7.0, 37°C (mimicking the physiological pH). The percentage of NPEA released was calculated and the $t_{1/2}$ was determined. The following **figures 3.35**, **3.36**, **3.37**, **3.38** and **3.39** represent the graphic data corresponding to compounds **(68)**, **(69)**, **(70)**, **(85)** and **(94)** respectively.
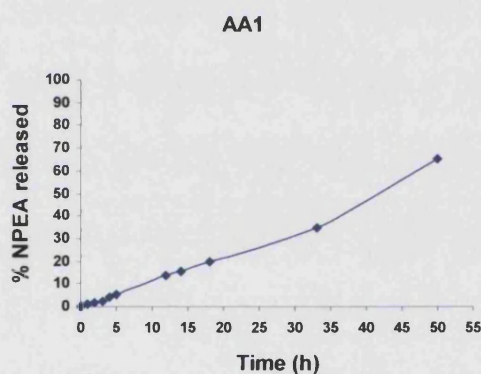
Figure 3.35   *Time courses of chemical cyclisation of compound* ***(68)*** *at pH 7.0 (37°C) of the two trials, as monitored by consumption of the starting material.*
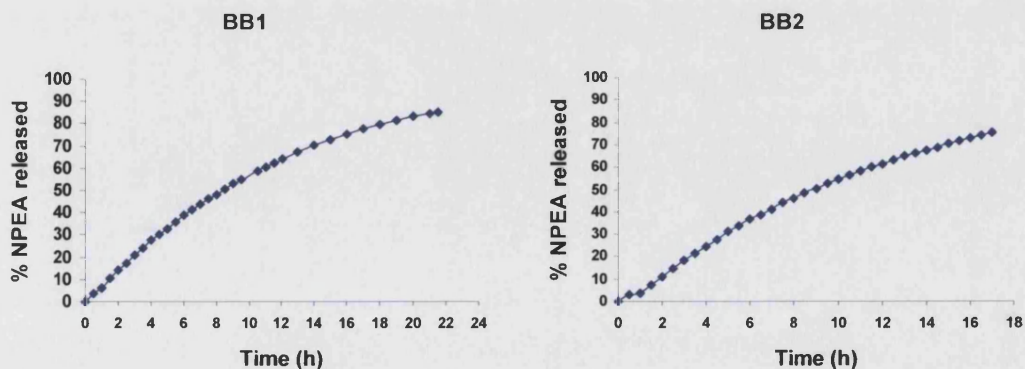
Figure 3.36   *Time courses of chemical cyclisation of compound* ***(69)*** *at pH 7.0 (37°C) of the two trials, as monitored by consumption of the starting material.*

102
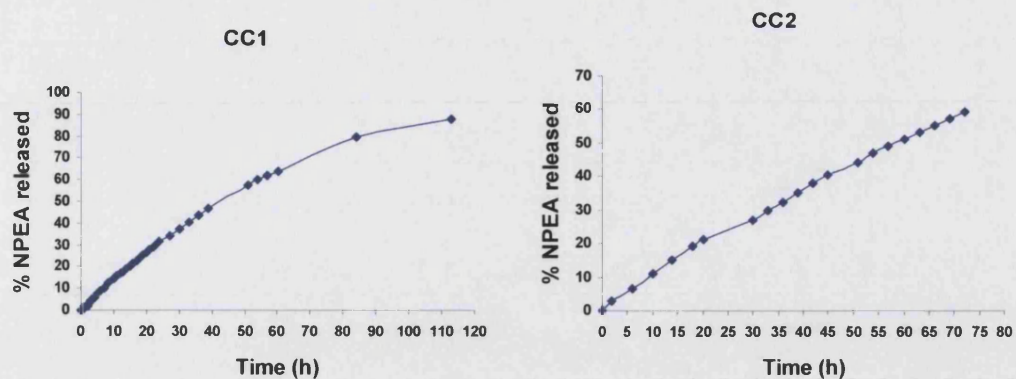
Figure 3.37 *Time courses of chemical cyclisation of compound* ***(70)*** *at pH 7.0 (37°C) of the two trials, as monitored by consumption of the starting material.*
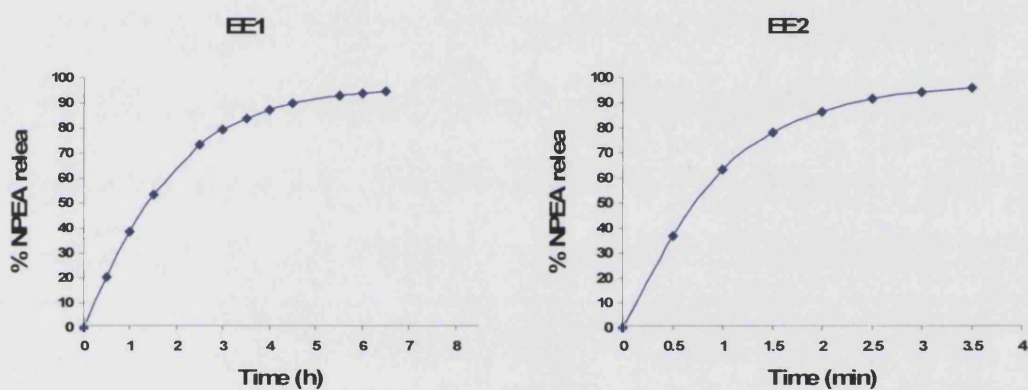
Figure 3.38 *Time courses of chemical cyclisation of compound* ***(85)*** *at pH 7.0 (37°C) of the two trials, as monitored by consumption of the starting material.*
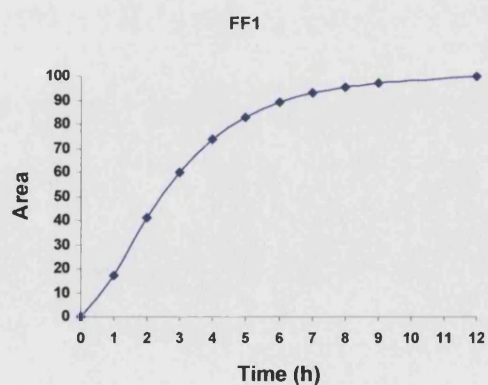
Figure 3.39 *Time courses of chemical cyclisation of compound* ***(94)*** *at pH 7.0 (37°C) of the two trials, as monitored by consumption of the starting material.*

C   *Release studies at pH 6.0*

At this pH, only compound **(85)** was studied, since this is the compound which cyclised most rapidly at the other pH values. The graphic results are presented in **Figures 3.40**.
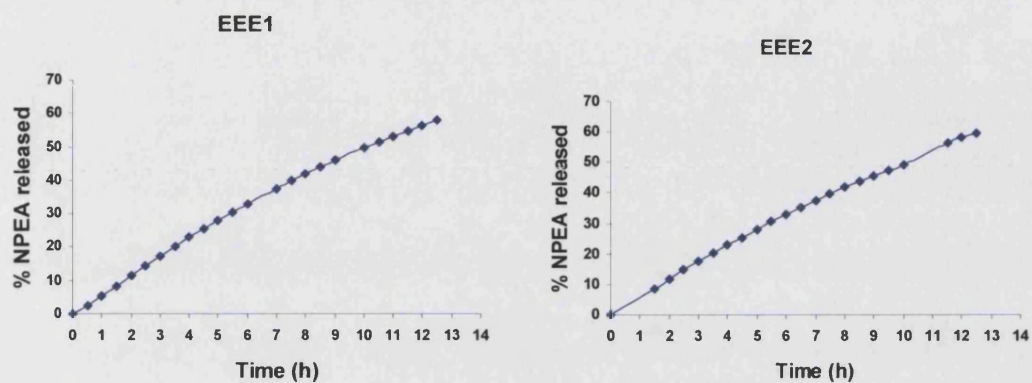
Figure 3.40   *Time courses of chemical cyclisation of compound* ***(85)*** *at pH 6.0 (37°C) of the two trials, as monitored by consumption of the starting material.*
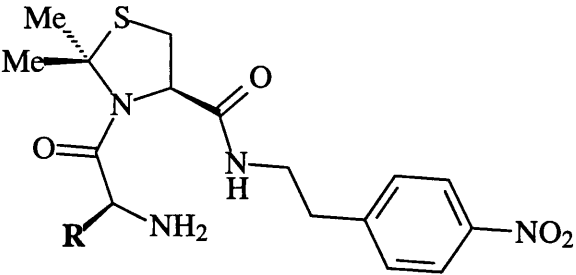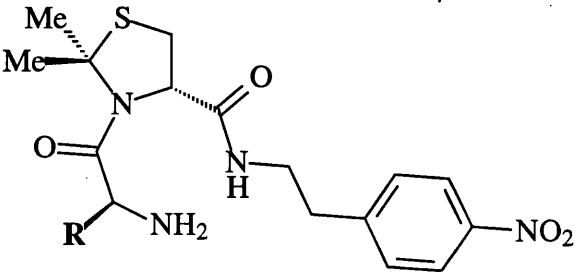
Aminoacyldimethylthiazolidine molecular clips	Derivatives (R)	Approx. half lives (t½), 37°C		
		pH 8.0	pH 7.0	pH 6.0
	H (68)	10-11 h	42 h	ND
	CH₃ (69)	3-4 h	8-9	ND
	CH(CH₃)₂ (70)	26-27 h	~ 45 h	ND
	CH₂Ph (71)	28-29 h	ND	ND
	CH(CH₃)₂ (85)	15-20 min	45-75 min	10 h
	CH₂CH(CH₃)₂ (94)	60-90 min	2.5 h	ND

Table 3.3   *The approximate times required for 50% of the molecular clips to cyclise and release 50% of the model drug (t½) at various pH values in phosphate buffer-acetonitrile mixture.*

The results presented in (Table 3.3) indicate the effect of the size of the side-chain and the relative configuration on the rate of DKP formation and liberation of the model drug (NPEA). In the design of the molecular clip, the side-chain R group of the terminal amino acid is designed to clash sterically with the geminal 2,2-dimethyl moiety of the thiazolidine ring, thus forcing the clip into 100% cis (Z) amide conformation (Scheme

3.12). Consequently, DKP formation and drug expulsion would be enhanced. As a result, one might expect that compounds with more bulky R group would cyclise more quickly. However, on the contrary, the cyclisation process was found to be slower for the L-aminoacyl-*R*-thiazolidines with bulky side-chains. Examination of the X-ray crystallographic structures of the DKPs derived from L-Ala **(99)** and L-Val **(100)** in the previous section **(3.3)** helped in the explanation of these results.

The mechanism of DKP formation is suggested in **(Scheme 3.12)**. As one might expect, as the size of the R group of the amino-acids increases, the equilibrium between the two amide conformations *Z* **(110)** and *E* **(111)** will be in favour of the *Z* conformer **(110)**. Conformer **(112)** is also disfavoured due the steric clash between the R group and the drug. In compound **(110)**, the amino group is pointed towards the carbonyl atom promoting cyclisation through formation of the tetrahedral intermediate **(113)**. This then eliminates the model drug R`NH$_2$ to give the DKP **(114)**. The question arises of which step is rate-determining.
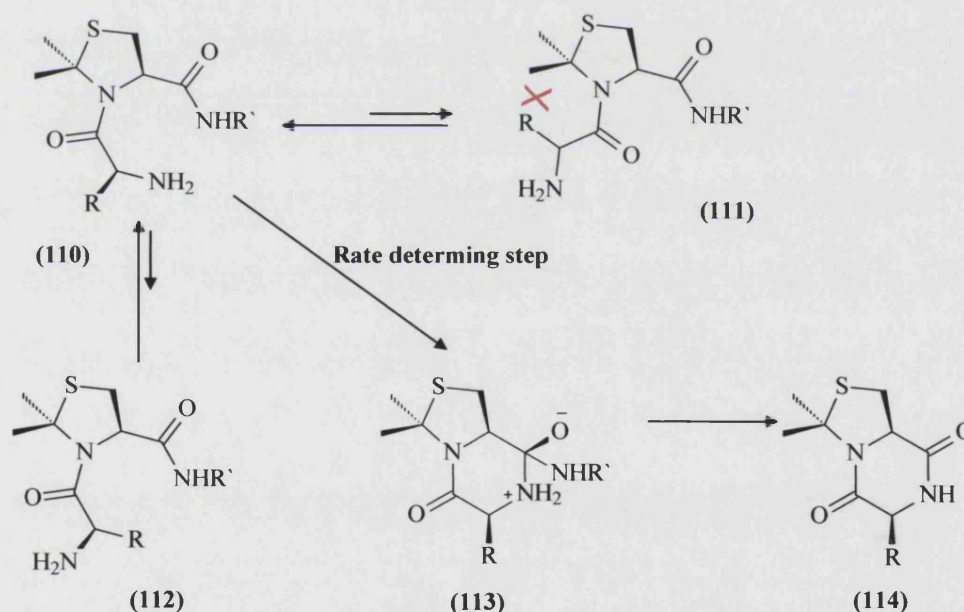
Scheme 3.12 *Mechanism of DKP formation (R= H, Me, Pr^i, CH$_2$Ph and CH$_2$Pr^i, R`= NPEA).*

The intermediate **(113)** is expected to have a twisted-chair conformation due to the presence of four sp^3 and two contiguous sp^2 hybridised atoms. In this twisted-chair conformation, the R group in the L,*R* diastereoisomers **(68)**, **(69)**, **(70)** and **(71)** will be pointed upward and thus clash sterically with the "up" methyl group of the geminal

106

dimethyl unit. Thus, if the formation of (113) is rate-determining, increase of the bulk of R will slow the overall reaction. This is the rank order observed. Therefore, the formation of (113) is suggested to be rate-determining. However, on the other hand, in the L,S diastereoisomers (85) and (94), the R group will be pointed downward and thus no steric clash will exist with either of the geminal dimethyls; as a result, the rate of cyclization will be faster. In the L,R diastereoisomers, the rate of DKP formation increases as the size of the side-chain R group decreases. Interestingly, the rate of DKP formation is faster in the L,S diastereoisomer as the R group of the side chain was more locally bulky (Val vs. Leu). The origin of this effect is not clear, as the R group is far from the geminal dimethyls in the intermediate but it may be connected with the proportion of the reactive Z-amide conformer of the starting material.

As shown in the X-ray crystallographic study, the L,R DKPs exist in a flattened boat conformation, having two sp^3 atoms separating two sets of two trigonal sp^2 atoms. In this conformation, the side-chain R is far from the geminal dimethyls, so the effect of steric bulk should be insignificant in the final elimination step leading to the DKP. Within the set of L,R compounds, the bulk of the R group has a profound effect on reaction rate, so the final elimination step cannot be rate-determining. However, structures of the DKPs of the L,S diastereoisomers were not available but the ring is proposed to be almost planar (vide supra). This planarity again places the R group far from the geminal dimethyls, so the final elimination step is again unlikely be rate-determining.

A study of the effects of pH, buffer and temperature on the cyclisation reaction of Ala-Pro-NH$_2$ to the cyclo-AlaPro DKP has been reported.[121] The effect of the size of the R group was not studied. This report is more relevant to the present study, as the leaving group is an amine (ammonia), unlike many studies on DKP formation[70,118] where the leaving group is oxygen-based and consequently a better leaving group. In Ala-Pro-NH$_2$, the Pro ensured a sufficiently high cyclisation rate at all pHs. Capasso et al[121] considered parallel routes in which the intermediates differed in their protonation status at the heteroatoms concerned. The balance between the different pathways therefore depended on the pH of the solution and affected which step was rate-determining. Interestingly, only effects on steps after the formation of intermediates corresponding to (113) were considered. However, in our study, the side-chains R had a profound effect

on the overall rate and this steric effect could only be exerted on the initial cyclisation step forming intermediate **(113)**.

As a conclusion, increasing the size of R group in the L,*R* diastereoisomers would, on one hand, shift the equilibrium between the two conformations (*Z* and *E*) towards the energetically favourable *Z* conformation **(110)** and, on the other hand, slow the rate-determining step in DKP formation. In the other diastereoisomeric L,*S* series, a bulky R group would shift the conformational equilibrium in the starting material towards *Z* but not as effectively as in the L,*R* series. However, in this series, comparison of the rates of cyclisation of **(85)**, **(94)** and **(68)** (as could also be considered as a member of both series with R = H) shows that cyclisation is faster with more bulky R groups. Since the R group is equatorial in the intermediate and is far from the geminal dimethyl in the DKP, the *E* → *Z* interconversion may now be rate-limiting. Alternatively, large R may influence the relative energies of the conformations around the carbonyl—C_α bond so that the reacting conformer with NH_2 pointed towards the secondary amide electrophile is more accessible with large R.

It is noteworthy that with the change of the pH from 8.0 to 7.0, the half-lives of the cyclisations increased by 2-4 fold. This is due to the presence of the equilibrium between the protonated and the unprotonated forms of the primary amine. The pK_a of AlaProNH$_2$ is 7.8;[121] the pK_a of these molecular clips should be similar. This pK_a is within the pH range studied. At the three different pH values studied, the degree of protonation will vary markedly, consequently affecting the overall rate of cyclisation. At pH 6.0, where the amino group is highly protonated, the rate should be much slower, as seen with compound **(85)** (pH 8.0 $t_{1/2}$ = 15 min; pH 7.0 $t_{1/2}$ = 45 min; pH 6.0 $t_{1/2}$ = 10 h) **(Table3.3)**.

3.5   Synthesis of the PSA-cleavable peptide linker

The HPLC study on the relative rates of DKP formation and expulsion of the model drug in the previous section showed that the clip derived from L-Val and S-dimethylthiazolidine cyclised most rapidly. Thus, this clip was chosen for studies on development of the PSA-cleavable peptide linker.

Following optimisation of the self-immolative molecular clip, the synthesis of PSA-cleavable peptide linker is the next target. On the basis of the literature,[114] two peptide sequences SSKLQ and SKLQ will be synthesised and examined. Since the HPLC study highlighted the fact that the DKP formation from (85) was very rapid under basic conditions, this compound could not be used as a synthetic intermediate for acylation with activated amino-acids or peptides. (Scheme 3.13)
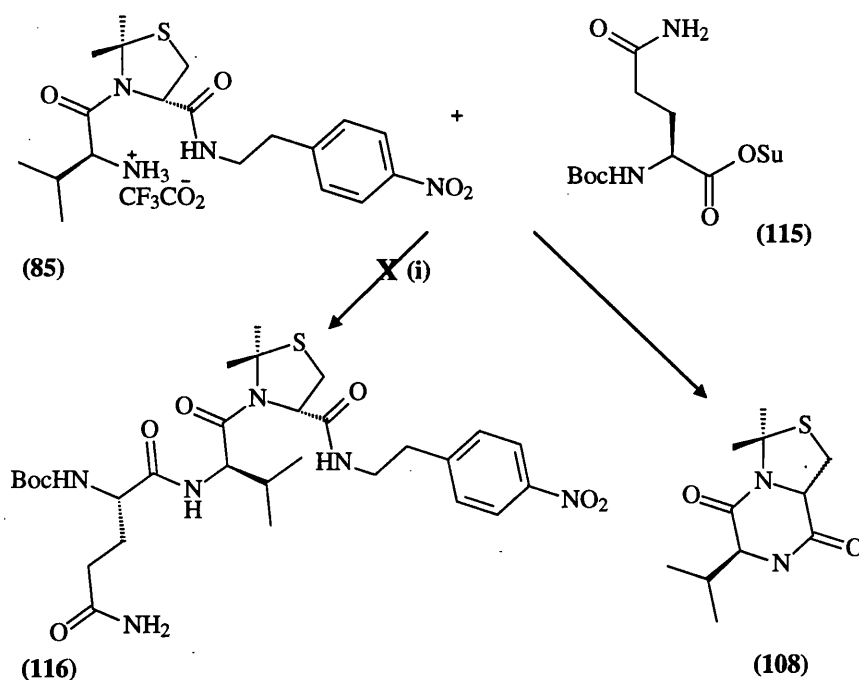
Scheme 3.13   Proposed route towards the synthesis of compound (116). (i) Et_3N, CH_2Cl_2.

Since it is the dimethylthiazolidine that is driving the rapid cyclisation and DKP formation, a series of experiments was conducted to test whether it would be possible to construct a peptide containing D-Cys and later build the thiazolidine ring.

Generally speaking, ψPro derivatives are used as temporary protecting groups in peptide synthesis. It has been reported that coupling of amino-acid derivatives to a growing peptide chain containing N-terminal serine-derived oxazolidine (Ser^{ox}) or threonine-derived oxazolidine (Thr^{ox}) results in low reaction yields. Consequently, the pre-formation of ψPro-containing dipeptides is readily accomplished by *in situ* N-acylation with amino acid halides or N-carboxyanhydrides (**Route B, Scheme 3.1**). Interestingly, successful acid-catalyzed oxazolidine ring formation was achieved by the reaction of N-protected dipeptide derivatives (**117**) with 2,2-dimethoxypropane (DMP) upon refluxing (**Scheme 3.14**). Furthermore, it is noteworthy that racemization sometimes observed in the coupling of peptide derivatives, is suppressed by the presence of this ring system.[133] Notably no thiazolidine ring formation from Aaa-Cys dipeptides has been reported.
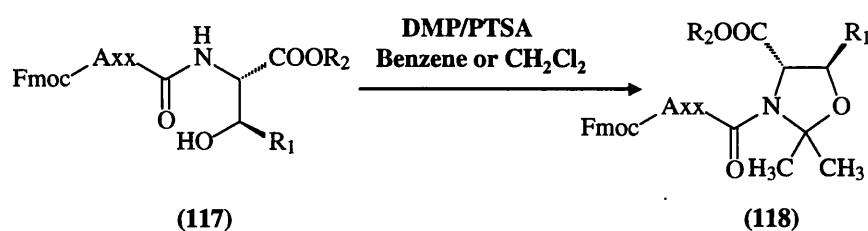
Scheme 3.14 Oxazolidine formation in dipeptide derivatives (R_1 = H, CH_3; R_2 = H, CH_3, allyl, succinimide; Axx = Ala, Val).

Consequently, the strategy now was to gain advantage of the possible recyclisation of the cysteine moiety to the thiazolidine ring. A model experiment using glutathione (GSH), which is a tripeptide composed of glutamate, cysteine and glycine was executed. The rationale of this experiment is to set up the conditions required for ring-closure of a cysteine moiety incorporated into a peptide chain (**Scheme 3.15**). Glutathione (**119**) was esterified with methanol in the presence of hydrogen chloride. Evaporation afforded crude (**120**). Consequent simultaneous protection of the thiol and amine moieties with benzoyl groups was an attractive proposition because of the ability of selective S-deprotection.[154] Benzoylation of (**120**) was attempted by stirring with benzoyl chloride in the presence of excess triethylamine in dichloromethane. Recrystallisation afforded pure (**121**) as a white solid in 20% yield.

(119) (120)

(i)

(ii)

(121)

(iii)

(122)

(iv)

(123)
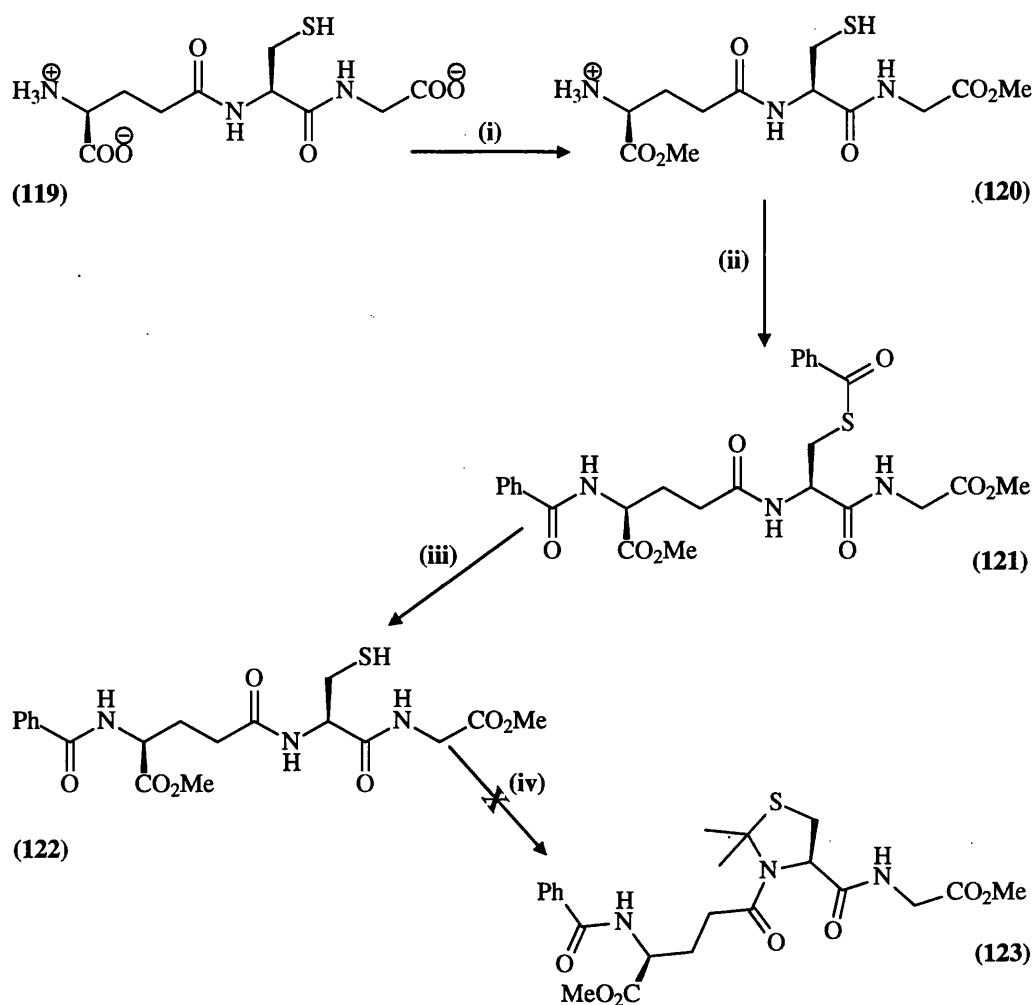
Scheme 3.15 *Proposed route toward the chemical synthesis of compound (123). (i) HCl, MeOH; (ii) PhCOCl, Et₃N, CH₂Cl₂; (iii) MeOH, 30°C, 48 h; (iv) (CH₃)₂CO, DMP, PTSA or TOSEC, DMAP.*

Selective deprotection of the benzoyl thioester was attained by methanolysis upon stirring with methanol in the presence of triethyamine. Evaporation and recrystallisation afforded (122) as a white solid in 57% yield. All attempts of cyclocondensation failed. Several attempts by refluxing with acetone in the presence of 2,2-dimethoxypropane, toluenesulfonic acid as an acid catalyst for different times were unsuccessful to drive the cyclisation process. The product was usually identified by ^{1}H NMR to be the starting material. Mass spectrometry suggested that some of the disulfide (m/z 877 for M + H) may have been formed. So far, no clue was known for the obstruction of the cyclisation process.

An alternative cysteine-containing unit with amide bonds on the N- and C- terminals was also studied. Three pathways were investigated to synthesise compounds of this type (**Scheme 3.16, 3.17, 3.18**). The principle of the three pathways starts with the use of cystine, in which the S-S bridge linkage can be cleaved later on to yield the corresponding cysteine moieties.
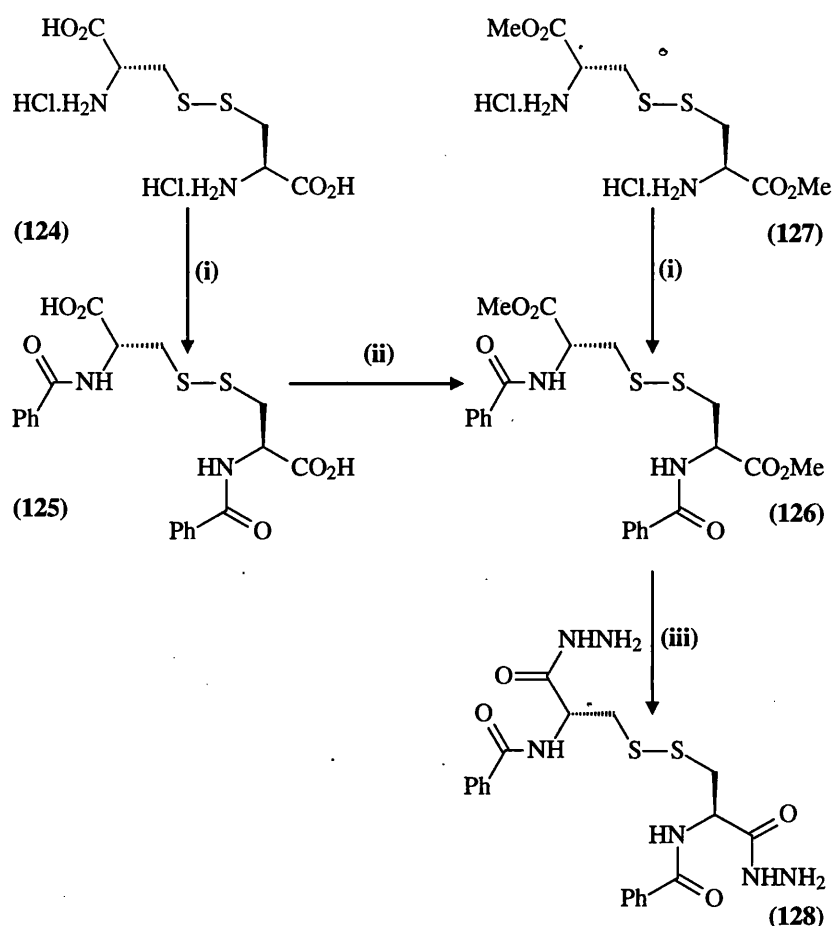
Scheme 3.16 *Different routes towards the chemical synthesis of (128). (i) PhCOCl, aq. NaOH; (ii) H₂SO₄, MeOH; (iii) NH₂NH₂, MeOH.*

On the basis of (**Scheme 3.16**), benzoylation of L-cystine (**124**)[155] with benzoyl chloride under Schotten-Baumann conditions afforded (**125**) in 54% yield. The ^{1}H NMR spectrum indicates the presence of one signal for the two cysteine moieties in cystine, due to the symmetry of the compound. Consequent esterfication of (**125**) by boiling with sulphuric acid in methanol afforded (**126**) in a quantitative yield. It is noteworthy that compound (**126**) can be synthesised directly from L-cystine dimethyl ester dihydrochloride (**127**) in 67% yield, which is higher than that of the two-step synthesis process. Reaction of (**126**) with hydrazine hydrate[156] in methanol for 16 h afforded (**128**) in 60% yield. The hydrazides formed could have been converted to the corresponding acyl azides for coupling with amine

Pathway A
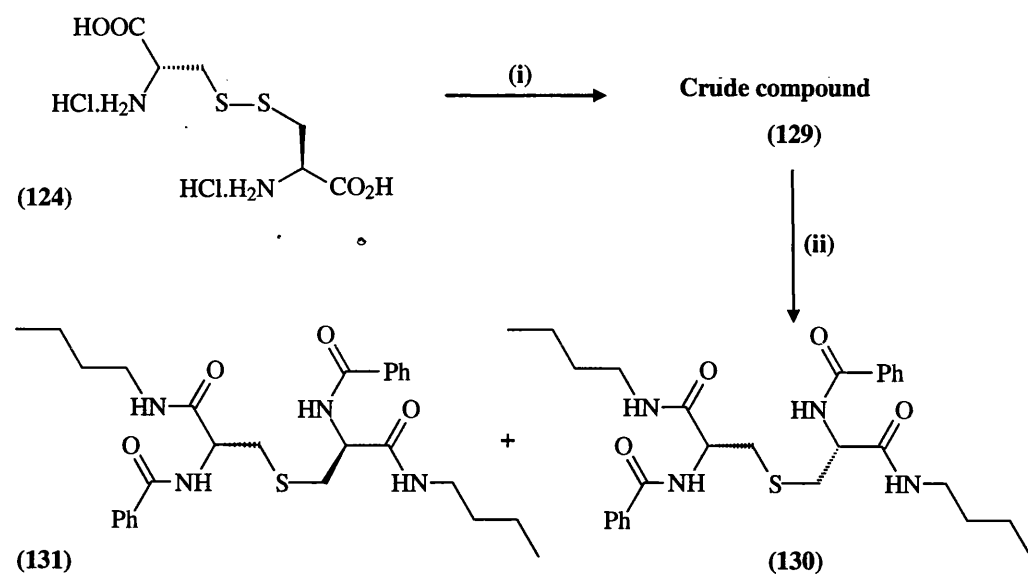
Pathway B
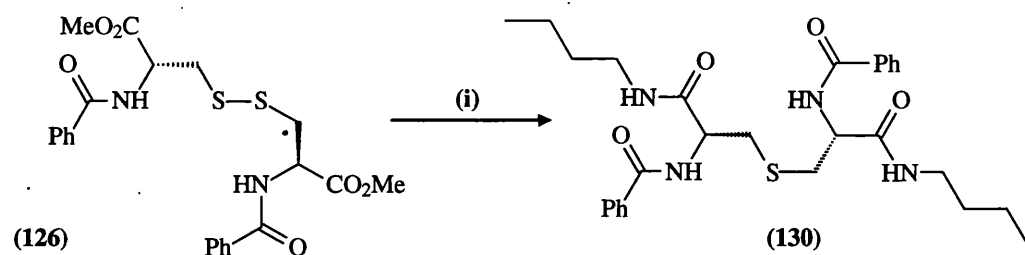
Scheme 3.17 *Two different approaches for the synthesis of (130). (i) 1- BuNH$_2$, -78°C, 2-reflux for 5 h; (ii) aq. NaOAc, Et$_2$O, PhCOCl, 0°C, 4 h.*

On the basis of **(Pathway A, Scheme 3.17)**, L-cystine **(124)** was boiled under reflux with butylamine for 5 h and afforded crude mixture **(129)**.[155,157] Benzoylation of crude **(129)** with benzoyl chloride afforded two diastereoisomers **(130)** and **(131)**. The ^{1}H NMR spectra of each of these compounds confirmed the presence of the benzoyl group, the butylamide and the cysteine. In these spectra, the characteristic differential signal was corresponding to the Cys β–H protons, which is presented as a pair of double doublets for compound **(130)** and a single doublet for **(131)**. Surprisingly, mass spectroscopy showed these compounds to contain only one sulfur per two amino-acid units. Compound **(131)** also showed $[\alpha]_D^{20}$ + 0.0° (c 0.003, CHCl$_3$), which is consistent with a meso stereoisomer. The structures **(130)** and **(131)** are therefore proposed for these compounds.

However, it has been reported that disulfides undergo facile monodesulfurisation on treatment with an aminophosphine.[158] This desulfurisation process is stereospecific in that inversion of configuration occurs at one of the carbon atoms α to the disulfide group. However, since the diastereomeric products are formed in similar amounts, a different mechanism is likely (**Scheme 3.17**). Elimination of RSS⁻ would give N-benzoyldehydroalanine N-butylamide. RSS⁻ would then lose one sulfur to give the thiolate which attacks the dehydroalanine in a Michael reaction. Since the Michael electrophile is achiral, the addition will give equal amounts of the *R,S* and *R,R* isomers.

We were, however, surprised to encounter that the straightforward acylation process of (**126**) by dissolving in anhydrous butylamine at -78°C and boiling under reflux for 5 h, resulting in the isolation of solely one diastereoisomer (**130**) in 8% yield (**Pathway B, Scheme 3.17**).
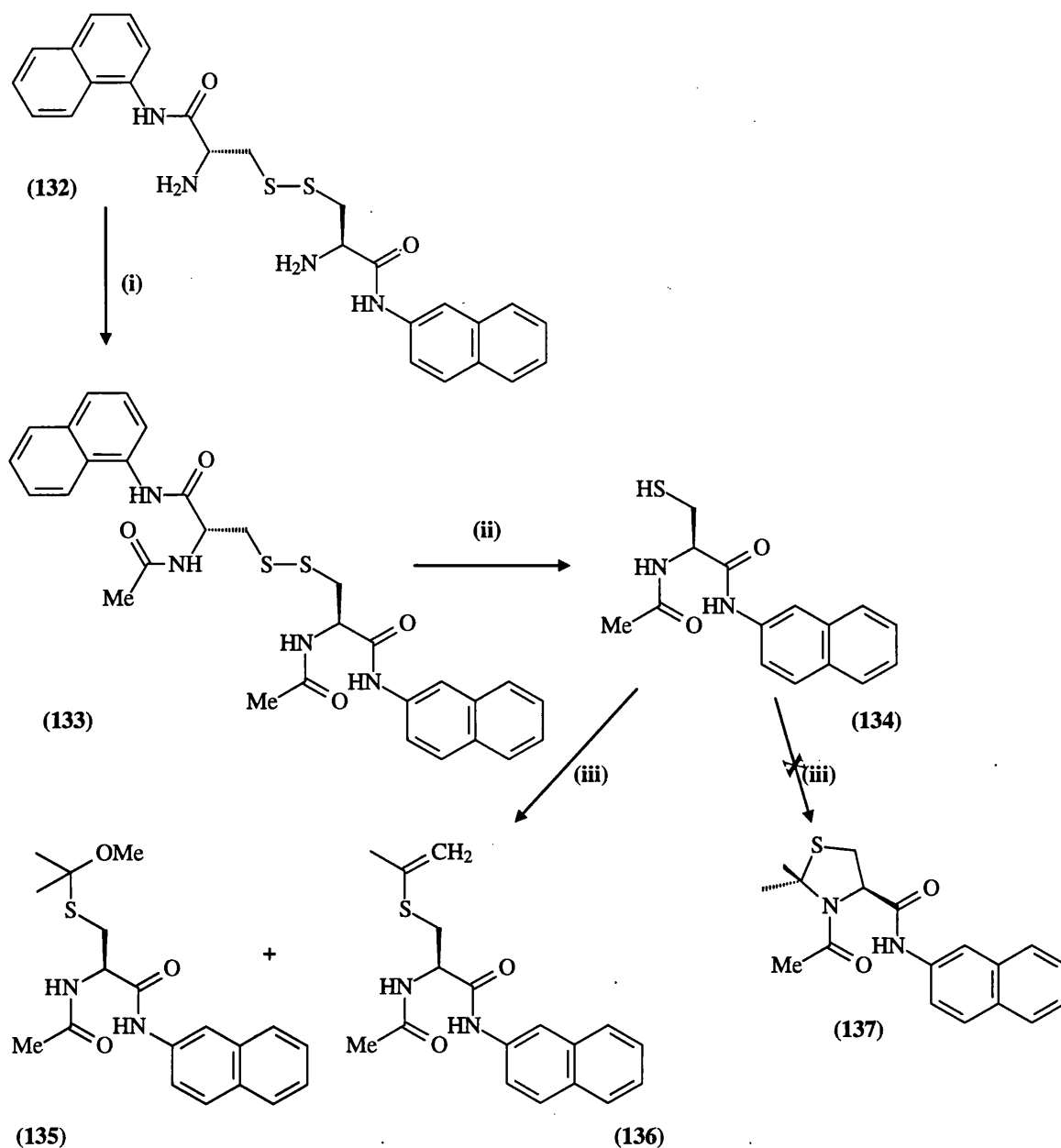
Scheme 3.18 *Proposed chemical approach for the synthesis of (137).(i) Ac₂O, Et₃N; (ii) propane-1,3-dithiol, Pr^{i}₂NEt, THF; (iii) (CH₃)₂CO, DMP, PTSA, CH₂Cl₂.*

An alternative method was based on the use of the highly expensive commercially available L,L-cystine bis(naphth-2-yl)amide **(132).** This compound was acetylated with acetic anhydride and afforded **(133)** in 92% yield as a white solid. This approach is very convenient because the structure is confirmed and fulfils the required features, being now appropriately modified on both the C- and N- terminals. Compound **(133)** was cleaved swiftly to **(134)** with excess propane-1,3-dithiol[159] in THF. The rate of the process was considerably enhanced by the addition of a hindered tertiary amine (Pr^{i}₂NEt), which aids in an intermediate formation of

the appropriate thiolate anions. The by-product, 1,2-dithiacyclopentane, has been reported[160] to be unstable and to give rise to intractable insoluble polymers. Cyclocondensation of (134) was attempted by refluxing with acetone in the presence of 2,2-dimethoxypropane and toluenesulfonic acid or BF_3 as an acid catalyst. None of the desired compound (137) was formed. The products identified by ^1H NMR were the monothioacetal (135) and the thioenol ether (136), both potential intermediates in the desired process. It may be possible to rationalise such results on the basis of lack of nucleophilicity of the amide.

As a conclusion, the concept of constructing a peptide sequence in which cysteine moiety is at the penultimate position with the drug attached, followed by cyclocondensation to form the thiazolidine ring, proved to be unsuccessful. So, an alternative approach should be considered.

The new approach will be based on the successful constructing of the aminoacyl-Me_2Thiazolidine unit (Scheme 3.19). In this suggested route, acidolysis of (82) will be performed with trifluoroacetic acid in dichloromethane to afford (138). The latter would subsequently be coupled with BocGlnOPFP to afford (139). The rationale of this pathway is based on the stability of the carboxylic acid functionality toward any nucleophilic attack relative to the pentafluorophenyl active esters which proved to undergo · spontaneous intramolecular cyclization to the DKP following the deprotection process. However, an unexpected cyclisation took place in the deprotection reaction, forming the DKP (108).
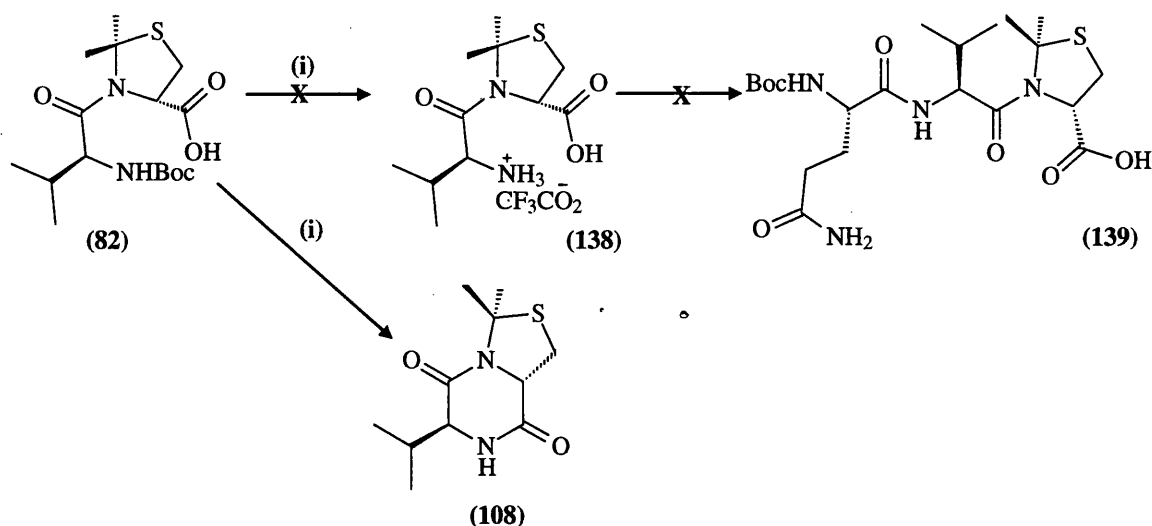
Scheme 3.19 *Proposed chemical approach for the synthesis of (138). (i) 20% CF_3CO_2H / CH_2Cl_2.*

So far, the strategy has been to synthesise the clip or clip-drug units, then to attach the peptide. A new strategy was investigated in which dipeptides or oligopeptides are attached to the dimethylthiaproline, avoiding intermediates which may form DKPs. Direct coupling of the heptapeptide Ac-Hyp-Ser-Ser-Chg-Gln-Ser-Ser-OH with 4-O-prolyl ester of dAc-VIN was reported **(Scheme 1.3)**; however, the preceding experiment **(Scheme 3.2)** proves that amino-acyl coupling of compound **(51)** resulted in ring-opening. This, in turn will prohibit the possibility of initial drug and subsequent amino acid coupling to the Me2ThPro moiety.

Alternatively, a new strategy based upon the method of coupling dipeptide acid fluorides to Me2Thiazolidine unit was attempted. The rationale of this tactic is based upon barring the intramolecular cyclisation process by insertion of an amino acid moiety between the nucleophilic N and the electrophilic carbonyl moiety **(Scheme 3.20)**. Generally speaking, dipeptide acid fluorides coupling were not reported at the time of the experiment. However, very recently, Carpino *et al.*[161] have reported a new method for dipeptide acid fluoride generation and utilisation in the segment coupling process. It is noteworthy that the acid fluoride of side-chain-unprotected Gln-containing dipeptides was not reported. On the other hand, synthesis of acid fluorides of trityl-side-chain-protected Gln-containing dipeptides proved to be successful. The rationale of this route was based on the advantage of reactive acid fluorides coupling with the hindered Me2thiazolidine unit.
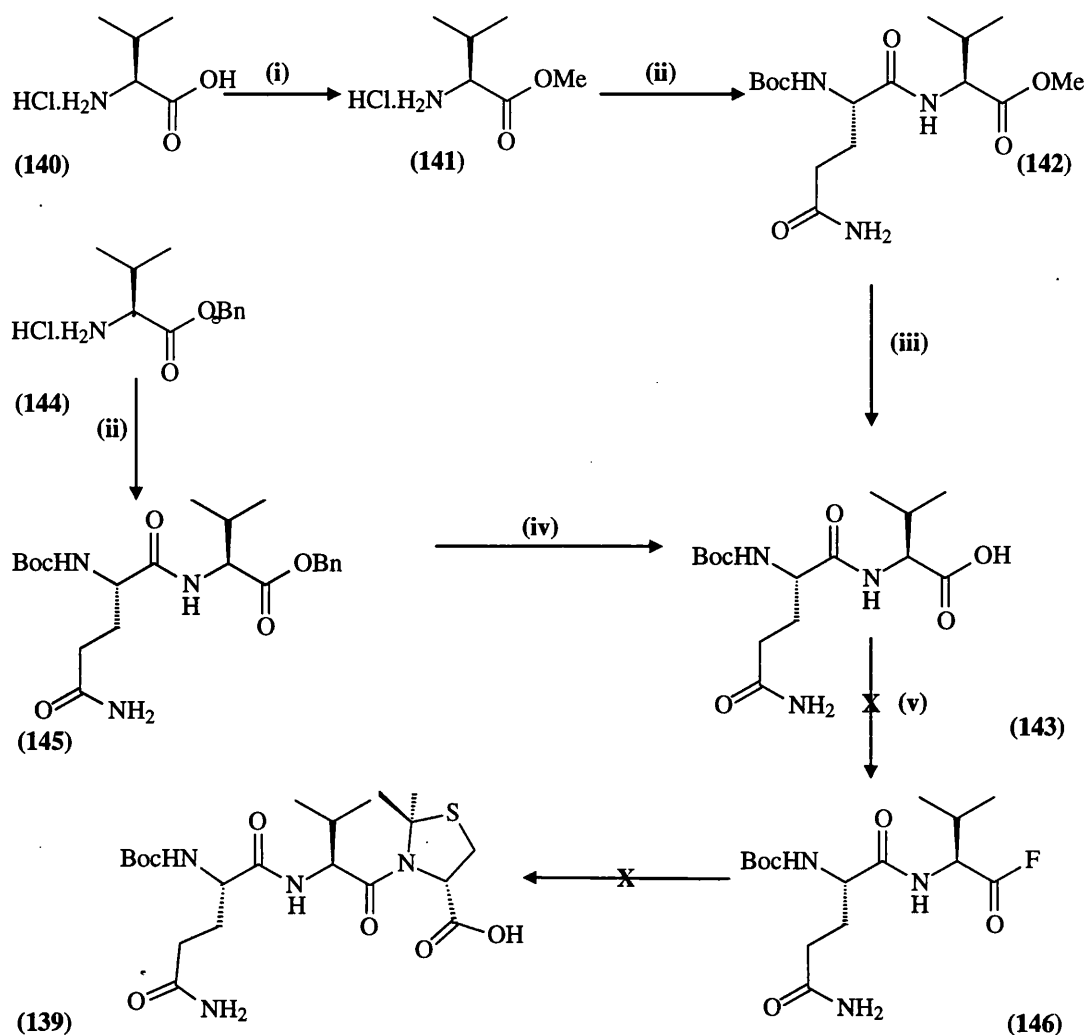
Scheme 3.20 *Proposed chemical approach for the synthesis of (139). (i) SOCl₂, MeOH, 40°C; (ii) BocGlnOH, HOBt, DCC, CH₂Cl₂, Pr^{i}₂NEt; (iii) NaOH, MeOH; (iv) 10% Pd/C, MeOH; (v) Cyanuric fluoride, pyridine, CH₂Cl₂, -10°C.*

This route starts with the conventional esterification[162] of **(140)** by stirring in MeOH with thionyl chloride at 40°C for 24 h. A quantitative yield of **(141)** was obtained. Subsequent coupling of N$^\alpha$-Boc-L-glutamine with **(141)** using the DCC/1-hydroxybenzotriazole method[163] afforded **(142)** in 71% yield. Alkaline hydrolysis of **(142)** was achieved by stirring in methanol with sodium hydroxide for 2 h. Following evaporation of the solvent, water was added and neutralised to protonate the carboxylate anion which was then extracted with EtOAc. This process afforded a very low yield of **(143)**. However, TLC indicated its presence in the aqueous layer. It may be possible to rationalise this result as being due to the high aqueous solubility of the polar Gln-containing dipeptides. Salting-out by the saturation of the aqueous layer with sodium chloride, followed by extraction with ethyl acetate, proved to enhance the yield. The best yield obtained for **(143)** was 64%. Furthermore, an alternative

118

method of ester hydrolysis with LiOH[164] was not that good, because of the need to use H_2O in the working up procedures.

However, there is a need for a versatile and facile procedure to prepare (143) in a good yield. Therefore, an alternative method based on the use of the benzyl ester (144) instead of (140) was applied. The rationale of this substitution was based upon the ease of hydrogenolysis of the benzyl group, from which the product can be isolated without aqueous washing.[165] Thus coupling of Boc-L-glutamine with L-valine benzyl ester (144) using the DCC/1-hydroxybenzotriazole method[163] afforded (145) in 71% yield. Debenzylation with hydrogen and palladium afforded (143) in 94% yield.

Attempts to convert (143) with cyanuric fluoride to its acyl fluoride in the presence of pyridine appeared to be positive by TLC detection but no product could be isolated. It may be possible that the work-up procedure drives the acid fluoride into the aqueous layer because of the high solubility of Gln residue. However, the solubility problem may be overcome by the inclusion of various protecting groups on the Gln side-chain. These derivatives are available commercially but are very expensive. So, it was necessary first to confirm that dipeptides can, in general, be converted to their acyl fluorides. Therefore, it was decided to synthesise analogues in which Gln was substituted with the hydrophobic phenylalanine. Interestingly, this substitution proved to be virtuous (Scheme 3.21). This experiment, on one hand, will examine the effectiveness of the concept of acid fluoride synthesis of dipeptides and, on the other hand, will explain the unsuccessful synthesis of Gln-containing dipeptides acid fluorides. The synthesis pathway starts with the coupling of Boc-L-Phe with L-ValOMe (141) using the DCC/1-hydroxybenzotriazole method.[163] Recrystallisation afforded BocPheValOMe (147) in 33% yield. Subsequent alkaline hydrolysis afforded the corresponding BocPheValOH (148) in 88% yield. Treatment of this dipeptides with cyanuric fluoride applying the usual methodology afforded crude (149), which coupled with 2-(4-nitrophenyl)-ethylamine, affording (150) in 10% overall yield. From these results, it is clear that synthesis of acid fluorides of dipeptides with cyanuric fluoride methodology is not an efficient process.
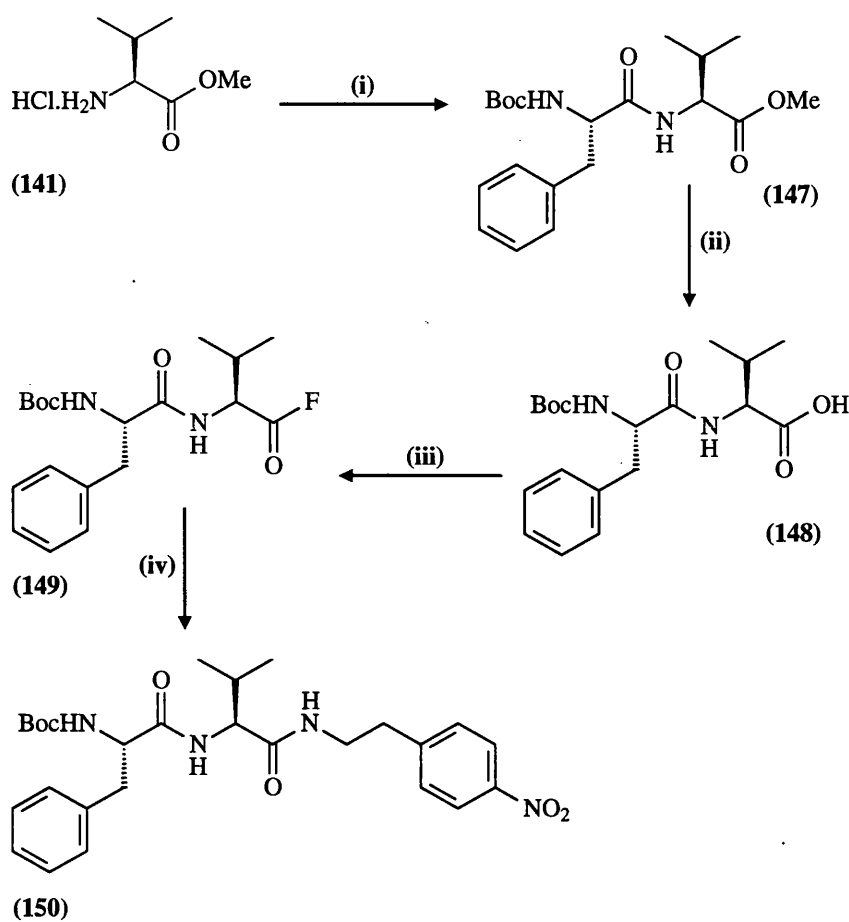
Scheme 3.21 Chemical synthesis of (150).(i) BocPheOH, HOBt, DCC, CH_2Cl_2; (ii) aq. NaOH, CH_3OH; (iii) Cyanuric fluoride, pyridine, CH_2Cl_2; (iv) 4-nitrophenylethylamine hydrochloride, Et_3N, DMAP, CH_2Cl_2.

Other coupling methods were examined in turn. The first trial was the use of the mixed anhydride coupling method (**Scheme 3.22**). Two attempts were executed. In the first attempt, compound (**143**) was stirred in dry DMF with isobutyl chloroformate[166,167,168] and N-ethylmorpholine at -18°C under argon for 1 h, after which a solution of (**81**) and diisopropylethylamine in DMF was added. The mixture was then allowed to warm gradually to 20°C and stirred for 16 h. Following work-up, ^1H NMR analysis indicated the failure of this coupling reaction. The next attempt was a "one-pot" process in which (**143**) was treated with 4-nitrophenyl chloroformate (**Scheme 3.22**), with the intention of forming the 4-nitrophenyl active ester.[169,170] However, consequent coupling of this active ester with (**81**) was not successful. Another coupling approach based on the DCC/1-hydroxybenzotriazole method[167] was unsuccessful. Furthermore, the common coupling agent 2-ethoxy-1-(ethoxycarbonyl)-1,2-dihydroquinoline (EEDQ)[171] was also used without any success. It is

noteworthy that all these experiments were attempted several times, for different periods, with or without DMAP catalyst.
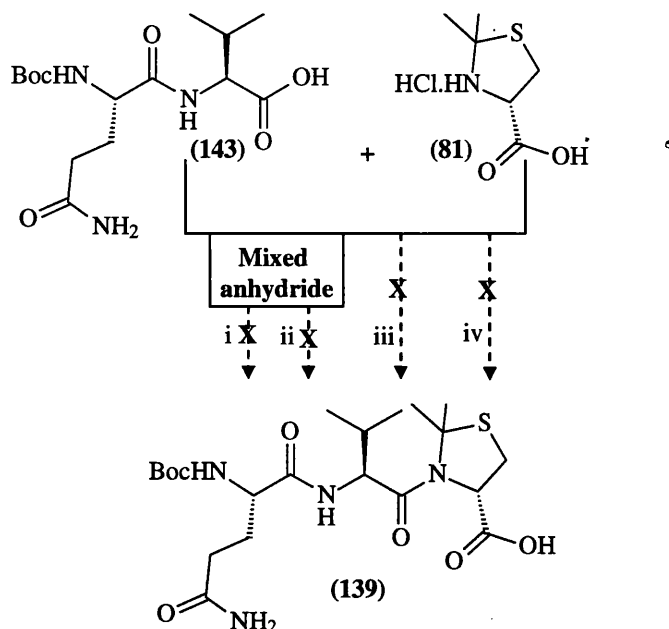
Scheme 3.22 *Proposed different chemical approaches for the synthesis of (139). (i) isobutyl chloroformate, N-ethylmorpholine, Pr^i$_2$NEt, DMF, -18°C; (ii) 4-nitrophenylchloroformate, Pr^i$_2$NEt, DMF, DMAP, -18°C; (iii) HOBt, DCC, Pr^i$_2$NEt, DMF; (iv) EEDQ, Pr^i$_2$NEt, DMAP, DMF.*

In view of the reported high reactivity of pentafluorophenyl ester coupling with thiazolidines,[172] it was worthy to test them in the dipeptide coupling process with the Me$_2$thiazolidine unit. This attempt was executed despite the previous unsuccessful coupling of PFP esters to the thiazolidine-N-(nitrophenylethyl)amide (51) where the thiazolidine ring opens (Scheme 3.1). However, a model experiment was executed by using an Fmoc-protected amino acid to provide a good chromophore to follow. Fmoc-Val-OPFP (86) was successfully coupled with the 2,2-dimethylthiazolidine-4-carboxylic acid (81) (Scheme 3.6). This result suggests that the ring-opening may be associated with the presence of the amide and that coupling of dipeptide active esters with the thiazolidinecarboxylic acid should preserve the heterocycle.

However, the required presence of Gln in the dipeptide will lower its solubility in moderately polar organic solvents, probably due to hydrogen bonds through the Gln side-chain amide.[173]

However, solubility may be increased by the inclusion of various protecting groups on the Gln-side chain. These derivatives are available commercially but are very expensive.

As a part of the ongoing synthetic strategy, a new tactic was employed to circumvent the solubility problem of Gln. This tactic was based on the substitution of Gln with pyroglutamate (Pyg). Pyg can act as a lipophilic synthon for Gln.[174] Interestingly, N-Boc protected pyroglutamate (151) undergoes a ring-opening reaction with Grignard reagents[175] and with lithium enolates through attack of these powerful nucleophiles with the ring carbonyl.[176] Also, it has been reported that the reaction of (151) with at least two equivalents of an alcohol in the presence of KCN in THF opens the ring to form the Glu γ-esters[177] but the reaction time needed was long (24 h). In this reaction, alcohol nucleophile will displace the cyanide in the highly reactive acyl cyanide intermediate, delivering the acyclic product. Amines behave as good nucleophiles.[174] Therefore, reaction of (151) with amines should yield the corresponding carboxamide derivatives. More specifically, reaction of (151) with ammonia in wet THF is expected to yield BocGlnOBn. On this basis, a model experiment was executed by the reaction of (151) with ammonia in wet THF, which gave (152). (Scheme 3.23)
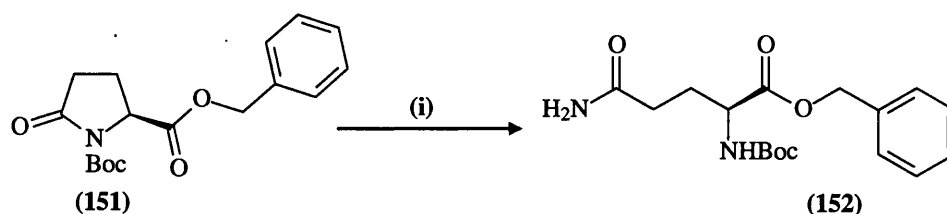
Scheme 3.23 Proposed chemical synthesis of (152). (i) aq. NH₃, THF.

A complete monomeric model for PSA-triggered release of NPEA was then constructed. The dipeptides BocPygValOPFP (157) was assembled according to the route in (Scheme 3.24). L-PygOH (153) contains a lactam moiety, which is responsible for the very low reactivity of the NH function. To introduce the Boc group to the poorly nucleophilic lactam nitrogen, it was first necessary to protect the carboxylic acid of (153)[178,179] as the benzyl ester. This was achieved by alkylation of the carboxylate anion with benzyl choride. The crude ester was then treated with di-*tert*-butyl dicarbonate (Boc₂O), triethylamine and DMAP in dichloromethane at 0°C for 1 h and at RT for 16 h to give the BocPygOBn (151). Hydrogenolysis of (151) afforded (154) in 93% yield. Coupling with ValOBn (144) by the DCC/1-

hydroxybenzotriazole method afforded the dipeptide (155) in 71% yield. Subsequent hydrogenolysis afforded BocPygValOH (156) in a quantitative yield. Formation of the PFP active ester (157) was achieved with pentafluorophenyl trifluoroacetate (TFAOPFP). This reagent has been shown to be particularly useful in the preparation of activated carboxylic acids via a mixed carboxylic-trifluoroacetic anhydride type of intermediate.[180,181] Others have shown that TFAOPFP could be used to protect amines as the corresponding trifluoroacetyl derivatives. Thus, TFAOPFP can be used for one-pot protection/activation of amino-acids. Therefore, recently many studies were conducted, all aimed at evaluating the scope of this chemistry. One of the advantages of TFAOPFP over the traditional DCC/PFPOH method is the high purity of the product.
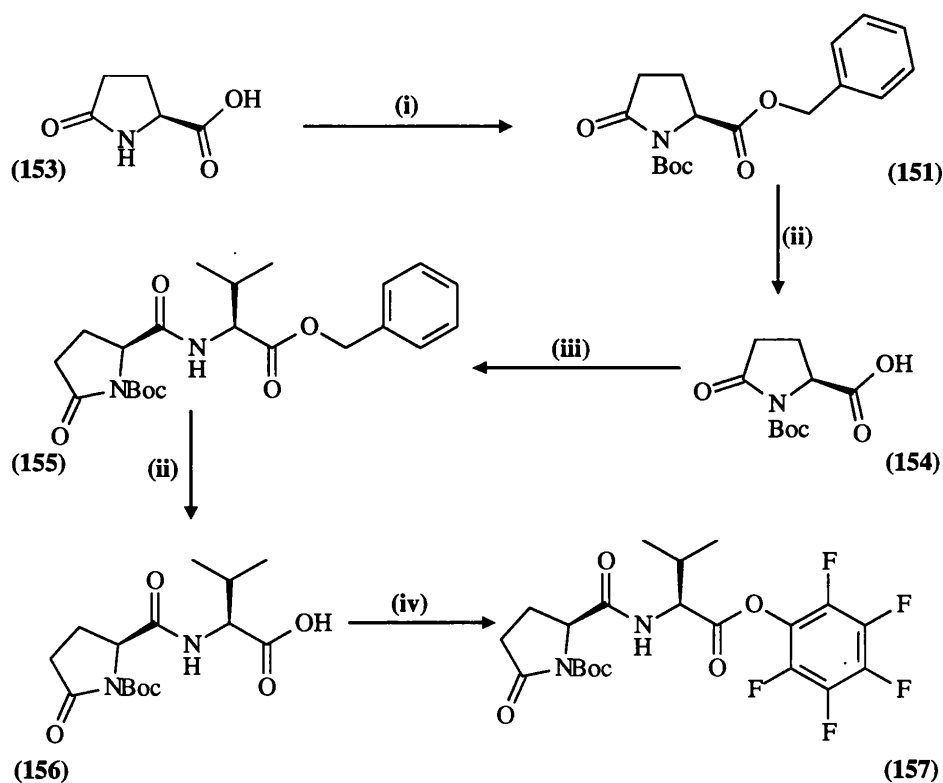
Scheme 3.24 *Synthetic steps towards the formation of compound (157) (i) A- Benzyl chloride, Et3N, THF, 5 d. B- Boc2O, Et3N, DMAP, CH2Cl2, 0°C; (ii) 10% Pd/C, MeOH; (iii) A- HOBt, DCC, CH2Cl2, 0°C, 1 h. B- L-ValOBn, Pr^i2NEt, DCM, 24 h;(iv) TFAPFP, pyridine, DMF.*

The next step forward was the preparation of the molecular clip-drug portion (Scheme 3.25). The synthesis pathway starts with the coupling of the dipeptides active ester (157) with S-2,2-dimethylthiazolidine-4-carboxylic acid (81) and diisopropylethylamine in dry DMF for 16 h.

123

Interestingly, the coupling reaction proceeded swiftly. Recrystallistion proved unsuccessful. However, chromatography afforded two compounds; **(158a)** in 42% and **(158b)** in 10% yield.
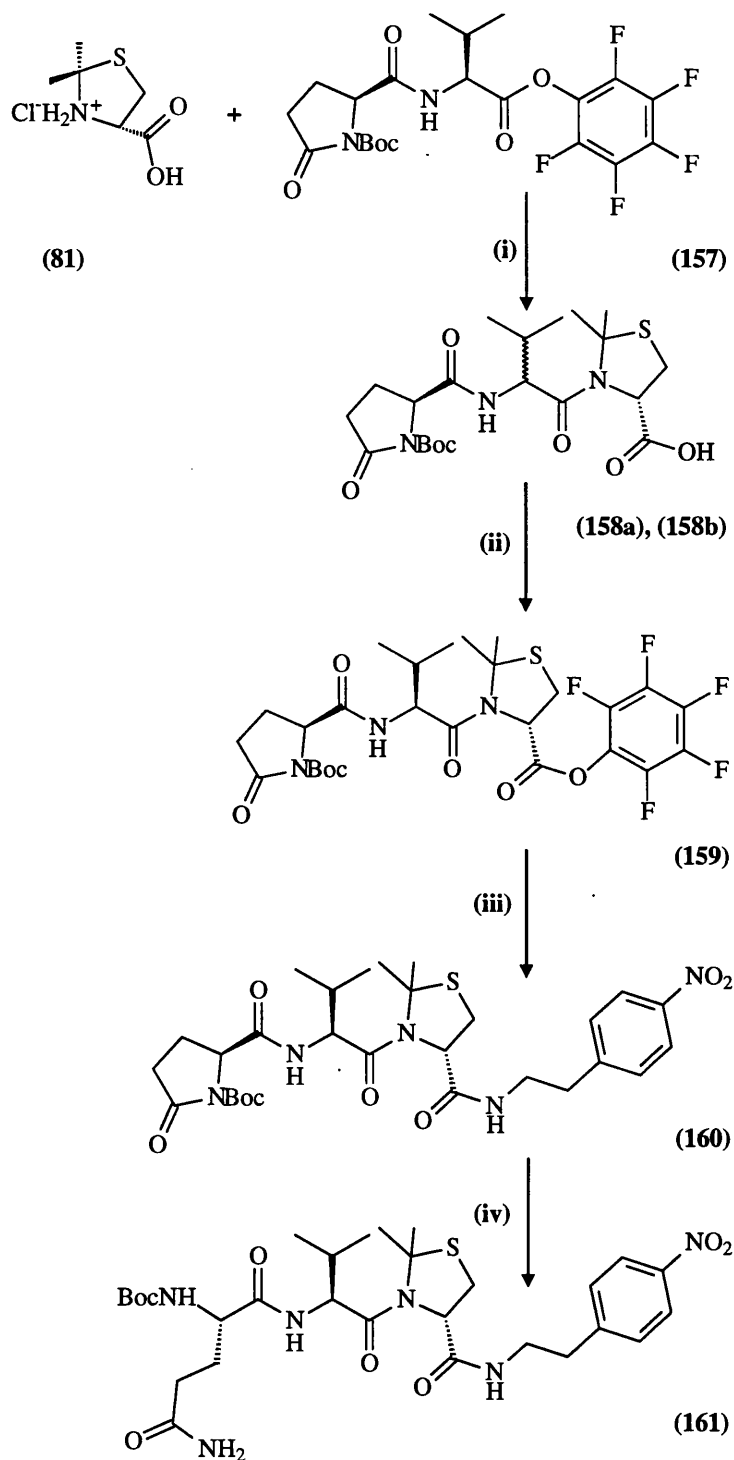
Scheme 3.25 *Synthetic steps towards the formation of compound (161). (i) Compound (81), Pr$^i_2$NEt, DMF; (ii) TFAPFP, pyridine, DMF; (iii) 4-nitrophenylethylamine hydrochloride, Et$_3$N, CH$_2$Cl$_2$; (iv) aq. NH$_3$, THF.*

On the bases of ^{1}H NMR and mass spectroscopic analysis, compound (158a) and (158b) are diastereoisomers. Whereas the usual couplings with active esters of carbamate-protected (Boc, Cbz, Fmoc) single amino-acids normally occur without racemisation, coupling of active esters of amino-acids with amides at the nitrogen often give partly racemised products. This racemisation occurs through formation of intermediate oxazolidinones, in which the "α-proton" is highly acidic. Dipeptides, of course, have an amide bond between the two amino-acids.

The apparent difference in the NMR spectra of (158a) and (158b) can be seen with the signal of Val α-H, which is presented as triplet at δ 4.25 in (158a) and as double doublet at δ 4.78 in (158b). It was expected that the major compound (158a) would be the required Boc-L-Pyg-L-Val-Me$_2$thiazolidinecarboxylic acid diastereoisomer and that the minor compound (158b) would be the epimer Boc-L-Pyg-D-Val-Me$_2$thiazolidinecarboxylic acid. It was planned that an X-ray structure be determined for a suitably crystalline intermediate later in the sequence, to confirm the stereochemistry.

Subsequent reaction of (158a) by pentafluorophenyl trifluoroacetate (TFAOPFP) granted (159) in 93% yield, which was then coupled with 2-(4-nitrophenyl)ethylamine (41) and afforded (160) in a 69% yield. Crystallisation of (160) afforded large, but severely twinned, crystals, which, after several efforts, were found unsuitable for X-ray analysis. Luckily, ring-opening of the pyroglutamine in (160) to Gln was attained successfully by stirring for 18 h with excess ammonia in wet THF and afforded (161) quantitatively.
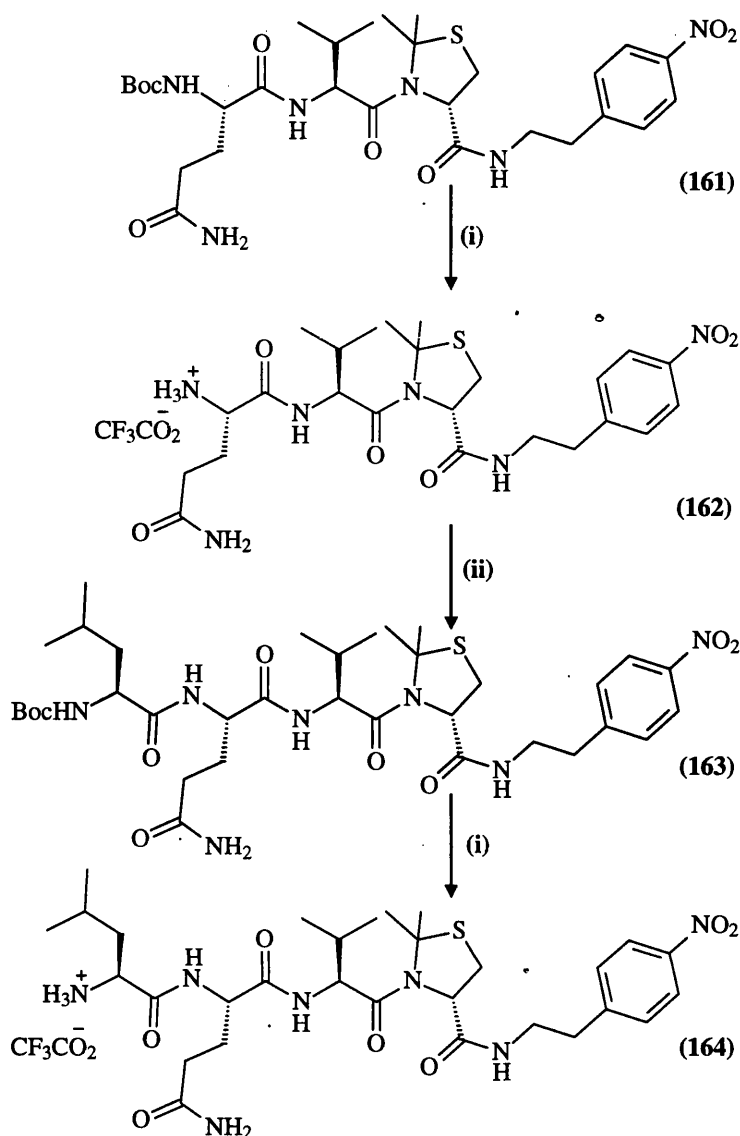
Scheme 3.26 *Synthetic steps towards the formation of compound (164). (i) 20% CF₃CO₂H / CH₂Cl₂; (ii) BocLeuOSu, Et₃N, DMF, THF, DMAP.*

Deprotection of **(161)** afforded **(162)** quantitatively **(Scheme 3.26)**. Compound **(162)** was then subsequently coupled through the active ester method with the hydroxysuccinimide ester BocLeuOSu and afforded **(163)** as a white solid in 92% yield. The ^{1}H NMR spectrum of this compound was complex but the presence of characteristic signals for the Leu α-H and Leu-Me₂ at the expected chemical shifts and correct integration confirmed the structure. Subsequent deprotection afforded **(164)** quantitatively.

126
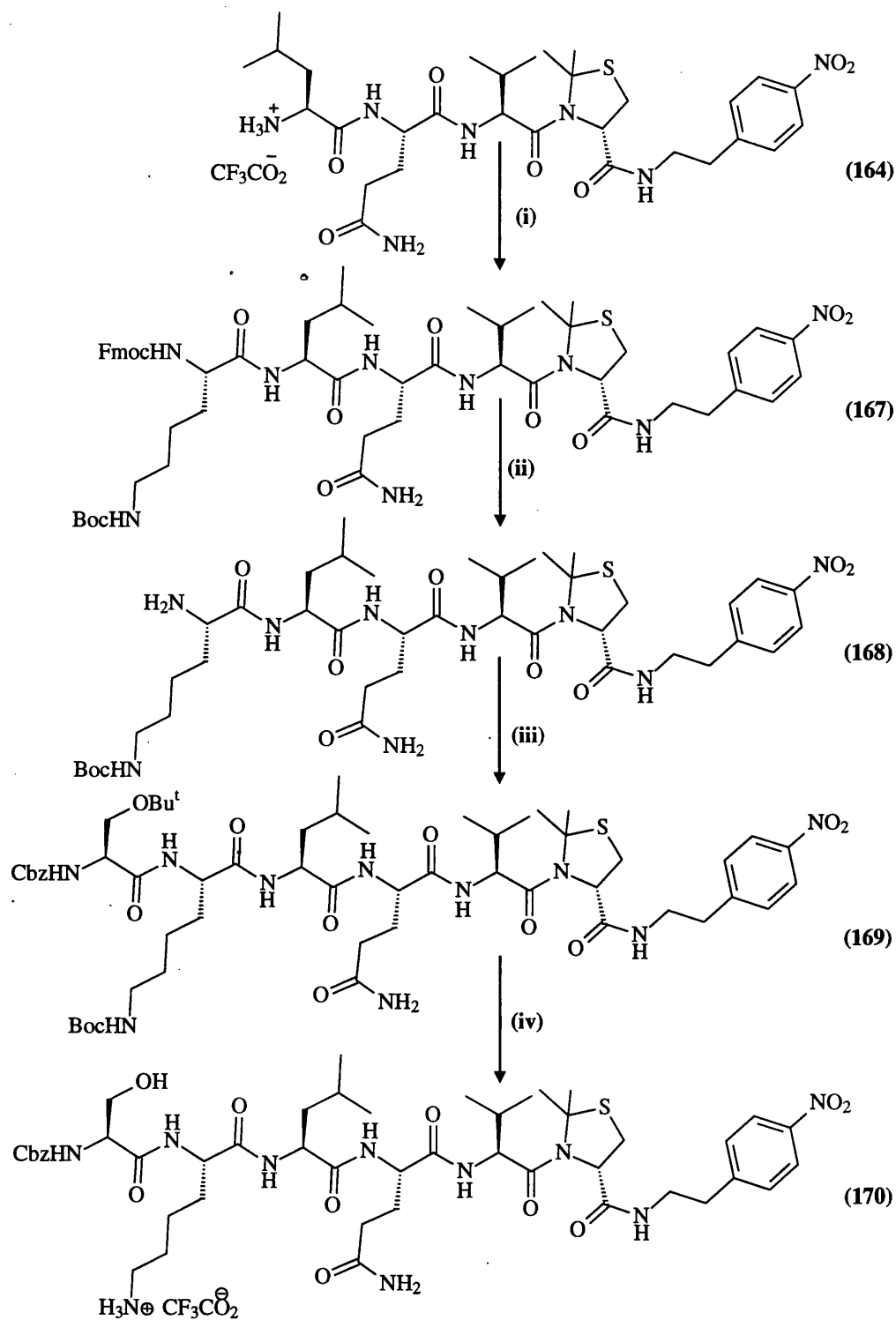
Scheme 3.27 *Synthetic steps towards the formation of compound (170). (i) FmocLysOPFP, Et₃N, DMF, THF, DMAP; (ii) 10% Et₂NH / CH₂Cl₂; (iii) CbzSer(Buᵗ)OSu, Et₃N, DMF, THF, DMAP; (iv) 20% CF₃CO₂H / CH₂Cl₂.*

The next step toward the synthesis of target **(167)** **(Scheme 3.27)** required the activation of the carboxylic acid of N^α-Fmoc-N^ε-Boc-L-Lys **(165)** **(Scheme 3.28)**. Activation was granted

with pentafluorophenol/DCC method and afforded (166) in 59%. It is noteworthy that orthogonal protecting groups of lysine were needed.
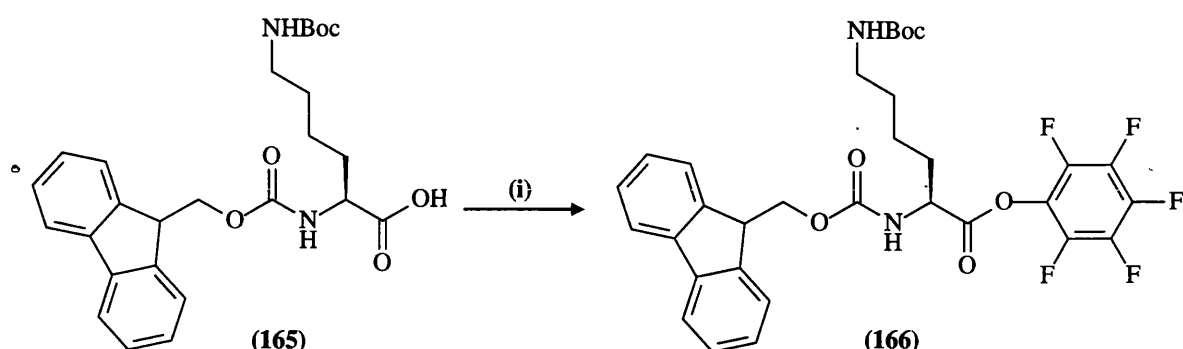
Scheme 3.28 Chemical synthesis of (166). (i) PFPOH, DCC, EtOAc, THF.

The N^ε side chain should be Boc protected to provide consistency for selective deprotection of the whole target peptide, since the next coupling step will involve the O-*tert*-butyl derivative of Ser. N^α was chosen to be Fmoc-protected. This is an attractive proposition because of the opportunity for selective deprotection. Fmoc group can be removed by treatment with secondary amines such as piperidine[182] and diethylamine.[183] However, Boc group proved to be stable under these alkaline conditions. It is important to maintain N^ε protection, to avoid any involvement of the nucleophilic amino motif in the next coupling step and also any possible cyclisation. The coupling of N^α-Fmoc-N^ε-Boc-L-LysOPFP (166) with (164) gave crystalline (167) in 95% yield (Scheme 3.27). Characteristic signals of the Fmoc moiety were seen in the ^{1}H NMR spectrum. Removal of the Fmoc protecting group was conducted with a 10% solution of diethylamine in dichloromethane, affording (168) in a 90% yield. From here, couplings with orthogonally protected serine derivatives were essential.

Since the cleavage of two peptide sequences (SSKLQV and SKLQV) by PSA were to be studied, the synthetic pathways diverged at this point. Two parallel couplings of (168) were granted by using CbzSer(Bu^t) (Scheme 3.27) and FmocSer(Bu^t) (Scheme 3.29).

As a part of the ongoing strategy, the side chain protection of Lys and Ser amino acids should possess the same characteristics. The protecting group should be cleaved swiftly under the same conditions. Therefore, the serine side-chain protecting group should be acid-labile, such as the *tert*-butyl (Bu^t) ether. On the other hand, on the way to synthesise SKLQV target (170) (Scheme 3.27), the N^α- protecting group of serine was chosen to be Cbz. Unlike Fmoc, the Cbz protecting moiety is known to be stable under the alkaline conditions (pH = 7.4) under

which the release study of the model drug by PSA will be conducted later. In addition, the Cbz moiety will provide a UV-detectable tag during the release study. However, in the route to target **(174)** **(Scheme 3.29)**, one more coupling step with another Ser residue is required. This, in turn, suggested the use of an orthogonal protecting group which is not acid-labile and, at the same time, could be cleaved under mild conditions, which do not affect the integrity of the thiazolidine ring. The Fmoc protecting group has been proved earlier to serve these purposes well and can be removed swiftly without damaging the thiazolidine ring.

To achieve target **(170)** **(Scheme 3.27)**, coupling of compound **(168)** with CbzSer(Bu^t)OSu was executed, giving crystalline **(169)** in 51% yield. Again, these crystals were not of good enough quality for X-ray analysis. Subsequent simultaneous deprotection of Lys and Ser protecting groups was executed with 20% trifluoroacetic acid in dichloromethane and afforded **(170)** quantitatively.

The synthesis pathway to target **(173)** **(Scheme 3.29)** starts with the coupling of compound **(168)** with FmocSer(Bu^t)OSu, affording **(171)** in 62% yield. The subsequent removal of the Fmoc protecting group was conducted with diethylamine to give **(172)** in 88% yield. The following coupling with CbzSer(Bu^t)OSu and FmocSer(Bu^t)OSu afforded **(173)** **(Scheme 3.29)** and **(175)** **(Scheme 2.31)** in 62% and 43% yield, respectively. Consequent deprotection of **(173)** afforded **(174)** quantitatively.

Compound **(175)** could have been coupled with the polymer to construct a complete polymeric prodrug model.
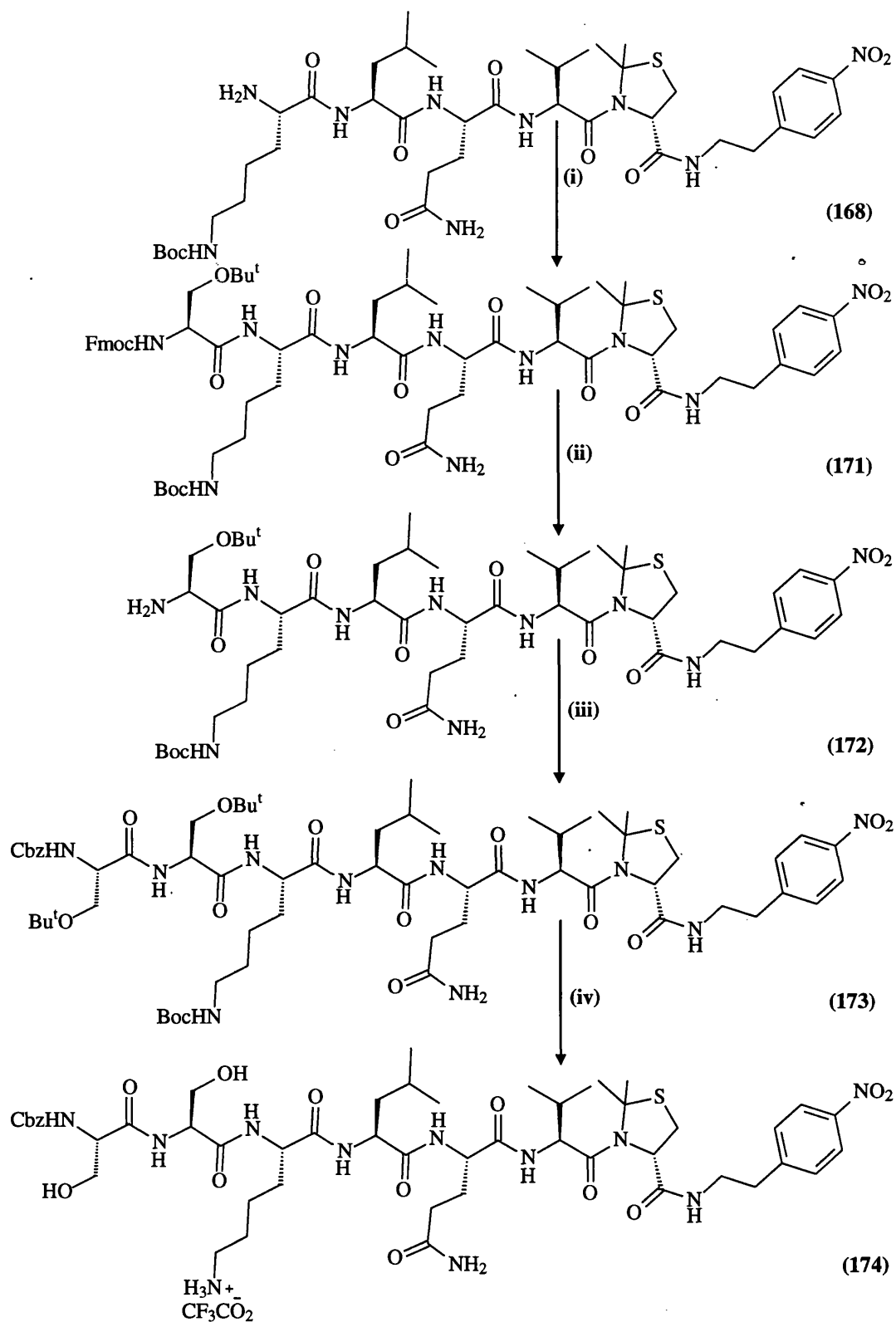
Scheme 3.29 *Synthetic steps towards the formation of compound (174). (i) FmocSer(Buᵗ)OSu, Et₃N, DMF, THF, DMAP;(ii) 10% Et₂N/CH₂Cl₂ (ii) CbzSer(Buᵗ)OSu, Et₃N, DMF, THF, DMAP; (iv) 20% CF₃CO₂H / CH₂Cl₂.*

130

Scheme 3.30 *Chemical synthesis of compound (175). (i) FmocSer(But)OSu, Et₃N, DMF,* $Scheme 3.30$
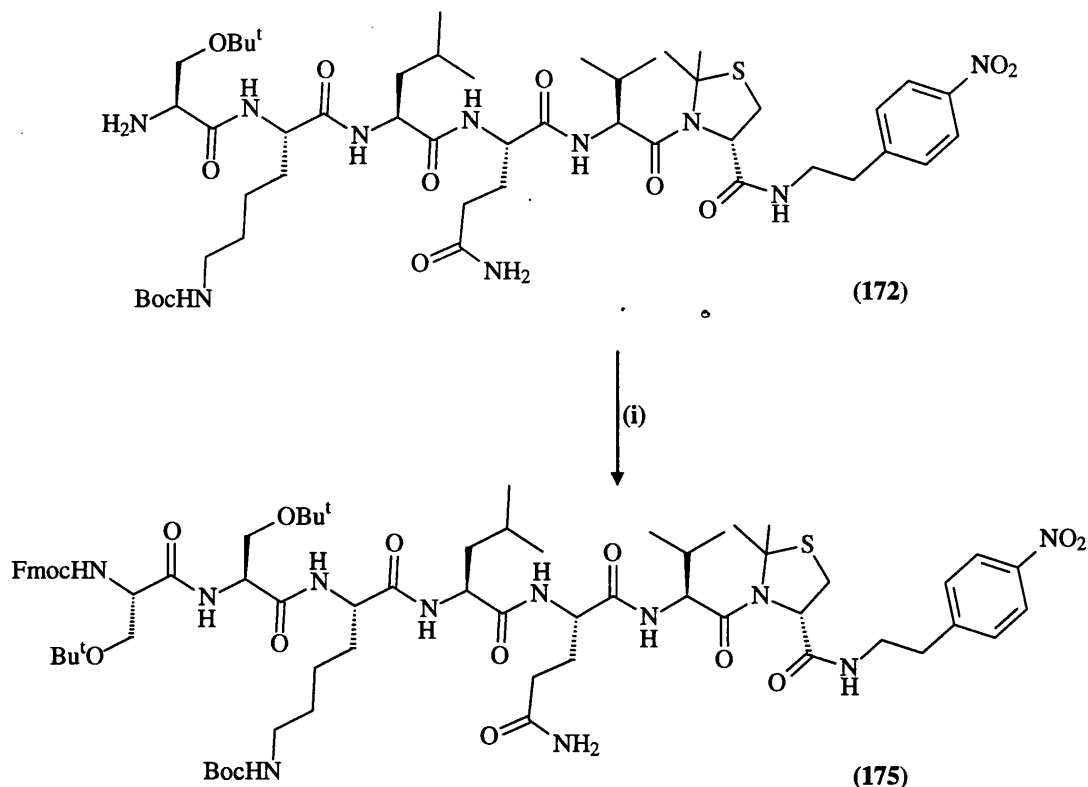
Scheme 3.30   Chemical synthesis of compound (175). (i) FmocSer(But)OSu, Et₃N, DMF, THF, DMAP.

In conclusion, syntheses of the CbzSKLQV and CbzSSKLQV sequences attached to the thiazolidine-N-nitrophenyl amide unit have been achieved in satisfactory overall yield through active ester couplings. These will provide substrates to test for cleavage by PSA and for subsequent DKP formation and release of the model drug. The success of these synthetic sequences was largely due to development of methods to couple dipeptides to the thiazolidine nitrogen and to use of Pyg as a more soluble synthon for Gln.

An alternative known pathway to solve the solubility problem of Gln during peptide synthesis is the use of N-side-chain-protected derivatives. These derivatives were available commercially but are very expensive. As a result, an alternative pathway was investigated briefly using the Gln(Trt) derivative **(Scheme 3.31)**. The protecting trityl moiety is removed under the same conditions as *tert*-butyl ether and Boc. As a test of the use of Gln(Trt), a dipeptide was synthesized. Therefore, coupling of ValOBn **(174)** with Gln(Trt) was conducted using the DCC/1-hydroxybenzotriazole method.[163] Chromatography afforded **(176)** in 54% yield. Subsequent hydrogenolysis afforded **(177)** in 56% yield, without cleavage of the trityl group.
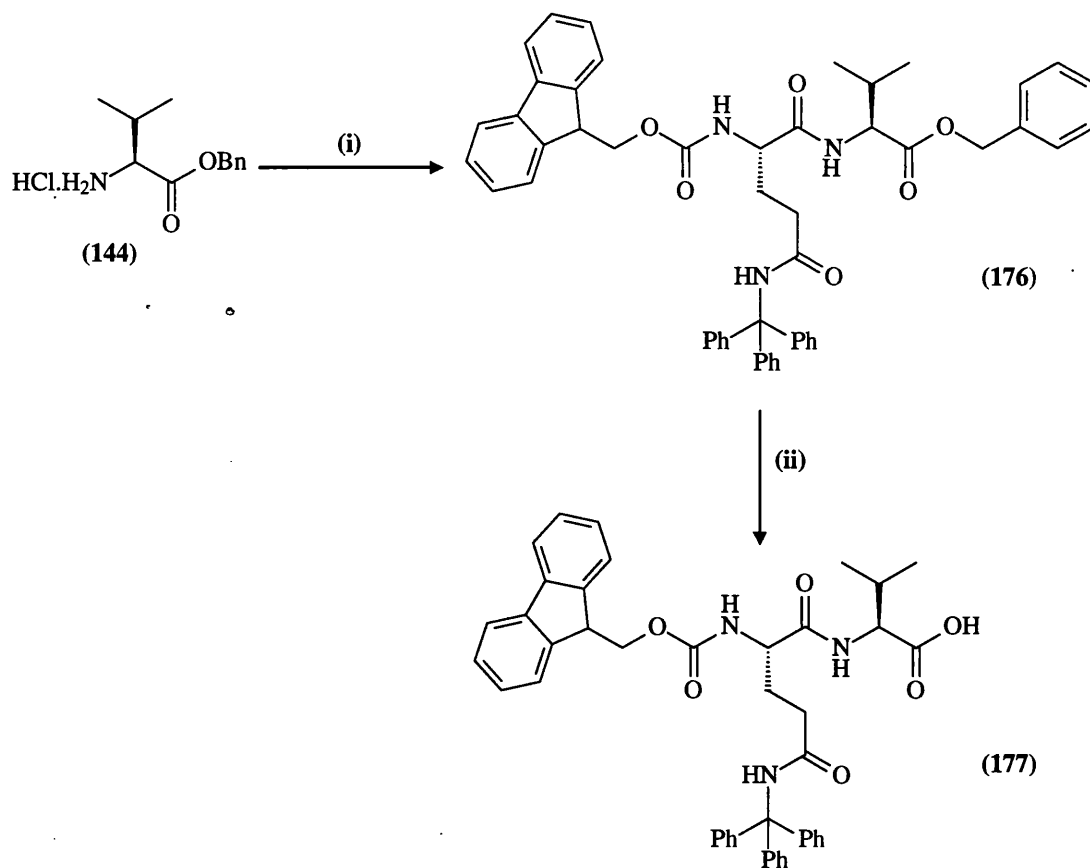
Scheme 3.31 *Synthetic steps towards the formation of compound (177). (i)*
FmocGln(Tr)OH, HOBt, DCC, CH₂Cl₂, Pr^i₂NEt; (ii)10% Pd/C, MeOH.

132

3.6   Synthesis of PSA-specific substrate analogue

The next plan was to synthesise SKLQVOMe as an analogue of the PSA-specific substrate SKLQ. The cleavage study of this sequence will add to the body of knowledge; on one hand, confirmation of the activity of the enzyme in cleaving the sequence and, on the other hand, the ability of the enzyme to cleave the Q----V amide bond. This will help later in interpretation of the release study from targets **(170)** and **(174)**.

In the design of a synthetic method for target **(184)** **(Scheme 3.33)**, solution-phase synthesis methodology was applied. The route to the pentapeptide **(184)** is illustrated in **scheme 3.32** and **3.33**. The active ester coupling method was employed predominantly for the stepwise elongation process. BocGlnValOMe **(142)** was deprotected with trifluoroacetic acid, giving GlnValOMe **(178)**. This dipeptide ester does not form the corresponding DKP readily, since it is in the *trans* peptide conformation. The remaining amino-acid units were added using BocLeuOSu, N^{α}-Fmoc-N^{ε}-Boc-L-LysOPFP and CbzSer(Bu^t)OSu, as before. Only one diastereoisomer was seen in the NMR spectra of all intermediates, indicating that no racemisation had taken place during the sequence.
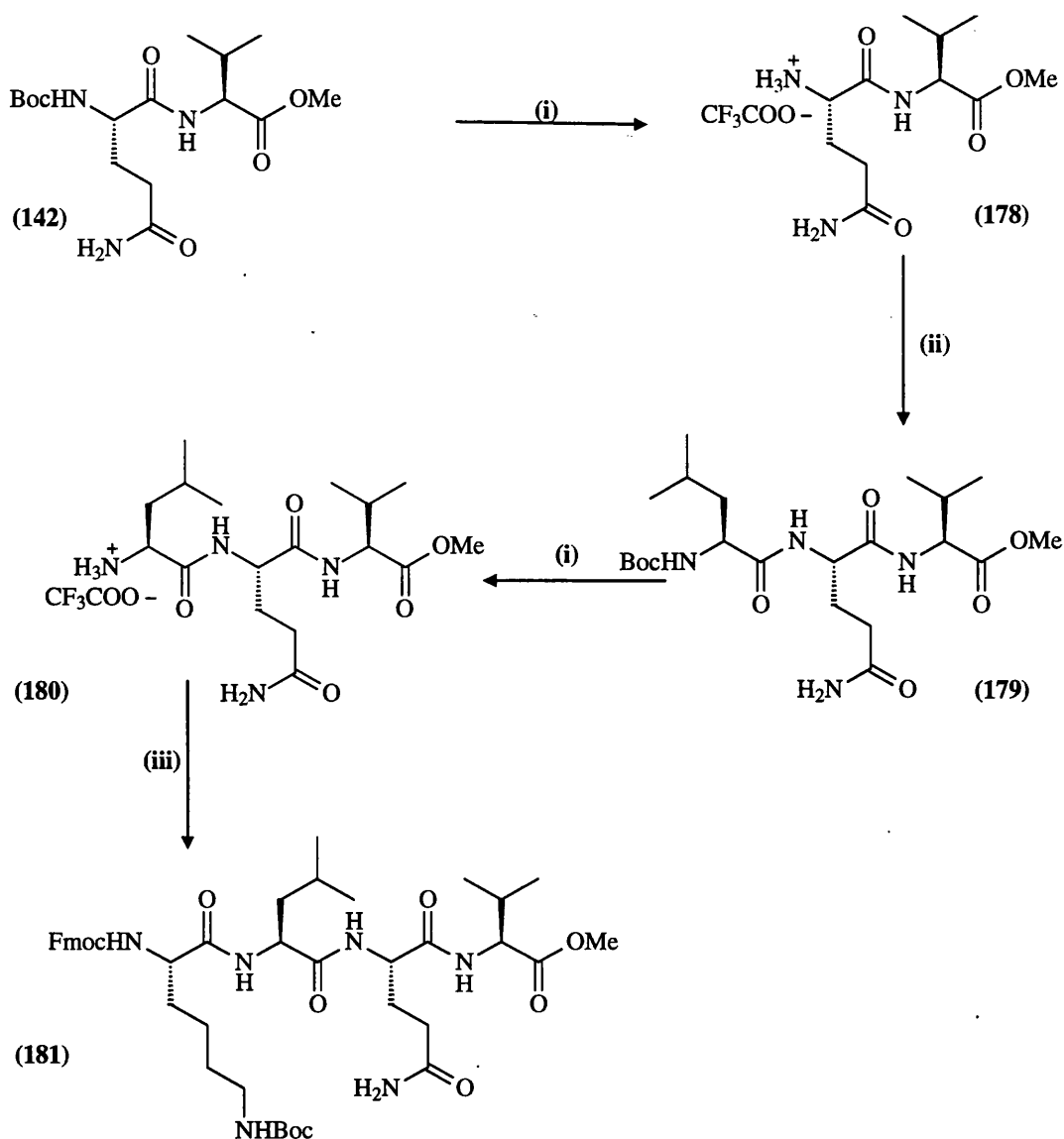
Scheme 3.32 *Synthetic steps toward the formation of compound (181). (i) 50% CF₃CO₂H /* CH_2Cl_2*; (ii) BocLeuOSu, Et₃N, DMF, THF, DMAP; (iii) FmocLysOPFP, Et₃N, DMF, THF, DMAP*

As the peptide sequence grows, in the stage of tetrapeptide **(181)** **(Scheme 3.32)** and **(Scheme 3.33)**, limited solubility of the product was observed. This is attributed to the trans-amide bond conformation adopted by the amino acids, which results in inter-molecular H-bond formation and consequent aggregation. However, in this synthetic pathway, limited solubility was an advantage because of the ability of washing solids **(181)** with ethyl acetate and with aqueous solutions to remove by-products without any loss of compound. Analysis of the 1-D ^{1}H NMR spectrum was difficult for the tetra- and penta-peptides. Therefore, the H-H coupling relationships were assigned through the two dimensional COSY spectra.
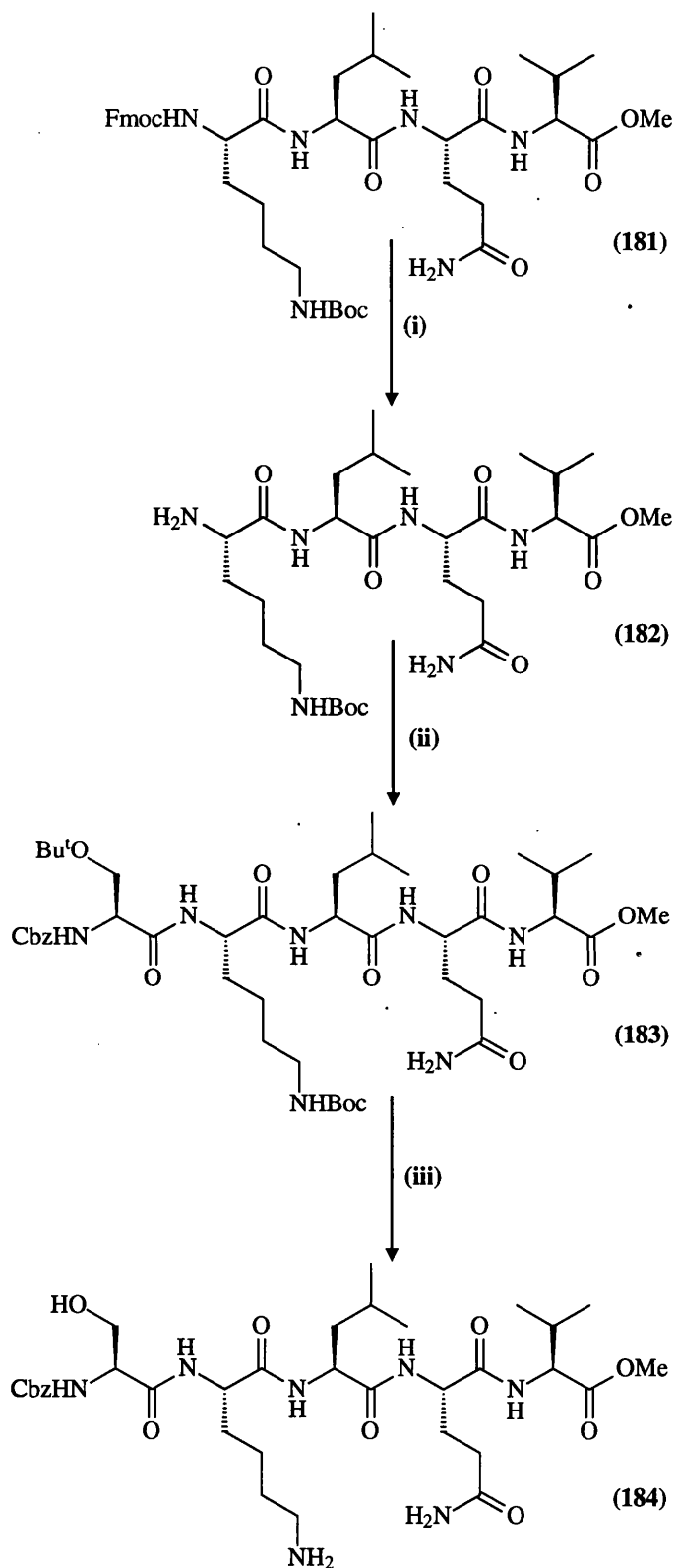
Scheme 3.33 *Synthetic steps toward the formation of compound (184). (i) 10% Et₂NH/DMF; (ii) CbzSer(Buᵗ)OSu, Et₃N, DMF, THF, DMAP; (iii) 30% CF₃CO₃H/CH₂Cl₂.*

135

3.7 Assaying of the PSA-cleavable peptide linker in the monomeric model prodrug.

The synthesized peptide-clip-drug models (170), (174) and the synthesized PSA substrate analogue (184) were assayed for PSA hydrolysis. In brief, peptide conjugates were mixed with PSA at a molar ratio of 100:1, respectively, in 50 mM TRIS.HCl and 140 mM NaCl at pH 7.4.[70] The reaction was incubated for different intervals at 37°C. The reactions were then quenched with $ZnCl_2$ (10 mM final concentration). The chromatogram was monitored at λ_{220}. Results are reported as the time required for PSA to hydrolyze 50% of the initial substrate. The instrumentation and the chromatographic method were similar to those used in **Section 3.4**. PSA enzyme was bought from Aldrich.

The constructed models $CbzSSKLQVMe_2ThProNPEA$ and $CbzSSKLQVMe_2ThPro-NPEA$ will now be evaluated for cleavage by PSA, liberating $ValMe_2ThProNPEA$ and hence, NPEA. Also, the PSA analogue substrate CbzSKLQVOMe will be assayed to evaluate the activity of the enzyme.

The first step in this study is the analysis of the authentic fragments of the peptide sequence CbzSKLQV and CbzSSKLQV attached to the thiazolidine-N-nitrophenyl amide and the fragments of the CbzSKLQVOMe target. The corresponding retention times (Rt) are shown in (**Table 3.4**) and (**Table 3.5**) respectively.

Standard Compounds	Comp. No	Ret. Time (min), pH 7.40, 37°C
NPEA	(41)	3.9
S Val DKP	(108)	6.8
Val-thiazolidine-N-nitrophenyl amide	(85)	13.9
GlnVal-thiazolidine-N-nitrophenyl amide	(162)	8.2
LeuGlnVal-thiazolidine-N-nitrophenyl amide	(164)	13.9
LysLeuGlnVal-thiazolidine-N-nitrophenyl amide	(168)	8.3
CbzSerLysLeuGlnVal-thiazolidine-N-nitrophenyl amide	(170)	5.4
CbzSerSerLysLeuGlnVal-thiazolidine-N-nitrophenyl amide	(174)	17.4

Table 3.4   *Retention times of the target compounds (170), (174) and the intermediate fragments.*

Standard Compounds	Compound number	Ret. Time (min) at pH 7.4, 37°C
Val-OMe	(141)	4.5
GlnValOMe	(178)	3.8
LeuGlnValOMe	(180)	4.5
LysLeuGlnValOMe	(182)	3.9
CbzSerLysLeuGlnValOMe	(184)	5.7

Table 3.5   *Retention times of the target compounds (184) and the intermediate fragments.*

Since the retention time of the fragments Val-thiazolidine-N-nitrophenyl amide (85) and LeuGlnVal-thiazolidine-N-nitrophenyl amide (164) were identical, the consequence assaying of the cleavage site would be verified by the identification of the DKP and the model drug (NPEA) peaks for the target compounds (170) and (174). Also, in the target compound (184) similar retention times were recorded for the fragments ValOMe (141) and LeuGlnValOMe (180). Thus, assaying of PSA cleavage site would be by the

identification of a ValOMe peak. It is noteworthy that different mobile phase gradients were unsuccessful to give different retension times for the fragments.

HPLC analysis of the incubation of (170) with PSA indicated that the enzymatic cleavage took place between either the L↓Q or S↓K amino-acid residues and not between Q↓V as was expected.[68] However, the addition of another Ser amino acid, as in compound (174), proved not to make any difference, either to the rate of cleavage or to the site of cleavage. Interestingly, cleavage of CbzSKLQVOMe (184) also took place at L↓Q.

The HPLC evidence showed that cleavage of (170) has taken place at L↓Q or at S↓K. However, when samples were collected from the HPLC, concentrated and subjected to mass spectroscopic analysis, no useful spectra could be obtained. Therefore, the specific site of cleavage is still uncertain.

As a conclusion, PSA enzyme proved to be active and managed to cleave the constructed sequences. However, the cleavage did not take place in the correct site (Q↓V), either in the constructed CbzSKLQVThPro-NPEA and CbzSSKLQVThPro-NPEA targets or in the close substrate analogue CbzSKLQVOMe. Therefore, one might conclude that the Me$_2$Thiazolidine moiety had no effect on the PSA specificity. On the other hand, the difference in the steric environments of Val and of Leu may account for this shifting in the site of cleavage.

The percentage cleavage of the targets (170), (174) and (184) is presented in (Figure 3.41), (Figure 3.42) and (Figure 3.43) respectively. From these figures it is clear that the rate of cleavage is relatively slow. It is noteworthy that the difference in percentage cleavage between the two trials is due to the use of two batches of the enzyme.
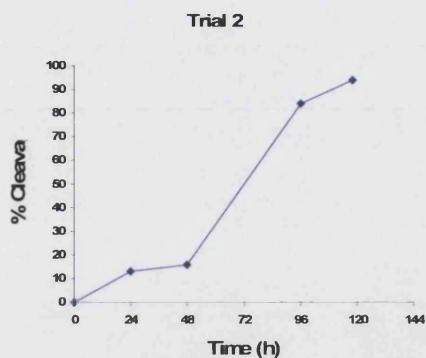
Figure 3.41 *A plot of the % cleavage of CbzSKLQV(2,2-dimethylthiazolidine)-N-nitrophenyl amide (170) in the presence of PSA versus time.*
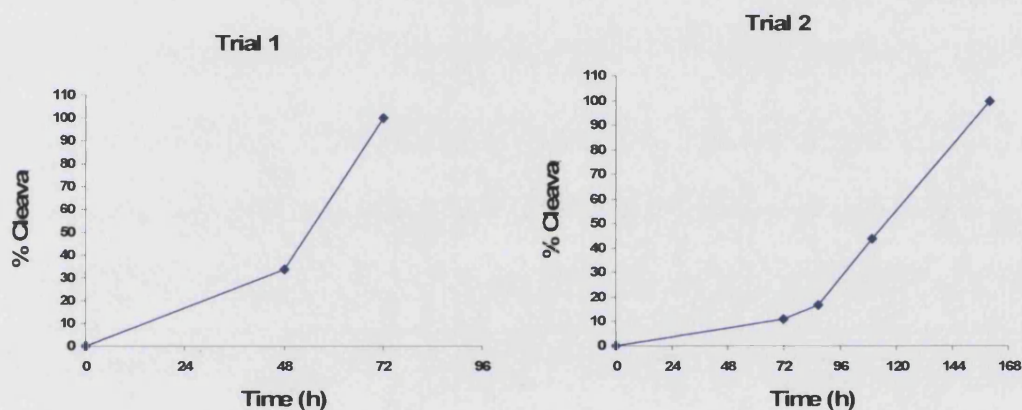
Figure 3.42 *A plot of the % cleavage of CbzSSKLQV(2,2-dimethylthiazolidine)-N-nitrophenyl amide (174) in the presence of PSA versus time.*
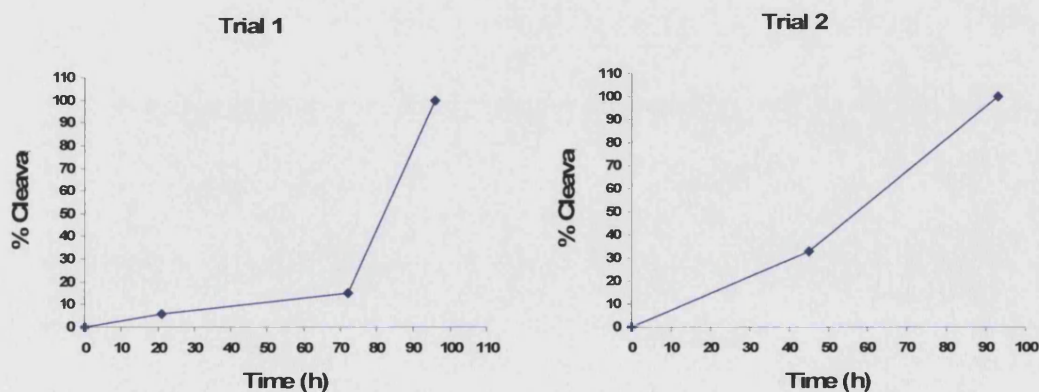
Figure 3.43 *A plot of the % cleavage of CbzSKLQVOMe (184) in the presence of PSA versus time.*

As a conclusion, future work in our lab will be performed to increase the body of knowledge. A new target in which Val amino acid residue in the L S-diastereoisomer will be replaced by Leu will be synthesised. Also, another peptide sequence Ac-Hyp-Ser-Ser-CHg-Gln-Ser-Ser-OH [74] ($T_{1/2}$ ~ 12 min at 37°C) will be synthesized to improve the rate of the cleavage.

Conclusion

PSA-Activated prodrugs

In conclusion, synthetic strategies have been successfully investigated for the development of the tripartite prodrugs, CbzSSKLQVMe$_2$ThProNPEA, CbzSKLQVMe$_2$ThProNPEA and CbzSKLQVOMe.

A putative approach toward the synthesis of the self-immolative molecular clips was developed. Various derivatives were synthesized. The conformation of these derivatives was studied by various spectroscopic methods and the preferred conformation was determined to be the Z for all derivatives. Furthermore, no loss of stereochemical integrity was found to take place during any of the coupling reaction throughout the synthetic process. Notably, incorporation of a 2-C disubstituted thiazolidine moiety offers a simple and attractive means to constrain selectively in the peptide bonds, i.e. to induce cis amide.

The X-ray crystallographic studies on the DKPs **(99)** and **(100)** derived from L-Ala-*R*-dimethylthiazolidinecarboxylic acid and L-Val-*R*-dimethylthiazolidinecarboxylic acid showed that the DKP ring is in a boat conformation, with the thiazolidine in a half-chair. The geminal methyl groups at position-3 are in equatorial and axial positions; the amino-acid side chain occupies a *pseudo*-equatorial position. This conformation was also likely to be adopted in solution.

The rates of intramolecular cyclization of the molecular clips and the consequent drug liberation were studied for the L, *R* and the L, *S* diastereoisomers. The effect of the size of the amino acid side chain on each series was also investigated. Interestingly, a change in the rate-determining step provides insights on the general effect of the size of the amino-acid side chain.

A PSA cleavable peptide sequence analogue has been synthesized using suitable orthogonal protecting groups and an effective ester coupling strategy. In addition, a novel synthesis of the tripartite system (peptide-clip-drug) has been realised. The six-amino acid peptide SSKLQ↓Lwas document to be hydrolysed specifically by PSA to liberate the

active drug. However, assaying of the PSA cleavage of our tripartite system realized that the cleavage has took place most probably between L↓Q, thus no drug was released.

Nitric oxide synthase inhibitors

Introduction

5.1 Nitric oxide - a puzzling molecule

In 1772, Joseph Priestly discovered nitric oxide (NO).[184] This naturally occurring free radical has been established in large number of mammalian tissues. It is a double-edged sword, beneficial as a messenger or modulator for immunological self-defence but at the same time, potentially toxic upon excessive production.[185] It plays peculiar roles and is involved in a myriad of biological processes including neuronal function, vascular tone and the cytotoxic function of macrophages.[186] These roles played by NO give the prospect of developing of new drugs to tackle important diseases. For example, drugs that release NO, improve blood flow to the heart muscle due to vascular smooth muscle relaxation. Also, NO controls blood flow into the corpus cavernosum of the penis; this role has been exploited by the anti-impotence drug Viagra®. On the other hand, overproduction of NO leads to chronic diseases, such as rheumatoid arthritis, may contribute to brain damage and could led to fatal conditions, such as septic shock.[187]

5.1.1 Biosynthesis

The biosynthesis of NO consists of two steps. First, L-arginine, the physiological substrate, is converted to N^G-hydroxyarginine in a reaction catalysed by Nitric Oxide Synthase (NOS). In the second step, N^G-hydroxyarginine is oxidised by NOS to form citrulline and NO.[188] This five-electron-transfer reaction involves the utilisation of NADPH and O_2 as substrates, as well as flavin adenine dinucleotide (FAD), flavin mononucleotide (FMN), tetrahydrobioterin (BH_4) and haem as cofactors.[189]

The NOSs are a family of haem-containing oxygenases.[190] Three genetically distinct isoforms have been characterised. These isoforms share an overall ≈50% amino acid sequence identity with one another. They were originally isolated from neuronal, immunocyte and endothelial cell sources. Their nomenclature was initially based on the cell type from which they were originally purified, cloned and characterised; hence, the designations for neuronal (nNOS), immunocyte (iNOS) and endothelial (eNOS). Later on,

143

it has been discovered that the different NOS isoforms have a much wider distribution than was previously thought. For example, nNOS is also expressed in the skeletal muscle, iNOS is expressed in many tissues after immunoactivation and eNOS is also expressed in brain. This discovery of a more general tissue distribution of the archetypal neuronal, inducible and endothelial NOS isoforms has led to a proposed numerical designation in order of their discovery (NOS1, NOS2, and NOS3, respectively).[191]

NOS isoforms have also been characterised and distinguished by their Ca^{2+}/calmodulin-(CaM) dependence and by whether they are expressed constitutively (cNOS) or induced following exposure to cytotoxins or endotoxins (iNOS).[192] nNOS and eNOS are constitutive and regulated by their dependence on Ca^{2+} concentration, while iNOS does not depend on Ca^{2+} concentration since it is tightly bound to CaM.[189] The main differences between the constitutive and the inducible isoforms are the amount and duration of production of NO. The total amount of NO generated per cell by cNOS is low when compared with that formed by iNOS and the flux of NO generated by cNOS is of short duration. On the other hand, iNOS generates considerably higher concentrations of NO for periods of hours-to-days and is essentially unregulated, once expressed.[193]

Therefore, the physiological *versus* pathophysiological role of NO is correlated to the presence and activity of specific isoforms of NOS. These isoenzymes are distinct from each other by their amino acid sequences, thus the active site of the three isoenzymes might be different enough to allow selective inhibition towards a therapeutic benefit.[194]

NOSs have two major domains, the reductase domain (C-terminal) and the oxygenase domain (N-terminal). The reductase domain shows very high similarity to cytochrome P450 reductase and contains sequences for binding sites for NADPH, FAD and FMN. The oxygenase domain binds to the haem and BH_4. The oxygenase and reductase domain are joined by a calmodulin-binding site, which serves as a 'switch'. The shuttle of electrons from NADPH to the oxygenase domain depends on Ca^{2+}/CaM^{184} (**Figure 5.1**).

Reductase domain   **Oxygenase domain**
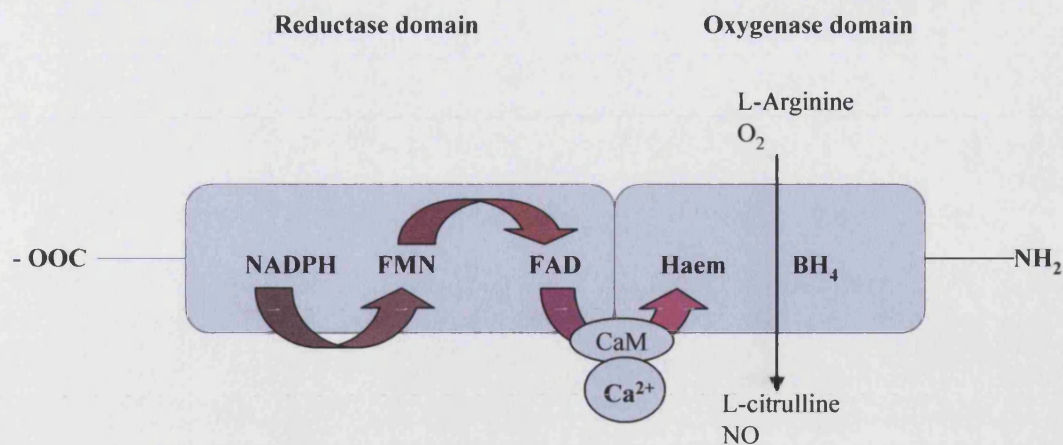
Figure 5.1   *Domains and cofactors of NO synthase.*

5.1.2 Chemical biology

L-arginine is bound near the haem cofactor, the iron of which is bound to NOS through the sulfur (S) of the active-site cysteine. The haem iron is then reduced to the ferrous form (Fe^{2+}) by an electron transfer from NADPH. One O_2 is bound to the haem and a second electron is delivered from NADPH, *via* flavin, to form a perferryl haem species. This is a potent hydroxylating agent, reacting with the arginine to form N^G-hydroxyarginine.[195]

Further reaction of this intermediate takes place with the original haem cofactor, which again receives one electron from NADPH and binds O_2. This electron is later delivered from the intermediate as H; this radical then attacks the peroxyhaem species in the resulting intermediate radical, leading to the formation of L-citrulline, NO, and water (H_2O) **(Figure 5.2)**.[195]
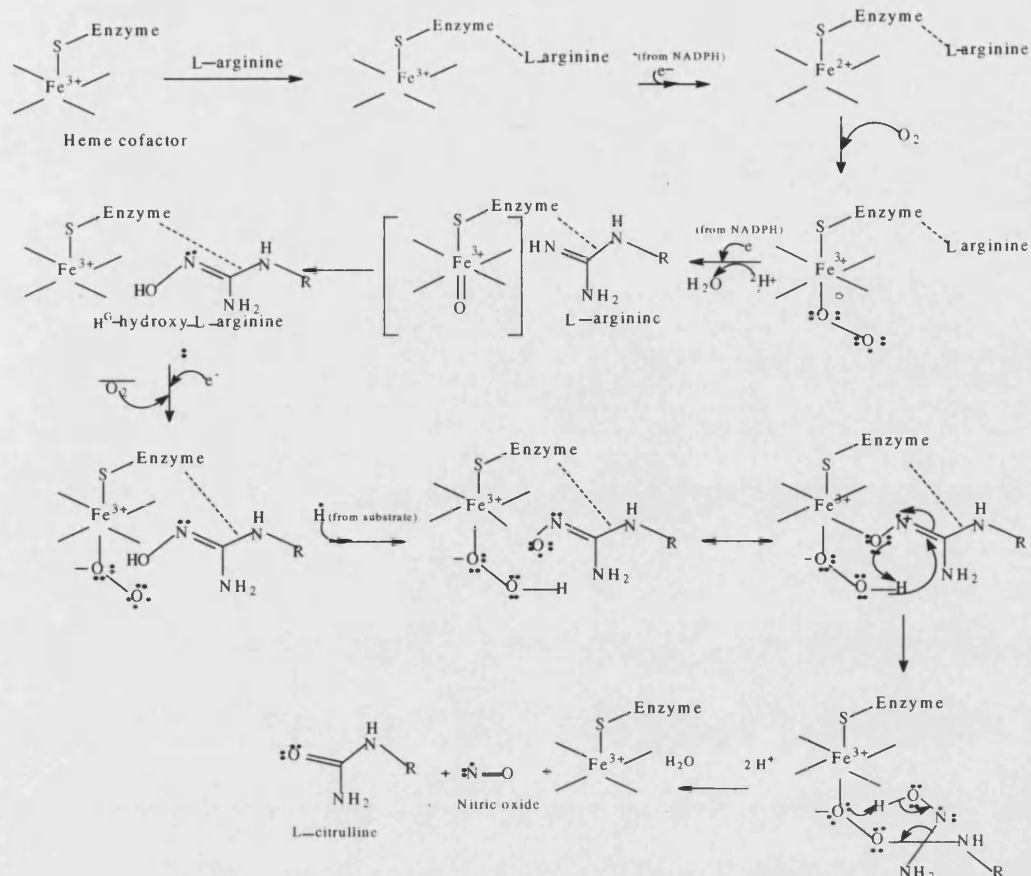
Figure 5.2 *Proposed mechanism for the synthesis of NO.*[195]

5.1.3 Nitric oxide: the good, superoxide the bad, and peroxynitrite the ugly

In biological media, NO reacts with superoxide anion radical ($O_2^{\cdot-}$) to produce peroxynitrite ($ONOO^-$), which is not a free radical but a highly potent oxidant. This peroxynitrite induces peroxidation of lipids, disrupts protein structure through nitration of tyrosine, oxidises –SH residues in proteins, depletes antioxidants and causes breaks in DNA strands.[196] This modification has considerable effects on protein and enzyme function and contributes to pathophysiological dysfunction.

5.1.4 Isoenzyme-specific inhibitors

It is hoped that NOS inhibitors will offer a high degree of potency and selectivity to suppress specific NOS isoform activity. For example, selective nNOS inhibitors might help to alleviate ischaemic brain damage[187] and might be useful in the treatment of septic shock,[193] chronic inflammatory diseases such as rheumatoid arthritis, adverse immune reactions associated with transplantation[187] and cancer.[197]

146

5.1.5 NOS inhibitors

NOS inhibitors are usually classified into two main categories, amino-acid derivatives and non-amino-acid derivatives (**Figure 5.3**).

5.1.5.1 Amino-acid-based NOS inhibitors
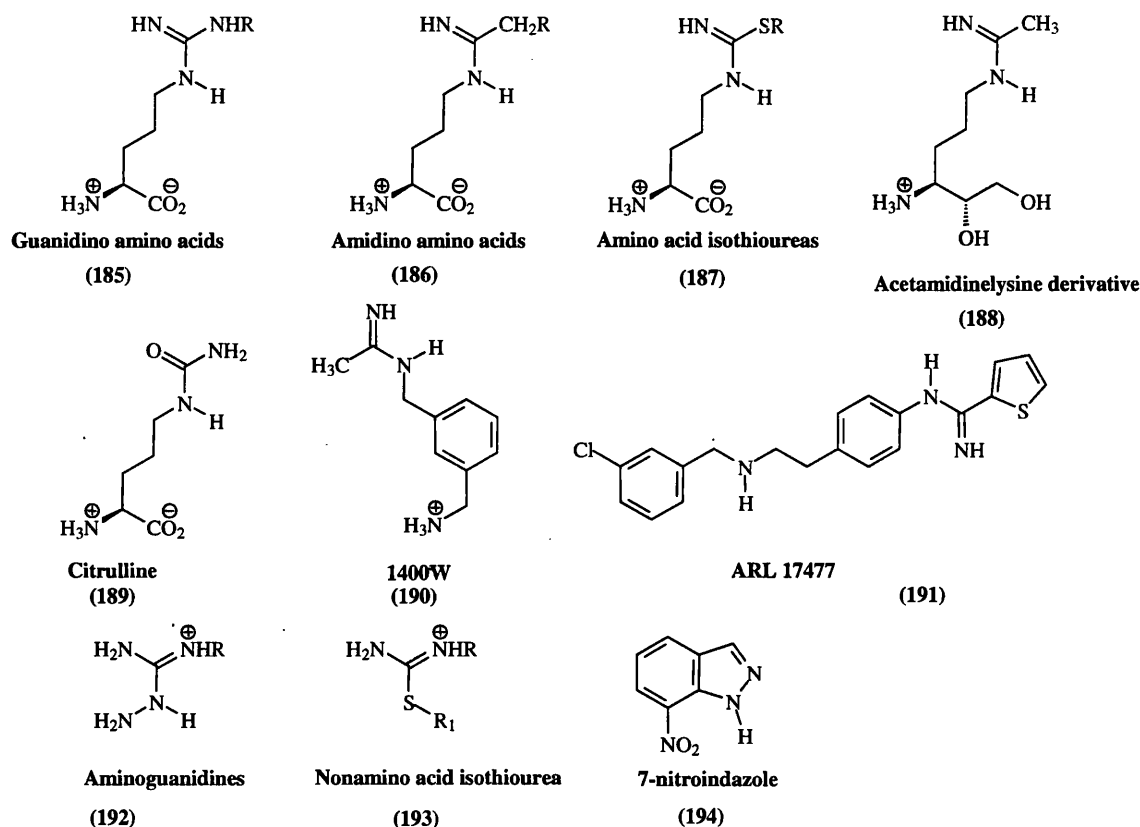
Figure 5.3   *Structures of amino-acid and non-amino-acic inhibitors of NOS.*

A   *Guanidino amino-acids (185)*

These are analogues of the NOS substrate L-arginine and have minimal selectivity.[189]

B   Amidino amino-acids (186)

These are analogues of the NOS substrate L-arginine and show higher degrees of selectivity. It has been noticed that none of the saturated derivatives shows significant isoform selectivity while, in contrast, the unsaturated derivative (vinyl-L-NIO) showed a marked selectivity for nNOS and could be classified as a potent mechanism-based inactivator of nNOS.[193]

C   Amino-acid isothioureas (187)

Griffith and Furfine have reported that these NOS inhibitors are potent with selective inhibition for nNOS.[189] S-methyl- and S-ethyl-L-citrulline are reversible and time-dependent inhibitors. Obviously, the proposed mechanisms for this time-dependence is not yet understood.[198] Also, the sulphur, which replaces the guanidium nitrogen atom, binds in close proximity to haem iron.

D   Acetamidine lysine derivative (188)

This compound resembles an amidino-amino-acid. However, the carboxylate group is replaced by vicinal glycol. Halliman et al.[199] found that additional iNOS selectivity (with a slight penalty in potency) resulted from this replacement. Interestingly, inversion of the stereochemical configuration at the secondary alcohol abolishes NOS inhibitory activity.

E   Citrullines (189)

Urea citrullines are inactive as inhibitors. However, the thiourea derivatives are potent and bind to the active site of the enzyme through the sulfur atom in close proximity to haem.

5.1.5.2 Non–amino-acid-based NOS inhibitors

A   N-(3-(Aminomethyl)benzyl)acetamidine (1400W) (190)

This is a monoamidine monoamine analogue.[193] It is the most selective iNOS inhibitor reported to date, with an irreversible or an extremely slowly reversible mechanism-based inactivation.[198] The inhibition was dependent on NADPH and its binding was competitive with L-arginine. The amidine moiety of 1400W binds in the guanidine-binding pocket of the substrate site.[198] Studies showed that 1400W had a similar toxicity profile to the bis-isothioureas. However, such toxic effects appeared only after exceeding a relatively high threshold plasma concentration of drug and not at normal doses.[198]

B   ARL 17477 (191)

This is a heterocyclic substituted amidine, which is reported to be the most selective nNOS inhibitor at present (IC_{50} = 35 nM against rat nNOS), being at least 100-fold selective for nNOS over eNOS and iNOS.[193]

C   Isothioureas (193)

They are non-amino-acid analogues of L-arginine. The simple alkyl derivative were extremely potent,[194] with little isoform selectivity. Their binding is competitive with L-arginine and is reversible. However, the acetylenic isothiourea, S-propargylisothiourea, shows NADPH-dependent mechanism-based inactivation. The pharmacological use of (iso)thioureas is limited due to their acute toxicity.[193]

D   Indazoles (194)

7-Nitroimidazole is a selective nNOS inhibitor. This selectivity may be due to differences in its uptake or metabolism in different tissues or to its mode of inhibition, since it competes with BH_4 and L-arginine binding. Thus its nNOS selectivity could be attributed to the relatively low concentrations of the substrate and BH_4 in certain tumours.[187]

5.1.6 Structure-activity relationships (SARs)

The NOS enzymes interact with the guanidinium region of L-arginine throughout NO biosynthesis **(Figure 5.4)**. Therefore, the first NOS inhibitors reported bind to the oxygenase domain and interact with the guanidinium region of L-arginine-binding site within NOS.[193] Also, it has been found that several modifications to the guanidino group are tolerated by the enzyme and showed higher binding affinity, giving rise to a number of
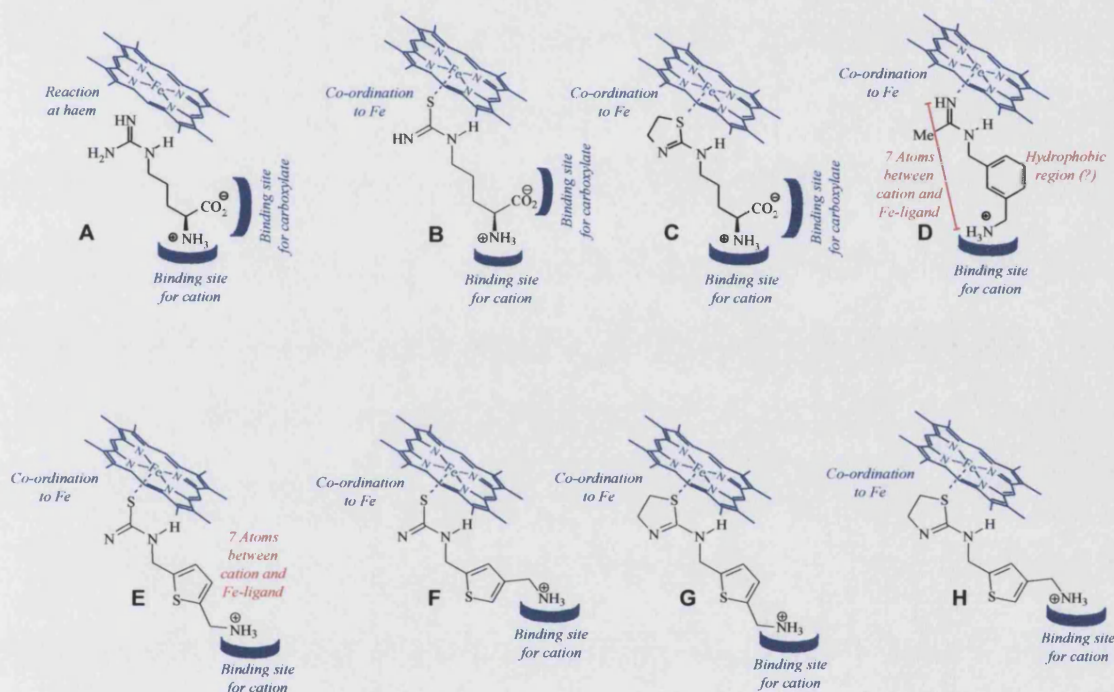
Figure 5.4   *Models for binding of the substrate;* **B** *the potent with little isoform selectivity thiocitrulline;* **C** *the potent non-isoform-selective Nδ-(4,5-dihydrothiazol-2-yl)ornithine;* **D** *the iNOS selective inhibitor 1400W;* **E, F, G and H** *a proposed potential analogue.*
NOS inhibitors.[189]

Aspects of the SARs underlying the isoform selectivity can be gleaned from examination of the structure and possible mode of binding in the active sites of known inhibitors. 1400W is a highly potent NOS inhibitor with a selectivity of 5000 for iNOS versus eNOS.[200] This finding constitutes the largest selectivity reported for iNOS. Some features in its structure were the benzene ring (which may fit in a hydrophobic pocket) and the

150

absence of the amino-acid carboxylate. In respect of the aromatic ring, (±)-6-cyclohexylmethyl-2-iminopiperidine with its iNOS-selectivity supports the hydrophobic ring role;[201] also one may speculate that the function of the benzene ring is to maintain the correct relative conformation of the acetamidine and the amine groups which bind to the haem iron and in a cation-binding pocket, respectively.

The role of the carboxylate anion is more debatable. When the CO_2^- is removed from the dihydrothiazole C, inhibitory potency was diminished[202] *ca.* 10-fold. When the amidine group was joined directly to the benzene ring[189] (6-atom bridge) in 1400W, it shows nNOS inhibition selectivity.

5.1.7 Role in tumours

In the 1950s, Tomlinson and Gray observed that the diffusion limitation of O_2 led to the presence of hypoxic cells in tumours.[53] In general, hypoxia usually resulted from two mechanisms: diffusion-limited or chronic hypoxia (resulting from reduced oxygen diffusion from regions distant from the tumour blood vessels) and acute hypoxia (due to the transient occlusion of blood vessels). Hypoxic cells are about three times more resistant to radiotherapy than normoxic cells and tumour hypoxia has been purported to be an important biological factor in the failure of radical radiotherapy to achieve local control. Therefore, to enhance tumour sensitivity to radiotherapy, methods to enhance tumour blood supply, thus increasing the amount of oxygen delivered to the tumour, have been investigated.

NO, as a vasoactive agent, was generally thought to enhance tumour blood flow and so increase the amount of oxygen delivered to tumours; this would enhance the sensitivity of tumour cells to radiotherapy by decreasing the hypoxic state. However, NOS inhibitors actually increase tumour hypoxia and induce 3-5 fold increases in tumour resistance to radiotherapy.

Actually, the potential effect of vasodilators on tumour perfusion is a controversial topic, when the vascular bed in tumour and normal tissue are in parallel, an increase in the blood flow in normal tissue due to vasodilatation would shunt away the blood flow to the tumour. This effect is called the "steal" effect. In contrast, when the blood vessels in tumours and

normal tissue are in series, changes in perfusion would be similar because the blood, which leaves normal tissue vascular bed directly, flows into tumours. However, in many tumours, series and parallel types may be mixed or combined, and so modification of tumour perfusion vary depending on the relative contribution of both types.[203]

However, in human tumours, high NOS activities have been identified in comparison with surrounding tissue. Also, the expression of NOS is related to tumour grade. So, inhibition of NOS decreases tumour blood flow, increases tumour hypoxia and consequently stops tumour growth. Also, increase in tumour hypoxia is a target in itself, as it will allow increased activation of bioreductive prodrugs of cytotoxins and NOS inhibitors.[204] Many of these compounds undergo bioreductive metabolism of an aromatic nitro compound into the active amine derivative.[205]

5.2 Aim

To design and synthesis a novel NOS inhibitors with isoform selectivity, based on information from known substrates and previously synthesised inhibitors.

5.3 Research proposal

Most of the NOS inhibitors described to date are analogues of the substrate L-arginine. These inhibitors bind to the guanidinium region of the arginine-binding site and are competitive inhibitors with reported potency but little isoform selectivity. However, the amino-acid moiety is not a requirement for either selectivity or potency.[198]

The target compounds will illustrate the possibility of switching isoform selectivity through subtle changes in the spatial relationship between the haem-ligating headgroup and the remote functionalities. Inhibitors containing a rigid planar benzene ring are known.[198,206] An attractive approach would be the synthesis of a new target in which the benzene ring is replaced with the approximately isosteric thiophene. This rigidity introduced would then maximise the interaction with the enzyme binding site and, more importantly, differentiate between various NOS isoforms.

Information from potent but non-isoform-selective NOS inhibitors suggested that thiourea is good head groups for haem-iron-binding. Therefore, the design would be a hybrid of the aromaticity of the 1400W and the thiourea functionality of the L-thiocitrulline inhibitor; each carries the CO_2Me motif in a "meta-like" arrangement with thiourea on the thiophene seeking for better potency and selectivity than the lead compounds.

The structures of the designed target compounds are shown in (**Figure 5.5**). In fact, we will explore whether the isoform selectivity shown by 1400W could be translated into analogous compounds carrying sulfur haem-ligating head group.

(195)   (196)   (197)

R_1 = Thiourea head group
R_2 = CO_2Me
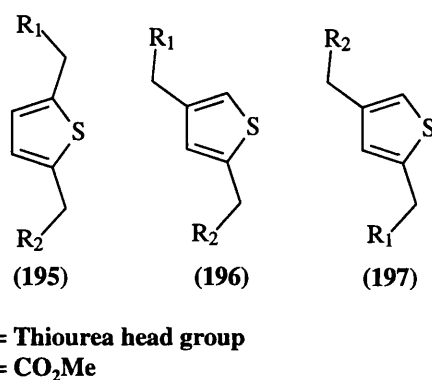
Figure 5.5   *Proposed structure of the target compounds*

5.4   Discussion

5.4.1   2,5-Disubstituted thiophenes

Retrosynthetic analysis suggested that one of the key intermediates in the synthesis of the targets would be 2,5-bis(aminomethyl)thiophene, which is reported in the literature[207] to be synthesised from 2,5-bis(hydroxymethyl)thiophene (**200**) (**Scheme 5.1**).

Alcohols are mostly prepared from carbonyl compounds by reduction with metal hydrides, such as $LiAlH_4$, $LiBH_4$, and $NaBH_4$. $LiAlH_4$[208] is one of the few reagents that can reduce a carboxylic acid directly. Reduction of commercially available thiophene-2,5-dicarboxylic acid (**198**) with $LiAlH_4$ gave the diol with great difficulty, owing to its considerable solubility in water, which impeded the work-up. Treatment of (**198**) with borane.THF complex, which is a selective reducing agent for carboxylic acids,[209] afforded only an

unidentifiable solid product. As an alternative to direct reduction, acids are often converted into alcohols by a two-step process: esterification and reduction using milder reducing agent. Consequently, compound (198) was esterified with a large excess of methanol and catalytic H_2SO_4 to afford compound (199) (74%). Treatment of (199) with four equivalents of $LiBH_4$ in dry THF, followed by quench with acetic acid and acetylation *in situ* with acetyl chloride and triethylamine, gave a mixture of two compounds. The acetylation enabled isolation of the very water-soluble alcohols from the boron residues as their acetate esters. Removal of the protecting acetates with methanol and ammonia, afforded a mixture of compounds which were then separated by chromatography to afford the mono-alcohol (201) and the required diol (200) in low yields. Use of greater excesses of $LiBH_4$ and longer reaction times did not improve the proportion of (200) produced.
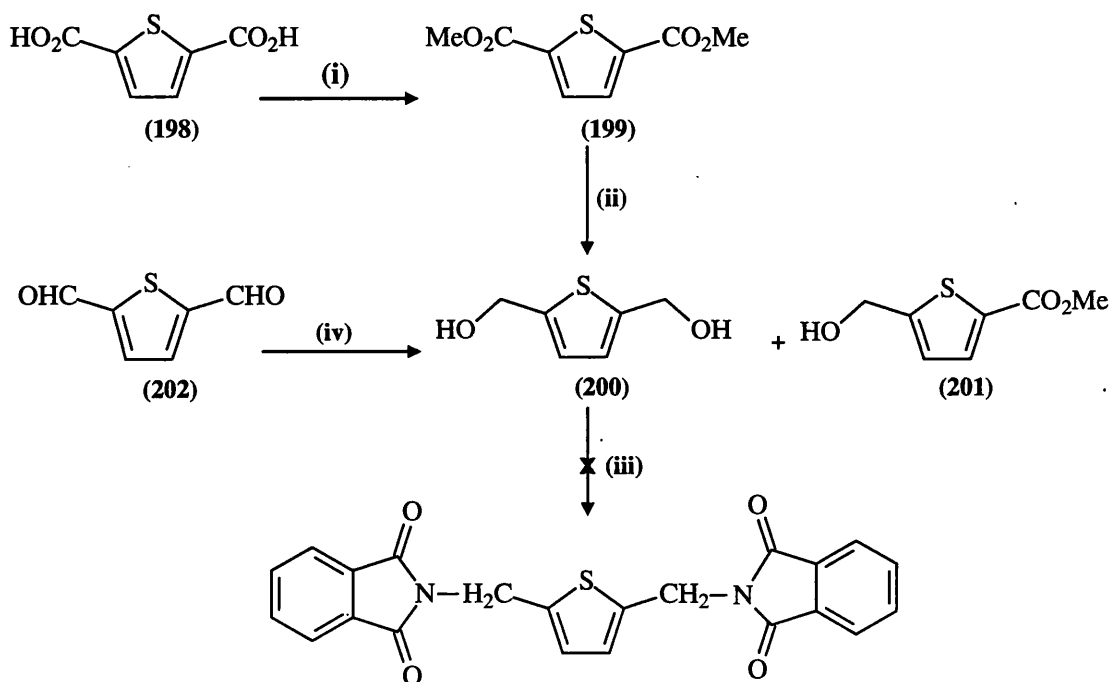
Scheme 5.1 *Chemical synthesis of compound (200). (i) H_2SO_4, MeOH; (ii) A- $LiBH_4$, Dry THF, B- CH_3COCl, Et_3N, C-MeOH, NH_3; (iv) $NaBH_4$, THF.*

An alternative method was the direct reduction of thiophene-2,5-dicarboxaldehyde (202), which is available commercially but is expensive, using the milder reagent $NaBH_4$[210] afforded the diol (200) in 76% yield (Scheme 5.1).

The Mitsunobu reaction provides a convenient route for the synthesis of amines from alcohols through the intermolecular reaction between alcohols and phthalimide on

treatment with diethyl azodicarboxylate (DEAD) and triphenylphosphine under dry conditions.[211] Indeed, the literature preparation of 2,5-bis(aminomethyl)thiophene used this method.[207] However, prolonged treatment of (200) with two equivalents of DEAD, phthalimide and triphenylphosphine failed to give the required bis(phthalimide). The Mitsunobu reaction is very sensitive to traces of water. However, the starting diol (200) is highly viscous and hygroscopic oil which resisted rigorous drying and this may explain the lack of reaction (Scheme 5.1).
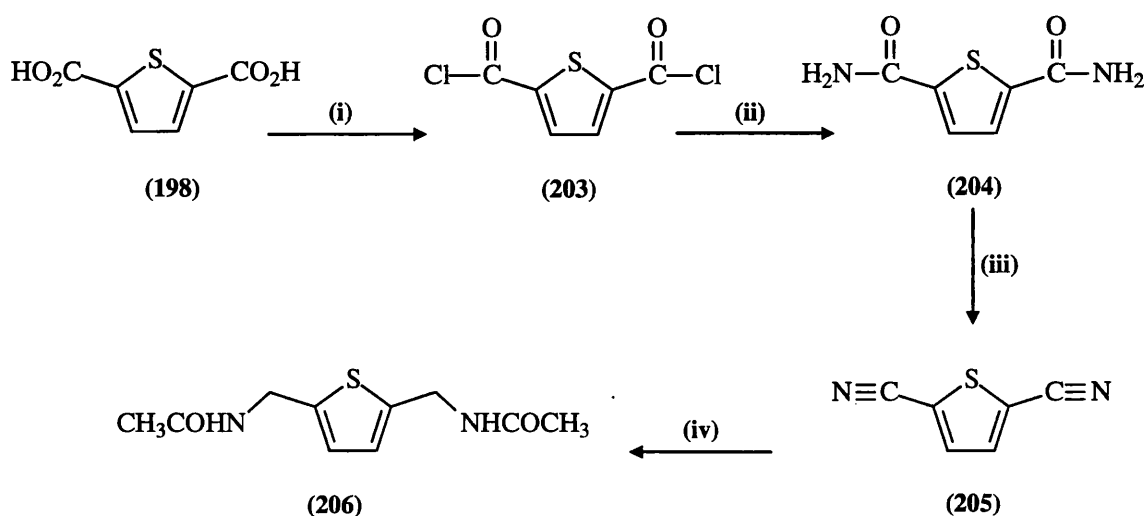
Scheme 5.2 Chemical synthesis of compound (206). (i) $SOCl_2$, DMF; (ii) NH_3, THF; (iii) $POCl_3$; (iv) 1-$BH3.Me_2S$, Dry THF, MeOH; 2- CH_3COCl.

In another approach (Scheme 5.2), the two nitrogens of the target diamine were introduced at the amide oxidation level. The dicarboxylic acid (198) was converted to the bis(acid chloride) (203) with thionyl chloride / DMF. Treatment of crude (203) with ammonia gave the diamide (204) in 74% yield as a white solid. Reduction of (204) was attempted using LiAlH₄ but the diamide was found to be insoluble in the solvents (THF, diethyl ether, 1,2-dimethoxyethane, etc.), which are compatible with this reagent. An attempt to extract the diamine into solution in 1,2-dimethoxyethane using a Soxhlet apparatus for several days was not successful. Alternatively, the diamide (204) was converted to the corresponding dinitrile (205) by dehydration with refluxing POCl₃. This dinitrile (205) is much less polar than the the diamide (204) and was readily soluble in THF. However, reduction using LiAlH₄ failed due to the highly polar nature of the diamine product, which impeded isolation from inorganic lithium aluminium salts. As a result, reduction using borane-methyl sulfide complex, one of the most efficient reagents for the reduction of nitriles,[212]

was used. Treatment of (205) with BH$_3$.Me$_2$S, followed by acetylation of the diamine *in situ*, afforded the diacetamide (206) in 9% yield. Interestingly, the diacetamide (206) was isolated from the aqueous layer.
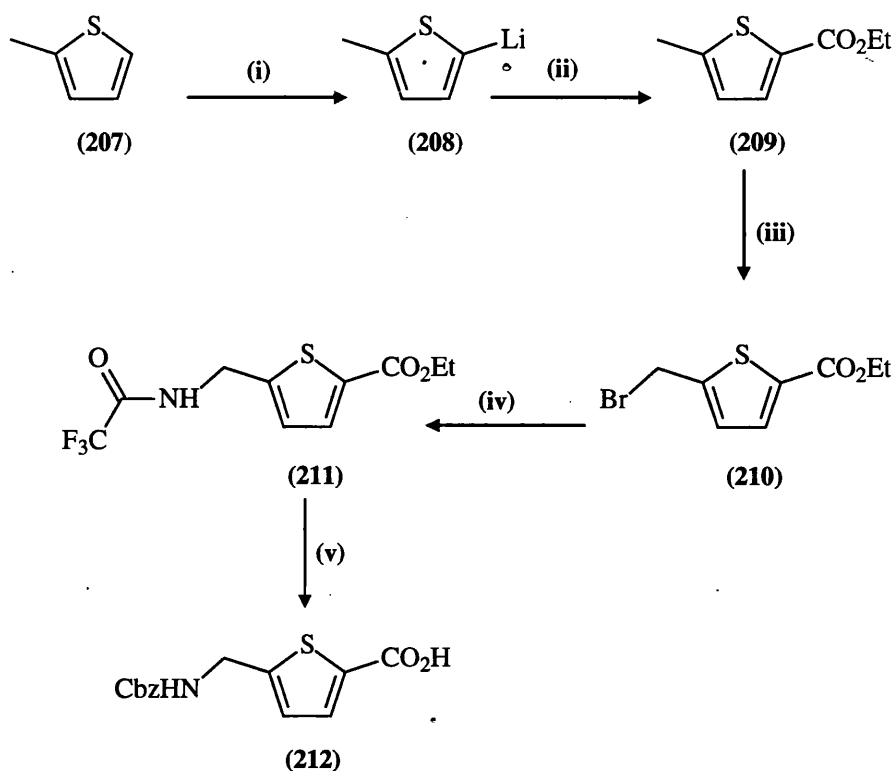
Scheme 5.3 *Chemical synthesis of compound (212). (i) Butyllithium, THF, 0°C;(ii) EtO$_2$CCl, THF, 0°C; (iii) N-bromosuccinimide, aq. HClO$_4$, hexane; (iv) CF$_3$CONH$_2$, KOBu^t, THF; (v) NaOH, H$_2$O, MeOH.*

After these several unsuccessful attempts to synthesise 2,5-bis(aminomethyl)thiophene, new synthetic pathway was investigated (Scheme 5.3). This pathway, although longer, differentiated the 2- and 5- substituents at an early stage. The commercially available 2-methylthiophene (207) was converted to the thienylmetallo compound (208); abstraction of the relatively acidic thiophene 2-proton by butyl lithium would give an appropriate nucleophile for the reaction with a reactive carbonyl electrophile. Lithiation of (207) with butyl lithium at 0°C, followed by quench with ethyl chloroformate (a reactive carboxy electrophile equivalent) gave the required ester (209) in 68% optimised yield. A similar lithiation of (207) with butyl lithium, followed by quenching with methyl chloroformate, afforded a mixture of products. Thus the precise nature of the trapping electrophile was important.[213]

A radical bromination[214] of (209) by treatment with one equivalent of N-bromosuccinimide afforded a mixture of ethyl 5-bromomethylthiophene-2-carboxylate (210), ethyl 4-bromo-5-methylthiophene-2-carboxylate and ethyl 4-bromo-5-bromomethylthiophene-2-carboxylate, in addition to the starting material. Changes in reaction time, solvent and radical initiating agent did not divert the reaction towards side-chain bromination particularly: As the Rf values of these materials are very similar, separation by column chromatography gave pure (210) in the low yield of 13%.

N-Alkylation of the potassium salt of trifluoroacetamide is an alternative to the Gabriel synthesis of primary and secondary amines.[215] These methods were of similar scope but removal of the blocking trifluoroacetyl group is relatively easy. Treatment (210) with the potassium salt of trifluoroacetamide (strong nucleophile) gave the N-alkyltrifluoroacetamide (211) in 62% yield. The trifluoroacetamide group was then hydrolysed with NaOH to the corresponding amine. However, under these alkaline conditions, the ester in (211) also hydrolysed to the corresponding carboxylic acid salt. In the same reaction flask, reaction of resulting amine with benzyl chloroformate was carried out using the Schotten-Baumann technique. In this way, the Cbz protecting group was introduced for the amine. The carboxylic acid salt was converted to the corresponding acid upon acidification of the aqueous layer. Compound (212) was isolated in excellent yield.

Compound (212) (Scheme 5.4) was esterified with methanol in the presence of H_2SO_4 to afford compound (213) in (88%). The Cbz protecting group of (213) was cleaved by treatment with hydrogen bromide[216] to give the amine salt (214). The corresponding free amine was then converted to the isothiocyanate (215) by treatment with two equivalents of thiophosgene in the presence of $CaCO_3$. Ammonia was added across of the electrophilic isothiocyanate to give the thiourea (216) in excellent yield. Treatment of (212) with BH_3.THF complex afforded a mixture of (217) and (218). The alcoholic compound (217) could have been converted to the corresponding amine through mitsunobu reaction.
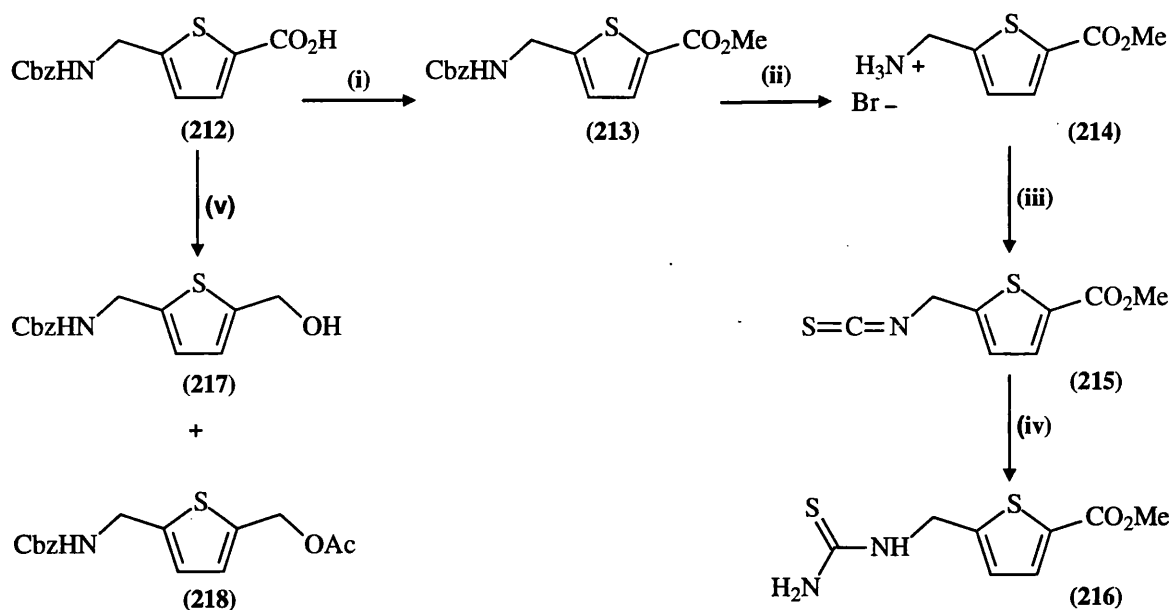
Scheme 5.4   *Chemical synthesis of compound (216). (i) H₂SO₄, MeOH; (ii) 30% HBr in AcOH; (iii) SCCl₂, CaCO₃, H₂O, CHCl₃; (iv) NH₃, CH₂Cl₂; (v) BH₃.THF complex,, THF, AcOH.*

Scheme 5.4   Chemical synthesis of compound (216). (i) H_2SO_4, $MeOH$; (ii) 30% HBr in AcOH; (iii) $SCCl_2$, $CaCO_3$, H_2O, $CHCl_3$; (iv) NH_3, CH_2Cl_2; (v) BH_3.THF complex,, THF, AcOH.

5.4.2   2,4-Disubstituted thiophenes

Retrosynthetic analysis suggested that 3-methylthiophene **(219)** (**Scheme 5.5**) would be an ideal starting material, by analogy with the 2,5-disubstituted series. Detty and Hays[217] have reported two direct approaches for formylation of **(219)** which usually afford mixture of 2,3- and 2,4-disubstituted products. The ratio of the isomers depends on the bulkiness of the substituent at position 3 and on the method of preparation.
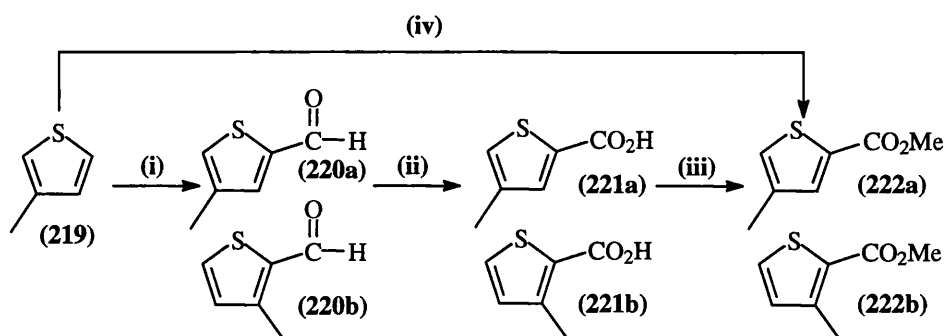
Scheme 5.5   *Chemical synthesis of compound (222a) and (222b). (i) Butylithium, DMF, Et₂O; (ii) Ag₂O, aq. NaOH; (iii) MeOH, H₂SO₄; (iv) Butyllithium, MeO₂CCl, THF, 0°C.*

Scheme 5.5   Chemical synthesis of compound $(222a)$ and $(222b)$. (i) Butylithium, DMF, Et_2O; (ii) Ag_2O, aq. NaOH; (iii) MeOH, H_2SO_4; (iv) Butyllithium, MeO_2CCl, THF, $0°C$.

158

Firstly, standard Vilsmeier reactions led predominantly to the 2,3-disubstituted product (**220b**). For 3-methylthiophene, the preferential site of attack by the electrophilic species is the 2-position, leading predominantly to 2,3-disubstituted products. However, it has been shown that, as the steric bulk of the 3-substituent increases, more of the 2,4-disubstituted products are formed and the 2,3:2,4 ratio decreases.[217] Secondly, lithiation, followed by treatment with dimethylformamide appears to have the opposite regioselectivity and to afford mainly the required (**220a**) isomer. In contrast to the literature report, about successful separation of the two isomers *via* chromatography on silica gel, the mixture of (**220a**) and (**220b**) could not be separated preparatively using various eluant systems.

Thus the sequence proceeded with the mixture of the two isomers. Compounds (**220a,b**) were oxidised by silver oxide to the corresponding acids (**221a,b**). These were esterified with excess methanol and H_2SO_4 to afford a mixture of compounds (**222a,b**) (**Scheme 5.5**). Interestingly, this new lithiation approach also provided a direct synthesis of (**222a,b**), in that the lithiated 3-methylthiophene reacted with methyl chloroformate to give the isomeric esters in approximately the same ratio as of the aldehydes formed by DMF quench of the anion. However, attempts using ethyl chloroformate gave a complex mixture, in contrast to the reaction with lithiated 2-methylthiophene (**Scheme 5.3**).
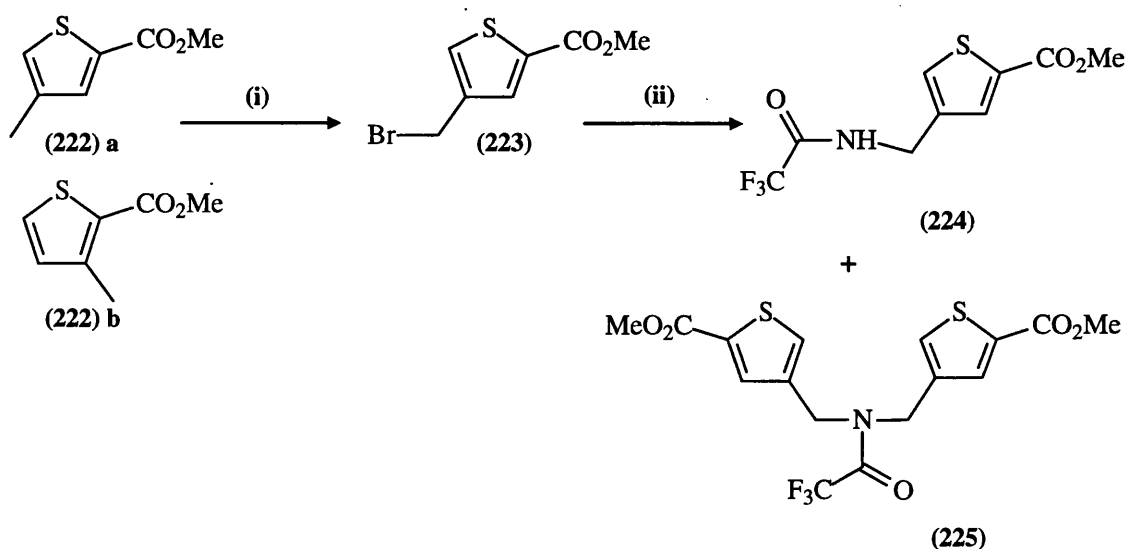
Figure 5.6 *Chemical synthesis of compound (224). (i) N-Bromosuccinimide, Dibenzoyl peroxide, CCl₄; (ii) CF₃CO₂H, KOBuᵗ, THF.*

Side-chain bromination of (222a) was achieved in <50% yield by treatment with one equivalent of N-bromosuccinimide (NBS), using dibenzoyl peroxide[218] as radical initiator. (Scheme 5.6). However, a mixture of unreacted starting material, ring-brominated products, and side-chain brominated (and polybrominated) products were produced. Repeated attempts using two equivalents of NBS gave higher percentages of ring-brominated products. Separation of the mixture *via* chromatography afforded 4.5% of (223). Treatment with the potassium salt of trifluoroacetamide produced a mixture of unreacted starting material, the required secondary amide (224) and the dialkylated trifluoroacetamide (225). Separation by chromatography afforded (224) in 35% yield and (225) in 5% yield (Scheme 5.6). Repeated experiments used a combination of nucleophile and increasing the mixing time, but neither consumed all the starting material, or avoided dialkylation. As a result of the previous low isolated yield of pure (223), treatment of crude (223) with the potassium salt of trifluoroacetamide was investigated and gave an improved overall yield of (224). As expected, the contaminating methyl 3-bromomethylthiophene-2-carboxylate did not react with this nucleophile, allowing easier separation from the product amide (224).

The simultaneous removal of the trifluoroacetyl blocking group and reduction of the ester was attempted using LiBH₄. Ninhydrin indicated the formation of a primary amine but, on work-up, nothing was found in the organic layer. However, the aqueous layer contained a trace of (226) (Scheme 5.7) as white solid mixed with inorganic salts, as shown by NMR.

As for the 2,5-disubstituted series, hydrolysis of the trifluoroacetamide and the ester was carried out simultaneously using sodium hydroxide. In the same reaction flask, a Schotten-Baumann reaction was carried out using benzyl chloroformate, giving, after acid work-up, the Cbz compound (227) in 82% yield. This was esterified with methanol and H_2SO_4 to give the ester (228) in high yield. As before, the protecting Cbz group of (228) was cleaved quantitatively upon treatment with hydrogen bromide[216] in acetic acid. Compound (229) was then converted to the isothiocyanate (230) with thiophosgene in the presence of $CaCO_3$. Reaction of (230) with ammonia gave the thiourea (231) in excellent yield (Scheme 5.7).
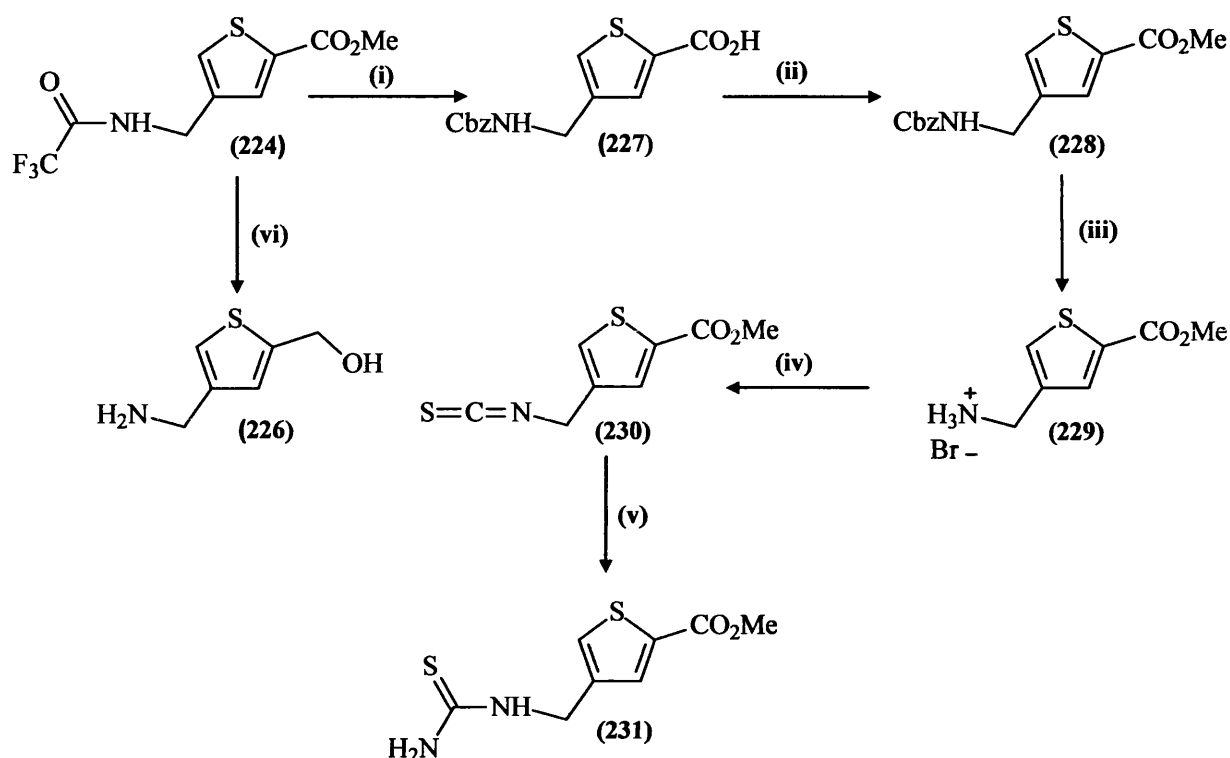
Scheme 5.7 *Chemical synthesis of compound (231). (i) 1- NaOH, H₂O, MeOH, 2-BnO₂CCl; (ii) H₂SO₄, MeOH; (iii) 30% HBr in AcOH; (vi) SCCl₂, CaCO₃, H₂O, CHCl₃; (v) NH₃, CH₂Cl₂; (vi) LiBH₄, THF.*

5.5 Biological Evaluation and conclusion

Neither **(216)** nor **(231)** showed any inhibitory effect against iNOS or cNOS. In contrast, they showed significant stimulatory effects on iNOS, as shown in **(Table 5.1)** below; this stimulation was evident only without preincubation of the enzyme with the agents. These compounds have been evaluated by Dr Claire Goodyer according to the method published previously.[204,219]

The biochemical origin and mechanism of this stimulation is unclear, although a similar but weaker stimulation was reported by Ulhaq *et al.*[204] for S-2-amino-5-(3-nitro-1,2,4-triazol-1-yl)pentanoic acid hydrochloride, S-2-nitro-5-(3-nitro-1,2,4-triazol-1-yl)pentanoic acid hydrochloride and S-2-amino-5-(2-cyanoimidazol-1-yl)pentanoate hydrochloride on iNOS and nNOS and similar stimulatory values were reported recently by Goodyer *et al.*[206] for N-(4-aminophenylmethyl)thiourea, 3-(thioureidomethyl)benzoic acid, and 4-(thiouridomethyl)benzoic acid. Goodyer *el al* have also reported that introduction of an N`-

(2-hydroxyethyl) motif into the methoxyarylthiourea targets introduce an increase in the stimulatory values for the iNOS isoform at a preincubation time of zero.[206]

Furthermore, 3-phenyl-3,4-dihydro-1-isoquinolinamine has been reported to be a weak inhibitor of iNOS and nNOS.[220] However, analogues compounds 6-phenyl-4-amino-6,7-dihydrothienopyridines, in which the benzo ring has been replaced by a thieno ring fusion are potent iNOS and nNOS inhibitors.[221]
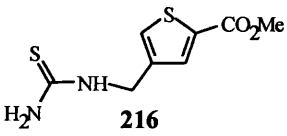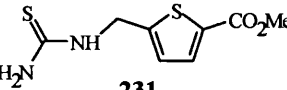
Compound	% Inhibition of iNOS		% Inhibition of cNOS	
	T = 0 min	T = 10 min	T = 0 min	T = 10 min
216	- 62 ± 2	4 ± 3	1 ± 4	- 3 ± 3
231	- 37 ± 27	8 ± 11	- 6 ± 1	- 6 ± 7

Table 5.1 *Inhibition results for compounds (216) and (231) against hiNOS and rat brain cNOS at 100 µM concentration, Values are expressed as means ± SEM (n=2). T=0 refers to no pre-incubation of the compound with the enzyme. T=10 refers to a ten-minute pre-incubation time of the compound with the enzyme.*

From the previous reports on this marked NOS stimulation effects of some compounds, one might expect that these compounds interact with the active site of the enzyme through more than one binding site under different conditions; binding to one site would have a stimulatory effect while binding to the other would have inhibitory effect. The binding to the allosteric stimulatory site is expected to be fast, this would then explain the stimulation effects reported without preincubation.

Interestingly, these compounds may have some therapeutic value in increasing NO biosynthesis. However, the reported switch in this stimulation effect after incubation to a weak inhibition effect may hinder their use in clinical trial.[206]

Experimental

6.1 HPLC instrumentation and conditions

The chromatographic equipment comprised a Dionex autosampler (Model ASl – 100 / ASl – 100T), Dionex pump (Model P 580), Dionex column thermostat for HPLC and GPC (Model 585) and a Dionex UV/VIS detector (Model UVD 170S/340S).

6.2 HPLC Chromatographic conditions

A C_{18} Hypersil (Thermoquest BDS) column (250 × 4.6 mm) was used. The mobile phase was composed of a mixture (65/35, v/v) of acetonitrile and 0.066 M phosphate buffer, adjusted to pH 6.0, pH 7.0, and pH 8.0 with 19 M potassium hydroxide using a Hanaa pH meter (Model 210). The phosphate buffer was filtered in a Vacuubrand GmbH vacuum system (Model ME 4) with a Schleicher and Schuell filter membrane (pore size and diameter of 0.45 and 47mm). The flow rate during the assays was 0.8 ml min^{-1} and detection being accomplished at $\lambda = 275$ nm and $\lambda = 225$ nm. The incubations and analyses were carried out at 37°C. The times between injections varied depending on the speed of drug release.

6.3 Spectroscopic instrumentation

^{1}H NMR spectra were recorded on Varian GX270 or EX400 spectrometers of samples in $CDCl_3$, unless otherwise stated. ^{19}F NMR spectra were referenced to $CFCl_3$. IR spectra were recorded on a Perkin-Elmer 782 spectrometer as KBr discs, unless otherwise stated. Mass spectra were obtained using fast atom bombardment (FAB) ionisation in the positive ion mode, unless otherwise stated. Chromatography was performed with silica 33-70 μm.

6.4 Experimental abbreviations and conditions

DCC refers to dicyclohexylcarbodiimide, THF refers to tetrahydrofuran, DMF refers to dimethylformamide, HOBt refers to 1-hydroxybenzotriazole, DMAP refers to 4-dimethylaminopyridine. THF was dried with Na. Solutions in organic solvents were dried with $MgSO_4$. Solvents were evaporated under reduced pressure. The aqueous $NaHCO_3$ and brine were saturated. Experiments were conducted at ambient temperature, unless

otherwise stated.

R-2,2-Dimethyltetrahydrothiazole-4-carboxylic acid hydrochloride (47)
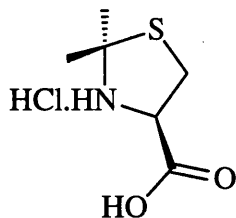
L-Cys.HCl.H$_2$O (3.5 g, 20 mmol) and 2,2-dimethoxypropane (50 mL) was boiled under reflux in acetone (250 mL) for 6 h. The resulting solid was collected by filtration to afford **47** (3.45 g, 87%) as a white solid: mp 125-130°C (lit[135] mp 165-168°C); IR ν_{max} 3412 (NH), 2600, (OH), 1744 (C=O) cm^{-1}; NMR (D$_2$O) δ_H 1.58 (3 H, s, Me), 1.59 (3 H, s, Me), 3.31 (1 H, dd, *J* = 12.1, 8.2 Hz, 5-H), 3.45 (1 H, dd, *J* = 12.1, 8.2 Hz, 5-H), 4.63 (1 H, t, *J* = 8.2 Hz, 4-H).

R-3-(1,1-Dimethylethoxycarbonyl)-2,2-dimethyltetrahydrothiazole-4-carboxylic acid (48)
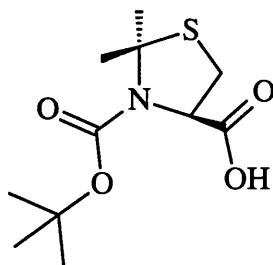
Pr$^i_2$NEt (722 mg, 5.6 mmol) was stirred with **47** (1.0 g, 5.1 mmol) and di-*t*-butyl dicarbonate (1.45 g, 6.6 mmol) in dry MeCN (10 ml) for 2 d. The evaporation residue, in Et$_2$O, was filtered through Celite$^®$. The evaporation residue was dissolved in CH$_2$Cl$_2$ and washed with aq. H$_2$SO$_4$ (100 mM, cold), H$_2$O and brine. Drying, evaporation of the organic layer and recrystallisation of the residue (hexane) afforded **48** (150 mg, 11%) as a white solid: mp 112-114°C (lit[135] mp 114-114.5°C); NMR (CDCl$_3$; 20°C) δ_H 1.43 (4.5 H, brs) and 1.53 (4.5 H, brs) (Bu^t), 1.80 (4.5 H, m) and 1.87 (1.5 H, brs) (2 × Me), 3.1-3.28 (2 H, m, 5-H$_2$), 4.83 (1 H, m) and 4.98 (1 H, m) (4-H); NMR ((CD$_3$)$_2$SO; 20°C) δ_H 1.35 (5.4 H, brs) and 1.43 (3.6 H, brs) (Bu^t), 1.70 (brs) and 1.73 (brs) and 1.75 (brs) (2 × Me), 3.03 (d, *J* = 12.1 Hz) and 3.34 (m) (5-H$_2$), 4.67 (0.6 H, dd, *J* = 4.0, 12.1 Hz) and 4.74 (0.4 H, brd, *J* = 5.0 Hz) (4-H); NMR ((CD$_3$)$_2$SO; 80°C) δ_H 1.41 (9 H, s, Bu^t), 1.73 (3 H, s, 2-Me), 1.77 (3

H, s, 2-Me), 3.05 (1 H, dd, J = 12.1, 3.0 Hz, 5-H), 3.35 (1 H, dd, J = 12.1, 6.9 Hz, 5-H), 4.72 (1 H, dd, J = 6.9, 3.0 Hz, 4-H).

Pentafluorophenyl$R$-3-(1,1-dimethylethoxycarbonyl)-2,2-dimethyltetrahydrothiazole-4-carboxylate (49)
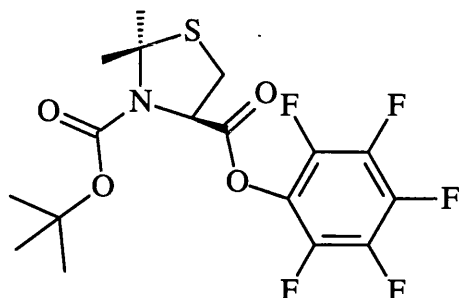
Compound **48** (1.10 g, 4.2 mmol) was stirred with pentafluorophenol (850 mg, 4.6 mmol) and DCC (850 mg, 4.6 mmol) in EtOAc (10 mL) at 0°C under N_2 for 3 h. The mixture was filtered. The solvent was evaporated from the combined filtrate and EtOAc washings. The residue, in hexane, was filtered. Evaporation afforded **49** (1.62 g, 90%) as white needles: mp 107-109°C (lit[135] mp 104-105°C); NMR δ_H 1.46 (6.3 H, s, Bu^t), 1.52 (2.7 H, s, Bu^t), 1.80 (0.9 H, s, 2-Me), 1.83 (3 H, s, 2-Me), 1.90 (2.1 H, s, 2-Me), 3.28 (0.7 H, brd, J = 12.5 Hz, 5-H), 3.41 (0.3 H, m, 5-H), 3.47 (1 H, dd, J = 12.5, 7.0 Hz, 5-H), 4.05 (0.3 H, m, 5-H), 5.18 (0.7 H, dd, J = 6.6, 1.6 Hz, 4-H), 5.26 (0.3 H, dd, J = 6.6, 2.3 Hz, 4-H); NMR δ_F -162.2 (0.3 F, m, 4'-F), -161.8 (0.7 F, m, 4'-F), -157.8 (0.6 F, dd, J = 21.1, 17.2 Hz, 3',5'-F_2), -157.3 (1.4 F, dd, J = 21.1, 17.2 Hz, 3',5'-F_2), -152.6 (1.4 F, d, J = 17.2 Hz, 2',6'-F_2), -151.90 (0.6 F, d, J = 17.2 Hz, 2',6'-F_2).

R-2,2-Dimethyl-3-(1,1-dimethylethoxycarbonyl)-N-(2-(4-nitrophenyl)ethyl)tetrahydrothiazole-4-carboxamide (50)
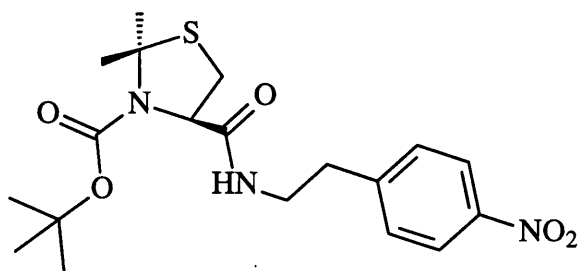
4-Nitrophenylethylamine hydrochloride (85 mg, 420 µmol) was stirred with Et_3N (85 mg, 840 µmol) and **49** (180 mg, 420 µmol) in CH_2Cl_2 (2.0 mL) for 2 h. Evaporation and chromatography (CHCl$_3$ / MeOH 9:1) afforded **50** (160 mg, 93%) as a viscous yellow oil:

IR (Nujol) v_{max} 3325 (NH), 1681 (C=O), 1519 (NO$_2$), 1346 (NO$_2$) cm^{-1}; NMR δ_H 1.43 (9 H, s, Bu^t), 1.70 (3 H, s, 2-Me), 1.75 (3 H, s, 2-Me), 2.95 (2 H, m, ArCH$_2$), 3.23 (2 H, m, 5-H$_2$), 3.53 (1 H, m) and 3.68 (1 H, m) (NHCH$_2$), 4.74 (1 H, m, 4-H), 7.42 (2 H, d, J = 8.6 Hz, Ar 2,6-H$_2$), 8.18 (2 H, d, J = 8.6 Hz, Ar 3,5-H$_2$); NMR δ_C 19.6, 28.7, 36.0, 40. 7, 67.5, 82.0, 93.7, 110.0, 124.0, 129.9, 146.9, 171.3; MS m/z 410.1764 (M + H) (C$_{19}$H$_{28}$N$_3$O$_5$S requires 410.1750), 354 (M -Me$_2$C=CH$_2$), 336 (M - Bu^{t}O), 310 (M - Boc); Found: H, 6.59; N, 9.94. C$_{19}$H$_{27}$N$_3$O$_5$S requires H, 6.65; N, 10.27%.

R-2,2-Dimethyl-N-(2-(4-nitrophenyl)ethyl)tetrahydrothiazole-4-carboxamide tri-fluoroacetate (51)
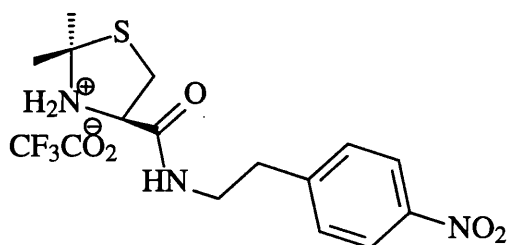
Compound **50** (1.30 g, 3.2 mmol) was stirred with CF$_3$CO$_2$H (20 mL) and CH$_2$Cl$_2$ (10 mL) for 2 h. Evaporation afforded **51** (1.35 g, quant.) as a highly hygroscopic viscous oil: NMR δ_H 1.82 (3 H, s, 2-Me), 1.93 (3 H, s, 2-Me), 2.97 (2 H, m, ArCH$_2$), 3.20 (1 H, dd, J = 12.5, 6.2 Hz, 5-H), 3.59 (1 H, dd, J = 12.5, 8.2 Hz, 5-H), 3.64 (2 H, m, NHCH$_2$), 5.22 (1 H, dd, J = 8.2, 6.2 Hz, 4-H), 7.35 (2 H, d, J = 8.6 Hz, Ar 2,6-H$_2$), 7.56 (1 H, brt, J = 5.9 Hz, NH), 8.15 (2 H, d, J = 8.6 Hz, Ar 3,5-H$_2$), 9.76 (3 H, br, N$^+$H$_2$); MS m/z 310.1238 (M + H) (C$_{14}$H$_{20}$N$_3$O$_3$S requires 310.1225).

tert-Butyl N-(fluorocarbonylmethyl)carbamate (52)
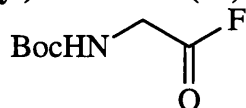
BocGlyOH (1.0 g, 5.7 mmol) was stirred with pyridine (450 mg, 5.7 mmol) in dry CH$_2$Cl$_2$ (30 mL) and added slowly to cyanuric fluoride (1.54 g, 11.4 mmol) in dry CH$_2$Cl$_2$ (10 mL), then stirred for 3 h. The mixture was washed with ice-water (3 × 50 mL). Drying and evaporation afforded crude **52** (800 mg): NMR δ_H 1.47 (9 H, s, Bu^t), 4.11 (2 H, t, J = 5.5 Hz, CH$_2$), 5.05 (1 H, br, NH); NMR δ_F 30.21 (1 F, s, CO$_2$F).

tert-Butyl S-N-(1-fluorocarbonyl-2-methylpropyl)carbamate (54)
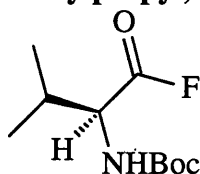
BocValOH (2.5 g, 11 mmol) was stirred with pyridine (910 mg, 11.5 mmol) in dry CH_2Cl_2 (30 mL) and added slowly to cyanuric fluoride (3.1 g, 23.0 mmol) in dry CH_2Cl_2 (30 mL). Stirring continued under nitrogen at -10°C for 2 h. The mixture was washed with ice-water (3 × 100 mL). Drying and evaporation afforded crude **54** (2.22 g) as a white solid: mp 38-42°C (lit[136] mp 36-38°C); NMR δ_H 0.99 (3 H, d, J = 7.0 Hz, Val-Me), 1.04 (3 H, d, J = 6.6 Hz, Val-Me), 1.46 (9 H, s, Bu^t), 2.25 (1 H, m, Val β-H), 4.40 (1 H, dd, J = 8.6, 4.7 Hz, Val α-H), 4.96 (1 H, brd, NH); NMR δ_F 32.29 (1 F, s, CO_2F)

tert-Butyl S-N-(1-fluorocarbonyl-2-phenylethyl)carbamate (55)
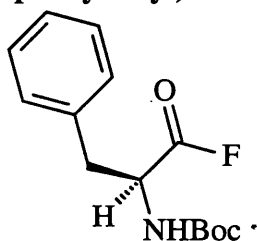
BocPheOH (2.5 g, 9.4 mmol) was stirred with pyridine (744 mg, 9.4 mmol) in dry CH_2Cl_2 (30 mL) and added slowly to cyanuric fluoride (2.54 g, 18.80 mmol) in dry CH_2Cl_2 (30 mL). The mixture was stirred under nitrogen at -10°C for 2 h. The mixture was washed with ice-water (3 × 100 mL). Drying and evaporation afforded crude **55** (1.53 g, 57 %): NMR δ_H 1.42 (9 H, s, Bu^t), 3.15 (1 H, dd, J = 14.4, 6.0 Hz, Phe β-H), 3.17 (1 H, dd, J = 14.4, 6.0 Hz, Phe β-H), 4.74 (1 H, brd, J = 6.0 Hz, Phe α-H), 4.86 (1 H, d, J = 6.6 Hz, NH), 7.10-7.30 (5 H, m, $Ph-H_5$); NMR δ_F 29.21 (1 F, s, CO_2F).

R-2,2-Dimethyl-3-(N-(1,1-dimethylethoxycarbonyl)glycyl)tetrahydrothiazole-4-carboxylic acid (56)
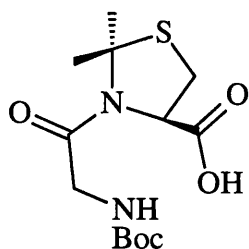
BocGlyF[53] (810 mg, 4.6 mmol) was stirred with **47** (1.00 g, 5.1 mmol) and Pr$^i_2$NEt (1.24 g, 9.6 mmol) in dry DMF (100 mL) for 3 h. The evaporation residue, in EtOAc, was washed with cold 5% aq. citric acid and brine. Drying, evaporation and chromatography (EtOAc / Et$_2$O / AcOH 13:6:1) afforded **56** (560 mg, 35%) as a pale buff solid: mp 152-155°C: IR v_{max} 3385 (NH), 2933 (OH), 1748 (C=O), 1672 (C=O), 1625 (amide I), 1539 (amide II) cm^{-1}; NMR ((CD$_3$)$_2$SO) δ_H 1.38 (9 H, s, Bu^t), 1.74 (3 H, s, 2-Me), 1.76 (3 H, s, 2-Me), 3.28 (2 H, m, 5-H$_2$), 3.50 (1 H, dd, J = 17.0, 6.2 Hz) and 3.87 (1 H, dd, J = 17.0, 5.5 Hz) (Gly-H$_2$), 5.10 (1 H, m, 4-H), 6.78 (1 H, t, J = 6 Hz, NH); MS m/z 319.1339 (M + H) (C$_{13}$H$_{23}$N$_2$O$_5$S requires 319.1328), 263 (M - Me$_2$C=CH$_2$); Found: C, 47.80; H, 6.72; N, 8.85; C$_{13}$H$_{22}$N$_2$O$_5$S 0.5H$_2$O requires C, 47.99; H, 6.51; N, 8.61%.

tert-Butyl S-N-(1-(fluorocarbonyl)ethyl)carbamate (53) and R-2,2-dimethyl-3-(N-(1,1-dimethylethoxycarbonyl)-L-alanyl)tetrahydrothiazole-4-carboxylic acid (57)
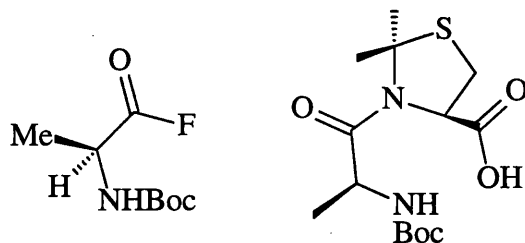
BocAlaOH (2.0 g, 11 mmol) was stirred with pyridine (840 mg, 10.6 mmol) in dry CH$_2$Cl$_2$ (30 mL) and added slowly to cyanuric fluoride (2.86 g, 21.1 mmol) in dry CH$_2$Cl$_2$ (30 mL). Stirring continued for 3 h. The mixture was washed with ice-water (3 × 100 mL). Drying and evaporation afforded crude **53** (1.74 g) as a white solid. This material (1.74 g, 9.1 mmol) was stirred with **47** (2.0 g, 10 mmol) and Pr$^i_2$NEt (2.5 g, 19 mmol) in dry DMF (100 mL) for 16 h. The evaporation residue, in EtOAc, was washed with cold 5% aq. citric acid and brine. Drying, evaporation and chromatography (EtOAc / Et$_2$O / AcOH 49:49:2) afforded **57** (680 mg, 30% from **47**) as a pale yellow solid: mp 93-94°C: IR v_{max} 3338 (NH), 1705 (C=O), 1655 (amide I), 1534 (amide II) cm^{-1}; NMR δ_H 1.31 (3 H, d, J = 6.8

Hz, Ala β-H₃), 1.40 (9 H, s, Buᵗ), 1.81 (3 H, s, 2-Me), 1.92 (3 H, s, 2-Me), 3.24 (1 H, dd, J = 12.1, 5.5 Hz, 5-H), 3.45 (1 H, d, J =12.1 Hz, 5-H), 4.53 (1 H, qn, J = 6.8 Hz, Ala α-H), 4.85 (1 H, d, J = 5.1 Hz, 4-H), 5.68 (1 H, d, J = 7.8 Hz, NH); MS m/z 333.1489 (M + H) ($C_{14}H_{25}N_2O_5S$ requires 333.1484), 277 (M - $Me_2C=CH_2$), 259 (M -Bu^tO).

R-2,2-Dimethyl-3-(N-(1,1-dimethylethoxycarbonyl)-L-valinyl)tetrahydrothiazole-4-carboxylic acid (58)
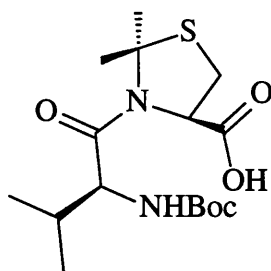
BocValF (1.61 g, 6.8 mmol) was stirred with **47** (1.50 g, 7.6 mmol) and Pr$^i_2$NEt (1.87 g, 14.4 mmol) in dry DMF (100 mL) for 16 h. The evaporation residue, in EtOAc, was washed with cold 5% aq. citric acid, cold H₂O and brine. Drying, evaporation and chromatography (hexane / EtOAc / AcOH 70:29:1) afforded **58** (730 mg, 27%) as a gummy solid: IR v_{max} 3338 (NH), 1705 (C=O), 1655 (amide I), 1534 (amide II) cm^{-1}; NMR δ_H 0.90 (3 H, d, J = 7.0 Hz, Val-Me), 1.0 (3 H, d, J = 6.6 Hz, Val-Me), 1.39 (9 H, s, Buᵗ), 1.82 (3 H, s, 2-Me), 1.88 (1 H, m, Val β-H), 1.92 (3 H, s, 2-Me), 3.21 (1 H, dd, J = 12.1, 5.3 Hz, 5-H), 3.44 (1 H, d, J =12.1 Hz, 5-H), 4.50 (1 H, dd, J = 9.4, 5.5 Hz, Val α-H), 5.02 (1 H, d, J = 5.3 Hz, 4-H), 5.60 (1 H, d, J = 9.4 Hz, NH), 8.52 (1 H, br, OH); MS m/z 361.1822 (M + H) ($C_{16}H_{29}N_2O_5S$ requires 361.1797), 305 (M - $Me_2C=CH_2$), 261 (M -Boc).

R-2,2-Dimethyl-3-(N-(1,1-dimethylethoxycarbonyl)-L-phenylalanyl)tetrahydro-thiazole-4-carboxylic acid (59)
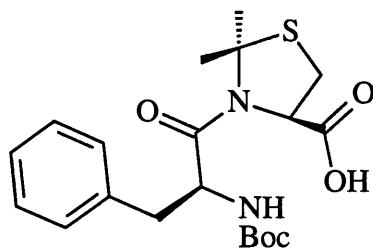
BocPheF (1.53 g, 5.4 mmol) was stirred with **47** (1.20 g, 6.0 mmol) and Pr$^i_2$NEt (1.47 g, 11.4 mmol) in dry DMF (100 mL) for 16 h. The evaporation residue, in EtOAc, was washed with cold 5% aq. citric acid and brine. Drying, evaporation and chromatography

(EtOAc / AcOH 99:1) afforded **59** (920 mg, 30%) as a pale yellow gum: NMR δ_H 1.29 (9 H, s, Bu^t), 1.68 (3 H, s, 2-Me), 1.77 (3 H, s, 2-Me), 2.80 (1 H, dd, J = 13.3, 7.1 Hz, Phe β-H), 2.88 (1 H, dd, J = 13.3, 6.1 Hz, Phe β-H), 2.97 (1 H, dd, J = 11.7, 5.9 Hz, 5-H), 3.12 (1 H, d, J = 11.7 Hz, 5-H), 4.34 (1 H, ddd, J = 9.0, 7.1, 6.1 Hz, Phe α-H), 4.68 (1 H, d, J = 5.9 Hz, 4-H), 6.50 (1 H, d, J = 9.0 Hz, NH), 7.26 (5 H, m, Ph-H$_5$); MS m/z 409.1812 (M + H) (C$_{20}$H$_{29}$N$_2$O$_5$S requires 409.1797), 353 (M - Me$_2$C=CH$_2$), 335 (M - Bu^{t}O), 309 (M – Boc).

Pentafluorophenyl   ***R*-2,2-dimethyl-3-(N-(1,1-dimethylethoxycarbonyl)glycyl)-tetrahydrothiazole-4-carboxylate (60)**
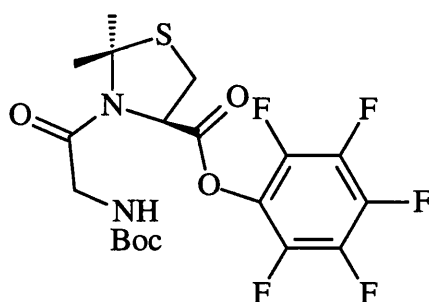
Compound **56** (450 mg, 1.4 mmol) was stirred with pentafluorophenol (290 mg, 1.6 mmol) and DCC (330 mg, 1.6 mmol) in EtOAc (5.0 mL) at 0°C under N$_2$ for 3 h. The mixture was filtered (Celite$^\circledR$) and the solid was washed with cold EtOAc. The evaporation residue, in hexane, was kept at 4°C for 16 h and filtered. Evaporation gave **60** (700 mg, 92%) as a colourless oil: NMR δ_H 1.45 (9 H, s, Bu^t), 1.88 (3 H, s, 2-Me), 1.92 (3 H, s, 2-Me), 3.45 (1 H, dd, J = 12.5, 5.5 Hz, 5-H), 3.51 (1 H, d, J = 12.1 Hz, 5-H), 3.67 (1 H, dd, J = 17.2, 3 Hz) and 4.13 (1 H, dd, J = 17.2, 6.6 Hz) (Gly-H$_2$), 5.20 (1 H, d, J = 5.3 Hz, 4-H), 5.37 (1 H, br, NH); NMR δ_F -161.3 (2 F, m, 3',5'-F$_2$), -156.4 (1 F, t, J = 21.4 Hz, 4'-F), -152.0 (2 F, d, J = 16.8 Hz, 2',6'-F$_2$); MS m/z 485.1185 (M + H) (C$_{19}$H$_{22}$F$_5$N$_2$O$_5$S requires 485.1170), 429 (M - Me$_2$C=CH$_2$), 411 (M - Bu^{t}O), 385 (M - Boc).

Pentafluorophenyl   R-2,2-dimethyl-3-(N-(1,1-dimethylethoxycarbonyl)-L-alanyl)-tetrahydrothiazole-4-carboxylate (61)
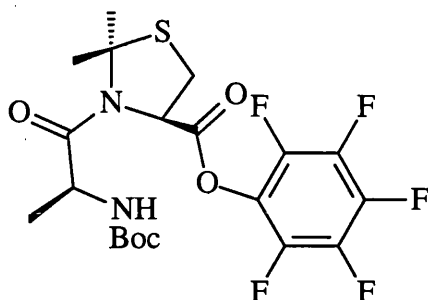
Compound **57** (400 mg, 1.2 mmol) was stirred with pentafluorophenol (240 mg, 1.3 mmol) and DCC (270 mg, 1.3 mmol) in EtOAc (10 mL) at 0°C under N_2 for 3 h. The mixture was filtered (Celite®) and the solid was washed with cold EtOAc. The evaporation residue, in hexane, was kept at 4°C for 16 h and filtered. Evaporation gave **61** (530 mg, 89%) as a colourless oil: NMR δ_H 1.36 (2.1 H, d, J = 6.6 Hz, Ala β-H$_3$), 1.37 (0.9 H, d, J = 6.6 Hz, Ala β-H$_3$), 1.39 (6.3 H, s, Bu^t), 1.43 (2.7 H, s, Bu^t), 1.85 (2.1 H, s, 2-Me), 1.94 (2.1 H, s, 2-Me), 2.05 (0.9 H, s, 2-Me), 2.09 (0.9 H, s, 2-Me), 3.33 (0.3 H, dd, J = 12.7, 2.9, 5-H), 3.40 (0.7 H, dd, J = 12.5, 5.5 Hz, 5-H), 3.46 (0.3 H, m, 4-H), 3.49 (0.7 H, d, J = 12.1 Hz, 4-H), 4.39 (0.7 H, qn, J = 7 Hz, Ala α-H), 4.79 (0.3 H, qn, J = 7 Hz, Ala α-H), 5.19 (0.7 H, d, J = 5.5 Hz, 4-H), 5.24 (0.3 H, br, NH), 5.40 (0.7 H, d, J = 7.8 Hz, NH), 5.57 (0.3 H, dd, J = 6.6, 3.1 Hz, 4-H); NMR δ_F –161.7 (0.6 F, m, 3',5'-F$_2$), -161.6 (1.4 F, dt, J = 21.0, 18.4 Hz, 3',5'-F$_2$), -157.1 (0.3 F, t, J = 21.0 Hz, 4'-F), -156.7 (0.7 F, t, J = 21.0 Hz, 4'-F), -151.9 (0.6 F, d, J = 17.1 Hz, 2',6'-F$_2$), -150.8 (1.4 F, d, J = 17.1 Hz, 2',6'-F$_2$); MS m/z 499.1335 (M + H) ($C_{20}H_{24}F_5N_2O_5S$ requires 499.1326), 443 (M - Me$_2$C=CH$_2$), 425 (M - Bu^{t}O).

Pentafluorophenyl   2,2-dimethyl-3-(N-(1,1-dimethylethoxycarbonyl)-L-valinyl)tetra-hydrothiazole-4-carboxylate (62)
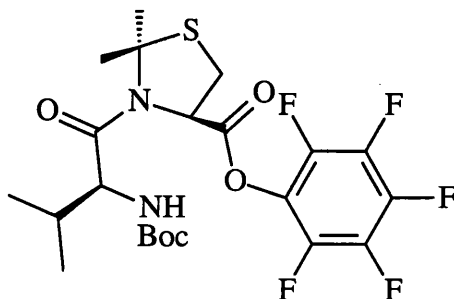
Compound **58** (500 mg, 1.4 mmol) was stirred with pentafluorophenol (280 mg, 1.5 mmol) and DCC (320 mg, 1.5 mmol) in EtOAc (10 mL) at 0°C under N_2 for 3 h. The mixture was

filtered (Celite®) and the solid was washed with cold EtOAc. The evaporation residue, in hexane, was kept at 4°C for 16 h and filtered. Evaporation gave **62** (680 mg, 93%) as a colourless oil: IR v_{max} 3440 (NH), 1718 (C=O), 1669 (amide I), 1521 (amide II) cm^{-1}; NMR δ_H 0.94 (2.1 H, d, J = 6.6 Hz, Val-Me), 0.99 (2.1 H, d, J = 6.6 Hz, Val-Me), 1.03 (0.9 H, d, J = 7.0 Hz, Val-Me), 1.10 (0.9 H, d, J = 7.0 Hz, Val-Me), 1.33 (6.3 H, s, Bu^t), 1.43 (2.7 H, s, Bu^t), 1.86 (2.1 H, s, 2-Me), 1.91 (0.7 H, m, Val β-H), 1.95 (2.1 H, s, 2-Me), 1.99 (1.8 H, s, 2 × 2-Me), 3.32 (0.3 H, dd, J = 12.5, 3.5 Hz, 5-H), 3.40 (0.7 H, dd, J = 12.1, 5.1 Hz, 5-H), 3.44 (0.3 H, d, J = 12.5, 6.4 Hz, 5-H), 3.50 (0.7 H, d, J = 12.1 Hz, 5-H), 4.28 (0.7 H, dd, J = 9.0, 6.2 Hz, Val α-H), 4.54 (0.3 H, dd, J = 9.8, 6.2 Hz, Val α-H), 5.12 (0.3 H, d, J = 10.2 Hz, NH), 5.24 (0.7 H, d, J = 9.0 Hz, NH), 5.38 (0.7 H, d, J = 5.1 Hz, 4-H), 5.62 (0.3 H, dd, J = 6.4, 3.5 Hz, 4-H); NMR δ_F -161.9 (1.4 F, dd, J = 22.4, 18.4 Hz, 3',5'-F$_2$), -161.6 (0.6 F, dd, J = 21.0, 17.1 Hz, 3',5'-F$_2$), -157.1 (0.7 F, dt, J = 22.4 Hz, 4'-F), -152.6 (0.3 F, d, J = 17.1 Hz, 4'-F), -151.8 (0.6 F, d, J = 17.1 Hz, 2',6'-F$_2$), -150.3 (1.4 F, d, J = 18.4 Hz, 2',6'-F$_2$); MS m/z 527.1660 (M + H) (C$_{22}$H$_{28}$F$_5$N$_2$O$_5$S requires 527.1639), 471 (M - Bu^{t}O), 427 (M – Boc), 328 (M – BocVal).

Pentafluorophenyl *R*-**2,2-dimethyl-3-(N-(1,1-dimethylethoxycarbonyl)-L-phenyl-alanyl)tetrahydrothiazole-4-carboxylate (63)**
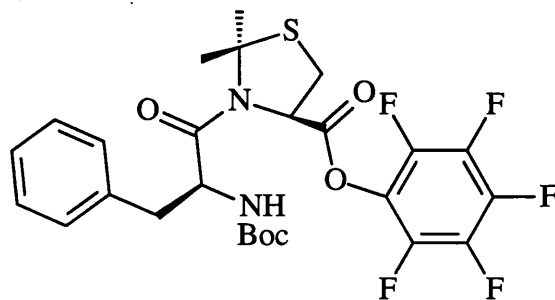
Compound **59** (400 mg, 1.0 mmol) was stirred with pentafluorophenol (150 mg, 800 μmol) and DCC (170 mg, 810 μmol) in EtOAc (10 mL) at 0°C under N$_2$ for 3 h. The mixture was filtered (Celite®) and the solid was washed with cold EtOAc. The evaporation residue, in hexane, was kept at 4°C for 16 h and filtered. Evaporation gave **63** (390 mg, 92%) as a white solid: mp 35-36°C: IR v_{max} 3442 (NH), 1792 (C=O), 1716 (C=O), 1659 (amide I), 1523 (amide II) cm^{-1}; NMR δ_H 1.39 (9 H, s, Bu^t), 1.77 (3 H, s, 2-Me), 1.86 (3 H, s, 2-Me), 2.40 (1 H, dd, J = 12.5, 5.5 Hz, 5-H), 2.89 (1 H, dd, J = 12.5, 10.9 Hz, Phe β-H), 3.00 (1 H, d, J = 12.5 Hz, 5-H), 3.25 (1 H, dd, 12.5, 3.9 Hz, Phe β-H), 4.37 (1 H, d, J = 5.5 Hz, 4-H), 4.51 (1 H, m, Phe α-H), 5.42 (1 H, d, J = 7.8 Hz, NH), 7.33 (5 H, m, Ph-H$_5$); NMR δ_F –

161.8 (2 F, dd, J = 21.0, 17.1 Hz, 3',5'-F$_2$), -156.9 (1 F, t, J = 21.0 Hz, 4'-F), -150.7 (1 F, d, J = 18.4 Hz, 2',6'-F$_2$); MS m/z 575.1635 (M + H) (C$_{26}$H$_{28}$F$_5$N$_2$O$_5$S requires 575.1639), 519 (M - Me$_2$C=CH$_2$), 501 (M - Bu^{t}O), 475 (M – Boc).

R-2,2-Dimethyl-3-(N-(1,1-dimethylethoxycarbonyl)glycyl)-N-(2-(4-nitrophenyl)ethyl)-tetrahydrothiazole-4-carboxamide (64)
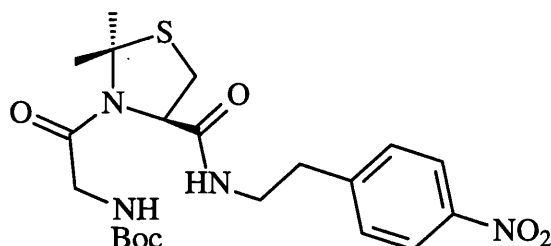
4-Nitrophenylethylamine hydrochloride (270 mg, 1.3 mmol) was stirred with Et$_3$N (270 mg, 2.7 mmol) and **60** (650 mg, 1.3 mmol) in CH$_2$Cl$_2$ (5.0 mL) for 2 h. Evaporation and chromatography (EtOAc) afforded **64** (470 mg, 76%) as a white solid: mp 65-66°C; NMR ((CD$_3$)$_2$SO) δ_H 1.38 (9 H, s, Bu^t), 1.72 (3 H, s, 2-Me), 1.74 (3 H, s, 2-Me), 2.91 (2 H, t, J = 7.4 Hz, ArCH$_2$), 3.10 (1 H, d, J = 12.9 Hz, 5-H), 3.20 (1 H, dd, J = 16.4, 5.5 Hz, Gly-H), 3.31 (1 H, m, 5-H), 3.39 (1 H, m) and 3.47 (1 H, m) (NHCH$_2$), 3.67 (1 H, dd, J = 16.4, 5.5, Gly-H), 4.79 (1 H, d, J = 5.5 Hz, 4-H), 6.67 (1 H, t, J = 5.5 Hz, Gly-NH), 7.50 (2 H, d, J = 8.8 Hz, Ar 2,6-H$_2$), 8.07 (1 H, t, J = 5.5 Hz, NH), 8.13 (2 H, d, J = 8.8 Hz, Ar 3,5-H$_2$); MS m/z 467.1943 (M + H) (C$_{21}$H$_{31}$N$_4$O$_6$S requires 467.1964), 411 (M - Me$_2$C=CH$_2$), 393 (M - Bu^{t}O), 367 (M -Boc).

R-2,2-Dimethyl-3-(N-(1,1-dimethylethoxycarbonyl)-L-alanyl)-N-(2-(4-nitrophenyl)-ethyl)tetrahydrothiazole-4-carboxamide (65)
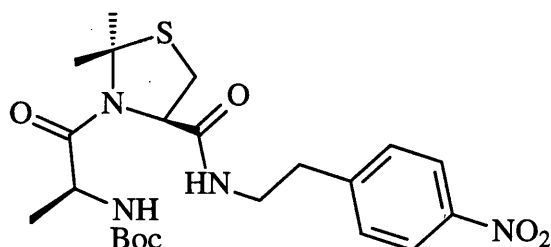
4-Nitrophenylethylamine hydrochloride (210 mg, 1.1 mmol) was stirred with Et$_3$N (210 mg, 2.1 mmol) and **61** (530 mg, 1.1 mmol) in CH$_2$Cl$_2$ (5.0 mL) for 2 h. Evaporation and chromatography (EtOAc / hexane 4:1) afforded **65** (380 mg, 75%) as a white solid: mp 156-158°C: IR v_{max} 3319 (NH), 1696 (C=O), 1657 (C=O), 1601 (amide I), 1520 (amide II)

cm^{-1}; NMR ((CD$_3$)$_2$SO) δ_H 1.12 (3 H, d, J = 7.0 Hz, Ala β-H$_3$), 1.37 (9 H, s, Bu^t), 1.61 (3

H, s, 2-Me), 1.71 (3 H, s, 2-Me), 2.95 (2 H, m, ArCH$_2$), 3.24 (1 H, dd, J =12.1, 5.5 Hz, 5-

H), 3.32 (2 H, m, 5-H and ArCH$_2$CH), 3.53 (1 H, m, ArCH$_2$CH), 3.84 (1 H, m, Ala α-H),

4.73 (1 H, d, J = 5.5 Hz, 4-H), 7.06 (1 H, d, J =5.9 Hz, NH), 7.49 (2 H, d, J = 8.8 Hz, Ar

2,6-H$_2$), 8.13 (2 H, d, J = 8.8 Hz, Ar 3,5-H$_2$) 8.13 (1 H, br, NH); MS m/z 481.2142 (M + H)

(C$_{22}$H$_{33}$N$_4$O$_6$S requires 481.2121), 425 (M - Me$_2$C=CH$_2$), 381 (M - Boc).

**R-2,2-Dimethyl-3-(1,1-dimethylethoxycarbonyl)-L-valinyl)-N-(2-(4-nitro-
phenyl)ethyl)tetrahydrothiazole-4-carboxamide (66)**
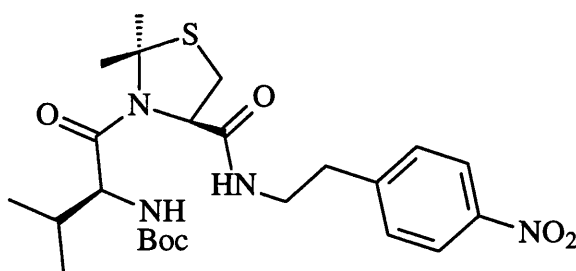
4-Nitrophenylethylamine hydrochloride (230 mg, 1.1 mmol) was stirred with Et$_3$N (230

mg, 2.3 mmol) and **62** (600 mg, 1.1 mmol) in CH$_2$Cl$_2$ (7.0 mL) for 2 h. Evaporation and

chromatography (EtOAc / hexane 1:1) afforded **66** (420 mg, 73%) as a white solid: mp

233.8°C (DSC); IR v_{max} 3331 (NH), 1700 (C=O), 1653 (amide I), 1519 (amide II) cm^{-1};

NMR δ_H 0.95 (3 H, d, J = 6.6 Hz, Val-Me), 1.01 (3 H, d, J = 6.6 Hz, Val-Me), 1.44 (9 H, s,

Bu^t), 1.65 (3 H, s, 2-Me), 1.81 (3 H, s, 2-Me), 1.87 (1 H, m, Val β-H), 3.02 (2 H, m,

ArCH$_2$), 3.12 (1 H, dd, J = 12.1, 5.5 Hz, 5-H), 3.50 (1 H, m, ArCH$_2$CH), 3.63 (1 H, d, J =

12.1 Hz, 5-H), 3.75 (1 H, m, Val α-H), 3.79 (1 H, m, ArCH$_2$CH), 4.67 (1 H, d, J =5.5 Hz,

4-H), 4.90 (1 H, d, J = 7.8 Hz, NHBoc), 7.38 (2 H, d, J = 8.8 Hz, Ar 2,6-H$_2$), 7.98 (1 H, br,

NHCH$_2$), 8.14 (2 H, d, J = 8.8 Hz, Ar 3,5-H$_2$); MS m/z 509.2434 (M + H) (C$_{24}$H$_{37}$N$_4$O$_6$S

requires 509.2434), 453 (M - Bu^{t}O), 409 (M - Boc), 310 (M – BocVal).

R-2,2-Dimethyl-3-(N-(1,1-dimethylethoxycarbonyl)-L-phenylalanyl)-N-(2-(4-nitro-phenyl)ethyl)tetrahydrothiazole-4-carboxamide (67)
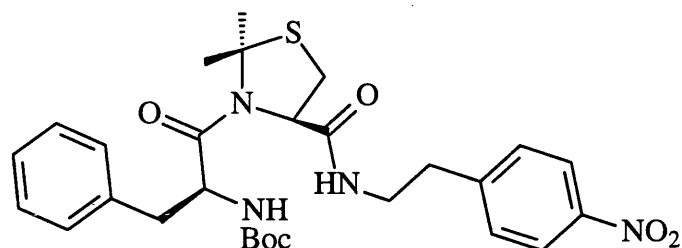
4-Nitrophenylethylamine hydrochloride (160 mg, 800 μmol) was stirred with Et$_3$N (158 mg, 1.6 mmol) and **63** (450 mg, 800 μmol) in CH$_2$Cl$_2$ (5.0 mL) for 2 h. Evaporation and chromatography (EtOAc / hexane 1:1) afforded **67** (410 mg, 95%) as a white solid: mp 45-46°C: IR v_{max} 3442 (NH), 1699 (C=O), 1652 (amide I), 1518 (amide II) cm^{-1}; NMR δ_H 1.43 (9 H, s, Bu^t), 1.58 (3 H, s, 2-Me), 1.60 (3 H, s, 2-Me), 2.30 (1 H, dd, J = 11.7, 5.9 Hz, Phe β-H), 2.89 (2 H, m, Phe β-H + 5-H), 2.97 (2 H, t, J = 7.0 Hz, ArCH$_2$), 3.20 (1 H, d, J = 11.7 Hz, 5-H), 3.41 (1 H, m, ArCH$_2$CH), 3.69 (1 H, m, ArCH$_2$CH), 3.74 (1 H, d, J = 5.5 Hz, 4-H), 4.13 (1 H, m, Phe α-H), 4.98 (1 H, d, J = 5.9 Hz, Phe NH), 7.18 (2 H, m, Phe 2',6'-H$_2$), 7.33 (3 H, m, Phe 3',4',5'-H$_3$), 7.35 (2 H, d, J = 8.8 Hz, Ar 2,6-H$_2$), 8.10 (2 H, d, J = 8.8 Hz, Ar 3,5-H$_2$), 8.10 (1 H, m, NH); MS m/z 557.2433 (M + H) (C$_{28}$H$_{37}$N$_4$O$_6$S requires 557.2434), 501 (M - Me$_2$C=CH$_2$), 457 (M - Boc).

R-2,2-Dimethyl-3-glycyl-N-(2-(4-nitrophenyl)ethyl)tetrahydrothiazole-4-carboxamide trifluoroacetate (68)
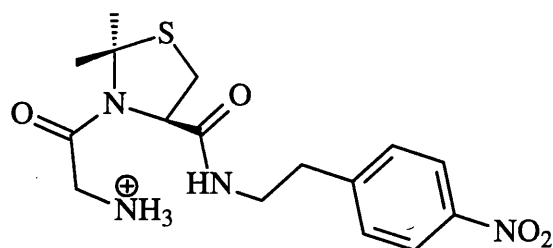
Compound **64** (50 mg, 110 μmol) was stirred in CF$_3$CO$_2$H (400 μL) and CH$_2$Cl$_2$ (1.6 mL) for 45 min. Evaporation afforded **68** (53 mg, quant.) as a highly hygroscopic colourless gum: NMR ((CD$_3$)$_2$SO) δ_H 1.76 (3 H, s, 2-Me), 1.78 (3 H, s, 2-Me), 2.90 (2 H, t, J = 6.6 Hz, ArCH$_2$), 3.18 (1 H, m, Gly-H), 3.20 (d, J = 12.3 Hz, 5-H), 3.34 (1 H, dd, J = 12.3, 5.9 Hz, 5-H), 3.42 (2 H, brq, NHCH_2), 3.89 (1 H, m, Gly-H), 4.85 (1 H, d, J = 6.1 Hz, 4-H), 7.50 (2 H, d, J = 8.8 Hz, Ar 2,6-H$_2$), 8.02 (3 H, br, N$^+$H$_3$), 8.15 (2 H, d, J = 8.8 Hz, Ar 3,5-H$_2$), 8.26 (1 H, t, J = 6.2 Hz, NH); MS m/z 367.1448 (M + H) (C$_{16}$H$_{24}$N$_4$O$_4$S requires

367.1400), 310 (M – Gly), 225 (M – $CH_2CH_2C_6H_4NO_2$).

3-(L-Alanyl)-R-2,2-dimethyl-N-(2-(4-nitrophenyl)ethyl)tetrahydrothiazole-4-carbox-amide trifluoroacetate (69)
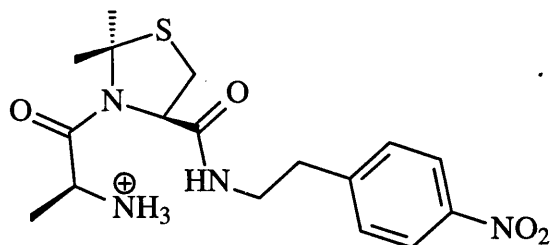
Compound **65** (20 mg, 40 µmol) was stirred with CF_3CO_2H (200 µL) and CH_2Cl_2 (800 µL) for 20 min. Evaporation afforded **69** (quant.) as a pale buff solid: mp 119-121°C: IR ν_{max} 3410 (NH), 1655 (C=O), 1600 (amide I), 1517 (amide II) cm^{-1}; NMR ((CD$_3$OD) δ_H 1.34 (3 H, d, J = 6.6 Hz, Ala β-H$_3$), 1.69 (3 H, s, 2-Me), 1.72 (3 H, s, 2-Me), 2.85 (1 H, dt, J = 12.9, 6.6 Hz) and 2.89 (1 H, dt, J = 12.9, 6.6 Hz) (ArCH$_2$), 3.10 (1 H, dd, J =12.9, 1.6 Hz, 5-H), 3.33 (2 H, m, 5-H, NCHH), 3.54-3.61 (1 H, dt, J = 13.7, 6.6 Hz, NCHH), 3.68 (1 H, q, J = 7.0 Hz, Ala α-H), 4.74 (1 H, dd, J = 5.9, 1.6 Hz, 4-H), 7.39 (2 H, d, J = 9.0 Hz, Ar 2,6-H$_2$), 8.07 (2 H, d, J = 9.0 Hz, Ar 3,5-H$_2$); MS m/z 381.1603 (M + H) (C$_{17}$H$_{25}$N$_4$O$_4$S requires 381.1597).

R-2,2-Dimethyl-N-(2-(4-nitrophenyl)ethyl)-3-(L-valinyl)tetrahydrothiazole-4-carbox-amide trifluoroacetate (70)
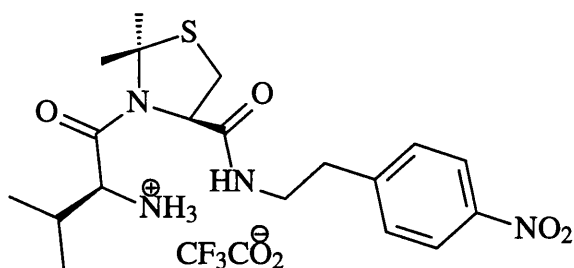
Compound **66** (70 mg, 140 µmol) was stirred in CF_3CO_2H (600 µL) and CH_2Cl_2 (2.4 mL) for 15 min. Evaporation afforded **70** (quant.) as a highly hygroscopic viscous oil: NMR ((CD$_3$)$_2$SO) δ_H 0.95 (3 H, d, J = 6.6 Hz, Val-Me), 1.00 (3 H, d, J = 6.6 Hz, Val-Me), 1.80 (3 H, s, 2-Me), 1.82 (3 H, s, 2-Me), 2.10 (1 H, m, Val β-H), 2.98 (2 H, t, J = 7.0 Hz, ArCH$_2$), 3.32 (1 H, dd, J = 12.3, 2.3 Hz, 5-H), 3.45 (1 H, dd, J = 12.3, 5.9 Hz, 5-H), 3.53 (3 H, m, NCH$_2$ and Val α-H), 4.95 (1 H, dd, J =5.9, 2.3 Hz, 4-H), 7.57 (2 H, d, J = 8.6 Hz,

Ar 2,6-H$_2$), 8.16 (3 H, br, N$^+$H$_3$), 8.23 (2 H, d, J = 8.6 Hz, Ar 3,5-H$_2$), 8.33 (1 H, t, J = 5.9 Hz, NH); MS m/z 409.1911 (M + H) (C$_{19}$H$_{29}$N$_4$O$_4$S requires 409.1910).

R-2,2-Dimethyl-N-(2-(4-nitrophenyl)ethyl)-3-(L-phenylalanyl)tetrahydrothiazole-4-carboxamide trifluoroacetate (71)
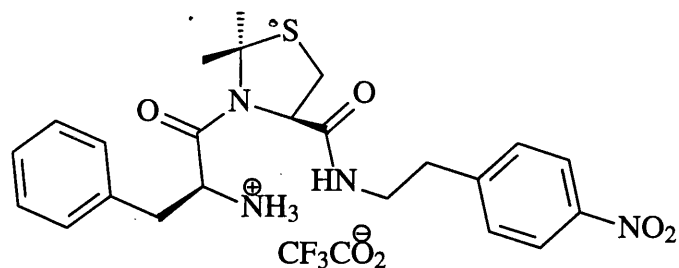
Compound **67** (5 mg, 9 µmol) was stirred in CF$_3$CO$_2$H (100 µL) and CH$_2$Cl$_2$ (400 µL) for 15 min. Evaporation afforded **71** (quant.) as a highly hygroscopic viscous oil: NMR((CD$_3$)OD) δ$_H$ 1.64 (3 H, s, 2-Me), 1.70 (3 H, s, 2-Me), 2.55 (1 H, dd, J = 12.5, 5.9 Hz, 5-H), 2.90 (2 H, t, J = 7.0 Hz, ArCH$_2$), 2.95 (1 H, dd, J = 13.3, 8.6 Hz, Phe β-H), 3.08 (1 H, d, J = 12.5 Hz, 5-H), 3.10 (1 H, dd, J = 13.3, 5.6 Hz, Phe β-H), 3.42 (2 H, m, ArCH$_2$CH$_2$), 4.08 (1 H, m, Phe α-H), 4.20 (1 H, d, J = 5.9 Hz, 4-H), 7.27 (2 H, m, Phe 2',6'-H$_2$), 7.36 (3 H, m, Phe 3',4',5'-H$_3$), 7.50 (2 H, d, J = 8.6 Hz, Ar 2,6-H$_2$), 8.18 (2 H, d, J = 8.6 Hz, Ar 3,5-H$_2$), 8.23 (1 H, t, J = 6.6 Hz, NH), 8.38 (3H, br, N$^+$H$_3$); MS m/z 457.1907 (M + H) (C$_{23}$H$_{29}$N$_4$O$_4$S requires 457.1910).

R-2,2-Dimethyl-3-(N-(1,1-dimethylethoxycarbonyl)-D-alanyl)tetrahydrothiazole-4-carboxylic acid (73a) and R-2,2-dimethyl-3-(N-(1,1-dimethylethoxycarbonyl)-L-alanyl)tetrahydrothiazole-4-carboxylic acid (73b)
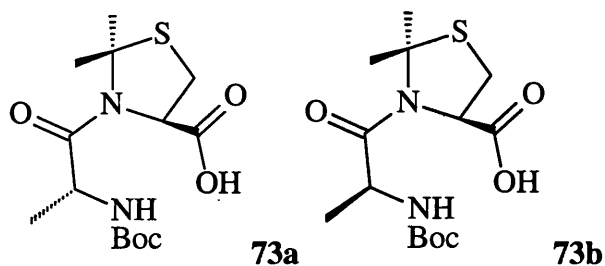
A mixture of Boc(D-Ala)F **72a** (308 mg, 1.6 mmol) and Boc(L-Ala)F **72b** (132 mg, 700 µmol) was stirred with xx (500 mg, 2.5 mmol) and Et$_3$N (480 mg, 4.8 mmol) in dry DMF (50 mL) for 16 h. The evaporation residue, in EtOAc, was washed with cold 5% aq. citric acid and brine. Drying and evaporation afforded a mixture of **73a** and **73b** (300 mg, 36%) as a white solid: IR ν$_{max}$ 3316 (NH), 1748 (C=O), 1718 (C=O), 1643 (amide I), 1660

(amide I), 1540 (amide II), 1512 (amide II) cm^{-1}; NMR δ_H 1.30 (1.2 H, d, J = 2.7 Hz, Ala β-H$_3$ (L,R-diastereoisomer)), 1.32 (1.8 H, d, J = 3.1 Hz, Ala β-H$_3$ (D,R-diastereoisomer)), 1.40 (3.6 H, s, Bu^t (L,R-diastereoisomer)), 1.42 (5.4 H, s, Bu^t (D,R-diastereoisomer)), 1.81 (1.2 H, s, 2-Me (L,R-diastereoisomer)), 1.84 (1.8 H, s, 2-Me (D,R-diastereoisomer)), 1.87 (1.8 H, s, 2-Me (D,R-diastereoisomer)), 1.91 (1.2 H, s, 2-Me (L,R-diastereoisomer)), 3.23 (0.4 H, dd, J = 11.7, 5.3 Hz, 5-H (L,R-diastereoisomer)), 3.34 (0.6 H, dd, J = 12.1, 5.3 Hz, 5-H (D,R-diastereoisomer)), 3.40 (0.6 H, d, J = 12.1 Hz, 5-H (D,R-diastereoisomer)), 3.45 (0.4 H, d, J = 11.7 Hz, 5-H (L,R-diastereoisomer)), 4.25 (0.6 H, qn, J = 6.6 Hz, Ala α-H (D,R-diastereoisomer)), 4.53 (0.4 H, qn, J = 7.0 Hz, Ala α-H (L,R-diastereoisomer)), 4.87 (0.4 H, d, J = 5.3 Hz, 4-H (L,R-diastereoisomer)), 5.36 (0.6 H, d, J = 8.6 Hz, NH (D,R-diastereoisomer)), 5.59 (0.6 H, d, J = 5.3 Hz, 4-H (D,R-diastereoisomer)), 5.79 (0.4 H, d, J = 8.2 Hz, NH (L,R-diastereoisomer); MS m/z 333.1494 (M + H) (C$_{14}$H$_{25}$N$_2$O$_5$S requires 333.1484), 277 (M - Me$_2$C=CH$_2$).

Pentafluorophenyl R-2,2-dimethyl-3-(N-(1,1-dimethylethoxycarbonyl)-D-alanyl)tetra-hydrothiazole-4-carboxylate (74a) and pentafluorophenyl R-2,2-dimethyl-3-(N-(1,1-dimethylethoxycarbonyl)-L-alanyl)tetrahydrothiazole-4-carboxylate (74b)
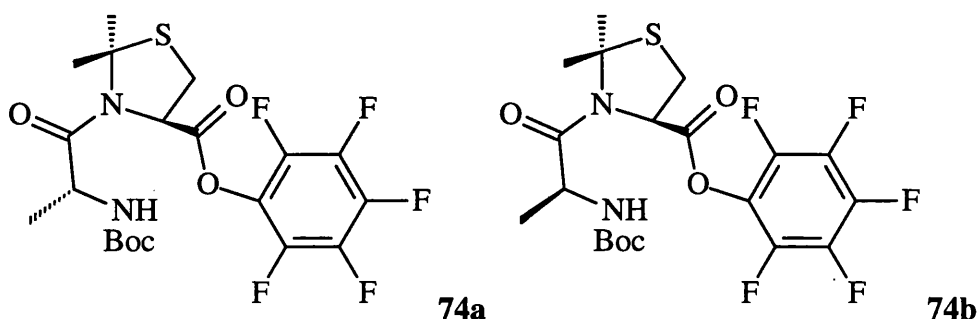
Mixture (**73a and 73b**) (250 mg, 800 μmol) was stirred with pentafluorophenol (160 mg, 900 μmol) and DCC (180 mg, 900 μmol) in EtOAc (5.0 mL) at 0°C under N$_2$ for 3 h. The mixture was filtered (Celite®) and the solid was washed with cold EtOAc. The evaporation residue, in hexane, was kept at 4°C for 16 h and filtered. Evaporation gave **74a and 74b** (320 mg, 80%) as a colourless gum; NMR δ_H 1.30 (2.1 H, d, J = 6.6 Hz, Ala-Me (D,R-diastereoisomer)), 1.37 (0.9 H, d, J = 6.6 Hz, Ala-Me (L,R-diastereoisomer)), 1.39 (2.7 H, s, Bu^t (L,R-diastereoisomer)), 1.43 (6.3 H, s, Bu^t (D,R-diastereoisomer)), 1.85 (0.9 H, s, 2-Me (L,R-diastereoisomer)), 1.87 (2.1 H, s, 2-Me (D,R-diastereoisomer)), 1.89 (2.1 H, s, 2-Me (D,R-diastereoisomer)), 1.94 (0.9 H, s, 2-Me (L,R-diastereoisomer)), 3.37 (0.3 H, dd, J = 12.5, 3.5 Hz, 5-H (L,R-diastereoisomer)), 3.40 (0.7 H, dd, J = 12.5, 5.7 Hz, 5-H (D,R-

diastereoisomer)), 3.49 (1 H, d, J =12.5 Hz, 5-H), 4.22 (0.7 H, qn, J = 7.0 Hz, Ala α-H

(D,R-diastereoisomer)), 4.38 (0.3 H, m, Ala α-H (L,R-diastereoisomer)), 5.01 (0.7 H, d, J

= 9.0 Hz, NH (D,R-diastereoisomer)), 5.19 (0.7 H, d, J = 5.7 Hz, 4-H (D,R-

diastereoisomer)), 5.58 (0.3 H, d, J = 3.5 Hz, 4-H (L,R-diastereoisomer)), 6.13 (0.3 H, d, J

= 3.9 Hz, NH (L,R-diastereoisomer)); NMR δ_F −163.8 (2 F, t, J = 21.0 Hz, 3',5'-F_2), -162.1

(2 F, t, J = 21.0 Hz, 3',5'-F_2), −161.5 (2 F, m, 3',5'-F_2), -161.1 (2 F, t, J = 22.4 Hz, 3',5'-

F_2), 156.4 (1 F, t, J = 21.0 Hz, 4'-F), -156.6 (1 F, t, J = 21.0 Hz, 4'-F), 157.1 (1 F, t, J =

21.0 Hz, 4'-F), -157.8 (1 F, t, J = 21.0 Hz, 4'-F), -150.9 (2 F, d, J = 17.1 Hz, 2',6'-F_2), -

151.9 (2 F, d, J = 17.1 Hz, 2',6'-F_2) -152.1 (2 F, d, J = 18.4 Hz, 2',6'-F_2), -152.6 (2 F, d, J

= 17.1 Hz, 2',6'-F_2); MS m/z 499.1340 (M + H) ($C_{20}H_{24}F_5N_2O_5S$ requires 499.1326), 443

(M - $Me_2C=CH_2$), 425 (M - Bu^tO).

R-2,2-Dimethyl-3-(N-(1,1-dimethylethoxycarbonyl)-D-alanyl)-N-(2-(4-nitrophenyl)-
ethyl)tetrahydrothiazole-4-carboxamide (75a) and R-2,2-dimethyl-3-(N-(1,1-dimethyl-
ethoxycarbonyl)-L-alanyl)-N-(2-(4-nitrophenyl)ethyl)tetrahydrothiazole-4-
carboxamide (75b)
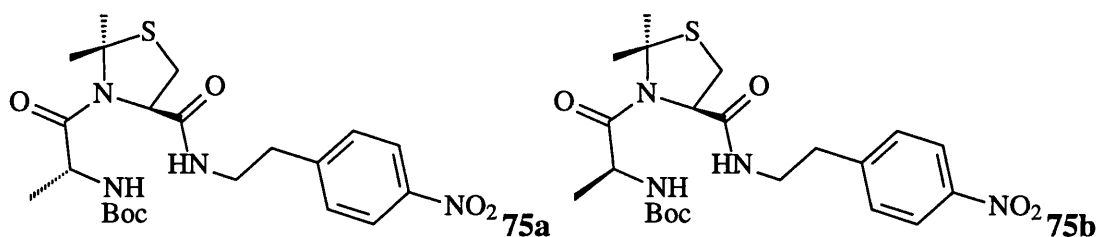
4-Nitrophenylethylamine hydrochloride (120 mg, 600 μmol) was stirred with Et_3N (120

mg, 1.20 mmol) and **74a and 74b** (300 mg, 600 μmol) in CH_2Cl_2 (3.0 mL) for 2 h.

Evaporation and chromatography (EtOAc / hexane 4:1) afforded **75a and 75b** (220 mg,

76%) as a white solid: mp 69-80°C: NMR ((CD_3)$_2$SO) δ_H 0.93 (1.8 H, d, J = 6.6 Hz, Ala-

Me (D,R-diastereoisomer)), 1.11 (1.2 H, d, J = 6.6 Hz, Ala-Me (L,R-diastereoisomer)),

1.36 (3.6 H, s, Bu^t (L,R-diastereoisomer)), 1.37 (5.4 H, s, Bu^t (D,R-diastereoisomer)), 1.59

(1.2 H, s, 2-Me (L,R-diastereoisomer)), 1.68 (1.8 H, s, 2-Me (D,R-diastereoisomer)), 1.70

(1.8 H, s, 2-Me (D,R-diastereoisomer)), 1.71 (1.2 H, s, 2-Me (L,R-diastereoisomer)), 2.88

(0.8 H, m, $ArCH_2$ (L,R-diastereoisomer)), 2.95 (1.2 H, m, $ArCH_2$ (D,R-diastereoisomer)),

3.00-4.00 (5 H, m, 5-H_2, $ArCH_2\underline{CH_2}$, Ala α-H), 4.72 (0.4 H, d, J = 4.1 Hz, 4-H (L,R-

diastereoisomer)), 5.25 (0.6 H, d, J = 4.3 Hz, 4-H (D,R-diastereoisomer)), 7.05 (0.4 H, d, J

= 5.9 Hz, NH (L,R-diastereoisomer)), 7.13 (0.6 H, d, J = 7.4 Hz, NH (D,R-

diastereoisomer)), 7.49 (0.8 H, d, J = 8.2 Hz, Ar 2,6-H_2 (L,R-diastereoisomer)), 7.51 (1.2

H, d, J = 8.6 Hz, Ar 2,6-H$_2$ (D,R-diastereoisomer)), 8.13 (2 H, d, J = 8.6 Hz, Ar 3,5-H$_2$), 8.17 (1 H, d, J = 5.9 Hz, Ala NH); MS m/z 481.2128 (M + H) (C$_{22}$H$_{33}$N$_4$O$_6$S requires 481.2121), 425 (M - Me$_2$C=CH$_2$), 381 (M - Boc).

S-2,2-Dimethyl-3-(N-(1,1-dimethylethoxycarbonyl)-D-valinyl)tetrahydrothiazole-4-carboxylic acid (77)
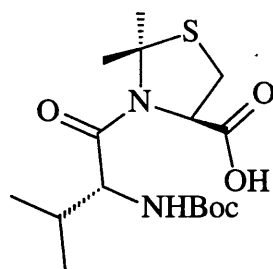
BocD-Val F (270 mg, 1.1 mmol) was stirred with **47** (250 mg, 1.1 mmol) and Pr$^i_2$NEt (310 mg, 2.4 mmol) in dry DMF (10 mL) for 16 h. The evaporation residue, in EtOAc, was washed with cold 5% aq. citric acid, cold H$_2$O and brine. Drying, evaporation and chromatography (hexane / EtOAc / AcOH 49:49:2) afforded **77** (200 mg, 50%) as a colourless gum: IR (film) v_{max} 3329 (NH), 1714 (C=O), 1657 (amide I), 1462 (amide II) cm^{-1}; NMR δ_H 0.92 (3 H, d, J = 6.4 Hz, Val-Me), 0.94 (3 H, d, J = 6.4 Hz, Val-Me), 1.43 (9 H, s, Bu^t), 1.85 (3 H, s, 2-Me), 1.89 (3 H, s, 2-Me), 2.05 (1 H , m, Val β-H), 3.27 (1 H, dd, J = 12.1, 5.7 Hz, 5-H), 3.40 (1 H, d, J = 12.1 Hz, 5-H), 3.86 (1 H, t, J = 9.8 Hz, Val α-H), 5.42 (1 H, d, J = 9.8 Hz, NH), 5.66 (1 H, d, J = 5.7 Hz, 4-H); MS m/z 361.1810 (M + H) (C$_{16}$H$_{29}$N$_2$O$_5$S requires 361.1797), 305 (M - Me$_2$C=CH$_2$).

Pentafluorophenyl R-2,2-dimethyl-3-(N-(1,1-dimethylethoxycarbonyl)-D-valinyl)-tetrahydrothiazole-4-carboxylate (78)
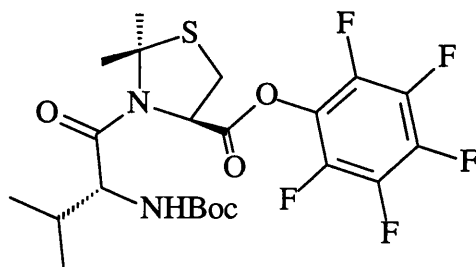
Compound **77** (200 mg, 560 μmol) was stirred with pentafluorophenol (113 mg, 610 μmol) and DCC (126 mg, 610 μmol) in EtOAc (10 mL) at 0°C under N$_2$ for 3 h. The mixture was filtered (Celite$^®$) and the solid was washed with cold EtOAc. The evaporation residue, in hexane, was kept at 4°C for 16 h and filtered. Evaporation gave **78** (120 mg, 41%) as a

colourless oil; NMR δ_H 0.89 (2.1 H, d, J = 6.8 Hz, Val-Me), 0.98 (2.1 H, d, J = 6.8 Hz, Val-Me), 1.04 (0.9 H, d, J = 7.0 Hz, Val-Me), 1.10 (0.9 H, d, J = 7.0 Hz, Val-Me), 1.45 (6.3 H, s, Bu^t), 1.48 (2.7 H, s, Bu^t), 1.89 (3 H, s, 2-Me), 1.93 (3 H, s, 2-Me), 2.02 (1 H, m, Val β-H), 3.30 (1 H, m, 5-H), 3.54 (1 H, dd, J = 12.5, 6.2 Hz, 5-H), 3.83 (1 H, t, J = 9.0, 5-H), 5.03 (0.7 H, d, J = 9.8, Hz, 4-H), 5.08 (0.3 H, d, J = 9.0 Hz, 4-H), 5.62 (0.3 H, m, Val α-H), 5.67 (0.7 H, m, Val α-H), 6.2 (1 H, m, NH).   ·   °

R-2,2-Dimethyl-3-(1,1-dimethylethoxycarbonyl)-D-valinyl)-N-(2-(4-nitrophenyl)-ethyl)tetrahydrothiazole-4-carboxamide (79)
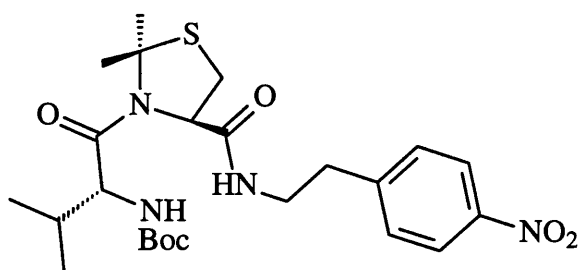
4-Nitrophenylethylamine hydrochloride (46 mg, 230 μmol) was stirred with Et$_3$N (47 mg, 460 μmol) and **78** (120 mg, 230 μmol) in CH$_2$Cl$_2$ (2 mL) for 2 h. Evaporation and chromatography (EtOAc / hexane 1:1) afforded **79** (20 mg, 17%) as a colourless gum: IR (film) ν_max 3320 (NH), 1702 (C=O), 1655 (amide I), 1514 (amide II) cm^{-1}; NMR δ_H 0.83 (3 H, d, J = 6.6 Hz, Val-Me), 0.92 (3 H, d, J = 6.6 Hz, Val-Me), 1.42 (7.2 H, s, Bu^t), 1.55 (1.8 H, s, Bu^t), 1.79 (2.4 H, s, 2-Me), 1.81 (2.4 H, s, 2-Me), 1.88 (0.6 H, s, 2-Me), 1.91 (0.6 H, s, 2-Me), 1.92 (1 H, m, Val β-H), 2.97 (2 H, t, J = 7.0 Hz, ArCH$_2$), 3.04 (1 H, d, J = 12.5 Hz, 5-H), 3.36 (1 H, dd, J = 12.5, 6.6 Hz, 5-H), 3.44 (1 H, m, ArCH$_2$CH), 3.80 (1 H, m, ArCH$_2$CH), 3.86 (1 H, t, J = 9.2 Hz, Val α-H), 4.85 (1 H, d, J = 9.2 H, ValNH), 5.07 (0.2 H, d, J = 6.6 Hz, 4-H), 5.36 (0.8 H, d, J = 6.6 Hz, 4-H), 6.03 (0.2 H, br, NHCH$_2$), 6.41 (0.8 H, br, NHCH$_2$), 7.35 (0.4 H, d, J = 8.8 Hz, Ar 2,6-H$_2$), 7.40 (1.6 H, d, J = 8.6 Hz, Ar 2,6-H$_2$), 8.15 (0.4 H, d, J = 8.8 Hz, Ar 3,5-H$_2$), 8.17 (1.6 H, d, J = 8.6 Hz, Ar 3,5-H$_2$); MS m/z 509.2437 (M + H) (C$_{24}$H$_{37}$N$_4$O$_6$S requires 509.2434).

S-2,2-Dimethyltetrahydrothiazole-4-carboxylic acid hydrochloride (81)
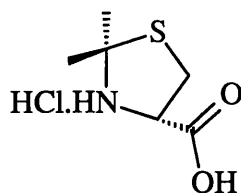
D-Cys.HCl.H₂O (2.00 g, 10 mmol) and 2,2-dimethoxypropane (30 mL) were boiled under reflux in acetone (200 mL) for 4 h. The resulting solid was collected by filtration to afford **81** (2.15 g, 78%) as a white solid: mp 166-170°C (lit[135] mp 165-168°C); IR ν_{max} 3412 (NH), 2600, (OH), 1743 (C=O) cm⁻¹; NMR (D₂O) δ_H 2.06 (6 H, s, 2 × Me), 2.92 (1 H, dd, J = 15.2, 3.9 Hz, 5-H), 3.00 (1 H, dd, J = 15.2, 5.9 Hz, 5-H), 4.06 (1 H, dd, J = 5.9, 3.9 Hz, 4-H).

S-2,2-Dimethyl-3-(N-(1,1-dimethylethoxycarbonyl)-L-valinyl)tetrahydrothiazole-4-carboxylic acid (82)
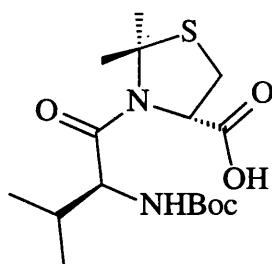
BocValF[53] (1.08 g, 4.6 mmol) was stirred with **81** (1.00 g, 5.1 mmol) and Prⁱ₂NEt (1.24 g, 9.6 mmol) in dry DMF (100 mL) for 16 h. The evaporation residue, in EtOAc, was washed with cold 5% aq. citric acid, cold H₂O and brine. Drying, evaporation and chromatography (hexane / EtOAc /AcOH 70:28:2) afforded **82** (630 mg, 35%) as a colourless gummy solid: : IR ν_{max} 3434 (NH), 2970 (OH), 1723 (C=O), 1605 (amide I), 1513 (amide II) cm⁻¹; NMR δ_H 0.87-0.95 (6 H, m, 2 × Val-Me), 1.43 (9 H, s, Buⁱ), 1.85 and 1.88 (6 H, s, 2 × 2-Me), 2.00 (1 H, m, Val β-H), 3.20-3.50 (2 H, m, 5-H + Val α-H), 3.85 (1 H, t, J = 10.0 Hz, 5-H), 5.36 (1 H, d, J = 10.02 Hz, 4-H), 5.68 (0.7 H, d, J = 5.1 Hz, NH), 8.63 (1 H, br, OH); MS *m/z* 361.1810 (M + H) (C₁₆H₂₉N₂O₅S requires 361.1797), 305 (M - Me₂C=CH₂).

Pentafluorophenyl   *S*-2,2-dimethyl-3-(N-(1,1-dimethylethoxycarbonyl)-L-valinyl)-tetrahydrothiazole-4-carboxylate (83)
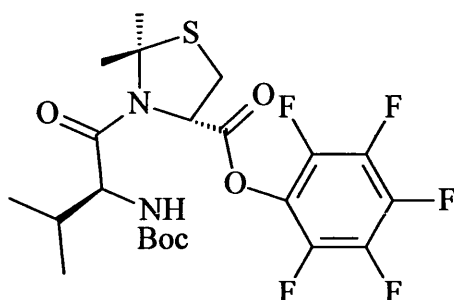
Compound **82** (500 mg, 1.4 mmol) was stirred with pentafluorophenol (280 mg, 1.5 mmol) and DCC (320 mg, 1.5 mmol) in EtOAc (10 mL) at 0°C under N_2 for 3 h. The mixture was filtered (Celite®) and the solution was washed with cold EtOAc. The evaporation residue, in hexane, was kept at 4°C for 16 h and filtered. Evaporation gave **83** (500 mg, 68%) as a colourless oil: NMR δ_H 0.88 (3 H, d, J = 6.6 Hz, Val-Me), 0.97 (3 H, d, J = 6.6 Hz, Val-Me), 1.45 (9 H, s, Bu^t), 1.88 (3 H, s, 2-Me), 1.92 (3 H, s, 2-Me), 3.55 (1 H, dd, J = 12.5, 6.6 Hz, 5-H), 3.82 (1 H, dd, J = 12.5, 9.8 Hz, 5-H), 5.08 (1 H, dd, J = 9.8, 6,6 Hz, 4-H), 5.61 and 5.66 (1 H, 2 × d, J = 4.5 Hz, Val α-H), 6.22 (1 H, brd, J = 4.5 Hz, NH); MS m/z 527.1656 (M + H) ($C_{22}H_{28}F_5N_2O_5S$ requires 527.1639), 471 (M - Bu^{t}O).

S-2,2-Dimethyl-3-(1,1-dimethylethoxycarbonyl)-L-valinyl)-N-(2-(4-nitro-phenyl)ethyl)tetrahydrothiazole-4-carboxamide   (84)
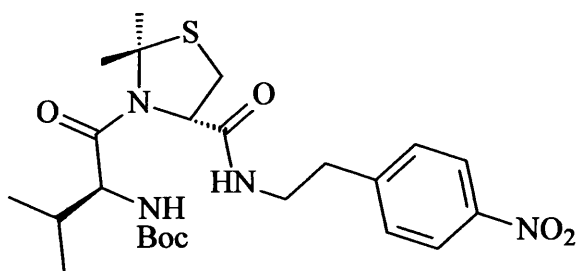
4-Nitrophenylethylamine hydrochloride (80 mg, 400 µmol) was stirred with Et$_3$N (80 mg, 800 µmol) and **83** (200 mg, 400 µmol) in CH_2Cl_2 (3.0 mL) for 2 h. Evaporation and chromatography (EtOAc / hexane 1:1) afforded **84** (100 mg, 49%) as an oil: IR v_{max} 3323 (NH), 1698 (C=O), 1605 (amide I), 1520 (amide II) cm^{-1}; NMR δ_H 0.83 (3 H, d, J = 6.6 Hz, Val-Me), 0.92 (3 H, d, J = 6.6 Hz, Val-Me), 1.42 (7.2 H, s, Bu^t), 1.55 (1.8 H, s, Bu^t), 1.80 (2.4H, s), 1.82 (2.4 H, s), 1.89 (0.6 H, s) and 1.91 (0.6 H, s) (2-Me$_2$), 1.95 (1 H, m, Val β-H), 2.81 (1.6 H, dt, J = 14.1 7.0 Hz, ArCH$_2$), 3.04 (0.8 H, d, J = 12.5 Hz, 5-H), 3.46 (1 H, dd, J = 12.5, 6.4 Hz, 5-H), 3.44 (1 H, m, ArCH$_2$C*H*), 3.77 (1 H, m, ArCH$_2$C*H*), 3.86

(1 H, t, J = 9.4 Hz, Val α-H), 4.92 (1 H, d, J = 9.4 Hz, Val NH), 5.07 (0.2 H, d, J = 6.4 Hz, 4-H), 5.36 (0.8 H, d, J = 6.4 Hz, 4-H), 6.09 (0.2 H, br, NHCH$_2$), 6.47 (0.8 H, t, J = 5.5 Hz, NHCH$_2$), 7.35 (0.4 H, d, J = 8.6 Hz, Ar 2,6-H$_2$), 7.40 (1.6 H, d, J = 8.4 Hz, Ar 2,6-H$_2$), 8.13 (0.4 H, d, J = 8.4 Hz, Ar 3,5-H$_2$), 8.16 (1.6 H, d, J = 8.6 Hz, Ar 3,5-H$_2$); MS m/z 509.2432 (M + H) (C$_{24}$H$_{37}$N$_4$O$_6$S requires 509.2434), 453 (M - Bu^{t}O).

S-2,2-Dimethyl-N-(2-(4-nitrophenyl)ethyl)-3-(L-valinyl)tetrahydrothiazole-4-carboxamide trifluoroacetate (85)
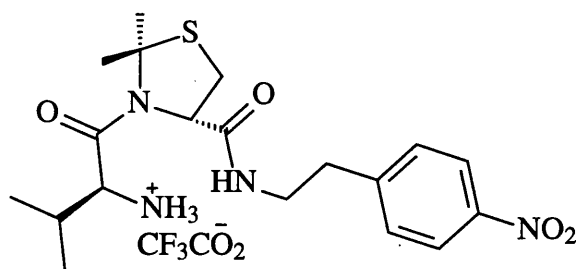
Compound **84** (5 mg, 9.8 μmol) was stirred in CF$_3$CO$_2$H (100 μL) and CH$_2$Cl$_2$ (400 μL) for 15 min. Evaporation afforded **85** (quant.) as a highly hygroscopic viscous oil: NMR ((CD$_3$)$_2$SO) δ$_H$ 0.82 (3 H, d, J = 7.4 Hz, Val-Me), 0.84 (3 H, d, J = 7.0 Hz, Val-Me), 1.80 (6 H, s, 2 × 2-Me), 2.02 (1 H, m, Val β-H), 2.88 (2 H, t, J = 7.0 Hz, ArCH$_2$), 3.08 (1 H, d, J = 12.1 Hz, 5-H), 3.38 (2 H, m, ArCH$_2$CH$_2$), 3.52 (1 H, dd, J = 12.1, 5.3 Hz, 5-H), 4.60 (1 H, m, Val α-H), 5.05 (1 H, d, J =5.3 Hz, 4-H), 7.49 (2 H, d, J = 8.6 Hz, Ar 2,6-H$_2$), 8.15 (2 H, d, J = 8.6 Hz, Ar 3,5-H$_2$), 8.23 (1 H, t, J = 5.9 Hz, NH); MS m/z 409.1911 (M + H) (C$_{19}$H$_{29}$N$_4$O$_4$S requires 409.1910).

N-(Fluoren-9-ylmethoxycarbonyl)-L-valine pentafluorophenyl ester (87)
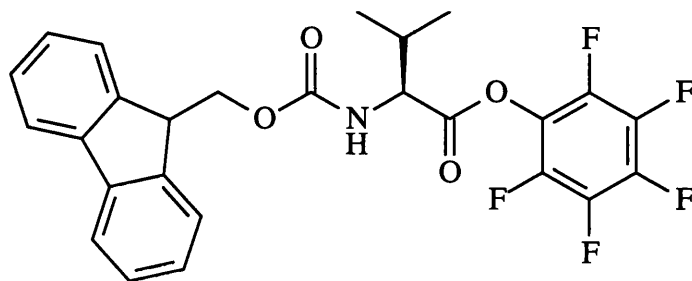
FmocValOH (2.0 g, 5.9 mmol) was stirred with pentafluorophenol (1.20 g, 6.5 mmol) and DCC (1.34 g, 6.5 mmol) in EtOAc (20 mL) at 0°C under N$_2$ for 4 h for 16 h. The mixture was filtered (Celite$^®$) and the solid was washed with cold EtOAc. Evaporation afforded **87** (2.10 g, 70%) as a white solid: mp 114-117°C (lit[141] mp 122-123°C); NMR δ$_H$ 1.03 (3 H, d, J = 6.6 Hz, Val-Me), 1.10 (3 H, d, J = 6.6 Hz, Val-Me), 2.40 (1 H, m, Val β-H), 4.24 (1

H, t, J = 6.6 Hz, C$\underline{H}$CH$_2$O), 4.46 (2 H, d, J = 6.6 Hz, CH$_2$O), 4.67 (1 H, dd, J = 9.4, 5.1

Hz, Val α-H), 5.27 (1 H, d, J = 9.4 Hz, NH), 7.30 (2 H, t, J = 7.4 Hz, Ar-H$_2$), 7.38 (2 H, t, J

= 7.4 Hz, Ar-H$_2$), 7.58 (2 H, d, J = 7.4 Hz, Ar-H$_2$), 7.75 (2 H, d, J = 7.4 Hz, Ar-H$_2$); NMR

δ_F −161.2 (2 F, t, J = 20.9 Hz, 3',5'-F$_2$), -156.6 (1 F, t, J = 20.9 Hz, 4'-F), -151.5 (2 F, d, J

= 18.0 Hz, 2',6'-F$_2$).

S-2,2-Dimethyl-3-(N-(fluoren-9-ylmethoxycarbonyl)-L-valyl)tetrahydrothiazole-4-carboxylic acid (88)
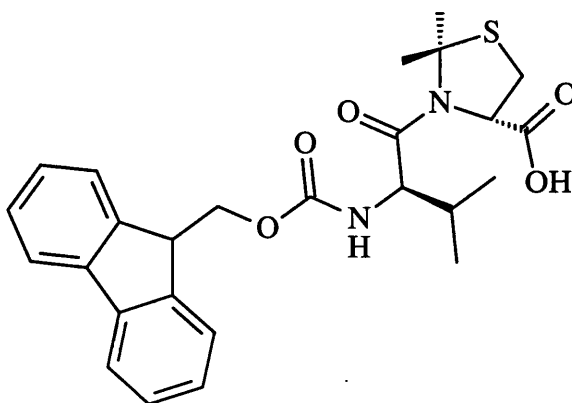
Compound **87** (1.16 g, 2.3 mmol) was dissolved in dry THF (10 mL) and added slowly to a solution of compound **81** (495 mg, 2.5 mmol) and Pr$^i_2$NEt (970 g, 7.5 mmol) in dry DMF (30 mL) at 0°C under N$_2$ for 3 h. The mixture was then gradually warmed to 20°C and stirred for 16 h. The evaporation residue, in EtOAc, was washed with cold 5% aq. citric acid and brine. Drying, evaporation and chromatography (petroleum ether / EtOAc /AcOH 25:25:1) afforded **88** (600 mg, 50%) as a white solid: mp 95-97°C; 0.92 (3 H, d, J = 7.0 Hz, Val-Me), 0.94 (3 H, d, J = 6.6 Hz, Val-Me), 1.84 (3 H, s, 2-Me), 1.89 (3 H, s, 2-Me), 2.10 (1 H, m, Val β-H), 3.25 (1 H, dd, J = 12.1, 5.3 Hz, 5-H), 3.35 (1 H, d, J =12.5 Hz, 5-H), 3.90 (1 H, t, J = 9.8 Hz, Val α-H), 4.20 (1 H, t, J = 7.0 Hz, CHCH$_2$O), 4.37 (1 H, dd, J = 10.7, 7.0 Hz, CHO), 4.45 (1 H, dd, J = 10.7, 7.0 Hz, CHO), 5.43 (1 H, d, J = 10.1 Hz, NH), 5.52 (1 H, d, J = 5.3 Hz, 4-H), 7.28 (2 H, t, J = 7.4 Hz, Ar-H$_2$), 7.38 (2 H, t, J = 7.4 Hz, Ar-H$_2$), 7.54 (2 H, d, J = 6.6 Hz, Ar-H$_2$), 7.75 (2 H, d, J = 7.4 Hz, Ar-H$_2$); MS m/z 483.1951 (M + H) (C$_{26}$H$_{31}$N$_2$O$_5$S requires 483.1954).

185

N-(1,1-Dimethylethoxycarbonyl)-L-leucine pentafluorophenyl ester (90)
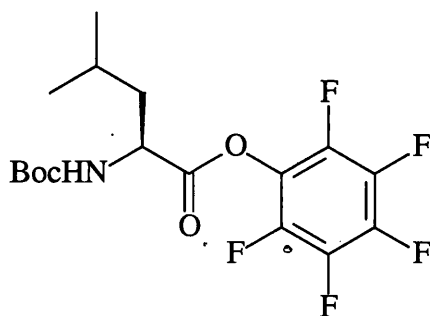
BocLeuOH (2.00 g, 8.0 mmol) was stirred with pentafluorophenol (1.62 g, 8.8 mmol) and DCC (1.82 g, 8.8 mmol) in dry EtOAc (20 mL) at 0°C under N_2 for 3 h. The mixture was filtered (Celite®) and the solid was washed with cold EtOAc. The filtrate was kept at 4°C for 16 h and filtered (Celite®). Evaporation gave **90** (2.50 g, 79%) as a solid: mp 49-53°C (lit[143] mp 48-50°C); NMR δ_H 1.02 (6 H, d, J = 6.3 Hz, 2 × Leu-Me), 1.47 (9 H, s, Bu^t), 1.67 (1 H, m, Leu β-H), 1.8 (2 H, m, Leu β-H, Leu γ-H), 4.41 (0.1 H, m, Leu α-H), 4.62 (0.9 H, m, Leu α-H), 5.75 (0.1 H, br, NH), 4.92 (0.9 H, d, J = 8.2 Hz, NH); NMR δ_F -162.1 (1.8 F, t, J = 21 Hz, 3',5'-F$_2$), -161.9 (0.2 F, t, J = 21.0 Hz, 3',5'-F$_2$), -157.6 (0.9 F, t, J = 22.4 Hz, 4'-F), -157.4 (0.1 F, t, J = 22.4 Hz, 4'-F), -152.7 (0.2 F, d, J = 19.7 Hz, 2',6'-F$_2$), -152.2 (1.8 F, d, J = 18.4 Hz, 2',6'-F$_2$); MS m/z 795 (2 M), 398.1394 (M + H) ($C_{17}H_{21}N_1O_4S$ requires 398.1391).

S-2,2-Dimethyl-3-(N-(1,1-dimethylethoxycarbonyl)-L-leucyl)tetrahydrothiazole-4-carboxylic acid (91)
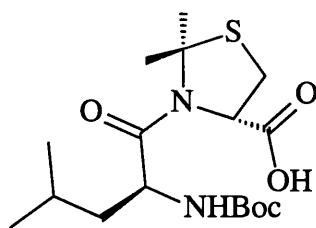
Compound **90** (1.5 g, 3.8 mmol) was stirred with **81** (833 mg, 4.2 mmol) and Pr$^i_2$NEt (1.63 g, 12.6 mmol) in dry DMF (40 mL) for 16 h. The evaporation residue, in EtOAc, was washed with cold 5% aq. citric acid, cold H_2O and brine. Drying and evaporation afforded crude **91** (2.4 g) as a gummy oil: NMR δ_H 0.81-0.90 (6 H, m, 2 × Leu-Me), 1.40 (9 H, s, Bu^t), 1.50-1.60 (2 H, m, Leu β-H$_2$, Leu γ-H), 1.83 (3 H, s, 2-Me), 1.86 (3 H, s, 2-Me), 3.28 (2 H, m, 5-H$_2$), 4.17 (1 H, m, Leu α-H), 5.30 (1 H, d, J = 5.90 Hz, NH), 5.70 (1 H, m, 4-H); MS m/z 375.1948 (M + H) ($C_{17}H_{31}N_2O_5S$ requires 375.1954), 319 (M – Me$_2$C=CH$_2$).

Pentafluorophenyl **S-2,2-dimethyl-3-(N-(1,1-dimethylethoxycarbonyl)-L-leucyl)-tetrahydrothiazole-4-carboxylate (92)**
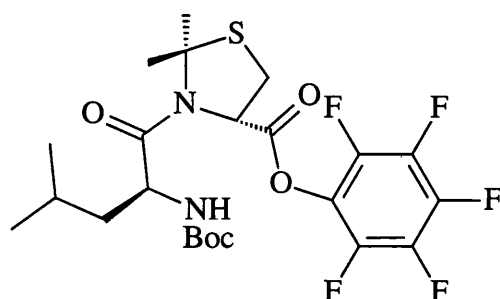
Compound **91** (1.50 g, 4.0 mmol) was stirred with pentafluorophenol (812 mg, 4.4 mmol) and DCC (908 mg, 4.4 mmol) in EtOAc (10 mL) at 0°C under N_2 for 3 h. The mixture was filtered (Celite®) and the solid was washed with cold EtOAc. The filtrate was kept at 4°C for 16 h and filtered (Celite®). Evaporation gave crude **92** (2.3 g) as a pale yellow oil: NMR δ_H 0.88 (3 H, d, J = 6.4 Hz, Leu-Me), 0.90 (3 H, d, J = 6.4 Hz, Leu-Me), 1.44 (9 H, s, Bu^t), 1.55-1.65 (2 H, m, Leu β-H$_2$, Leu γ-H), 1.86 (3 H, s, 2-Me), 1.91 (3 H, s, 2-Me), 3.47 (1 H, dd, J = 12.7, 9.4 Hz, 5-H), 3.54 (1 H, dd, J = 12.7, 4.8 Hz, 5-H), 4.17 (1 H, dt, J = 2.7, 8.7 Hz, Leu α-H), 4.96 (1 H, d, J = 9.4, 4.8 Hz, 4-H), 6.17 (1 H, d, J = 8.5 Hz, NH); NMR δ_F -161.5 (2 F, t, J = 17.1 Hz, 3',5'-F$_2$), -156.6 (1 F, t, J = 22.4 Hz, 4'-F), -152.1 (2 F, d, J = 18.4 Hz, 2',6'-F$_2$). MS m/z 541.1797 (M + H) ($C_{23}H_{30}N_2O_5F_5S$ requires 541.1796), 485 (M – Me$_2$C=CH$_2$), 441 (M – Boc).

S-2,2-Dimethyl-3-(1,1-dimethylethoxycarbonyl)-L-leucyl)-N-(2-(4-nitro-phenyl)ethyl)tetrahydrothiazole-4-carboxamide (93)
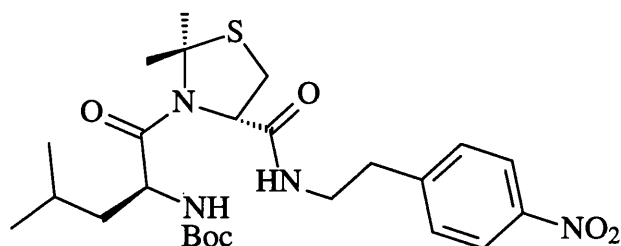
4-Nitrophenylethylamine hydrochloride (375 mg, 1.85 mmol) was stirred with Et$_3$N (375 mg, 3.7 mmol) and **92** (1.00 g, 1.85 mmol) in CH$_2$Cl$_2$ (5 mL) for 16 h. Evaporation and chromatography (EtOAc / hexane 1:1) afforded **93** (640 mg, 58%) as a white solid: mp 108-109°C; NMR δ_H 0.84 (2.4 H, d, J = 6.4 Hz, Leu-Me), 0.90 (2.4 H, d, J = 6.4 Hz, Leu-Me), 0.98 (1.2 H, d, J = 6.4 Hz, 2 × Leu-Me), 1.41 (7.2 H, s, Bu^t), 1.43 (1.8 H, s, Bu^t), 1.60-1.70 (3 H, m, Leu β-H$_2$, Leu γ-H), 1.78 (2.4 H, s, 2-Me), 1.80 (2.4 H, s, 2-Me), 1.84

(0.6 H, s, 2-Me), 1.85 (0.6 H, s, 2-Me), 2.97 (2 H, t, J = 7.0 Hz, ArCH$_2$), 3.05 (1 H, d, J = 12.3 Hz, 5-H), 3.45 (2 H, m, ArCH$_2$CH, 5-H), 3.85 (1 H, m, ArCH$_2$CH), 4.11 (0.8 H, m, Leu α-H), 4.30 (0.2 H, m, Leu α-H), 4.81 (0.8 H, d, J = 8.6 Hz, LeuNH), 4.92 (0.2 H, d, J = 8.6 Hz, LeuNH), 5.30 (0.2 H, d, J = 7.0 Hz, 4-H), 5.42 (0.8 H, d, J = 7.0 Hz, 4-H), 6.15 (1 H, t, J = 5.1 Hz, NHCH$_2$), 7.41 (2 H, d, J = 8.6 Hz, Ar 2,6-H$_2$), 8.15 (0.4 H, d, J = 8.6 Hz, Ar 3,5-H$_2$), 8.19 (1.6 H, d, J = 8.6 Hz, Ar 3,5-H$_2$); MS m/z 523.2596 (M + H) (C$_{25}$H$_{39}$N$_4$O$_6$S requires 523.2590), 467 (M – Me$_2$C=CH$_2$), 423 (M – Boc).

S-2,2-Dimethyl-N-(2-(4-nitrophenyl)ethyl)-3-(L-leucyl)tetrahydrothiazole-4-carbox-amide trifluoroacetate (94)
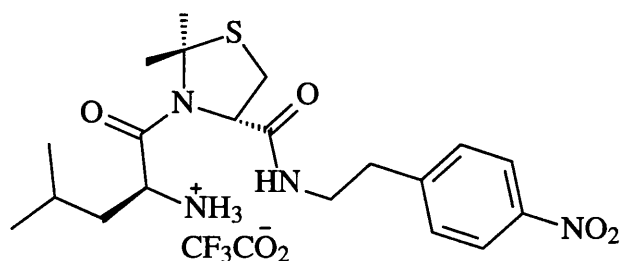
Compound **93** (5 mg, 9.6 μmol) was stirred in CF$_3$CO$_2$H (100 μL) and CH$_2$Cl$_2$ (400 μL) for 15 min. Evaporation afforded **94** (quant.) as highly hygroscopic viscous oil: NMR (CD$_3$OD) δ_H 0.90 (3 H, d, J = 4.7 Hz, Leu-Me), 0.98 (3 H, d, J = 4.3 Hz, Leu-Me), 1.60-1.70 (3 H, m, Leu β-H$_2$, Leu γ-H), 1.89 (3 H, s, 2-Me), 1.92 (3 H, s, 2-Me), 2.95-3.07 (3 H, m, 5-H, ArCH_2), 3.38-3.52 (2 H, m, ArCH$_2$CH, 5-H), 3.70 (1 H, m, ArCH$_2$CH), 3.95 (1 H, m, Leu α-H), 5.08 (1 H, d, J = 6.2 Hz, 4-H), 7.52 (2 H, d, J = 7.2 Hz, Ar 2,6-H$_2$), 8.20 (2 H, d, J = 7.2 Hz, Ar 3,5-H$_2$); MS m/z 423.2077 (M + H) (C$_{20}$H$_{31}$N$_4$O$_4$S requires 423.2066).

Pentafluorophenyl   3-(L-alanyl)-R-2,2-dimethyltetrahydrothiazole-4-carboxylate hydrochloride (96)
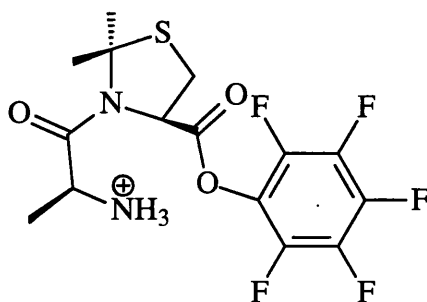
HCl was bubbled through **61** (90 mg, 180 μmol) in CH$_2$Cl$_2$ (5.0 mL) for 30 min.

Evaporation afforded **96** (quant.) as a highly hygroscopic yellow solid: IR v_{max} 3423 (NH), 1793 (C=O), 1670 (amide I), 1521 (amide II) cm^{-1}; NMR ((CD$_3$)$_2$SO) δ_H 1.20 (3 H, d, J = 7.0 Hz, Ala β-H$_3$), 1.74 (3 H, s, 2-Me), 1.77 (3 H, s, 2-Me), 3.17 (1 H, dd, J = 12.1, 10.2 Hz, 5-H), 3.25 (1 H, dd, J = 12.1, 6.6 Hz, 5-H), 4.10 (1 H, q, J = 7.0 Hz, Ala α-H), 4.68 (1 H, dd, J = 10.2, 6.6 Hz, 4-H), 6.30 (3 H, br, N$^+$H$_3$); MS m/z 215 (M – C$_6$F$_5$O).

Pentafluorophenyl   ***R*-2,2-dimethyl-3-(L-valinyl)tetrahydrothiazole-2-carboxylate hydrochloride (97)**
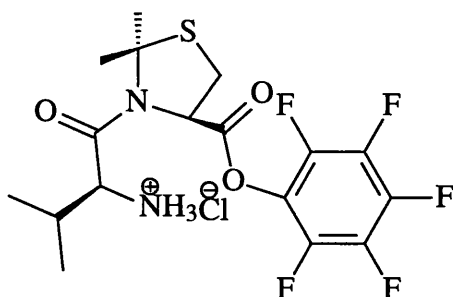
HCl was bubbled through **62** (150 mg, 300 μmol) in CH$_2$Cl$_2$ (5.0 mL) for 1 h. Evaporation afforded **97** (120 mg, 90%) as a white wax: IR v_{max} 3433 (NH), 1790 (C=O), 1667 (amide I), 1520 (amide II) cm^{-1}; NMR ((CD$_3$)$_2$SO) δ_H 0.82 (3 H, d, J = 6.6 Hz, Val-Me), 0.99 (3 H, d, J = 7.4 Hz, Val-Me), 1.75 (6 H, s, 2 × Me), 2.29-2.37 (1 H, d septet, J = 2.3, 7.0 Hz, Val β-H), 3.13 (1 H, dd, J = 11.5, 10.2 Hz, 5-H), 3.22 (1 H, dd, J =11.5, 6.2 Hz, 5-H), 3.89 (1 H, m, Val α-H), 4.60-4.64 (1 H, dd, J = 10.2, 6.2, Hz, 4-H), 5.94 (3 H, br, N$^+$H$_3$); NMR δ_F –171.5 (1F, tt, J = 23.7, 6.8 Hz, 4'-F$_2$), -165.1 (2 F, dd, J = 23.7, 19.6 Hz, 3',5'-F$_2$), -161.5 (2 F, dd, J = 19.6, 6.8 Hz, 2',6'-F$_2$); MS m/z 427 (M +H), 243 (M – C$_6$F$_5$O).

Pentafluorophenyl   ***R*-2,2-dimethyl-3-(L-phenylalanyl)tetrahydrothiazole-2-carboxylate hydrochloride (98)**
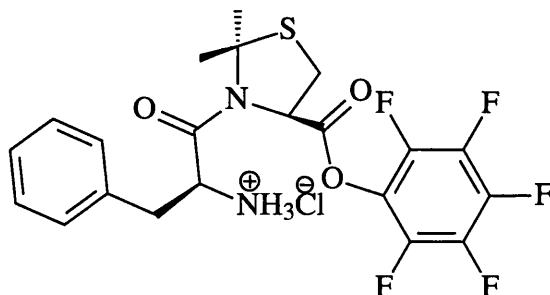
HCl was bubbled through **63** (130 mg, 230 μmol) in CH$_2$Cl$_2$ (6.0 mL) for 1.5 h. Evaporation afforded **98** (quant.) as a colourless highly hygroscopic viscous oil: IR v_{max}

3434 (NH), 1791 (C=O), 1669 (amide I), 1520 (amide II) cm^{-1}; NMR ((CD$_3$)$_2$SO) δ_H 1.66 (3 H, s, 2-Me), 1.74 (3 H, s, 2-Me), 2.75 (1 H, t, J = 11.3 Hz, 5-H), 3.04 (1 H, dd, J = 14.1, 4.5 Hz) and 3.06 (1 H, dd, J = 14.1, 4.5 Hz) (Phe β-H$_2$), 3.13 (1 H, dd, J = 11.3, 5.7 Hz, 5-H), 4.34 (1 H, t, J = 4.5 Hz, Phe α-H), 4.46 (3 H, br, N$^+$H$_3$), 4.60 (1 H, dd, J = 11.3, 5.7 Hz, 4-H), 7.25 (5 H, m, Ph-H$_5$) 8.31 (1 H, s, NH); NMR δ_F -171.5 (2 F, tt, J = 22.4, 6.6 Hz, 4'-F$_2$), -165.1 (1 F, dd, J = 22.4, 19.7 Hz, 3',5'-F$_2$), −161.8 (2 F, dd, J = 19.7, 6.6 Hz, 2',6'-F$_2$), MS m/z 475.1131 (M + H) (C$_{21}$H$_{20}$F$_5$N$_2$O$_3$S requires 475.1115), 291 (M − C$_6$F$_5$O).

6S,8aR-3,3,6-Trimethyltetrahydrothiazolo[3,4-a]pyrazine-5,8-dione (99)
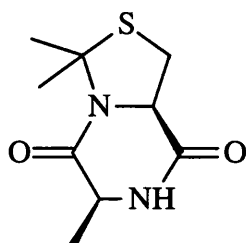
Compound **96** (190 mg, 480 μmol) was stirred with Et$_3$N (97 mg, 1.0 mmol) in CH$_2$Cl$_2$ (5.0 mL) for 5 min. Evaporation and chromatography (EtOAc) afforded **99** (15 mg, 15%) as a white solid: mp 155.8°C (DSC): IR v_{max} 3436 (NH), 1693 (C=O), 1652 (C=O) cm^{-1}; NMR δ_H 1.46 (3 H, d, J = 7.0 Hz, 6-Me), 1.85 (3 H, s, 3-Me), 1.89 (3 H, s, 3-Me), 3.25 (1 H, dd, J = 12.5, 6.6 Hz, 1-H), 3.30 (1 H, dd, J = 12.5, 10.2 Hz, 1-H), 4.07 (1 H, ddq, J = 0.8, 1.3, 7.0 Hz, 6-H), 4.57 (1 H, dddd, J = 10.2, 6.6, 1.3, 0.8 Hz, 8a-H), 7.28 (1 H, br, NH); MS m/z 368 (M + mNBA), 215.0862 (M + H) (C$_9$H$_{15}$N$_2$O$_2$S requires 215.0854); Found C, 50.43; H, 6.55; N, 12.9; C$_9$H$_{14}$N$_2$O$_2$S requires C, 50.45; H, 6.58; N, 13.07%.

6S,8aR-3,3-Dimethyl-6-(1-methylethyl)tetrahydrothiazolo[3,4-a]pyrazine-5,8-dione (100)
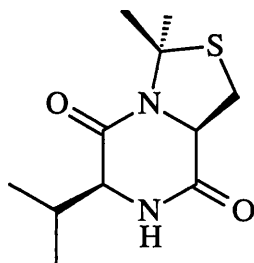
Compound **97** (90 mg, 190 μmol) was stirred with Et$_3$N (39 mg, 380 μmol) in CH$_2$Cl$_2$ (3.0 mL) for 10 min. Evaporation and chromatography (EtOAc) afforded **100** (40 mg, 87 %) as a white solid: mp 186.4°C (DSC): IR (film) v_{max} 3213 (NH), 1692 (C=O) cm^{-1}; NMR

((CD₃)₂SO) δ_H 0.83 (3 H, d, *J* = 7.0 Hz, CH*Me*), 1.0 (3 H, d, *J* = 7.0 Hz, CH*Me*), 1.76 (3 H, s, 3-Me), 1.77 (3 H, s, 3-Me), 2.34 (1 H, dseptet, *J* = 7.0, 2.3 Hz, C*H*Me₂), 3.14 (1 H, dd, *J* = 11.7, 10.2 Hz, 1-H), 3.23 (1 H, dd, *J* =11.7, 5.9 Hz, 1-H), 3.34 (1 H, br, NH), 3.89 (1 H, dd, *J* = 2.3, 1.2 Hz, 6-H), 4.64 (1 H, ddd, *J* = 10.2, 5.9, 1.2 Hz, 8a-H); MS *m/z* 396 (M + mNBA), 243.1168 (M + H) (C₁₁H₁₉N₂O₂S requires 243.1167).

6*S*,8a*R*-3,3-Dimethyl-6-phenylmethyltetrahydrothiazolo[3,4-*a*]pyrazine-5,8-dione (101)
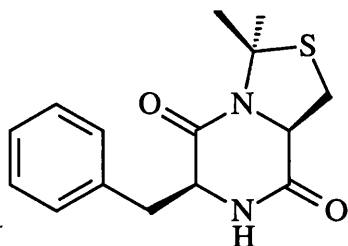
Compound **98** (80 mg, 170 μmol) was stirred with Et₃N (34.0 mg, 340 μmol) in CH₂Cl₂ (3.0 mL) for 1.5 h. Evaporation and chromatography (EtOAc) afforded **101** (40 mg, 81%) as a colourless gum: IR (film) v_max 3377 (NH), 1794 (C=O), 1688 (C=O) cm⁻¹; NMR δ_H 1.87 (3 H, s, 3-Me), 1.92 (3 H, s, 3-Me), 2.82 (1 H, dd, *J* = 14.4, 10.2 Hz, PhCH), 3.19 (1 H, dd, *J* = 12.1, 10.3 Hz, 1-H), 3.26 (1 H, dd, *J* = 12.1, 5.9 Hz, 1-H), 3.56 (1 H, dd, *J* = 14.4, 3.9 Hz, PhCH), 4.24 (1 H, ddd, *J* = 10.3, 3.9, 0.8 Hz, 6-H), 4.53 (1 H, dddd, *J* = 10.3, 5.9, 1.6, 0.8 Hz, 8a-H), 5.82 (1 H, s, NH), 7.21-7.37 (5 H, m, Ph-H₅); MS *m/z* 291.1169 (M + H) (C₁₅H₁₈N₂O₂S requires 291.1167).

Pentafluorophenyl *S*-2,2-dimethyl-3-(N-(L-valinyl)tetrahydrothiazole-2-carboxylate hydrochloride (106)
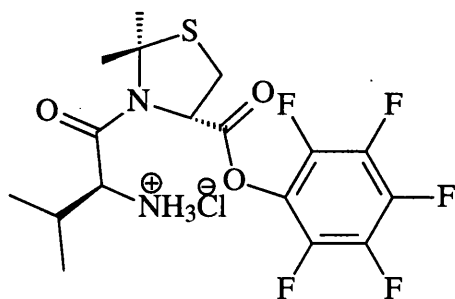
HCl was bubbled through **83** (110 mg, 200 μmol) in CH₂Cl₂ (5.0 mL) for 30 min. Evaporation afforded **106** (quant) as a pale yellow gummy solid: IR v_max 3412 (NH) cm⁻¹; NMR ((CD₃)₂SO) δ_H 0.88 (3 H, d, *J* = 6.6 Hz, Val-Me), 0.92 (3 H, d, *J* = 7.0 Hz, Val-Me),

191

1.78 (3 H, s, 2-Me), 1.82 (3 H, s, 2-Me), 2.06 (1 H, m, Val β-H), 3.11 (1 H, dd, J = 11.7, 10.9 Hz, 5-H), 3.22 (1 H, dd, J =11.7, 5.5 Hz, 5-H), 3.32 (3 H, br, N$^+$H$_3$), 4.64 (1 H, dd, J = 10.9, 5.5 Hz, 4-H), 5.19 (1 H, m, Val α-H); NMR δ$_F$ −171.46 (2 F, m, 3',5'-F$_2$), -165.12 (1 F, dt, J = 23.7 Hz, 4'-F), -161.53 (2 F, dd, J = 19.7, 6.6 Hz, 2',6'-F$_2$); MS m/z 427 (M + H), 243 (M − C$_6$F$_5$O).

6S,8aS-3,3-Dimethyl-6-(1-methylethyl)tetrahydrothiazolo[3,4-*a*]pyrazine-5,8-dione (108)
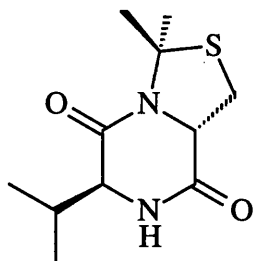
Compound **106** (90 mg, 190 μmol) was stirred with Et$_3$N (39 mg, 380 μmol) in CH$_2$Cl$_2$ (3.0 mL) for 10 min. Evaporation and chromatography (EtOAc) afforded **108** (28 mg, 61%) as a white solid: mp 180-182°C: NMR ((CD$_3$)$_2$SO) δ$_H$ 0.88 (3 H, d, J = 6.6 Hz, 6-CMe), 0.91 (3 H, d, J = 6.6 Hz, 6-CMe), 1.78 (3 H, s, 3-Me), 1.82 (3 H, s, 3-Me), 2.07 (1 H, m, 6-CH), 3.11 (1 H, dd, J = 11.7, 10.7 Hz, 1-H), 3.23 (1 H, dd, J =11.7, 5.5 Hz, 1-H), 3.40 (1 H, dd, J = 5.9, 3.5 Hz, 6-H), 4.64 (1 H, dd, J = 10.7, 5.5 Hz, 8a-H), 8.90 (1 H, d, J = 3.5 Hz, NH); MS m/z 396 (M + mNBA), 243.1176 (M + H) (C$_{11}$H$_{19}$N$_2$O$_2$S requires 243.1167); Found C, 54.60; H, 7.39; N, 11.4; C$_{11}$H$_{18}$N$_2$O$_2$S requires C, 54.52; H, 7.49; N, 11.56%.

Pentafluorophenyl   S-2,2-dimethyl-3-(N-(L-leucyl)tetrahydrothiazole-2-carboxylate trifluoroacetate   (107)   and   6S,8aS-3,3-Dimethyl-6-isopropylmethyltetrahydro-thiazolo[3,4-a]pyrazine-5,8-dione (109)

(107)   (109)
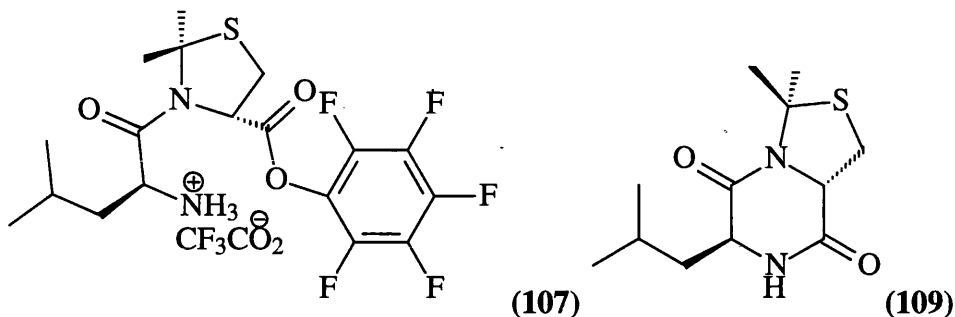
Compound **92** (700 mg, 1.30 mmol) was stirred with CF_3CO_2H (1 mL) and CH_2Cl_2 (4 mL) for 20 min. Evaporation afforded **107** (quant.) as a gummy solid. This material (554 mg, 1 mmol) was stirred with Et_3N (202 mg, 2 mmol) in CH_2Cl_2 (3.0 mL) for 30 min. Evaporation and chromatography (EtOAc) afforded **109** (150 mg, 59%) as a white solid: mp 153-155°C: NMR δ_H 0.95 (3 H, d, J = 6.6 Hz, CHCH_3), 1.00 (3 H, d, J = 6.6 Hz, CHCH_3), 1.60-1.78 (3 H, m, 6-CHCH_2CH), 1.88 (3 H, s, 3-Me), 1.89 (3 H, s, 3-Me), 3.23 (1 H, dd, J = 12.1, 10.7 Hz, 1-H), 3.32 (1 H, dd, J =12.1, 5.7 Hz, 1-H), 3.87 (1 H, dt, J = 10.0, 5.0 Hz, 6-H), 4.55 (1 H, dd, J = 10.7, 5.7 Hz, 8a-H), 6.29 (1 H, br, NH); MS m/z 257.1316 ($C_{12}H_{21}N_2O_2S$ requires 257.1324).

N-(N-(L-γ-glutamyl)-L-cysteinyl)glycine dimethyl ester hydrochloride (120), N-(S-Benzoyl-N-(N-benzoyl-γ-glutamyl)-L-cysteinyl)glycine dimethyl ester (121)

(120)

(121)
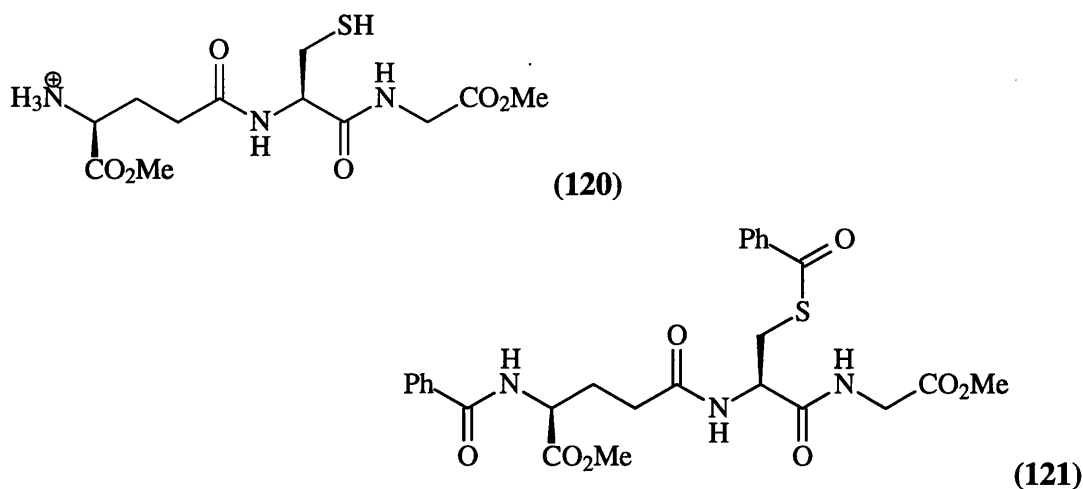
HCl was bubbled through glutathione **119** (1.5 g, 4.89 mmol) in MeOH (60 mL) for 1.5 h. The mixture was then stirred for 24 h. Evaporation afforded **crude 120** as a white solid. This material (1.75 g, 5.19 mmol) was stirred with benzoyl chloride (1.82 g, 13 mmol) and

Et$_3$N (2.10 g, 21 mmol) in CH$_2$Cl$_2$ (10 mL) under N$_2$ for 3 h. The organic layer was washed with H$_2$O and aq. HCl (1 M). Drying, evaporation and recrystallisation (EtOAc) afforded **121** (680 mg, 24 %) as a white solid: mp 189-192°C: IR v_{max} 3278 (NH), 1750 (C=O), 1662 (amide I), 1638 (amide I), 1581 (amide II), 1545 (amide II) cm^{-1}; NMR ((CD$_3$)$_2$SO) δ_H 1.99 (1 H, m, Glu β-H), 2.12 (1 H, m, Glu β-H), 2.32 (2 H, t, J = 7.8 Hz, Glu γ-H$_2$), 3.52 (1 H, dd, J = 13:3, 8.6 Hz, Cys β-H), 3.61 (3 H, s, CO$_2$Me), 3.65 (3 H, s, ° CO$_2$Me), 3.82 (1 H, dd, J = 13.3, 5.3 Hz, Cys β-H), 3.84 (1 H, dd, J = 17.2, 5.9 Hz) and 3.86 (1 H, dd, J = 17.2, 5.9 Hz) (Gly-H$_2$), 4.43 (1 H, m, Glu α-H), 4.61 (1 H, dt, J = 5.3, 8.6 Hz, Cys α-H), 7.45-7.92 (10 H, m, Ar), 8.36 (1 H, d, J = 8.6 Hz, Cys-NH), 8.51 (1 H, t, J = 5.9 Hz, Gly-NH), 8.79 (1 H, d, J = 7.4 Hz, Glu-NH); MS m/z 544.17636 (M + H) (C$_{26}$H$_{30}$N$_3$O$_8$S requires 544.17536), Found C, 56.90; H, 5.34; N, 7.62; C$_{26}$H$_{30}$N$_3$O$_8$S 0.25 H$_2$O requires C, 56.98; H, 5.42; N, 7.67%.

N-(N-(N-Benzoyl-γ-glutamyl)-L-cysteinyl)glycine dimethyl ester (122)
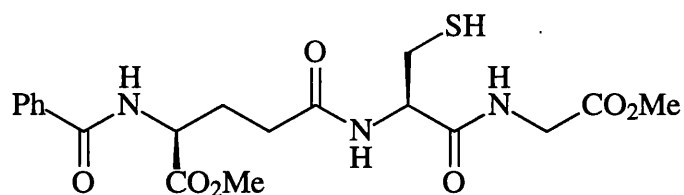
Compound **121** (100 mg, 180 μmol) in MeOH (10 mL) was stirred at 30°C for 48 h. The evaporation residue was recrystallised (hexane) to afford **122** (55 mg, 57%) as a white solid: 203-205°C; NMR ((CD$_3$)$_2$SO) δ_H 1.99 (1 H, m, Glu β-H), 2.09 (1 H, m, Glu β-H), 2.31 (2 H, m, Glu γ-H$_2$), 2.82 (1 H, dd, J = 13.5, 8.6 Hz, Cys β-H), 3.10 (1 H, dd, J = 13.5, 4.7 Hz, Cys β-H), 3.63 (3 H, s, Me), 3.64 (3 H, s, Me), 3.82 (2 H, d, J = 5.9 Hz, Gly-H$_2$), 4.45 (1 H, m, Glu α-H), 4.60 (1 H, dt, J = 4.7, 8.6 Hz, Cys α-H), 7.48-7.89 (5 H, m, Ph-H$_5$), 8.28 (1 H, d, J = 8.6 Hz, Cys-NH), 8.46 (1 H, t, J = 5.9 Hz, Gly-NH), 8.82 (1 H, d, J = 7.0 Hz, Glu-NH); MS m/z 440.1487 (M + H) (C$_{19}$H$_{26}$N$_3$O$_7$S requires 440.1491, 877 (2 × M).

N,N'-Dibenzoyl-L,L-cystine (125).

$$HO_2C$$
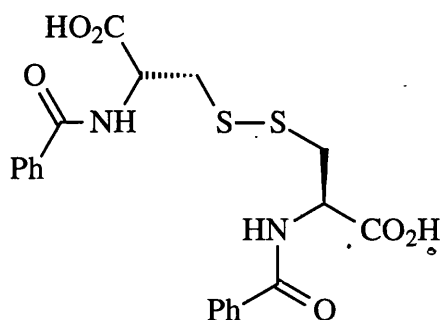
L-cystine hydrochloride **124** (2.50 g, 10.4 mmol) was stirred with benzoyl chloride (2.92 g, 21 mmol) and NaOH (2.10 g, 52.5 mmol) in H_2O (20 mL) for 20 h. The aq. phase was washed twice with Et_2O, acidified (1 M aq. HCl), filtered and washed with hot H_2O. Drying under vacuum afforded **125** (2.50 g, 54%) as a white solid: mp 179-181°C (lit[155] mp 178-180°C); NMR ((CD_3)$_2$SO) δ_H 3.08 (2 H, dd, J = 13.7, 9.4 Hz, 2 × β-H), 3.39 (2 H, dd, J = 13.7, 3.9 Hz, 2 × β-H), 4.69 (2 H, ddd, J = 9.4, 7.8, 3.9 Hz, 2 × α-H), 7.43-7.84 (10 H, m, 2 × Ph-H_5), 8.65 (2 H, d, J = 7.8 Hz, 2 × NH).

N,N'-Dibenzoyl-L-cystine dimethyl ester (126)

$$MeO_2C$$
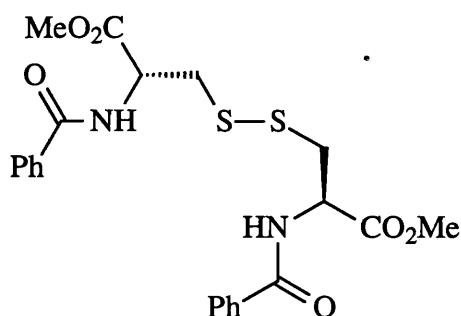
Compound **125** (500 mg, 1.1 mmol) was boiled under reflux with H_2SO_4 (1.0 mL) in MeOH (100 mL) for 24 h. Aq. $NaHCO_3$ was added until no further bubbling occurred. The evaporation residue was washed with H_2O. Drying under vacuum afforded **126** (530 mg quant.) as a white solid: mp 170-173°C (lit[222] mp 168-169°C); NMR ((CD_3)$_2$SO) δ_H 3.13 (2 H, dd, J = 13.7, 9.8 Hz, 2 × β-H), 3.27 (2 H, dd, J = 13.7, 4.7 Hz, 2 × β-H), 3.64 (6 H, s, 2 × Me), 4.74 (2 H, ddd, J = 9.8, 7.8, 4.7 Hz, 2 × α-H), 7.42-7.81 (10 H, m, 2 × Ph-H_5), 8.91 (2 H, d, J = 7.8 Hz, 2 × NH).

N,N-Dibenzoyl-L,L-cystine dihydrazide (128)
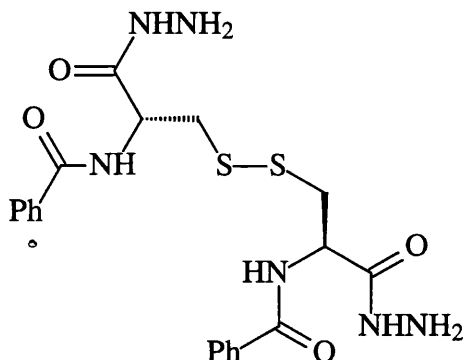
Compound **126** (500 mg, 1.1 mmol) was stirred with hydrazine hydrate (820 mg, 25 mmol) in MeOH (10 mL) for 16 h. The filtered solid was washed with MeOH. Drying afforded **128** (300 mg, 60%) as a white solid: mp 205-207°C (lit[223] mp 206-207°C);; NMR δ_H 3.02 (2 H, dd, J = 13.3, 9.8 Hz, 2 × β-H), 3.20 (2 H, dd, J = 13.3, 5.1 Hz, 2 × β-H), 4.73 (2 H, ddd, J = 9.8, 8.2, 5.1 Hz, 2 × α-H), 7.44 (2 H, t, J = 7.4 Hz, 2 × Ph 4-H), 7.52 (4 H, t, J = 7.4 Hz, 2 × Ph 3,5-H$_2$), 7.85 (4 H, d, J = 7.4 Hz, 2 × 2,6-H$_2$), 8.62 (2 H, d, J = 8.2 Hz, 2 × PhCONH), 9.37 (2 H, br, 2 × NHNH$_2$); MS m/z 477.1370 (M + H) (C$_{20}$H$_{25}$N$_6$O$_2$S$_2$ requires 477.1379).

L,L-Cystine bis(N-butyl)amide dihydrochloride (129)
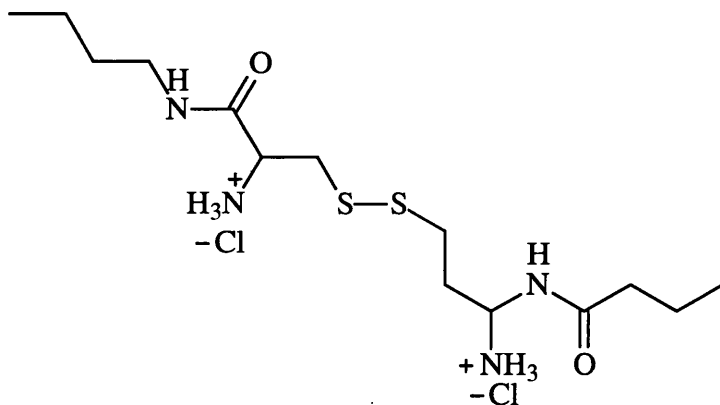
L,L-Cystine dimethyl ester dihydrochloride **124** (5.0 g, 15 mmol) was dissolved in anhydrous butylamine (100 mL) at -78°C. The solution was warmed to ambient temperature and heated under reflux for 5 h. Evaporation afforded a sticky yellow solid which was dissolved in MeOH and acidified (HCl). Evaporation afforded crude **129** (14.8 g) as a yellow viscous oil; MS m/z 351.1874 (M + H) (C$_{14}$H$_{31}$N$_4$O$_2$S$_2$ requires 351.1888).

R,R-Bis(2-benzoylamino-3-butylamino-3-oxopropyl)sulfide (130) and R,S-Bis(2-benzoylamino-3-butylamino-3-oxopropyl)sulfide (131)
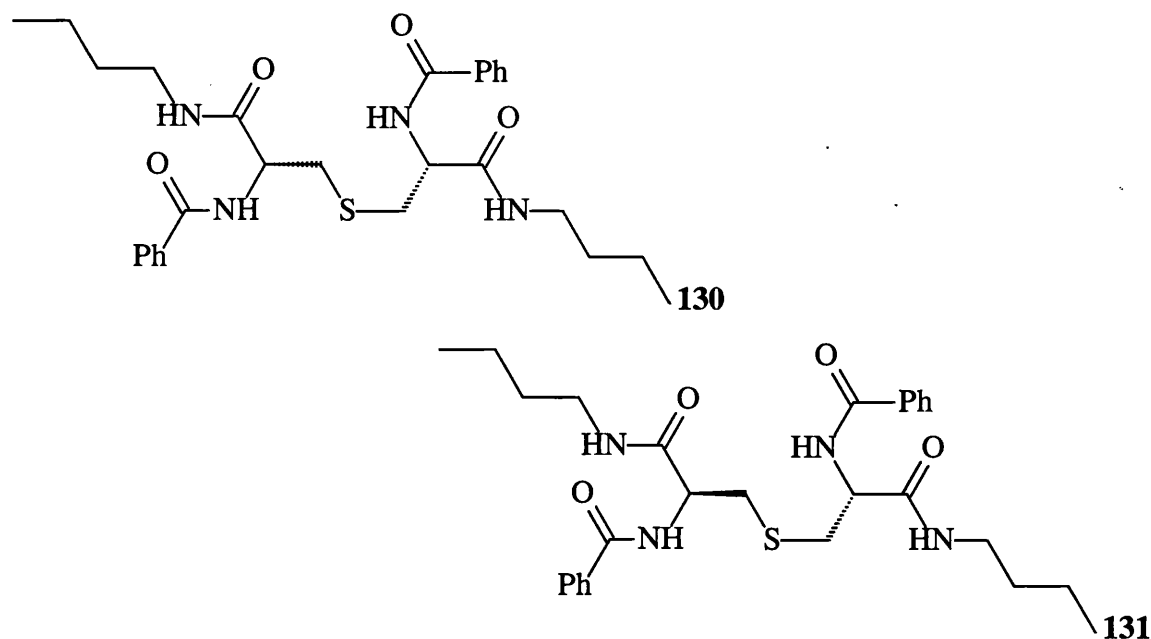
Crude **128** (14.7 mmol) was stirred with NaOAc (10 g) in H_2O (100 mL) and Et_2O (100 mL). Benzoyl chloride (9.1 g, 65 mmol) was added at 0°C and the mixture was stirred vigorously for 4 h. The Et_2O layer was separated. Drying, evaporation and chromatography (EtOAc / hexane 1:1) afforded **130** (500 mg, 951 μmol) as a white solid mp 154-156°C: $[\alpha]_D^{20}$ + 40.63° (c 3.2 × 10^{-3}, CHCl$_3$); IR ν_{max} 3286 (NH), 1634 (amide I), 1602 (amide I), 1557 (amide II), 1540 (amide II) cm^{-1}; NMR δ_H 0.90 (6 H, t, J = 7.0 Hz, 2 × Me), 1.41 (4 H, sextet, J = 7.0 Hz, 2 × CH_2Me), 1.58 (4 H, quintet, J = 7.0 Hz, 2 × NHCH$_2$CH_2), 3.01 (2 H, dd, J = 14.8, 6.2 Hz, 2 × 1-H), 3.07 (2 H, dd, J = 14.8, 6.2 Hz, 2 × 1-H), 3.33 (4 H, m, 2 × NHCH_2), 5.43 (2 H, q, J = 6.2 Hz, 2 × 2-H), 7.46-7.58 (8 H, m, 2 × Ar 3,4,5-H$_3$ + 2 × NH), 7.85 (4 H, m, 2 × Ar 2,6-H$_2$), 7.96 (2 H, t, J = 5.5 Hz, 2 × NHBu); MS m/z 527.2696 (M + H) (C$_{28}$H$_{39}$N$_4$O$_4$S requires 527.2692); Found: C, 62.30; H, 7.32; N, 10.37; C$_{28}$H$_{38}$N$_4$O$_4$S requires C, 63.85; H, 7.27; N, 10.63%. Further elution gave the other diastereoisomer **131** (310 mg, 589 μmol) as a white solid: mp 178-180°C: $[\alpha]_D^{20}$ + 0.0° (c 0.003, CHCl$_3$); IR ν_{max} 3287 (NH), 1633 (amide I), 1602 (amide I), 1560 (amide II), 1532 (amide II) cm^{-1}; NMR δ_H 0.93 (6 H, t, J = 7.4 Hz, 2 × Me), 1.40 (4 H, sextet, J = 7.4 Hz, 2 × CH_2Me), 1.56 (4 H, quintet, J = 7.4 Hz, 2 × NCH$_2$CH_2), 3.14 (4 H, d, J = 6.2 Hz, 2 × 1-H$_2$), 3.33 (4 H, m, 2 × NCH$_2$), 4.90 (2 H, q, J = 6.2 Hz, 2 × 1-H), 7.33 (2 H, t, J = 5.5 Hz, 2 × NHBu), 7.44 (6 H, m, 2 × Ph 3,5-H$_2$ + 2 × NH), 7.53 (2 H, m, 2 × Ph 4-H), 7.81 (4 H, m, 2 × Ph 2,6-H$_2$); MS m/z 527.2689 (M + H) (C$_{14}$H$_{31}$N$_4$O$_2$S$_2$ requires 527.2692).

N,N-Diacetyl-L,L-cystine bis-(naphth-2-yl)amide (133)
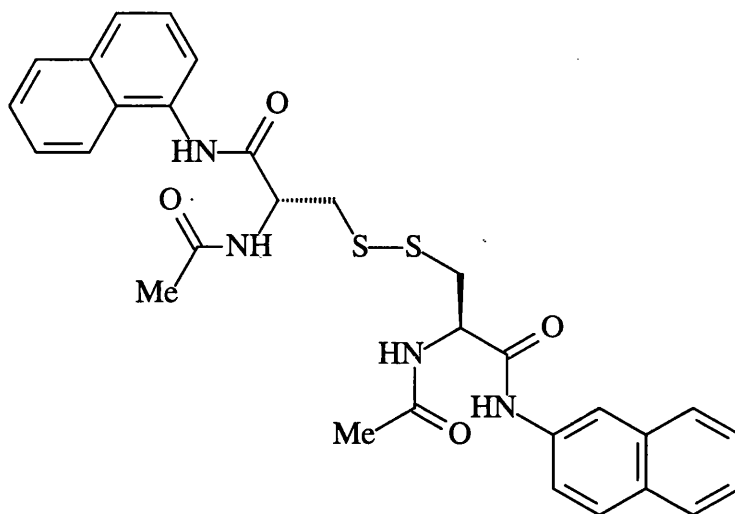
L,L-Cystine bis(naphth-2-yl)amide (500 mg, 1.0 mmol) was stirred with Ac_2O (7 mL) and Et_3N (206 mg, 2.0 mmol) for 16 h. The evaporation residue was washed with H_2O. Drying under vacuum afforded **133** (0.54 g, 92%) as a white solid: mp 250-252°C; IR v_{max} 3289 (NH), 1647 (amide I), 1604 (amide I), 1536 (amide II), 1505 (amide II) cm^{-1}; NMR ($(CD_3)_2SO$) δ_H 1.91 (6 H, s, 2 × Me), 3.03 (2 H, dd, J = 13.3, 8.4 Hz, 2 × β-H), 3.25 (2 H, dd, J = 13.3, 5.9 Hz, 2 × β-H), 4.78 (2 H, dt, J = 8.4, 5.9 Hz, 2 × α-H), 7.40 (2 H, dt, J = 1.2 Hz, 7.0 Hz) and 7.46 (2 H, dt, J = 1.2, 7.0 Hz) (2 × Ar 6,7-H_2), 7.63 (2 H, dd, J = 8.6, 2.0 Hz, 2 × Ar 3-H), 7.85 (6 H, m, 2 × Ar 4,5,8-H_3), 8.29 (2 H, d, J = 2.0 Hz, 2 × Ar 1-H), 8.45 (2 H, d, J = 7.8 Hz, 2 × NHAc), 10.41 (2 H, s, 2 × NH); MS m/z 575.1782 (M + H) ($C_{30}H_{31}N_4O_4S_2$ requires 575.1787); Found: C, 60.70; H, 5.31; N, 9.18; $C_{30}H_{30}N_4O_4S_2$ 1.0 H_2O requires C, 60.79; H, 5.44; N, 9.45%.

N-Acetyl-L-cysteine naphth-2-ylamide (134)
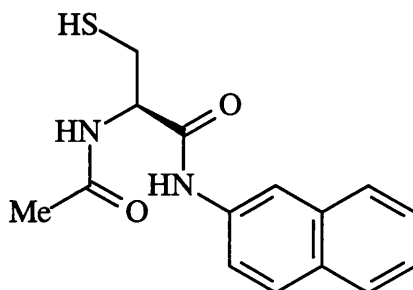
Compound **133** (250 mg, 0.44 mmol) was boiled under reflux with propane-1,3-dithiol (480 mg, 4.4 mmol) and Pr^i_2NEt (142 mg, 1.1 mmol) in THF (10 mL) for 48 h. The evaporation residue, in CH_2Cl_2, was washed twice with cold aqueous H_2SO_4 (1 M) and brine and was dried. The evaporation residue was washed with hexane and dried to afford

134 (190 mg, 150%) as a white solid: mp 204-207°C; IR v_{max} 3271 (NH), 1646 (amide I), 1542 (amide II), 1508 (amide II) cm^{-1}; NMR δ_H 1.94 (1 H, dd, J = 10.5, 7.0 Hz, SH), 2.15 (3 H, s, Me), 2.81 (1 H, ddd, J = 10.5, 7.4, 3.7, Hz, β-H), 3.24 (1 H, ddd, J = 7.4, 7.0, 3.7 Hz, β-H), 4.80 (1 H, dt, J = 3.7, 7.0 Hz, α-H), 6.61 (1 H, d, J = 6.6 Hz, NHAc), 7.47 (3 H, m, Ar-H$_3$), 7.79 (3 H, m, Ar-H$_3$), 8.19 (1 H, d, J = 2.0 Hz, Ar 1-H), 8.74 (1 H, brs, CONH); MS m/z 288.0932 (M) (C$_{15}$H$_{16}$N$_2$O$_2$S requires 288.0932).

N-Acetyl-S-(1-methoxy-1-methylethyl)cysteine naphth-2-ylamide (135) and N-acetyl-S-(1-methylethenyl)cysteine naphth-2-ylamide (136)
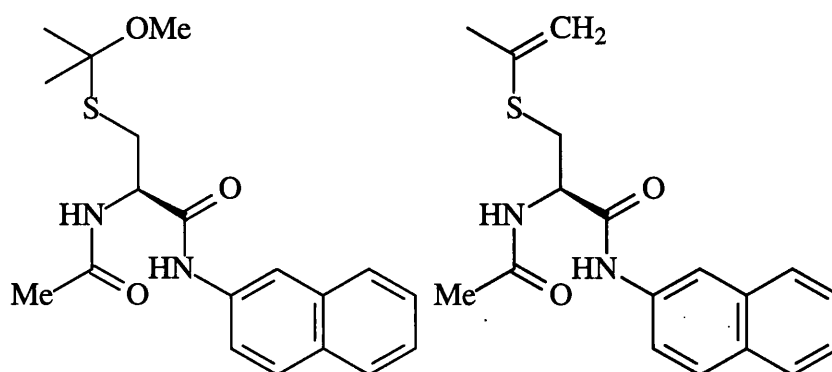
Compound **134** (50 mg, 0.17 mmol) was boiled under reflux in 2,2-dimethoxypropane (70 ml), 4-methylbenzenesulfonic acid hydrate (8.0 mg, 40 μmol) and CH$_2$Cl$_2$ (3 mL) for 3 h, after which CH$_2$Cl$_2$ (20 mL) and H$_2$O (10 mL) were added. The organic layer was extracted and washed with H$_2$O. Drying, evaporation and chromatography (EtOAc / hexane 9:1) afforded **135** (30 mg, 54%) as a colourless oil; NMR δ_H 2.03 (3 H, s, Me), 2.10 (3 H, s, COMe), 3.17 (1 H, dd, J = 14.1, 7.4 Hz, β-H), 3.30 (1 H, dd, J = 14.1, 6.2 Hz, β-H), 4.87 (1 H, dd, J = 7.4, 6.2 Hz, α-H), 5.04 (1 H, brs, =CH), 5.13 (1 H, s, =CH), 6.59 (1 H, d, J = 7.0 Hz, AcNH), 7.45 (3 H, m, Ar 3,6,7-H$_3$), 7.75 (3 H, m, Ar 4,5,8-H$_3$), 8.19 (1 H, d, J = 2.0 Hz, Ar 1-H), 8.85 (1 H, brs, NH); MS m/z 361.1589 (M + H) (C$_{19}$H$_{25}$N$_2$O$_3$S requires 361.1586). Further elution gave **136** (30 mg, 49%) as a white solid: mp 137-138°C; NMR δ_H 1.56 (3 H, s, Me), 1.58 (3 H, s, Me), 2.09 (3 H, s, COMe), 3.03 (1 H, dd, J = 13.7, 6.2 Hz, β-H), 3.10 (1 H, dd, J = 13.7, 6.2 Hz, β-H), 4.93 (1 H, dt, J = 7.8, 6.2 Hz, α-H), 7.01 (1 H, d, J = 7.8 Hz, AcNH), 7.39 (2 H, m, Ar 6,7-H$_2$), 7.46 (1 H, dd, J = 9.0, 2.0 Hz, Ar 3-H), 8.2 (1 H, d, J = 1.6 Hz, Ar 1-H), 9.2 (1 H, brs, NH); MS m/z 361.1589 (M + H) (C$_{19}$H$_{24}$N$_2$O$_3$S requires 361.1586).

L-Valine methyl ester hydrochloride (141)

$$\text{HCl.H}_2\text{N} \overset{}{\underset{}{\bigvee}} \text{OMe, O}$$
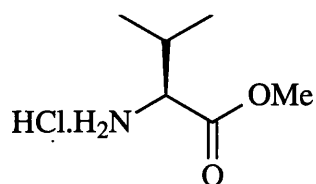
L-Valine (10.0 g, 85.5 mmol) was stirred with $SOCl_2$ (50 mL) in MeOH (500 mL) at 40°C for 24 h. Evaporation afforded **141** (11.1 g, 78%) as a white solid: mp 166-169°C (lit[162] mp 171-173°C); NMR ((CD$_3$)$_2$SO) δ_H 0.93 (3 H, d, J = 7.0 Hz, Val-Me), 0.98 (3 H, d, J = 7.0 Hz, Val-Me), 2.19 (1 H, m, Val β-H), 3.74 (3 H, s, OMe), 3.84 (1 H, m, Val α-H), 8.61 (3 H, br, N$^+$H$_3$).

N-(N-(1,1-Dimethylethoxycarbonyl)-L-glutaminyl)-L-valine methyl ester (142)
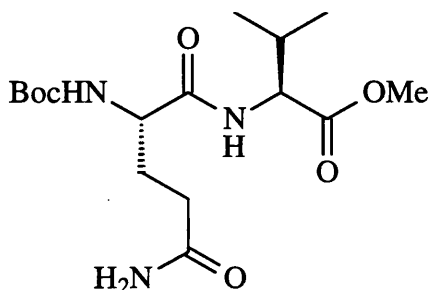
N-(1,1-Dimethylethoxycarbonyl)-L-glutamine (2.78 g, 11.3 mmol) was stirred with HOBt (1.68 g, 12.4 mmol) and DCC (3.49 g, 16.9 mmol) in CH_2Cl_2 (150 mL) at 0°C for 1 h. Pr$^i_2$NEt (2.92 g, 22.6 mmol) was added, followed by **141** (1.89 g, 11.3 mmol) in CH_2Cl_2 (50 mL) and the mixture was stirred for 24 h. The mixture was kept at 4°C for 16 h and filtered (Celite®). The filtrate was washed with aq. citric acid (10%), aq. NaHCO$_3$ and H$_2$O. Drying, evaporation and chromatography (EtOAc → EtOAc/MeOH 1:1) afforded **142** (2.90 g, 71%) as a white solid: mp 145-148°C; NMR δ_H 0.93 (3 H, d, J = 6.6 Hz, Val-Me), 0.96 (3 H, d, J = 6.6 Hz, Val-Me), 1.43 (9 H, s, Bu^t), 2.04 (2 H, m, Gln β-H$_2$), 2.21 (1 H, m, Val β-H), 2.42 (2 H, t, J = 6.6 Hz, Gln γ-H$_2$), 3.73 (3 H, s, OMe), 4.26 (1 H, brq, J = 7.4 Hz, Gln α-H), 4.48 (1 H, dd, J = 8.4, 5.1 Hz, Val α-H), 5.59 (1 H, d, J = 7.4 Hz, Gln-NH), 5.84 (1 H, s, CONH), 6.40 (1 H, s, CONH), 7.59 (1 H, d, J = 8.4 Hz, Val NH); MS m/z 741 (2M + Na), 719 (2M + H), 382 (M + Na), 360.2142 (M + H) (C$_{16}$H$_{30}$N$_3$O$_6$ requires 360.2135); Found C, 52.00; H, 7.82; N, 11.60; C$_{16}$H$_{29}$N$_3$O$_6$ requires C, 52.14; H, 7.82; N, 11.60%.

N-(N-(1,1-Dimethylethoxycarbonyl)-L-glutaminyl)-L-valine (143)
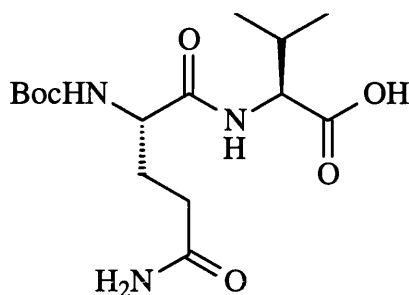
Compound **142** (890 mg, 2.5 mmol) was stirred with NaOH (2.0 g, 50 mmol) in MeOH (30 mL) for 2 h. H_2O (10 mL) was added and MeOH was evaporated. The aqueous solution was brought into neutrality with cold aq. citric acid (10%) and extracted several times with EtOAc. Also, the aqueous layer was saturated with NaCl and extracted further with EtOAc. Drying and evaporation of the combined extracts afforded **143** (550 mg, 64%) as a white solid: mp 86-89°C (lit[224]mp not reported); NMR $((CD_3)_2SO)$ δ_H 0.87 (6 H, d, J = 7.0 Hz, 2 × Val-Me), 1.37 (9 H, s, Bu^t), 1.66 (1 H, m, Gln β-H), 1.83 (1 H, m, Gln β-H), 2.10 (3 H, m, Gln γ-H$_2$,Val β-H), 3.94 (1 H, dt, J = 8.6, 5.5 Hz, Gln α-H), 4.15 (1 H, dd, J = 8.6, 5.5 Hz, Val α-H), 6.76 (1 H, s, CONH), 6.94 (1 H, d, J = 8.2 Hz, Gln NH), 7.25 (1 H, s, CONH), 7.75 (1 H, d, J = 8.6 Hz, Val NH); MS m/z 346.1975 (M + H) ($C_{15}H_{28}N_3O_6$ requires 346.1978).

N-(N-(1,1-Dimethylethoxycarbonyl)-L-phenylalanyl)-L-valine methyl ester (147)
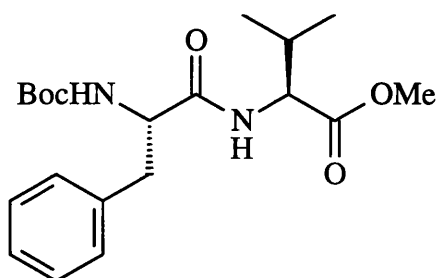
BocPheOH (10.0 g, 37.7 mmol) was stirred with HOBt (5.10 g, 37.7 mmol) and DCC (7.80 g, 37.7 mmol) in CH_2Cl_2 (250 mL) at 0°C for 1 h. Compound **141** (6.30 g, 37.7 mmol) in CH_2Cl_2 (100 mL) was added in the presence of Et_3N (7.60 g, 75.4 mmol) and the mixture was stirred for 48 h. The mixture was kept at 4°C for 16 h and filtered through Celite®. The solution was washed with 10% aq. citric acid, aq. $NaHCO_3$ and H_2O. Drying, evaporation and recrystallisation (EtOAc / hexane) afforded **147** (4.50 g, 33%) as a white solid: mp 115-118°C (lit [225] mp 115-117°C); NMR δ_H 0.84 (3 H, d, J = 7.0 Hz, Val-Me), 0.87 (3 H, d, J = 7.0 Hz, Val-Me), 1.42 (9 H, s, Bu^t), 2.11 (1 H, d septet, J = 5.0, 7.0 Hz,

Val β-H), 3.07 (2 H, d, J = 7.0 Hz, Phe β-H$_2$), 3.68 (3 H, s, OMe), 4.34 (1 H, brq, J = 6.6 Hz, Phe α-H), 4.46 (1 H, dd, J = 8.8, 5.1 Hz, Val α-H), 4.99 (1 H, br, Phe NH), 6.34 (1 H, d, J = 8.8 Hz, Val NH), 7.25 (5 H, m, Ph-H$_5$).

N-(N-(1,1-Dimethylethoxycarbonyl)-L-phenylalanyl)-L-valine (148)
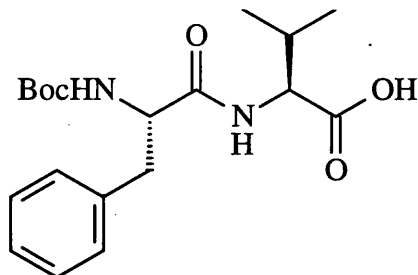
Compound **147** (1.0 g, 2.6 mmol) was stirred with NaOH (1.0 g, 26 mmol) in MeOH (15 mL) and H$_2$O (15 mL) for 1 h. The mixture was concentrated and EtOAc (25 mL) was added. The mixture was brought into neutrality with cold 10% aq. citric acid and extracted with EtOAc. Drying and evaporation afforded **148** (850 mg, 88%) as a white solid: mp 77-78°C (lit[226] mp 77-78°C); NMR δ_H 0.84 (3 H, d, J = 7.0 Hz, Val-Me), 0.91 (3 H, d, J = 7.0 Hz, Val-Me), 1.4 (9 H, s, Bu^t), 2.17 (1 H, d septet, J = 4.7, 6.7 Hz, Val β-H), 3.07 (2 H, m, Phe β-H$_2$), 4.34 (1 H, m, Phe α-H), 4.46 (1 H, dd, J = 8.4, 4.7 Hz, Val α-H), 5.10 (1 H, br, Phe NH), 6.55 (1 H, d, J = 8.4 Hz, Val NH), 7.25 (5 H, m, Ph-H$_5$).

N-(N-(N-1,1-Dimethylethoxycarbonyl)-L-phenylalanyl)-L-valine   N-(2-(4-nitro-phenylethyl)amide (150)
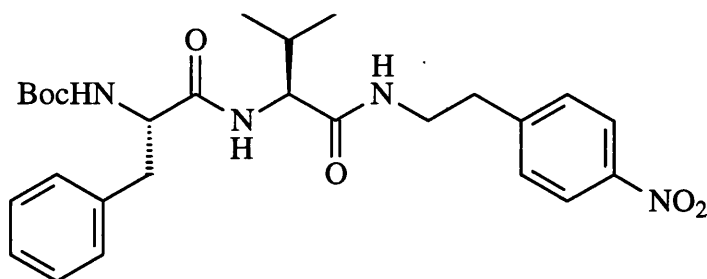
BocPheValOH **(148)** (200 mg, 55 μmol) was stirred with pyridine (44 mg, 55 μmol) in dry CH$_2$Cl$_2$ (5 mL) and added slowly to cyanuric fluoride (222 mg, 165 μmol) in dry CH$_2$Cl$_2$ (5 mL). The mixture was stirred under nitrogen at -10°C for 2 h. The mixture was washed with ice-water (3 × 20 mL). Drying and evaporation afforded crude **149** (40 mg, 14 %). This material (550 μmol) was dissolved in CH$_2$Cl$_2$ (3 mL) and added to 4-nitrophenylethylamine hydrochloride (168 mg, 830 μmol), Et$_3$N (172 mg, 1.7 mmol) and DMAP in CH$_2$Cl$_2$ (3 mL) under N$_2$. The mixture was stirred for 16 h and the evaporation

residue was washed with EtOAc (3mL) to afford **150** (100 mg, 36%) as a buff solid: mp 202-203°C; NMR ((CD$_3$)$_2$SO) δ_H 0.76 (6 H, d, J = 6.7 Hz, 2 × Val-Me), 1.28 (9 H, s, Bu^t), 1.85 (1 H, m, Val β-H), 2.71 (1 H, dd, J = 13.5, 10.6 Hz, Phe β-H), 2.85 (2 H, t, J = 7.0 Hz, ArCH$_2$), 2.91 (1 H, dd, J = 13.5, 4.1 Hz, Phe β-H), 3.34 (2 H, m, NCH$_2$), 4.07 (1 H, dd, J = 9.1, 7.0 Hz, Val α-H), 4.17 (1 H, ddd, J = 10.3, 8.5, 4.1 Hz, Phe α-H), 7.03 (1 H, d, J = 8.5 Hz, Phe NH), 7.12-7.26 (5 H, m, Ph-H$_5$), 7.47 (2 H, d, J = 8.8 Hz, Ar 2,6-H$_2$), 7.64 (1 H, d, J = 8.8 Hz, Val NH), 8.06 (1 H, t, J = 5.9 Hz, NH), 8.11 (2 H, d, J = 8.8 Hz, Ar 3,5-H$_2$); MS m/z 513.2714 (M + H) (C$_{27}$H$_{37}$N$_4$O$_6$ requires 513.2713), 457 (M – H$_2$C=CMe$_2$), 413 (M – Boc).

Phenylmethyl S-1-(1,1-dimethylethoxycarbonyl)-5-oxoyrrolidine-2-carboxylate (151)
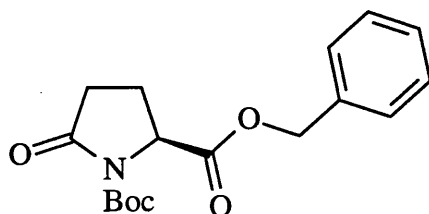
S-2-pyrrolidinone-5-carboxylic acid **153** (5.0 g, 39 mmol) was boiled under reflux with Et$_3$N (3.92 g, 39 mmol) and benzyl choride (5.4 g, 43 mmol) in THF (50 mL) for 5 d. After cooling, H$_2$O (50 mL) was added and the THF was evaporated. The evaporation residue was extracted with CH$_2$Cl$_2$ (3 × 50mL). Drying and evaporation afforded the crude benzyl pyroglutamate as oil. The oil was stirred with Et$_3$N (3.92 g, 38.8 mmol), Boc$_2$O (16.9 g, 77.6 mmol) and DMAP (2.8 g, 39 mmol) in CH$_2$Cl$_2$ (150 mL) at 0°C for 1 h and at 20°C for 16 h. The evaporation residue, in CH$_2$Cl$_2$, was washed with cold 5% aq.citric acid and brine. Drying and evaporation afforded **151** (9.0 g, 72%) as buff solid: mp 62-65C (lit.[179] mp 57-59°C); NMR δ_H 1.41 (9 H, s, Bu^t), 2.05 (1 H, ddt, J = 12.8, 10.3, 3.3 Hz, Pyg β-H), 2.32 (1 H, ddt, J = 12.8, 9.8, 9.4 Hz, Pyg β-H) , 2.47 (1 H, ddd, J = 17.6, 9.4, 3.5 Hz, Pyg γ-H), 2.60 (1H, ddd, J = 17.5, 10.3, 9.8 Hz, Pyg γ-H), 4.62 (1 H, dd, J = 9.4, 3.3 Hz, Pyg α-H), 5.18 (1 H, d, J = 12.1 Hz) and 5.20 (1 H, d, J = 12.1 Hz) (CH$_2$Ph), 7.34 (5 H, m, Ph-H$_5$).

S-1-(1,1-Dimethylethoxycarbonyl)-5-oxopyrrolidine-2-carboxylic acid (154)
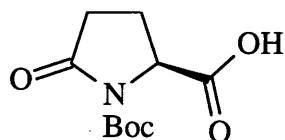
Compound **151** (15.0 g, 47 mmol) was stirred with 10% Pd/C (450 mg) in MeOH (300 mL) under H_2 for 6 h. Filtration (Celite®) and evaporation afforded **154** (10.0 g, 93%) as a white solid: mp 65-67°C (lit.[178] mp 77-80°C); NMR $((CD_3)_2SO)$ δ_H 1.42 (9 H, s, Bu^t), 1.90 (1 H, m, Pyg β-H), 2.30-2.55 (3 H, m, Pyg β,γ-H_3), 4.50 (1 H, dd, J = 9.4, 3.5 Hz, Pyg α-H).

N-(S-1-(1,1-Dimethylethoxycarbonyl)pyrrolidine-2-carbonyl)-L-valine phenylmethyl ester (155)
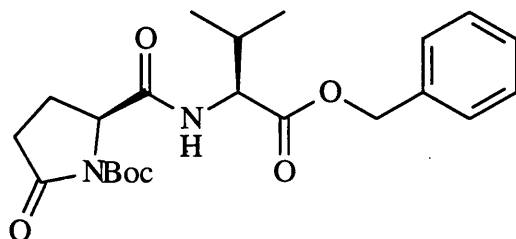
Compound **154** (10.0 g, 43.7 mmol) was stirred with HOBt (6.50 g, 48.1 mmol) and DCC (9.92 g, 48.1 mmol) in CH_2Cl_2 (200 mL) at 0°C for 1 h. L-ValOBn (16.60 g, 43.7 mmol) in CH_2Cl_2 (50 mL) was added in the presence of Pr^i_2NEt (11.30 g, 87.4 mmol) and the mixture was stirred for 24 h. The mixture was kept at 4°C for 16 h and filtered (Celite®). The solution was washed cold 5% aq. citric acid, aq. $NaHCO_3$ and H_2O. Drying, evaporation and chromatography (EtOAc) afforded **155** (13.0 g, 71%) as a white solid: mp 96-98°C; NMR δ_H 0.87 (3 H, d, J = 7.0 Hz, Val-Me), 0.93 (3 H, d, J = 7.0 Hz, Val-Me), 1.51 (9 H, s, Bu^t), 2.20 (3 H, m, Val β-H, Pyg β-H_2), 2.46 (1 H, ddd, J = 17.6, 8.5, 3.5 Hz, Pyg γ-H), 2.73 (1 H, dt, J = 17.6, 10.5 Hz, Pyg γ-H), 4.57 (1 H, dd, J = 7.8, 3.1 Hz, Pyg α-H), 4.60 (1 H, dd, J = 9.0, 4.7 Hz, Val α-H), 5.14 (1 H, d, J = 12.1 Hz) and 5.20 (1 H, d, J = 12.1 Hz) (CH_2Ph), 6.46 (1 H, d, J = 9.0 Hz, Val NH), 7.35 (5 H, m, Ph-H_5); MS m/z 859 (2 M + Na), 837 (2 M + H), 737 (2 M + H - Boc), 441 (M + Na), 419.2192 (M + H) ($C_{22}H_{31}N_2O_6$ requires 410.2182), 319 (M – Boc).

N-(S-1-(1,1-Dimethylethoxycarbonyl)pyrrolidine-2-carbonyl)-L-valine (156)
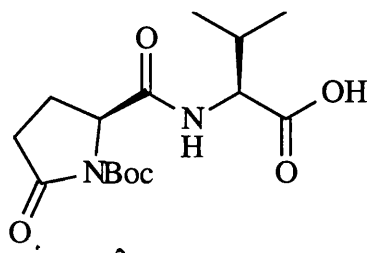
Compound **155** (7.50 g, 17.9 mmol) was stirred with 10% Pd/C (400 mg) in MeOH (300 mL) under H_2 for 16 h. Filtration (Celite®) and evaporation afforded **156** (5.60 g, quant.) as a white solid: mp 152-155°C; NMR ((CD_3)$_2$SO) δ_H 0.91 (3 H, d, J = 7.0 Hz, Val-Me), 0.92 (3 H, d, J = 7.0 Hz, Val-Me), 1.39 (9 H, s, Bu^t), 1.80 (1 H, m, Pyg β-H), 2.10 (1 H, octet, J = 7.0 Hz, Val β-H), 2.2-2.4 (3 H, m, Pyg β,γ-H$_3$), 4.16 (1 H, dd, J = 8.2, 7.0 Hz, Val α-H), 4.68 (1 H, dd, J = 9.0, 2.3 Hz, Pyg α-H), 8.32 (1 H, d, J = 8.6 Hz, NH); MS m/z 679 (2 M + Na), 657 (2 M + H), 557 (2 M + H - Boc), 351 (M + Na), 329.1721 (M + H) ($C_{15}H_{25}N_2O_6$ requires 329.1713), 229 (M − Boc).

N-(S-1-(1,1-Dimethylethoxycarbonyl)pyrrolidine-2-carbonyl)-L-valine pentafluorophenyl ester (157)
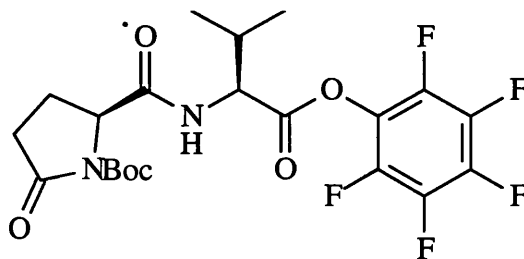
Compound **156** (200 mg, 610 μmol) was stirred with pentafluorophenyl trifluoroacetate (188 mg, 671 μmol) and pyridine (53 mg, 671 μmol) in dry DMF for 1 h. The mixture was diluted with EtOAc (20 mL) and washed with cold 5% aq. citric acid and 5% aq. $NaHCO_3$. Drying and evaporation afforded **157** (250 mg, 83%) as a highly colourless viscous oil; NMR δ_H 1.05 (3 H, d, J = 7.0 Hz, Val-Me), 1.07 (3 H, d, J = 6.6 Hz, Val-Me), 1.52 (9 H, s, Bu^t), 2.26 (2 H, m, Val β-H, Pyg β-H), 2.42 (1 H, m, Pyg β-H), 2.50 (1 H, m, Pyg γ-H), 2.75 (1 H, m, Pyg γ-H), 4.62 (1 H, dd, J = 7.8, 3.1 Hz, Pyg α-H), 4.89 (1 H, dd, J = 8.6, 5.1 Hz, Val α-H), 6.64 (1 H, d, J = 8.6 Hz, NH); NMR δ_F −161.2 (2 F, dd, J = 20.9, 18.0 Hz, 3',5'-F$_2$), -156.4 (1 F, t, J = 20.9 Hz, 4'-F), -151.6 (2 F, d, J = 18.0 Hz, 2',6'-F$_2$); MS m/z 495.1571 (M + H) ($C_{21}H_{24}N_2O_6F_5$ requires 495.1555), 395 (M − Boc), 494 (M + Na).

S-N-(N-(S-1-(1,1-Dimethylethoxycarbonyl)pyrrolidine-2-carbonyl)valyl)-2,2-dimethyltetrahydrothiazole-4-carboxylic acid (158a and b)
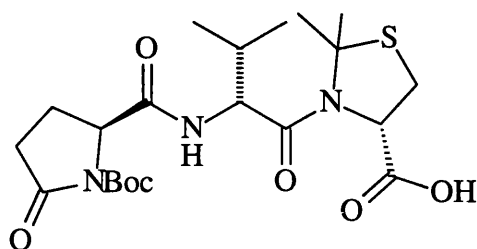
Compound **157** (750 mg, 1.52 mmol) was stirred with **81** (326 mg, 1.65 mmol) and Pr^i_2NEt (640 mg, 4.95 mmol) in dry DMF (100 mL) for 16 h. The evaporation residue, in EtOAc, was washed with cold 5% aq. citric acid and brine. Drying, evaporation and chromatography (EtOAc / AcOH 49:1) afforded **158a** (300 mg, 42%) as a white solid: mp 166-168°C; NMR δ_H 0.92 (3 H, d, J = 6.6 Hz, Val-Me), 0.95 (3 H, d, J = 6.6 Hz, Val-Me), 1.50 (9 H, s, Bu^t), 1.83 (3 H, s, 2-Me), 1.88 (3 H, s, 2-Me), 2.00-2.16 (2 H, m, Val β-H, Pyg β-H), 2.25 (1 H, m, Pyg β-H), 2.45 (1 H, ddd, J = 17.7, 9.4, 2.7 Hz, Pyg γ-H), 2.69 (1 H, dt, J = 17.7, 9.8 Hz, Pyg γ-H), 3.26 (1 H, dd, J = 12.1, 5.9 Hz, 5-H), 3.39 (1 H, d, J = 12.1 Hz, 5-H), 4.25 (1 H, t, J = 9.4 Hz, Val α-H), 4.55 (1 H, dd, J = 9.0, 2.0 Hz, Pyg α-H), 5.54 (1 H, d, J = 5.1 Hz, 4-H), 6.83 (1 H, d, J = 9.4 Hz, Val-NH); MS m/z 472.2129 (M + H) ($C_{21}H_{34}N_3O_7S$ requires 472.2117), 372 (M – Boc), 625 (M + mNBA + H), 742 (2 × (M –Boc)). Minor peaks were observed corresponding to a rotamer. Further elution gave **158b** (70 mg, 10%) as a white solid: mp 149-151°C; NMR δ_H 0.93 (3 H, d, J = 6.6 Hz, Val-Me), 1.01 (3 H, d, J = 6.6 Hz, Val-Me), 1.50 (9 H, s, Bu^t), 1.83 (3 H, s, 2-Me), 1.87 (3 H, s, 2-Me), 1.95 (2 H, m, Val β-H, Pyg β-H), 2.45 (1 H, m, Pyg β-H), 2.48 (1 H, ddd, J = 17.4, 9.4, 2.7 Hz, Pyg γ-H), 2.70 (1 H, dt, J = 17.4, 9.8 Hz, Pyg γ-H), 3.26 (1 H, dd, J = 11.7, 5.5 Hz, 5-H), 3.43 (1 H, d, J = 11.7 Hz, 5-H), 4.52 (1 H, dd, J = 9.4, 2.7 Hz, Pyg α-H), 4.78 (1 H, dd, J = 9.4, 6.6 Hz, Val α-H), 5.02 (1 H, d, J = 5.5 Hz, 4-H), 7.07 (1 H, d, J = 9.4 Hz, Val-NH); MS m/z 471.20002 (M - H) ($C_{21}H_{32}N_3O_7S$ requires 471.2039).

Pentafluorophenyl **S-N-(N-(S-1-(1,1-Dimethylethoxycarbonyl)-pyrrolidine-2-carbonyl)-L-valyl)-2,2-dimethyltetrahydrothiazole-4-carboxylate (159)**
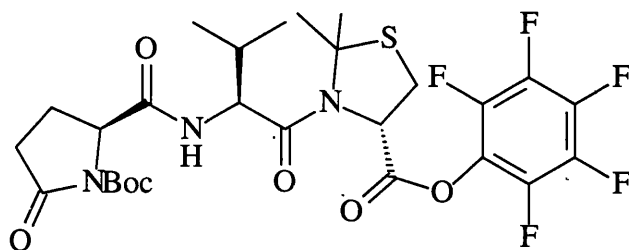
Compound **158a** (100 mg, 212 μmol) was stirred with pentafluorophenyl trifluoroacetate (65 mg, 233 μmol) and pyridine (18 mg, 233 μmol) in dry DMF (1 mL) for 1 h. The mixture was diluted with EtOAc (20 mL) and washed with cold 5% aq. citric acid and 5% aq. NaHCO$_3$. Drying, evaporation and recrystallisation (EtOAc / hexane) afforded **159** (125 mg, 93%) as a white solid: mp 150-152°C; NMR δ$_H$ 0.92 (3 H, d, J = 6.6 Hz, Val-Me), 0.96 (3 H, d, J = 6.6 Hz, Val-Me), 1.54 (9 H, s, Bu^t), 1.87 (3 H, s, 2-Me), 1.92 (3 H, s, 2-Me), 2.15 (2 H, m, Val β-H, Pyg β-H), 2.26 (1 H, m, Pyg β-H), 2.50 (1 H, ddd, J = 17.2, 9.0, 2.7 Hz, Pyg γ-H), 2.71 (1 H, ddd, J = 17.2, 10.5, 9.4 Hz, Pyg γ-H), 3.46 (2 H, m, 5-H$_2$), 4.12 (1 H, t, J = 8.6 Hz, Val α-H), 4.58 (1 H, dd, J = 9.0, 2.3 Hz, Pyg α-H), 6.14 (1 H, dd, J = 4.3, 2.3 Hz, 4-H), 6.83 (1 H, d, J = 8.6 Hz, Val NH); NMR δ$_F$ –161.1 (2 F, dd, J = 21.0, 18.4 Hz, 3',5'-F$_2$), -156.4 (1 F, t, J = 21.0 Hz, 4'-F), -151.4 (2 F, d, J = 17.1 Hz, 2',6'-F$_2$); MS m/z 1298 (2 M + Na), 1276 (2 M + H), 660.1779 (M + Na) (C$_{27}$H$_{32}$F$_5$N$_3$NaO$_7$ requires 660.1795), 560 (M + Na – Boc), 538 (M – Bu^{t}O).

S-3-(N-(S-1-(1,1-Dimethylethoxycarbonyl)pyrrolidine-2-carbonyl)-L-valyl)-2,2-dimethyl-N-(2-(4-nitrophenyl)ethyl)tetrahydrothiazole-4-carboxylamide (160)
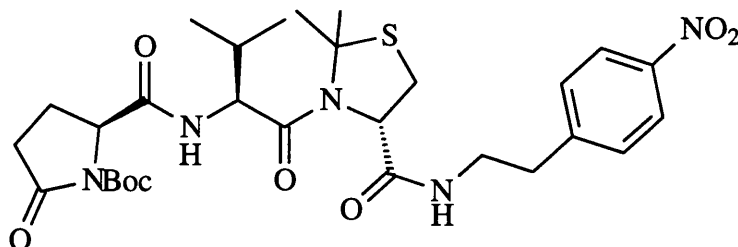
4-Nitrophenylethylamine hydrochloride (426 mg, 2.1 mmol) was stirred with Et$_3$N (425 mg, 4.2 mmol) and **159** (1.34 g, 2.1 mmol) in CH$_2$Cl$_2$ (10 mL) for 5 h. Evaporation and chromatography (EtOAc) afforded **160** (900 mg, 69%) as a buff solid: mp 115-117°C; NMR δ$_H$ 0.77 (3 H, d, J = 6.6 Hz, Val-Me), 0.83 (3 H, d, J = 6.6 Hz, Val-Me), 1.43 (9 H, s, Bu^t), 1.70 (3 H, s, 2-Me), 1.74 (3 H, s, 2-Me), 1.9-2.2 (3 H, m, Val β-H, Pyg β-H$_2$), 2.36

(1 H, ddd, J = 17.6, 9.4, 2.7 Hz, Pyg γ-H), 2.57 (1 H, m, Pyg γ-H), 2.90 (2 H, t, J = 7.4 Hz, ArCH$_2$), 2.93 (1 H, d, J = 12.5 Hz, 5-H), 3.28 (1 H, dd, J = 12.5, 6.6 Hz, 5-H), 3.40 (1 H, m, NHCH), 3.65 (1 H, m, NHCH), 4.13 (1 H, t, J = 8.2 Hz, Val α-H), 4.46 (1 H, dd, J = 9.0, 2.0 Hz, Pyg α-H), 5.24 (1 H, t, J = 6.6 Hz, 4-H), 6.39 (1 H, d, J = 8.2 Hz, Val NH), 6.50 (1 H,.t, J = 5.9 Hz, NHCH$_2$), 7.31 (2 H, d, J = 8.4 Hz, Ar 2,6-H$_2$), 8.08 (2 H, d, J = 8.4 Hz, Ar 3,5-H$_2$);. MS m/z 520.2225 (M - Boc) (C$_{24}$H$_{34}$N$_5$O$_6$S requires 520.2230).

S-3-(N-(N-(Dimethylethoxycarbonyl)-L-glutaminyl)-L-valyl)-2,2-dimethyl-N-(2-(4-nitrophenyl)ethyl)tetrahydrothiazole-4-carboxamide (161)
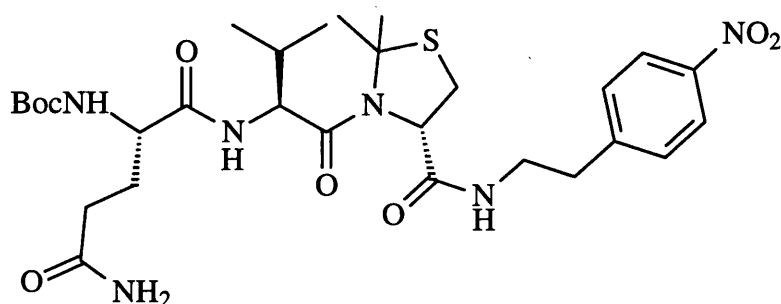
Compound **160** (100 mg, 162 μmol) was stirred in aq. NH$_3$ (35%, 1.0 mL) and THF (10 mL) for 18 h. Evaporation afforded **161** (quant.) as a white solid: mp 95-97°C; NMR δ$_H$ 0.84 (3 H, d, J = 6.6 Hz, Val-Me), 0.91 (3 H, d, J = 6.6 Hz, Val-Me), 1.42 (9 H, s, Bu^t), 1.77 (3 H, s, 2-Me), 1.79 (3 H, s, 2-Me), 2.0 (3 H, m, Val β-H, Gln β-H$_2$), 2.25 (1 H, m, Gln γ-H), 2.35 (1 H, m, Gln γ-H), 2.95-3.00 (3 H, m, 5-H, ArCH$_2$), 3.37 (1 H, dd, J = 12.5, 6.2 Hz, 5-H), 3.45 (1 H, m, NHCH), 3.75 (1 H, m, NHCH), 4.11 (2 H, m, Val α-H, Gln α-H), 5.35 (1 H, d, J = 6.2 Hz, 4-H), 5.50 (1 H, d, J = 7.4 Hz, NH), 5.69 (1 H, s, CONH), 6.21 (1 H, s, CONH), 6.50 (1 H, brt, NHCH$_2$), 7.27 (1 H, d, J = 8.2 Hz, NH), 7.38 (2 H, d, J = 8.6 Hz, Ar 2,6-H$_2$), 8.16 (2 H, d, J = 8.6 Hz, Ar 3,5-H$_2$); MS m/z 637.3020 (M + H) (C$_{29}$H$_{45}$N$_6$O$_8$S requires 637.3021), 537 (M − Boc).

S-2,2-Dimethyl-3-(N-(L-glutaminyl)-L-valyl)-N-(2-(4-nitrophenyl)ethyl)tetrahydrothiazole-4-carboxamide trifluoroacetate salt (162)
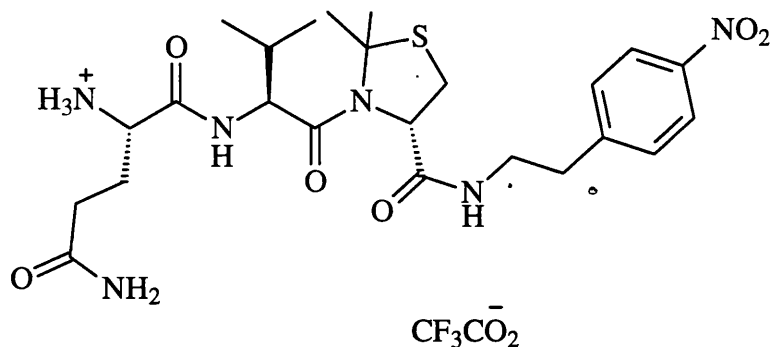
Compound **161** (300 mg, 472 μmol) was stirred in CF_3CO_2H (900 μL) and CH_2Cl_2 (3.6 mL) for 1 h. Evaporation and trituration with Et_2O afforded **162** (300 mg, 98%) as a white solid: mp 108-110°C; NMR (CD_3OD) δ_H 0.89 (3 H, d, J = 6.6 Hz, Val-Me), 0.91 (3 H, d, J = 6.6 Hz, Val-Me), 1.77 (3 H, s, 2-Me), 1.88 (3 H, s, 2-Me), 2.10 (3 H, m, Val β-H, Gln β-H_2), 2.40 (2 H, m, Gln γ-H_2), 2.99 (3 H, m, 5-H, ArCH_2), 3.37 (1 H, dd, J = 12.5, 6.2 Hz, 5-H), 3.51 (2 H, m, NHCH_2), 3.96 (1 H, t, J = 6.6 Hz, Gln α-H), 3.98 (1 H, d, J = 8.6 Hz, Val α-H), 5.38 (1 H, d, J = 5.5 Hz, 4-H), 7.48 (2 H, d, J = 8.8 Hz, Ar 2,6-H_2), 8.16 (2 H, d, J = 8.8 Hz, Ar 3,5-H_2); MS *m/z* 537.2495 (M + H) ($C_{24}H_{37}N_6O_6S$ requires 537.2493).

S-2,2-dimethyl-3-(N-(N-(N-(Dimethylethoxycarbonyl)-L-Leucyl)-L-glutaminyl)-L-valyl)-N-(2-(4-nitrophenyl)ethyl)tetrahydrothiazole-4-carboxamide (163)
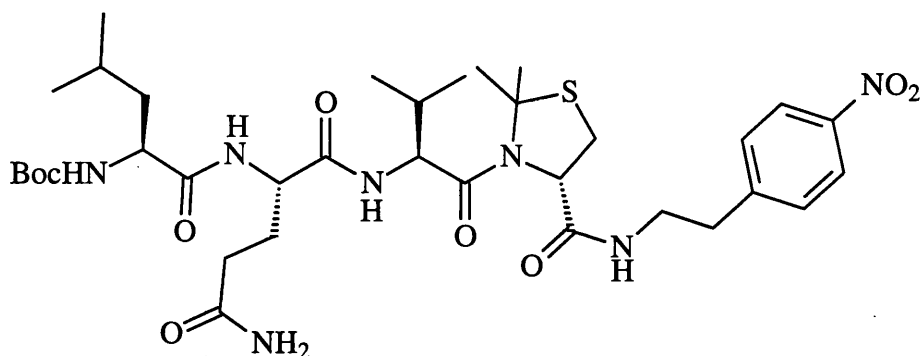
N-(1,1-Dimethylethoxycarbonyl)-L-leucine N-hydroxysuccinimide ester (157 mg, 477 μmol) in dry THF (2.0 mL) and added to compound **162** (310 mg, 477 μmol), Et_3N (97 mg, 954 μmol) and DMAP (1 mg) in dry DMF (1.5 mL) at 0°C and the mixture was stirred for 30 min. The mixture was then gradually warmed to 20°C and stirred for 24 h. The evaporation residue, in EtOAc, was washed with cold 5% aq. citric acid, H_2O and brine. Drying, evaporation and recrystallisation (EtOAc / hexane) afforded **163** (330 mg, 92%) as white solid: mp 109-111°C; NMR (CD_3OD) δ_H 0.85 (3 H, d, J = 6.6 Hz, Val-Me), 0.86 (3

H, d, J = 6.6 Hz, Val-Me), 0.93 (3 H, d, J = 6.6 Hz, Leu-Me), 0.95 (3 H, d, J = 6.6 Hz, Leu-Me), 1.45 (9 H, s, Bu^t), 1.52 (2 H, t, J = 7.0 Hz, Leu β-H$_2$), 1.79 (3 H, s, 2-Me), 1.88 (3 H, s, 2-Me), 1.70-2.10 (4 H, m, Val β-H, Leu γ-H, Gln β-H$_2$), 2.30 (2 H, m, Gln γ-H$_2$), 2.94-3.04 (3 H, m, 5-H, ArCH$_2$), 3.42 (1 H, dd, J = 12.1, 5.9 Hz, 5-H), 3.55 (2 H, brq, J = 5.5 Hz, NHCH_2), 3.95 (1 H, t, J = 9.0 Hz, Val α-H), 4.04 (1 H, t, J = 7.4 Hz, Leu α-H), 4.30 (1 H, brq, J = 6.6˙Hz, Gln α-H), 5.21 (1 H, d, J = 5.9 Hz, 4-H), 7.50 (2 H, d, J = 8.6 Hz, Ar 2,6-H$_2$), 8.07 (1 H, t, J = 5.5 Hz, NHCH$_2$), 8.16 (2 H, d, J = 8.6 Hz, Ar 3,5-H$_2$), 8.18 (2 H, m, 2 × NH); MS m/z 772 (M + Na), 750.3860 (M + H) (C$_{35}$H$_{56}$N$_7$O$_9$S requires 750.3901), 650 (M − Boc).

S-2,2-Dimethyl-3-(N-(N-(L-Leucyl)-L-glutaminyl)-L-valyl)-N-(2-(4-nitrophenyl)ethyl)tetrahydrothiazole-4-carboxamide (164)
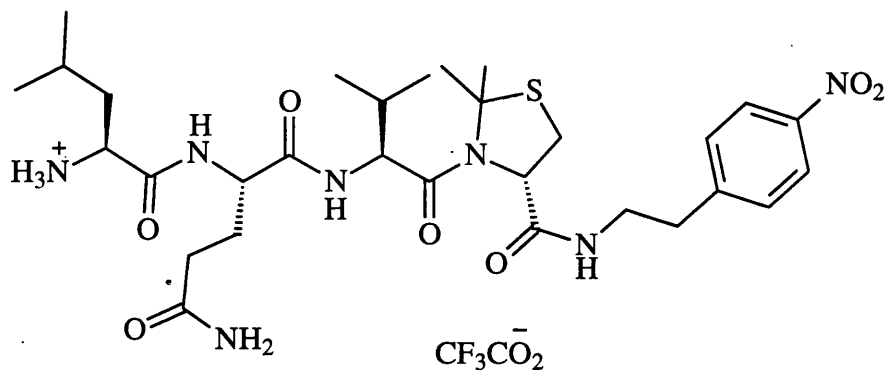
Compound **163** (300 mg, 401 μmol) was stirred in CF$_3$CO$_2$H (900 μL) and CH$_2$Cl$_2$ (3.6 mL) for 30 min. Evaporation and trituration with Et$_2$O afforded **164** (300 mg, 98%) as a white solid: mp 121-123°C; NMR (CD$_3$OD) δ$_H$ 0.76 (3 H, d, J = 7.0 Hz, Val-Me), 0.77 (3 H, d, J = 6.6 Hz, Val-Me), 1.00 (3 H, d, J = 5.5 Hz, Leu-Me), 1.01 (3 H, d, J = 5.5 Hz, Leu-Me), 1.54-1.74 (3 H, m, Leu β-H$_2$, Leu γ-H), 1.70 (3 H, s, 2-Me), 1.79 (3 H, s, 2-Me), 1.82-2.04 (3 H, m, Val β-H, Gln β-H$_2$), 2.20 (2 H, m, Gln γ-H$_2$), 2.89 (2 H, t, J = 6.6 Hz, ArCH$_2$), 2.91 (1 H, d, J = 12.1 Hz, 5-H), 3.30 (1 H, dd, J = 12.1, 5.9 Hz, 5-H), 3.50 (2 H, m, NHCH_2), 3.80 (1 H, brt, J = 8.2 Hz, Leu α-H), 3.87 (1 H, d, J = 9.4 Hz, Val α-H), 4.31 (1 H, t, J = 7.8 Hz, Gln α-H), 5.20 (1 H, d, J = 5.9 Hz, 4-H), 7.40 (2 H, d, J = 9.0 Hz, Ar 2,6-H$_2$), 7.97 (1 H, t, J = 5.5 Hz, NHCH$_2$), 8.06 (2 H, d, J = 9.0 Hz, Ar 3,5-H$_2$), 8.26 (1 H, d. J = 9.0 Hz, NH); MS m/z 650.3343 (M + H) (C$_{30}$H$_{48}$N$_7$O$_7$S requires 650.3336), 723 (M + Na).

N$^\varepsilon$-(1,1-dimethylethoxycarbonyl)-N$^\alpha$-(Fluoren-9-ylmethoxycarbonyl)-L-Lysyl pentafluorophenyl ester (166)
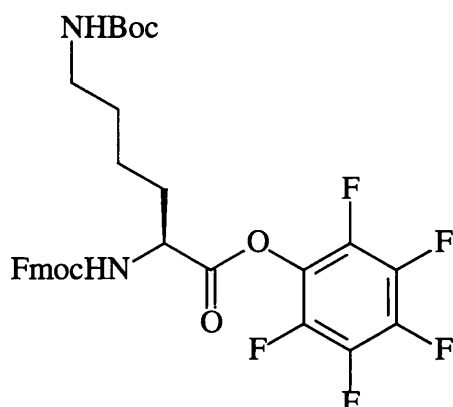
N$^\alpha$-Fmoc-N$^\varepsilon$-Boc-L-Lysine (1.0 g, 2.1 mmol) was stirred with pentafluorophenol (432 mg, 2.3 mmol) and DCC (483g, 2.3 mmol) in EtOAc (5 mL) and THF (5 ml) at 0°C under N$_2$ for 4 h for 16 h. The mixture was filtered (Celite$^\circledR$) and the precipitate was washed with cold EtOAc. Evaporation afforded **166** (2.10 g, 70%) as a white solid: mp 102-104°C (lit[181] mp 99-101°C); NMR δ_H 1.43 (9 H, s, Bu^t), 1.50-2.05 (8 H, m, Lys β-H$_2$, Lys γ-H$_2$, Lys δ-H$_2$, Lys ε-H$_2$), 4.23 (1 H, t, J = 7.0 Hz, CHCH$_2$O), 4.41 (1 H, dd, J = 10.5, 7.0 Hz, CHO), 4.49 (1 H, dd, J = 10.5, 7.0 Hz, CHO), 4.61 (1 H, br, NH), 4.69 (1 H, q, J = 7.8 Hz, Lys α-H), 5.57 (1 H, d, J = 7.0 Hz, NH), 7.29 (2 H, t, J = 7.4 Hz, Ar-H$_2$), 7.38 (2 H, t, J = 7.4 Hz, Ar-H$_2$), 7.58 (2 H, d, J = 7.4 Hz, Ar-H$_2$), 7.74 (2 H, d, J = 7.4 Hz, Ar-H$_2$); NMR δ_F –161.7 (2 F, t, J = 20.7 Hz, 3',5'-F$_2$), -157.1 (1 F, t, J = 20.7 Hz, 4'-F), -152.2 (2 F, d, J = 18.4 Hz, 2',6F$_2$).

S-2,2-Dimethyl-3-(N-(N-(N-(N$^\varepsilon$-(1,1-dimethylethoxycarbonyl)-N$^\alpha$-(fluoren-9-ylmethoxycarbonyl)-L-lysyl)-L-leucyl)-L-glutaminyl)-L-valyl)-N-(2-(4-nitrophenyl)ethyl)tetrahydrothiazole-4-carboxamide (167)
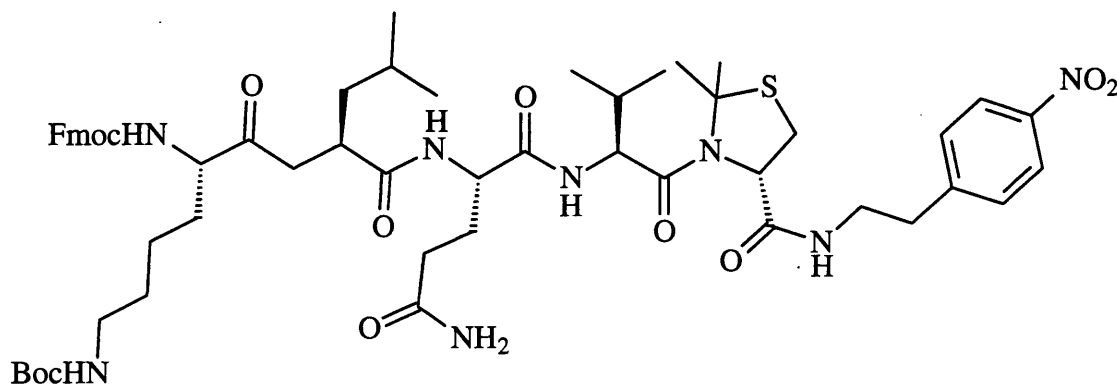
Compound **166** (290 mg, 380 μmol) in dry THF (1.5 mL) was stirred with compound **164**

(241 mg, 380 μmol), Et$_3$N (77 mg, 760 μmol) and DMAP (1 mg) in dry DMF (1.5 mL) at 0°C for 30 min. The mixture was then gradually warmed to 20°C and stirred for 16 h. The evaporation residue, in EtOAc, was washed with cold 5% aq. citric acid, H$_2$O and brine. Drying and recrystallisation (EtOAc / hexane) afforded **167** (395 mg, 95%) as a white solid: mp 72-75°C; NMR δ$_H$ 0.75-0.85 (12 H, m, 2 × Val-Me, 2 × Leu-Me), 0.92 (2 H, t, 7.4 Hz, Lys ε-H$_2$), 1.20-1.40 (6 H, m, Lys β-H$_2$, Lys γ-H$_2$, Lys δ-H$_2$), 1.43 (9 H, s, Bu^t), 1.50-1.65 (3 H, m, Leu β-H$_2$, Leu γ-H), 1.73 (3 H, s, 2-Me), 1.83 (3 H, s, 2-Me), 1.90-2.10 (3 H, m, Val β-H, Gln β-H$_2$), 2.30 (2 H, m, Gln γ-H$_2$), 2.78 (2 H, brd, CH$_2$O), 2.89-3.03 (4 H, m, 5-H$_2$, ArCH$_2$), 3.35 (1 H, m, NHC*H*CH$_2$), 3.65 (1 H, m, NHC*H*CH$_2$), 4.04 (1 H, t, *J* = 9.0 Hz, C*H*CH$_2$O), 4.15-4.50 (4 H, m, Val α-H , Gln α-H, Leu α-H, Lys α-H), 5.11 (1 H, m, 4-H), 7.24-7.55 (8 H, m, Ar-H$_8$), 7.72 (2 H, d, *J* = 7.4 Hz, Ar 2,6-H$_2$), 8.10 (2 H, d, *J* = 7.4 Hz, Ar 3,5-H$_2$); MS *m/z* 1100.5544 (M + H) (C$_{56}$H$_{78}$N$_9$O$_{12}$S requires 1100.5491), 1000 (M-Boc).

S-2,2-Dimethyl-3-(N-(N-(N-(N^ε-(1,1-dimethylethoxycarbonyl)-L-lysyl)-L-leucyl)-L-glutaminyl)-L-valyl)-N-(2-(4-nitrophenyl)ethyl)tetrahydrothiazole-4-carboxamide (168)
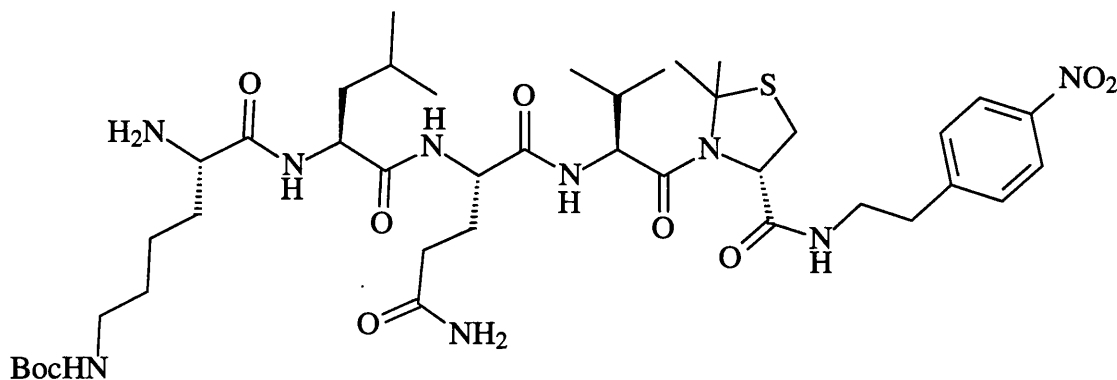
Compound **167** (250 mg, 227 μmol) was stirred in CH$_2$Cl$_2$ (4.5 mL) and diethylamine (500 μL) for 30 min. The evaporation residue was washed with Et$_2$O and dried to afford **168**(180 mg, 90%) as a white solid: mp 100-103°C; NMR (CD$_3$OD) 0.85 (3 H, d, *J* = 6.6 Hz, Val-Me), 0.86 (3 H, d, *J* = 6.6 Hz, Val-Me), 0.92 (3 H, d, *J* = 6.6 Hz, Leu-Me), 0.96 (3 H, d, *J* = 6.6 Hz, Leu-Me), 1.40-1.65 (18 H, m, Bu^t, Lys β-H$_2$, Lys γ-H$_2$, Lys δ-H$_2$, Leu β-H$_2$, Leu γ-H), 1.79 (3 H, s, 2-Me), 1.88 (3 H, s, 2-Me), 1.90-2.12 (3 H, m, Val β-H, Gln β-H$_2$), 2.30 (2 H, m, Gln γ-H$_2$), 2.96-3.04 (6 H, m, Lys ε-H$_2$, 5-H$_2$, ArCH$_2$), 3.40 (1 H, m, NHC*H*CH$_2$), 3.55 (1 H, m, NHC*H*CH$_2$), 3.92-4.42 (4 H, m, Val α-H , Gln α-H, Leu α-H, Lys α-H), 5.24 (1 H, d, *J* = 5.4 Hz, 4-H), 7.50 (2 H, d, *J* = 8.6 Hz, Ar 2,6-H$_2$), 8.15 (2 H, d,

J = 8.6 Hz, Ar 3,5-H$_2$); MS m/z 878.4831 (M + H) (C$_{41}$H$_{68}$N$_9$O$_{10}$S requires 878.4810), 778 (M – Boc).

S-2,2-Dimethyl-3-(N-(N-(N-N$^{\epsilon}$-(1,1-dimethylethoxycarbonyl)-N$^{\alpha}$-(O-(1,1-dimethylethyl)-N-(phenylmethoxycarbonyl)-L-serinyl)-L-lysyl)-L-leucyl)-L-glutaminyl)-L-valyl)-N-(2-(4-nitrophenyl)ethyl)tetrahydrothiazole-4-carboxamide (169)
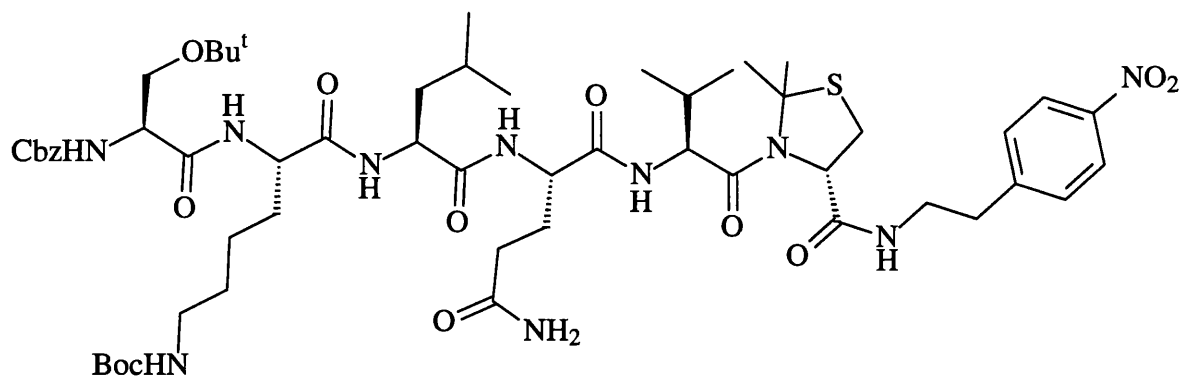
CbzSer(Bu^t)OSu (13.3 mg, 34 μmol) in dry THF (700 μL) was added to compound **168** (30 mg, 34 μmol), Et$_3$N (6.9 mg, 68 μmol) and DMAP (1 mg) in dry DMF (300 μL) at 0°C and the mixture was stirred for 30 min. The mixture was then gradually warmed to 20°C and stirred for 16 h. The evaporation residue, in EtOAc, was washed with cold 5% aq. citric acid, H$_2$O and brine. Drying and recrystallisation (EtOAc / hexane) afforded **169** (20 mg, 51%) as a white solid: mp 128-130°C; NMR (CD$_3$OD) 0.84 (3 H, d, J = 6.6 Hz, Val-Me), 0.86 (3 H, d, J = 6.6 Hz, Val-Me), 0.89 (3 H, d, J = 6.2 Hz, Leu-Me), 0.90 (3 H, d, J = 6.2 Hz, Leu-Me), 1.20 (9 H, s, SerOBu^t), 1.42 (9 H, s, Boc Bu^t), 1.45-1.75 (9 H, m, Lys β-H$_2$, Lys γ-H$_2$, Lys δ-H$_2$, Leu β-H$_2$, Leu γ-H), 1.79 (3 H, s, 2-Me), 1.88 (3 H, s, 2-Me), 1.90-2.15 (3 H, m, Val β-H, Gln β-H$_2$), 2.30 (2 H, m, Gln γ-H$_2$), 2.96-3.04 (4 H, m, Lys ε-H$_2$, ArCH$_2$), 3.42 (1 H, dd, J = 12.5, 5.9 Hz, 5-H), 3.55 (3 H, m, 5-H, NHCH$_2$), 3.76 (1 H, m, Ser β-H), 3.85 (1 H, m, Ser β-H), 3.95 (1 H, d, J = 9.4 Hz, Val α-H), 4.15-4.44 (4 H, m, Gln α-H, Leu α-H, Lys α-H, Ser α-H), 5.09 (1 H, d, J = 12.5 Hz) and 5.14 (1 H, d, J = 12.5 Hz) (CH$_2$Ph), 5.21 (1 H, d, J = 5.9 Hz, 4-H), 7.36 (5 H, m, Ph-H$_5$), 7.51 (2 H, d, J = 8.8 Hz, Ar 2,6-H$_2$), 8.06 (1 H, brt, J = 7 Hz, NH), 8.16 (2 H, d, J = 8.8 Hz, Ar 3,5-H$_2$); MS m/z 1155.6162 (M + H) (C$_{56}$H$_{87}$N$_{10}$O$_{14}$S requires 1155.6124), 1055 (M – Boc), 846 (M – Me$_2$thiazolidine-CONHCH$_2$CH$_2$PhNO$_2$).

S-2,2-Dimethyl-3-(N-(N-(N-(N-(phenylmethoxycarbonyl)-L-serinyl)-L-lysyl)-L-leucyl)-L-glutaminyl)-L-valyl)-N-(2-(4-nitrophenyl)ethyl)tetrahydrothiazole-4-carboxamide trifluoroacetate (170)
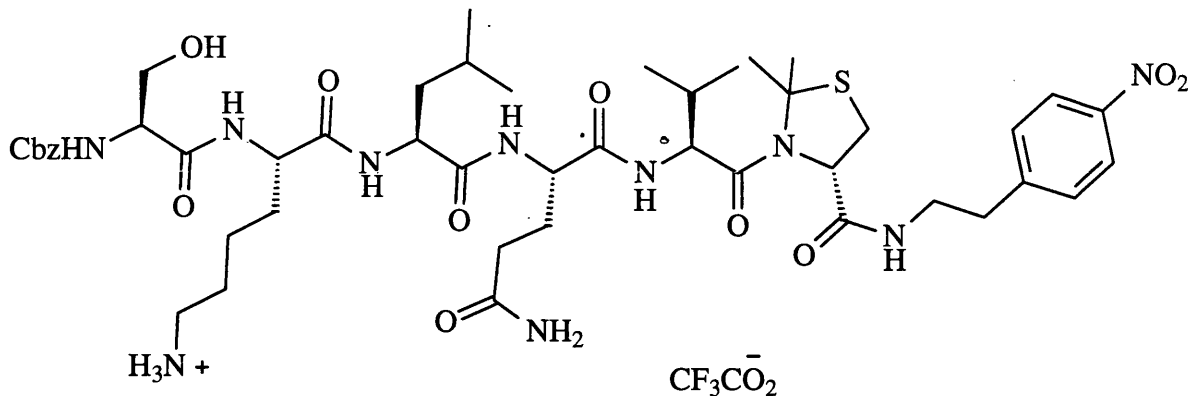
Compound **169** (5.0 mg, 4.3 μmol) was stirred in CF_3CO_2H (100 μL) and CH_2Cl_2 (400 μL) for 2 h. Evaporation and trituration with Et_2O afforded **170** (4.7 mg, 98%) as a white solid: mp 107-109°C; NMR (CD_3OD) 0.84 (3 H, d, J = 6.6 Hz, Val-Me), 0.85 (3 H, d, J = 6.6 Hz, Val-Me), 0.90 (3 H, d, J = 6.2 Hz, Leu-Me), 0.95 (3 H, d, J = 6.2 Hz, Leu-Me), 1.45-1.70 (9 H, m, Lys·β-H_2, Lys γ-H_2, Lys δ-H_2, Leu β-H_2, Leu γ-H), 1.78 (3 H, s, 2-Me), 1.88 (3 H, s, 2-Me), 1.90-2.15 (3 H, m, Val β-H, Gln β-H_2), 2.30 (2 H, t, J = 7.4 Hz, Gln γ-H_2), 2.39 (2 H, t, J = 7.0 Hz, ArCH_2), 2.98 (2 H, t, J = 6.5 Hz, Lys ε-H_2), 3.03 (1 H, J = 12.1 Hz, 5-H), 3.41 (1 H, dd, J = 12.1, 5.5 Hz, 5-H), 3.55 (2 H, m, NHCH_2), 3.75 (1 H, m, Ser β-H), 3.85 (1 H, m, Ser β-H), 3.95 (1 H, d, J = 9.4 Hz, Val α-H), 4.20-4.40 (4 H, m, Gln α-H, Leu α-H, Lys α-H, Ser α-H), 5.07 (1 H, d, J = 12.5 Hz) and 5.12 (1 H, d, J = 12.5 Hz) (CH_2Ph), 5.21 (1 H, d, J = 5.5 Hz, 4-H), 7.36 (5 H, m, Ph-H_5), 7.51 (2 H, d, J = 8.8 Hz, Ar 2,6-H_2), 8.06 (1 H, brt, J = 7 Hz, NH), 8.16 (2 H, d, J = 8.8 Hz, Ar 3,5-H_2); MS m/z 999.4964 (M + H) ($C_{57}H_{71}N_{10}O_{12}S$ requires 999.4974).

S-2,2-Dimethyl-3-(N-(N-(N-N$^\epsilon$-(1,1-dimethylethoxycarbonyl)-N$^\alpha$-(O-(1,1-dimethylethyl)-N-(fluoren-9-ylmethoxycarbonyl)-L-serinyl)-L-lysyl)-L-leucyl)-L-glutaminyl)-L-valyl)-N-(2-(4-nitrophenyl)ethyl)tetrahydrothiazole-4-carboxamide (171)
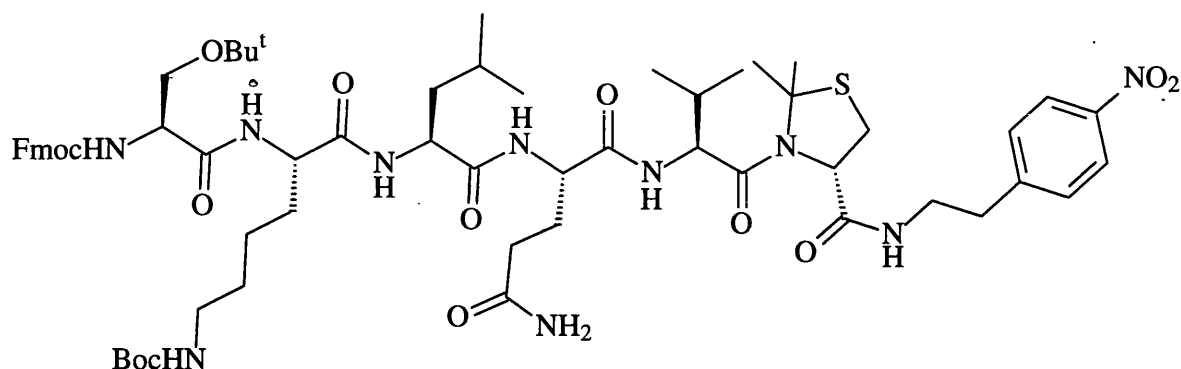
FmocSer(Bu^t)OSu (44 mg, 91 μmol) in dry THF (500 μL) was added to compound **168** (80 mg, 91 μmol), Et$_3$N (18.4 mg, 182 μmol) and DMAP (1 mg) in dry DMF (500 μL) at 0°C and the mixture was stirred for 30 min. The mixture was then gradually warmed to 20°C and stirred for 16 h. The evaporation residue, in EtOAc, was washed with cold 5% aq. citric acid, H$_2$O and brine. Drying and recrystallisation (EtOAc / hexane) afforded **171** (70 mg, 62%) as a white solid: mp 184-186°C; NMR (CD$_3$OD) 0.85 (3 H, d, J = 6.6 Hz, Val-Me), 0.86 (3 H, d, J = 6.6 Hz, Val-Me), 0.90 (3 H, d, J = 6.2 Hz, Leu-Me), 0.95 (3 H, d, J = 6.2 Hz, Leu-Me), 1.18 (9 H, s, SerOBu^t), 1.43 (9 H, s, Boc Bu^t), 1.45-1.75 (9 H, m, Lys β-H$_2$, Lys γ-H$_2$, Lys δ-H$_2$, Leu β-H$_2$, Leu γ-H), 1.79 (3 H, s, 2-Me), 1.88 (3 H, s, 2-Me), 1.90-2.15 (3 H, m, Val β-H, Gln β-H$_2$), 2.30 (2 H, m, Gln γ-H$_2$), 2.96-3.02 (4 H, m, ArCH$_2$, Ser β-H$_2$), 3.15-3.25 (2 H, m, 5-H$_2$), 3.55 (2 H, m, Lys ε-H$_2$), 3.62 (2 H, m, NHCH$_2$), 3.94 (1 H, d, J = 9.4 Hz, CHCH$_2$O), 4.21-4.35 (5 H, m, Gln α-H, Leu α-H, Lys α-H, Ser α-H, fluorene 9-H), 5.20 (1 H, d, J = 5.1 Hz, 4-H), 7.30 (2 H, t, J = 7.4 Hz, Ar-H$_2$), 7.39 (2 H, t, J = 7.4 Hz, Ar-H$_2$), 7.50 (2 H, d, J = 8.6 Hz, Ar 2,6-H$_2$), 7.66 (2 H, J = 7.4 Hz, Ar-H$_2$), 7.80 (2 H, J = 7.4 Hz, Ar-H$_2$), 8.16 (2 H, d, J = 8.6 Hz, Ar 3,5-H$_2$); MS m/z 1243.6437 (M + H) (C$_{63}$H$_{91}$N$_{10}$O$_{14}$S requires 1243.6477).

S-2,2-Dimethyl-3-(N-(N-(N-N$^\varepsilon$-(1,1-dimethylethoxycarbonyl)-N$^\alpha$-(O-(1,1-dimethylethyl)-L-serinyl)-L-lysyl)-L-leucyl)-L-glutaminyl)-L-valyl)-N-(2-(4-nitrophenyl)ethyl)tetrahydrothiazole-4-carboxamide (172)
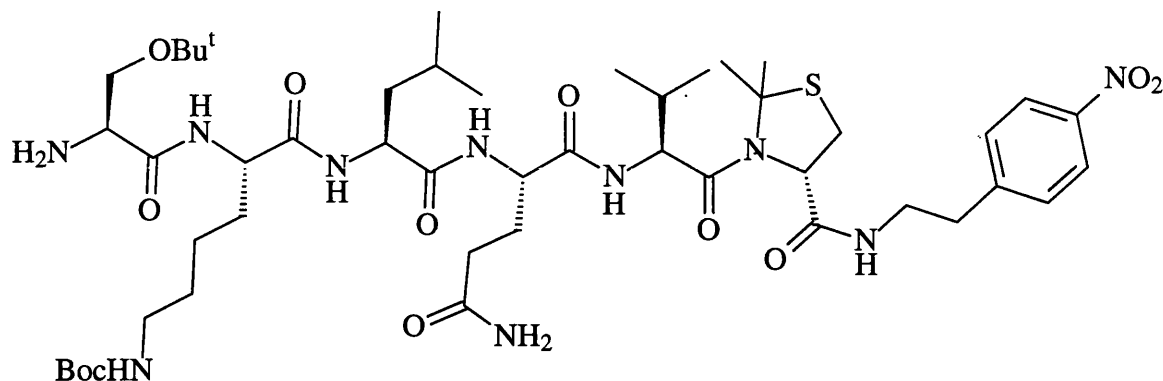
Compound **171** (70 mg, 56 μmol) was stirred in CH_2Cl_2 (1350 μL) and diethylamine (150 μL) for 30 min. The evaporation residue was washed with Et_2O and dried to afford **172** (50 mg, 88%) as a white solid: mp 94-96°C; NMR (CD_3OD) 0.85 (3 H, d, J = 6.6 Hz, Val-Me), 0.86 (3 H, d, J = 6.6 Hz, Val-Me), 0.92 (3 H, d, J = 6.2 Hz, Leu-Me), 0.96 (3 H, d, J = 6.2 Hz, Leu-Me), 1.31 (9 H, s, SerOBu^t), 1.44 (9 H, s, Boc Bu^t), 1.45-1.75 (9 H, m, Lys β-H$_2$, Lys γ-H$_2$, Lys δ-H$_2$, Leu β-H$_2$, Leu γ-H), 1.78 (3 H, s, 2-Me), 1.88 (3 H, s, 2-Me), 1.90-2.15 (3 H, m, Val β-H, Gln β-H$_2$), 2.30 (2 H,t, J = 7.0 Hz, Gln γ-H$_2$), 2.96-3.05 (5 H, m, 5-H, ArCH$_2$, Ser β-H$_2$), 3.42 (1 H, dd, J = 12.1, 5.3 Hz, 5-H), 3.55 (2 H, m, Lys ε-H$_2$), 3.58-3.55 (2 H, m, NHCH_2), 3.95 (1 H, d, J = 9.0 Hz, Val α-H), 4.20-4.40 (4 H, m, Gln α-H, Leu α-H, Lys α-H, Ser α-H), 5.21 (1 H, d, J = 5.3 Hz, 4-H), 7.51 (2 H, d, J = 8.6 Hz, Ar 2,6-H$_2$), 8.16 (2 H, d, J = 8.6 Hz, Ar 3,5-H$_2$); MS m/z 1021.5756 (M + H) ($C_{48}H_{81}N_{10}O_{12}S$ requires 1021.5762).

S-2,2-Dimethyl-3-(N-(N-(N-(N$^\varepsilon$-(1,1-dimethylethoxycarbonyl)-N$^\alpha$-(O-(1,1-dimethylethyl)-N-(O-(1,1-dimethylethyl)-N-(phenylmethoxycarbonyl)-L-serinyl)-L-serinyl)-L-lysyl)-L-leucyl)-L-glutaminyl)-L-valyl)-N-(2-(4-nitrophenyl)ethyl)tetrahydrothiazole-4-carboxamide (173)
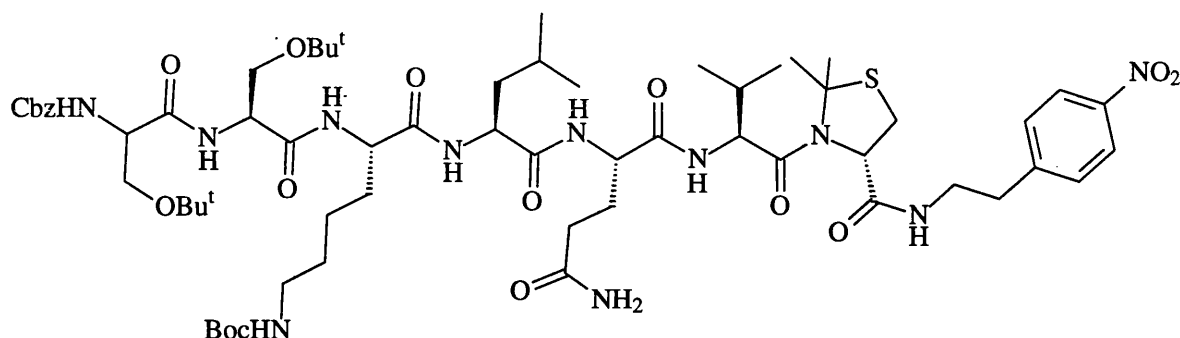
CbzSer(Bu^t)OSu (9.8 mg, 25 µmol) in dry THF (700 µL) was added to compound **172** (25 mg, 25 µmol), Et$_3$N (5.1 mg, 50 µmol) and DMAP (1 mg) in dry DMF (300 µL) at 0°C and the mixture was stirred for 30 min. The mixture was then gradually warmed to 20°C and stirred for 16 h. The evaporation residue, in EtOAc, was washed with cold 5% aq. citric acid, H$_2$O and brine. Drying and recrystallisation (EtOAc / hexane) afforded **173** (20 mg, 62%) as a white solid: mp 202-205; NMR (CD$_3$OD) 0.86 (3 H, d, *J* = 6.6 Hz, Val-Me), 0.89 (3 H, d, *J* = 6.6 Hz, Val-Me), 0.91 (3 H, d, *J* = 5.9 Hz, Leu-Me), 0.95 (3 H, d, *J* = 5.9 Hz, Leu-Me), 1.20 (18 H, s, 2 × SerOBu^t), 1.42 (9 H, s, Boc Bu^t), 1.45-1.75 (9 H, m, Lys β-H$_2$, Lys γ-H$_2$, Lys δ-H$_2$, Leu β-H$_2$, Leu γ-H), 1.80 (3 H, s, 2-Me), 1.88 (3 H, s, 2-Me), 1.90-2.15 (3 H, m, Val β-H, Gln β-H$_2$), 2.30 (2 H, m, Gln γ-H$_2$), 2.96-3.04 (4 H, m, Lys ε-H$_2$, ArCH$_2$), 3.45-3.8 (8 H, m, 5-H$_2$, NHC*H*$_2$, 2 × Ser β-H$_2$), 3.95 (1 H, d, *J* = 9.4 Hz, Val α-H), 4.15-4.80 (6 H, m, Gln α-H, Leu α-H, Lys α-H, 2 × Ser α-H), 5.09 (2 H, m,CH$_2$Ph), 5.21 (1 H, d, *J* = 5.5 Hz, 4-H), 7.35 (5 H, m, Ph-H$_5$), 7.51 (2 H, d, *J* = 8.8 Hz, Ar 2,6-H$_2$), 8.16 (2 H, d, *J* = 8.8 Hz, Ar 3,5-H$_2$); MS *m/z* 1199.6588 (M - Boc) (^{13}C$_1$^{12}C$_{57}$H$_{92}$N$_{11}$O$_{14}$S requires 1199.6579), 1297 (M − H.

S-2,2-Dimethyl-3-(N-(N-(N-(N-(N(N-(phenylmethoxycarbonyl)-L-serinyl)-L-serinyl)-L-lysyl)-L-leucyl)-L-glutaminyl)-L-valyl)-N-(2-(4-nitrophenyl)ethyl)tetrahydrothiazole-4-carboxamide trifluoroacetate (174)
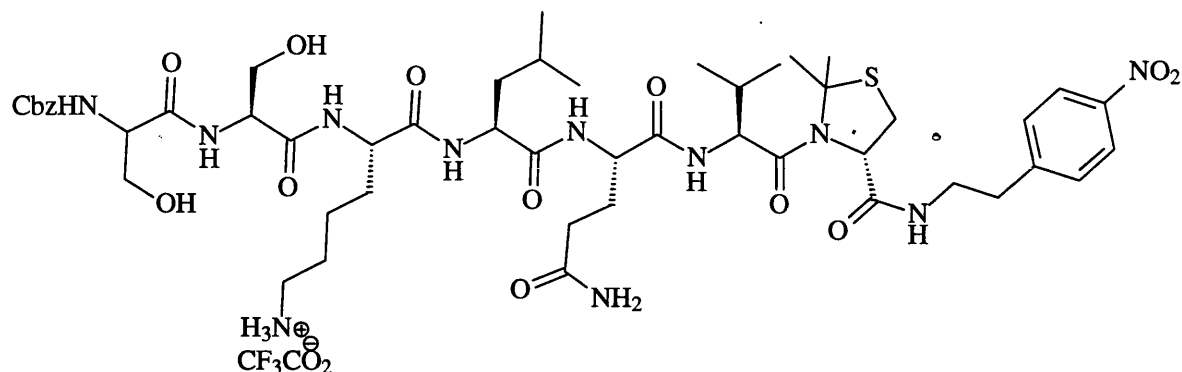
Compound **173** (5.0 mg, 3.9 µmol) was stirred in CF₃CO₂H (100 µL) and CH₂Cl₂ (400 µL) for 2 h. Evaporation afforded **174** (quant.) as a highly hygroscopic gummy solid. NMR (CD₃OD) 0.86 (3 H, d, *J* = 6.6 Hz, Val-Me), 0.89 (3 H, d, *J* = 6.6 Hz, Val-Me), 0.91 (3 H, d, *J* = 5.9 Hz, Leu-Me), 0.95 (3 H, d, *J* = 5.9 Hz, Leu-Me), 1.20 (18 H, s, 2 × SerOBuᵗ), 1.42 (9 H, s, Boc Buᵗ), 1.45-1.75 (9 H, m, Lys β-H₂, Lys γ-H₂, Lys δ-H₂, Leu β-H₂, Leu γ-H), 1.80 (3 H, s, 2-Me), 1.88 (3 H, s, 2-Me), 1.90-2.15 (3 H, m, Val β-H, Gln β-H₂), 2.30 (2 H, m, Gln γ-H₂), 2.96-3.04 (4 H, m, Lys ε-H₂, ArCH₂), 3.45-3.8 (8 H, m, 5-H₂, NHCH₂, 2 × Ser β-H₂), 3.95 (1 H, d, *J* = 9.4 Hz, Val α-H), 4.15-4.80 (6 H, m, Gln α-H, Leu α-H, Lys α-H, 2 × Ser α-H), 5.09 (2 H, m,CH₂Ph), 5.21 (1 H, d, *J* = 5.5 Hz, 4-H), 7.35 (5 H, m, Ph-H₅), 7.51 (2 H, d, *J* = 8.8 Hz, Ar 2,6-H₂), 8.16 (2 H, d, *J* = 8.8 Hz, Ar 3,5-H₂);

S-2,2-Dimethyl-3-(N-(N-(N-(Nᵉ-(1,1-dimethylethoxycarbonyl)-Nᵅ-(O-(1,1-dimethylethyl)-N-(O-(1,1-dimethylethyl)-N-(fluoren-9-ylmethoxycarbonyl)-L-serinyl)-L-serinyl)-L-lysyl)-L-leucyl)-L-glutaminyl)-L-valyl)-N-(2-(4-nitrophenyl)ethyl)tetrahydrothiazole-4-carboxamide (175)
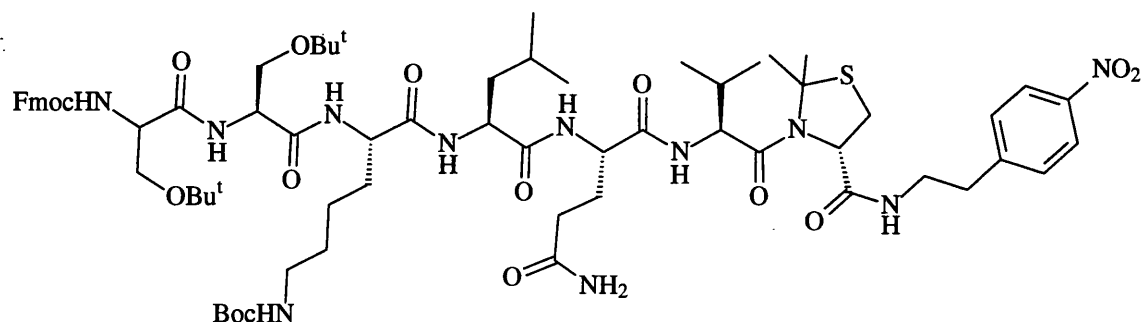
FmocSer(Buᵗ)OSu (12.0 mg, 25 µmol) in dry THF (700 µL) was added to compound **172** (25 mg, 25 µmol), Et₃N (5.1 mg, 50 µmol) and DMAP (1 mg) in dry DMF (300 µL) at 0°C

and the mixture was stirred for 30 min. The mixture was then gradually warmed to 20°C and stirred for 16 h. The solid evaporation residue was washed with Et$_2$O, cold 5% aq. citric acid and H$_2$O. Drying afforded **175** (15 mg, 43%) as a white solid: mp 168-170°C; MS m/z 1164 (M – Fmoc).

N-(N$^\alpha$-(Fluoren-9-ylmethoxycarbonyl)-N$^\delta$-(triphenylmethyl)-L-glutaminyl)-L-valine phenylmethyl ester (176)
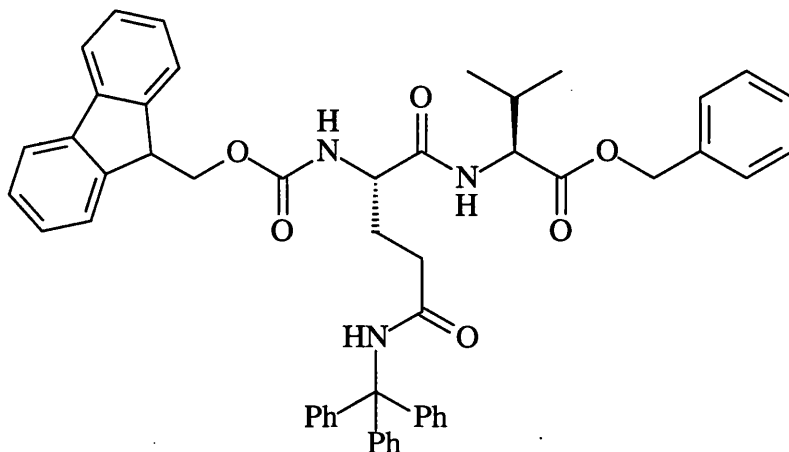
FmocGln(Trt)OH (2.99 g, 4.9 mmol) was stirred with HOBt (730 mg, 5.4 mmol) and DCC (1.11 g, 5.4 mmol) in CH$_2$Cl$_2$ (50 mL) at 0°C for 1 h. L-Valine benzyl ester (1.86 g, 4.9 mmol) in CH$_2$Cl$_2$ (50 mL) was added in the presence of Pr$^i_2$NEt (1.27 g, 9.8 mmol) and the mixture was stirred for 24 h. The mixture was kept at 4°C for 16 h and filtered (Celite$^\circledR$). The solution was washed cold 5% aq. citric acid, aq. NaHCO$_3$ and H$_2$O. Drying, evaporation and chromatography (EtOAc / hexane 2:3) afforded **176** (2.10 g, 54%) as a white solid: mp 110-113°C; NMR δ_H 0.72 (3 H, d, J = 6.6 Hz, Val-Me), 0.82 (3 H, d, J = 6.6 Hz, Val-Me), 1.95 (1 H, m, Gln β-H), 2.10 (2 H, m, Val β-H, Gln β-H), 2.52 (2 H, brt, J = 6.2 Hz, Gln γ-H$_2$), 4.19 (2 H, m, Gln α-H, C*H*CH$_2$O), 4.34 (2 H, m, CHC*H*$_2$O), 4.40 (1 H, dd, J = 7.8, 4.7 Hz, Val α-H), 5.03 (1 H, d, J = 12.1 Hz) and 5.13 (1 H, d, J = 12.1 Hz) (CH$_2$Ph), 5.89 (1 H, d, J = 7.0 Hz, Gln NH), 6.90 (1 H, s, CONHTr), 7.30 (21 H, m, 4 × Ph-H$_5$, NH), 7.37 (4 H, m, Ar-H$_4$), 7.56 (2 H, d, J = 7.6 Hz, Ar-H$_2$), 7.73 (2 H, d, J = 7.6 Hz, Ar-H$_2$) MS m/z 800.3701 (M + H) (C$_{51}$H$_{50}$N$_3$O$_6$ requires 800.3700), 621 (M – fluoreneCH$_2$), 243 (Ph$_3$C), 179 (fluorene-CH$_2$).

N-(Nα-(Fluoren-9-ylmethoxycarbonyl)-Nδ-(triphenylmethyl)-L-glutaminyl)-L-valine (177)
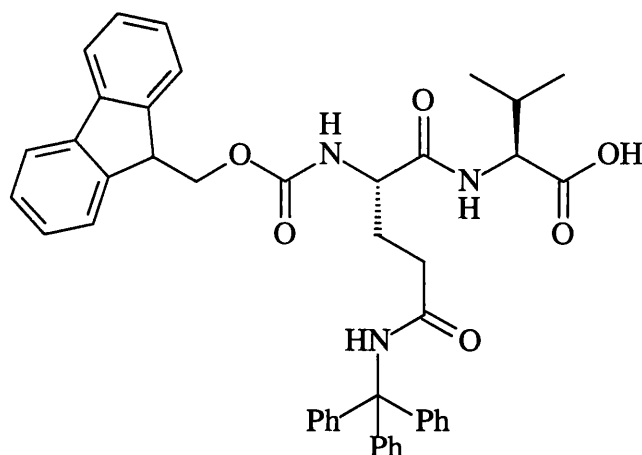
Compound 176(1.0 g, 1.2 mmol) was stirred with 10% Pd/C (40 mg) in MeOH (50 mL) and under H_2 for 24 h. Filtration (Celite®) and evaporation afforded 177 (500 mg, 56%) as a white solid: mp 120-122°C; NMR (CD_3OD) δ_H 0.94 (3 H, d, J = 7.0 Hz, Val-Me), 0.96 (3 H, t, J = 7.0 Hz, Val-Me), 1.84 (1 H, m, Gln β-H), 2.04 (1 H, m, Val β-H), 2.16 (1 H, m, Gln β-H), 2.45 (2 H, m, Gln γ-H_2), 4.20 (2 H, m, α-H, CHCH$_2$O), 4.31 (1 H, d, J = 5.1 Hz, α-H), 4.38 (2 H, d, J = 7.0 Hz, CHCH$_2$O), 7.17-7.31 (17 H, m, 3 × Ph-H$_5$, Ar-H$_2$), 7.36 (2 H, t, J = 7.3 Hz, Ar-H$_2$), 7.64 (2 H, d, J = 7.3 Hz, Ar-H$_2$), 7.78 (2 H, d, J = 7.3 Hz, Ar-H$_2$); MS m/z 710.3230 (M + H) ($C_{44}H_{44}N_3O_6$ requires 710.3233), 531 (M – fluoreneCH$_2$), 488 (M – Fmoc), 243 (Ph$_3$C), 179 (fluorene-CH$_2$).

N-(L-Glutaminyl)-L-valine methyl ester trifluoroacetate salt (178)
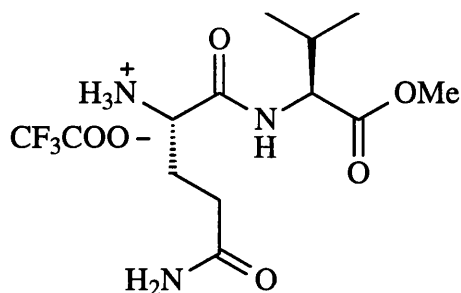
Compound 142 (1.00 g, 2.8 mmol) was stirred in CF_3CO_2H (3 mL) and CH_2Cl_2 (3 mL) for 45 min. Evaporation afforded crude 178 (quant.) as a highly hygroscopic yellow viscous oil: NMR ((CD_3)$_2$SO) δ_H 0.85 (6 H, d, J = 7.0 Hz, 2 × Val-Me), 1.88 (2 H, brq, J = 5.7 Hz, Gln β-H_2), 2.00 (1 H, m, Val β-H), 2.20 (2 H, t, J = 7.4 Hz, Gln γ-H_2), 3.59 (3 H, s, OMe), 3.87 (1 H, brq, J = 5.7 Hz, Gln α-H), 4.16 (1 H, dd, J = 7.8, 5.9 Hz, Val α-H), 6.93 (1 H, s, CONH), 7.42 (1 H, s, CONH), 8.14 (3 H, s, N$^+$H$_3$), 8.68 (1 H, d, J = 7.8 Hz, Val NH).

N-(N-(N-(1,1-Dimethylethoxycarbonyl)-L-leucyl)-L-glutaminyl)-L-valine methyl ester (179)
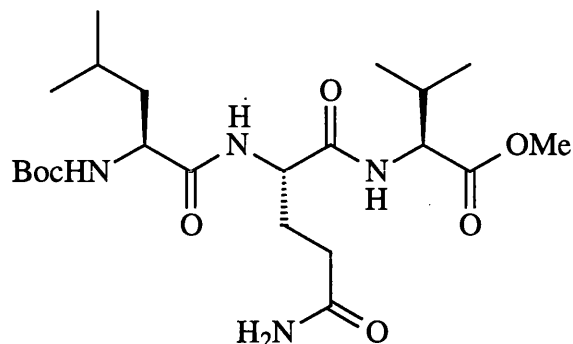
N-(1,1-Dimethylethoxycarbonyl)-L-leucine N-hydroxysuccinimide ester (1.14 g, 3.5 mmol) in dry THF (5 mL) was added to **178** (1.29 g, 3.5 mmol), Et$_3$N (708 mg, 7 mmol) and DMAP (1 mg) in dry DMF (5 mL) at 0°C during 30 min. The mixture was then gradually warmed to 20°C and was stirred for 24 h. The evaporation residue, in EtOAc, was washed with cold aq. citric acid (5%) and brine. Drying, evaporation and chromatography (EtOAc → EtOAc/MeOH 1:1) afforded **179** (900 mg, 54%) as a white solid: mp 135-139°C; NMR δ_H 0.83-0.87 (12 H, m, 2 × Val-Me, 2 × Leu-Me), 1.34 (9 H, s, Bu^t), 1.41 (1 H, m, Leu β-H), 1.57 (1 H, m, Leu γ-H), 1.70 (2 H, m, Gln β-H, Leu β-H), 1.85 (1 H, m, Gln β-H), 2.03 (1 H, m, Val β-H), 2.08 (2 H, m, Gln γ-H$_2$), 3.62 (3 H, s, OMe), 3.94 (1 H, dt, J = 8.2, 6.6 Hz, Leu α-H), 4.14 (1 H, dd, J = 7.8, 5.9 Hz, Val α-H), 4.34 (1 H, dt, J = 7.8, 5.5 Hz, Gln α-H), 6.77 (1 H, s, CONH), 6.95 (1 H, d, J = 8.2 Hz, Leu-NH), 7.25 (1 H, s, CONH), 7.82 (1 H, d, J = 7.8 Hz, Gln NH), 8.12 (1 H, d, J = 7.8 Hz, Val NH); MS m/z 495.2793 (M + Na) (C$_{22}$H$_{40}$N$_4$O$_7$ requires 495.2795), 395 (M + Na − Boc).

N-(N-(L-Leucyl)-L-glutaminyl)-L-valine methyl ester trifluoroacetate salt (180)
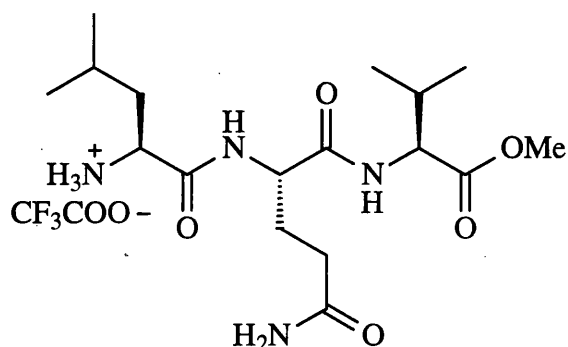
Compound **179** (650 mg, 1.4 mmol) was stirred in CF_3CO_2H (2 mL) and CH_2Cl_2 (2 mL) for 2 h. Evaporation afforded **180** (quant.) as a highly hygroscopic colourless viscous oil: NMR $((CD_3)_2SO)$ δ_H 0.85-0.87 (12 H, m, 2 × Val-Me, 2 × Leu-Me),, 1.26 (1 H, m, Leu β-H), 1.62 (1 H, m, Leu γ-H), 1.73 (2 H, m, Gln β-H, Leu β-H), 1.85 (1 H, m, Gln β-H), 2.04 (1 H, m, Val β-H), 2.15 (2 H, m, Gln γ-H$_2$), 3.62 (3 H, s, OMe), 3.80 (1 H, m, Leu α-H), 4.16 (1 H, dd, J = 8.2, 6.2 Hz, Val α-H), 4.42 (1 H, dt, J = 7.8, 5.5 Hz Gln α-H), 6.82 (1 H, s, CONH), 7.31 (1 H, s, CONH), 8.14 (3 H, br, N^+H_3), 8.28 (1 H, d, J = 8.2 Hz, Val NH), 8.66 (1 H, d, J = 7.8 Hz, Gln NH); MS m/z 525 (M + mNBA), 395 (M + Na), 373.2443 (M + H) ($C_{17}H_{33}N_4O_5$ requires 373.2451).

N-(N-(N-(N-(N^ϵ-(1,1-Dimethylethoxycarbonyl)-N^α-(fluoren-9-ylmethoxycarbonyl)-L-lysyl)-L-leucyl)-L-glutaminyl)-L-valine methyl ester (181)
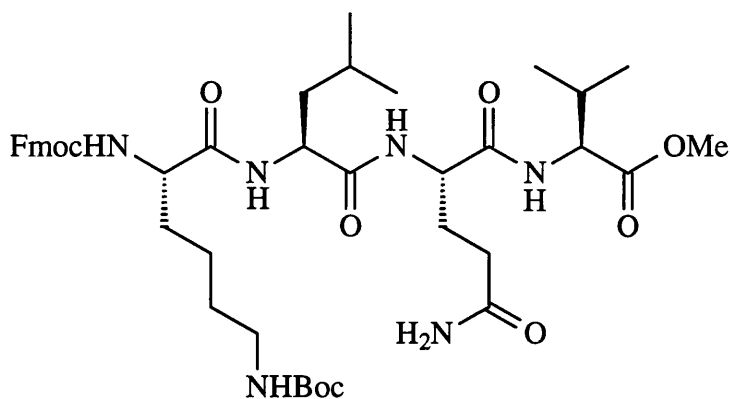
Compound **166** (700 mg, 1.10 mmol) in dry THF (5 mL) was added to **180** (826 mg, 1.7 mmol), Et$_3$N (344 mg, 3.4 mmol) and DMAP (1 mg) in dry DMF (3 mL) at 0°C during 30 min. The mixture was then slowly warmed to 20°C and stirred for 16 h. The evaporation residue was washed with EtOAc, cold aq. citric acid (5%) and H_2O. Drying afforded **181** (600mg, 68%) as a white solid: mp 200-202°C; NMR $((CD_3)_2SO)$ δ_H 0.80-0.86 (12 H, m, 2 × Val-Me, 2 × Leu-Me), 1.35 (9 H, s, Bu^t), 1.44-1.52 (6 H, m, Lys β,γ,δ-H$_6$), 1.54 (1 H, m,

Gln β-H), 1.57 (1 H, m, Gln β-H), 2.05 (1 H, m, Val β-H), 2.22 (2 H, m, Gln γ-H$_2$), 2.88 (2 H, m, Lys ε-H$_2$), 3.61 (3 H, s, OMe), 3.94-4.32 (7 H, m, Leu α-H, Gln α-H, Val α-H, Lys α-H, fluorene 9-H, CH$_2$O), 6.77 (2 H, m, CONH, NH), 7.23 (1 H, s, CONH), 7.30 (2 H, t, J = 7.4 Hz, Ar-H$_2$), 7.39 (2 H, t, J = 7.4 Hz, Ar-H$_2$), 7.46 (1 H, d, J = 8.2 Hz, NH), 7.69 (2 H, t, J = 7.4 Hz Ar-H$_2$), 7.86 (2 H, d, J = 7.4 Hz, Ar-H$_2$), 7.89 (1 H, d, J = 8.2 Hz, NH), 7.94 (1 H, d, J = 7.4 Hz, NH), 8.04 (1 H, d, J = 8.2 Hz; NH); MS m/z 823.4597 (M + H) (C$_{43}$H$_{63}$N$_6$O$_{10}$ requires 823.4606).

N-(N-(N^ε-(1,1-Dimethylethoxycarbonyl)-L-lysyl)-L-leucyl)-L-glutaminyl)-L-valine methyl ester (182)

Compound **181** (52 mg, 64 μmol) was stirred in DMF (900 μL) and diethylamine (100 μL) for 30 min. The evaporation residue was washed with Et$_2$O and dried to afford **182** (35 mg, 91%) as a white solid: mp 162-165°C; NMR (CD$_3$OD) δ$_H$ 0.94-0.98 (12 H, m, 2 × Val-Me, 2 × Leu-Me), 1.38-1.62 (17 H, m, Bu^t, Lys β,γ,δ-H$_6$, Gln β-H$_2$), 1.76 (1 H, m, Leu γ-H), 1.95 (1 H, m, Leu β-H), 2.08-2.20 (2 H, m, Val β-H, Leu β-H), 2.35 (2 H, t, J = 7.4 Hz, Gln γ-H$_2$), 3.04 (2 H, t, J = 6.6 Hz, Lys ε-H$_2$), 3.37 (1 H, t, J = 6.6 Hz, Lys α-H), 3.72 (3 H, s, OMe), 4.31 (1 H, d, J = 5.9 Hz, Val α-H), 4.38 (1 H, t, J = 7.4, Gln α-H), 4.45 (1 H, dd, J = 8.9, 5.1 Hz, Leu α-H); MS m/z 601.3948 (M + H) (C$_{28}$H$_{53}$N$_6$O$_8$ requires 601.3925).

N-(N-(N-(N-(Nᵉ-(1,1-Dimethylethoxycarbonyl)-Nᵃ-(O-(1,1-dimethylethyl)-N-(phenylmethoxycarbonyl)-L-serinyl)-L-lysyl)-L-leucyl)-L-glutaminyl)-L-valine methyl ester (183)

CbzSer(Buᵗ)OSu (19 mg, 48 μmol) in dry THF (700 μL) was added to **182** (29   mg,   48 μmol), Et₃N (9.8 mg, 96 μmol) and DMAP (1 mg) in dry DMF (300 μL) at 0°C. The mixture was stirred at 0°C for 30 min and at 20°C for 72 h. The evaporation residue, in EtOAc, was washed with cold aq. citric acid (5%) and H₂O and was dried to afford **183** (30 mg, 68%) as a white solid: mp 234-236°C; NMR ((CD₃)₂SO) δ_H 0.83-0.87 (12 H, m, 2 X Val-Me, 2 X Leu-Me), 1.10 (9 H, s, CH₂OBuᵗ), 1.25-2.11 (21 H, CO₂Buᵗ, Val β-H, Gln β-H₂, Leu β,γ-H₃, Lys β,γ,δ-H₆),   2.85 (2 H, t, J = 6.2 Hz, Gln γ-H₂), 3.32 (2 H, m, CH₂OBuᵗ), 3.44 (2 H, t, J = 5.5 Hz, Lys ε-H₂), 3.63 (3 H, s, OMe), 4.10-4.24 (5 H, Val α-H, Gln α-H, Leu α-H, Lys α-H, Ser α-H), 5.02 (1 H, d, J = 12.5 Hz) and 5.06 (1 H, d, J = 12.5 Hz) (CH₂Ph), 6.72-8.06 (13 H, m, 8 × NH, Ph-H₅); MS m/z 878.5264 (M + H) (C₄₃H₇₂N₇O₁₂ requires 878.5239).

N-(N-(N-(Nᵃ-(N-Phenylmethoxycarbonyl)-L-serinyl)-L-lysyl)-L-leucyl)-L-glutaminyl)-L-valine methyl ester trifluoroacetate salt (184)
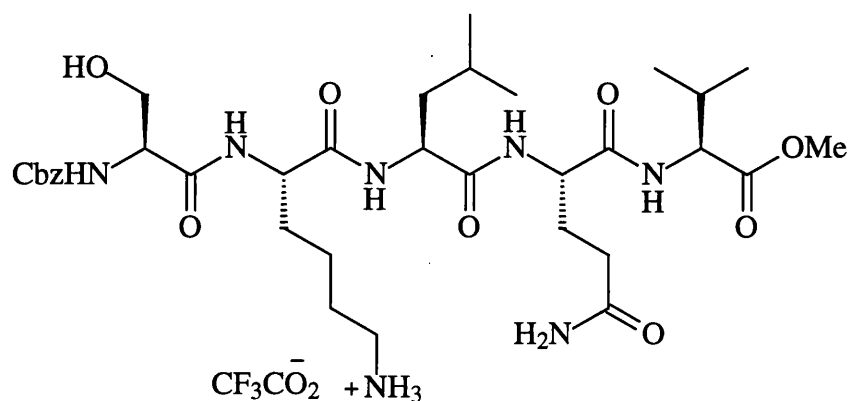
Compound **183** (3.0 mg, 3.4 μmol) was stirred in CF₃CO₂H (300 μL) and CH₂Cl₂ (700 μL)

for 4 h. Evaporation afforded **184** (quant.) as a highly hygroscopic colourless gum: NMR

$((CD_3)_2SO)$ δ_H 0.83 (3 H, d, J = 6.6 Hz, Val-Me), 0.87 (3 H, d, J = 6.2 Hz, Leu-Me), 0.89

(6 H, d, J = 5.9 Hz) (Val-Me, Leu-Me), 1.25-1.80 (10 H, m, Lys β,γ,δ-H$_6$, Leu β-H$_2$, Gln

β-H, Val β-H), 1.85 (1 H, m, Gln β-H), 2.04 (1 H, nonet, J = 6.2 Hz, Leu γ-H), 2.11 (2 H,

brt, J = 7 Hz, Gln γ-H$_2$), 2.85 (2 H, m, Lys ϵ-H$_2$), 3.57 (2 H,·brd, J = 5.5 Hz, Ser β-H$_2$),

3.63 (3 H, s, CO$_2$Me), 4.11 (1 H, brq, J = 7.4 Hz, Ser α-H), 4.15 (1 H, dd, J = 8.1, 6.2 Hz),

4.20-4.35 (3 H, m, Gln α-H, Leu α-H, Lys α-H), 5.00 (1 H, d, J = 12.5 Hz) and 5.04 (1 H,

d, J = 12.5 Hz) (CH$_2$Ph), 6.81 (1 H, s), 7.28 (1 H, s) (CONH$_2$), 7.32 (6 H, m, Ser NH,

Ph-H$_5$), 7.65 (3 H, br, NH$_3$), 7.91 (1 H, d, J = 5.9 Hz, NH), 7.93 (1 H, d, J = 7.4 Hz, NH),

8.04 (1 H, d, J = 7.8 Hz, Val NH), 8.10 (1 H, d, J = 8.2 Hz, NH); MS m/z 722.4099 (M +

H) ($C_{34}H_{56}N_7O_{10}$ requires 722.4089).

Dimethyl thiophene-2,5-dicarboxylate (199)
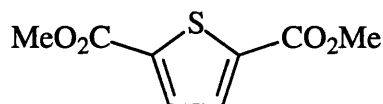
Thiophene-2,5-dicarboxylic acid **198** (900 mg, 5.2 mmol) was boiled under reflux with

H_2SO_4 (2.0 mL) in MeOH (150 mL) for 48 h. The evaporation residue, in CH$_2$Cl$_2$, was

washed with H$_2$O, aq. NaHCO$_3$ and brine. Drying and evaporation afforded **199** (770 mg,

74%) as a white solid: mp 147-149°C (lit[226] mp 147-151°C); NMR δ_H 3.92 (6 H, s, 2 ×

Me), 7.74 (2 H, s, 3,4-H$_2$).

2,5-Bis(hydroxymethyl)thiophene (200)
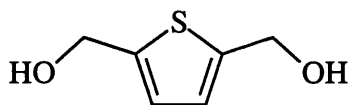
NaBH$_4$ (590 mg, 16 mmol) was stirred with **202** (1.0 g, 7.1 mmol) in H$_2$O (14 mL) and

THF (15 mL) for 24 h. The evaporation residue, in CH$_2$Cl$_2$, was extracted with H$_2$O. The

aqueous layer was saturated with NaCl and extracted with Et$_2$O. Drying and evaporation

afforded **200** (780 mg, 76%) as a pale buff viscous oil: NMR $((CD_3)_2SO)$ δ_H 4.55 (4 H, d, J

= 5.5 Hz, 2 × CH$_2$), 5.38 (2 H, t, J = 5.5 Hz, 2 × OH), 6.76 (2 H, s, 3,4-H$_2$).

Methyl 5-hydroxymethylthiophene-2-carboxylate (201)
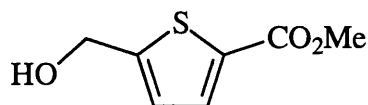
LiBH$_4$ (300 mg, 14 mmol) was added to **199** (500 mg, 2.5 mmol) in dry THF under Ar and the mixture was stirred for 2 d. AcOH was added dropwise until no further bubbling was observed. Acetyl chloride (2.0 mL) was added to the evaporation residue, followed by Et$_3$N (1.0 mL). The mixture was stirred for 16 h. The evaporation residue, in CH$_2$Cl$_2$, was washed with H$_2$O and dried. The evaporation residue was stirred with MeOH (15 mL) and aq. NH$_3$ (35%, 5.0 mL) for 16 h. Evaporation and chromatography (EtOAc / hexane 1:1) afforded **201** (150 mg, 34%) as a pale buff oil: IR (Nujol) v_{max} 2854 (OH), 1702 (C=O) cm^{-1}; NMR δ_H 3.80 (3 H, s, Me), 4.68 (2 H, d, J = 5.8 Hz, CH$_2$), 5.75 (1 H, t, J = 5.8 Hz, OH), 7.02 (1 H, dd, J = 3.7, 0.9 Hz, 4-H), 7.66 (1 H, d, J = 3.7 Hz, 3-H); MS (EI) m/z 172.0188 (M) (C$_7$H$_8$O$_3$S requires 172.0194), 141 (M - CH$_2$OH), 113 (M - CO$_2$Me); Found: H, 4.77. C$_7$H$_8$O$_3$S requires H, 4.68%.

Thiophene-2,5-dicarbonyl chloride (203)
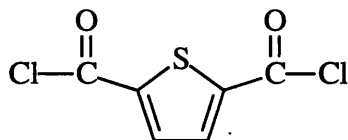
Thiophene-2,5-dicarboxylic acid **198** (1.00 g, 5.8 mmol) was boiled under reflux with DMF (30 μL) in SOCl$_2$ (3.45 g, 29 mmol) for 16 h. Evaporation afforded **203** (1.21 g, quant.): NMR δ_H 8.01 (2 H, s, 3,4-H$_2$).

Thiophene-2,5-dicarboxamide (204)
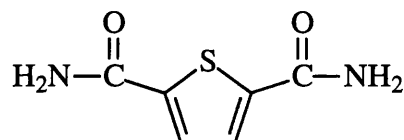
Compound **203** (6.44 g, 38 mmol) in THF (25 mL) was added dropwise to aq. NH$_3$ (35%, 50 mL). The solid was collected by filtration, washed with H$_2$O and dried to afford **204** (4.78 g, 74%) as a white solid: mp >350°C (lit.[226] no mp given); NMR ((CD$_3$)$_2$SO) δ_H 7.55 (2 H, s, 2 × NH), 7.68 (2 H, s, Hz, 3,4-H$_2$), 8.07 (2 H, s, 2 × NH).

Thiophene-2,5-dicarbonitrile (205)

$$N\equiv C-\text{(thiophene ring)}-C\equiv N$$
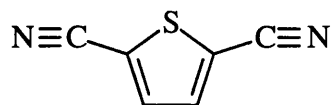
Compound **204** (4.70 g, 30 mmol) was boiled under reflux in $POCl_3$ (13 mL) for 3 h. CH_2Cl_2 (100 mL) was added, followed by aq. $NaHCO_3$ (CAUTION). The organic layer was washed with aq. $NaHCO_3$. Drying and evaporation afforded **205** (2.05 g, 51%) as a white solid: mp 102-103°C (lit.[227] mp 103°C); IR v_{max} 2361 (CN) cm^{-1}; NMR δ_H 7.67 (2 H, s, 3,4-H_2).

2,5-Bis(acetamidomethyl)thiophene (206)

$$CH_3COHN-\text{(thiophene ring)}-NHCOCH_3$$
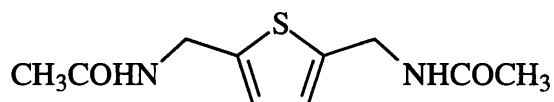
$BH_3.Me_2S$ in THF (2.0 M, 50 mL, 100 mmol) was added dropwise to **205** (1.00 g, 7.5 mmol) in dry THF (45 mL) at reflux. The mixture was boiled under reflux for 30 h and cooled to 20°C. MeOH (28 mL) was added and stirring continued for 30 h. Acetyl chloride (15.0 mL) was added to the evaporation residue, followed by Et_3N (1.0 mL). The mixture was stirred for 16 h. The evaporation residue, in EtOAc, was extracted with H_2O. The aqueous layer was saturated with NaCl and extracted with EtOAc. Drying, evaporation and chromatography ($CHCl_3$ / MeOH 13:1) afforded **206** (150 mg, 9%) as a white solid: mp 142-144°C; IR v_{max} 3254 (NH), 1648 (amide I), 1543 (amide II) cm^{-1}; NMR (CD_3OD) δ_H 1.94 (6 H, s, 2 × Me), 4.44 (4 H, s, 2 × CH_2), 6.78 (2 H, s, 3,4-H_2); MS m/z 227.0855 (M + H) $C_{10}H_{15}N_2O_2S$ requires 227.0854); Found: C, 53.10; H, 6.34; $C_{10}H_{14}N_2O_2S$ requires C, 53.08; H, 6.24%.

Ethyl 5-methylthiophene-2-carboxylate (209)

$$\text{(methyl-thiophene ring)}-CO_2Et$$
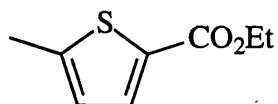
2-Methylthiophene (20.0 g, 204 mmol) was added slowly to butyl lithium (220 mmol) in dry THF (400 mL) at 0°C and the mixture was stirred at 0°C for 3 h before being added slowly to ethyl chloroformate (28.2 g, 260 mmol) in THF (200 mL) at 0°C. The mixture was stirred at 20°C for 16 h, and then poured onto ice. The organic layer was washed with H_2O, aq. HCl (1 M), aq. $NaHCO_3$, and H_2O. Drying, evaporation and distillation gave **209**

(23 g, 68%) bp~$_1$ 120°C (lit^{228}. bp$_5$ 87-89°C); NMR δ_H 1.33 (3 H, t, J = 7.0 Hz, CH$_2$CH_3), 2.48 (3 H, brs, 5-Me), 4.30 (2 H, q, J = 7.0 Hz, CH$_2$), 6.72 (1 H, dq, J = 3.7, 1.2 Hz, 4-H), 7.57 (1 H, d, J = 3.7Hz, 3-H).

Ethyl 5-bromomethylthiophene-2-carboxylate (210)
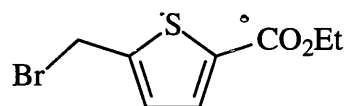
Compound **209** (1.00 g, 5.9 mmol) was stirred with N-bromosuccinimide (1.08 g, 6.1 mmol) and aq. HClO$_4$ (60%, 30 μL) in hexane (3.0 mL) for 24 h. The evaporation residue, in EtOAc, was washed with saturated aq. sodium sulphite solution. Drying, evaporation and chromatography (hexane / EtOAc 9:1) afforded **210** (160 mg, 11%) as a colourless oil: NMR δ_H 1.37 (3 H, t, J = 7.0 Hz, Me), 4.35 (2 H, q, J = 7.0 Hz, OCH$_2$), 4.68 (2 H, s, CH$_2$Br), 7.08 (1 H, dt, J = 3.9, 0.8 Hz, 4-H), 7.63 (1 H, d, J = 3.9 Hz, 3-H); MS m/z 251/249 (M + H), 170 (M + H − Br); Found: C, 38.60; H, 3.77; C$_8$H$_9$BrO$_2$S requires C, 38.55; H, 3.64%.

Ethyl 5-(trifluoroacetamidomethyl)thiophene-2-carboxylate (211)
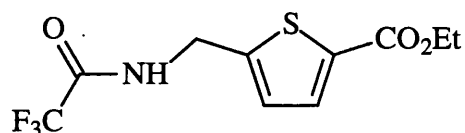
Trifluoroacetamide (410 mg, 3.6 mmol) in dry THF (2.0 mL) was added slowly to KOBu^t (410 mg, 3.6 mmol) in dry THF (2.0 mL). The mixture was stirred for 1 h, then added slowly to **210** (130 mg, 520 μmol) in dry THF (3.0 mL). The mixture was stirred for 15 h. The evaporation residue, in CH$_2$Cl$_2$, was washed with H$_2$O, aq. HCl (1 M) and H$_2$O. Drying and evaporation afforded **211** (90 mg, 62%) as a pale yellow solid: mp 65-66°C: IR ν_{max} 3333 (NH), 1719 (C=O), 1683 (C=O) cm^{-1}; NMR δ_H 1.37 (3 H, t, J = 7.0 Hz, Me), 4.34 (2 H, q, J = 7.0 Hz, OCH$_2$), 4.72 (2 H, d, J = 5.9 Hz, CH$_2$N), 7.03 (1 H, dt, J = 3.9, 0.8 Hz, 4-H), 7.67 (1 H, d, J = 3.5 Hz, 3-H); NMR δ_F -76.2 (3 F, s, CF$_3$); MS m/z 282.0413 (M + H) (C$_{10}$H$_{11}$F$_3$NO$_3$S requires 282.0412); Found C, 42.90; H, 3.49; N, 4.98; C$_{10}$H$_{10}$F$_3$NO$_3$S requires C, 42.68; H, 3.59; N, 4.98%.

5-(Benzyloxycarbonylaminomethyl)thiophene-2-carboxylic acid (212)
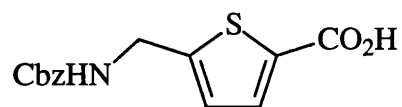
Compound **211** (3.50 g, 12.0 mmol) was boiled under reflux with NaOH (3.93 g, 98 mmol) in H_2O (50 mL) and MeOH (50 mL) for 16 h. The MeOH was evaporated. Benzyl chloroformate (5.10 mL, 36 mmol) was added at 0°C and the mixture was stirred vigorously for 4 h. The mixture was washed with Et_2O. The aqueous layer was acidified (aq. HCl) and extracted with EtOAc. Drying and evaporation afforded **212** (3.33 g, 92%) as a yellow solid: mp 142-145°C; IR v_{max} 3344 (NH), 2700 (OH), 1694 (C=O), 1547 (CONH), 1528 cm^{-1}; NMR ((CD_3)$_2$SO) δ_H 4.36 (2 H, d, J = 6.2 Hz, CH_2N), 5.04 (2 H, s, CH_2O), 6.98 (1 H, d, J = 3.5 Hz, 4-H), 7.3 (5 H, m, Ph-H_5), 7.55 (1 H, d, J = 3.5 Hz, 3-H), 8.02 (1 H, t, J = 6 Hz, NH); MS m/z 292.0644 (M + H) ($C_{14}H_{14}NO_4S$ requires 292.0640); Found: C, 57.50; H, 4.41; N, 4.63; $C_{14}H_{13}NO_4S$ requires C, 57.70; H, 4.50; N, 4.81%.

Methyl 5-(benzyloxycarbonylaminomethyl)thiophene-2-carboxylate (213)
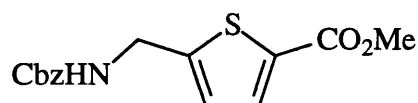
Compound **212** (500 mg, 1.7 mmol) was boiled under reflux with H_2SO_4 (1.0 mL) in MeOH (50 mL) for 2 d. Aq. $NaHCO_3$ was added until no further bubbling occurred. The suspension was filtered. The evaporation residue was washed with H_2O and dried to afford **213**(460 mg, 88%) as a white solid: mp 80-83°C; NMR δ_H 3.87 (3 H, s, Me), 4.55 (2 H, d, J = 5.9 Hz, CH_2N), 5.14 (2 H, s, CH_2O), 5.23 (1 H, br, NH), 6.95 (1 H, d, J = 3.5 Hz, 4-H), 7.31-7.36 (5 H, m, Ph-H_5), 7.64 (1 H, d, J = 3.5 Hz, 3-H); MS m/z 398 (M + glycerol + H), 306.0813 (M + H) ($C_{15}H_{16}NO_4S$ requires 306.0800), 259 (M - CO_2Me); Found C, 58.99; H, 5.00; N, 4.52; $C_{15}H_{15}NO_4S$ requires C, 58.98; H, 4.95; N, 4.59%.

Methyl 5-(aminomethyl)thiophene-2-carboxylate hydrobromide (214)
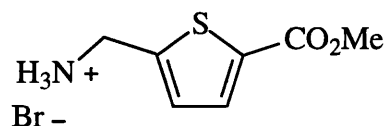
Compound **213** (100 mg, 330 μmol) in AcOH (1.0 mL) was stirred with HBr in AcOH (30%, 1.0 mL) for 20 min. The evaporation residue was washed (10 ×) with Et_2O and dried

to afford **214** (83 mg, quant.) as a white solid: mp 212-215°C; NMR ((CD$_3$)$_2$SO) δ_H 3.83 (3

H, s, Me), 4.31 (2 H, s, CH$_2$), 7.30 (1 H, d, J = 3.9 Hz, 4-H), 7.76 (1 H, d, J = 3.9 Hz, 3-H),

8.26 (3 H, br, N$^+$H$_3$); MS m/z 325 (M + mNBA + H), 172.0437 (M + H) (C$_7$H$_{10}$NO$_2$S

requires 172.0432); Found H, 4.01; N, 5.56; C$_7$H$_9$NO$_2$S requires H, 4.00; N, 5.56%.

Methyl 5-(isothiocyanatomethyl)thiophene-2-carboxylate (215)
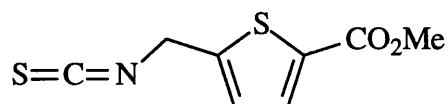
Compound **214** (210 mg, 830 μmol) was stirred with CaCO$_3$ (90 mg, 870 μmol) and

thiophosgene (200 mg, 1.7 mmol) in H$_2$O (1.5 mL) and CHCl$_3$ (10 mL) for 20 h. The

solvent was evaporated from the organic layer. Chromatography (hexane / EtOAc 7:3)

afforded **215** (110 mg, 62%) as a colourless oil: IR (Nujol) v$_{max}$ 2074 (NCS), 1711 (C=O)

cm^{-1}; NMR δ_H 3.87 (3 H, s, Me), 4.85 (2 H, s, CH$_2$), 7.03 (1 H, dt, J = 3.9, 0.8 Hz, 4-H),

7.76 (1 H, d, J = 3.9 Hz, 3-H); MS m/z 367 (M + mNBA + H), 214.0003 (M + H)

(C$_8$H$_8$NO$_2$S$_2$ requires 213.9997), 182 (M - S); Found: C, 44.90; H, 3.32; N, 6.55.

C$_8$H$_7$NO$_2$S$_2$ requires C, 45.05; H, 3.31; N, 6.57%.

Methyl 5-(thioureidomethyl)thiophene-2-carboxylate (216)
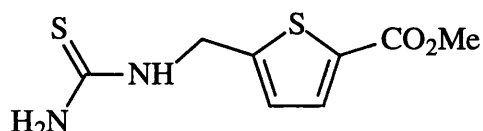
NH$_3$ was passed through **215** (60 mg, 280 μmol) in CH$_2$Cl$_2$ at 0°C for 20 min. The mixture

was stirred for 3 h at 0°C. Evaporation afforded **216** (65 mg, quant.) as a white solid: mp

131-132°C: IR v$_{max}$ 3398 (NH), 1703 (C=O), 1277 (C=S) cm^{-1}; NMR (CD$_3$OD) δ 3.84 (3

H, s, Me), 4.93 (2 H, d, J = 5.9 Hz, CH$_2$N), 7.06 (1 H, dt, J =3.7, 0.7 Hz, 4-H), 7.65 (1 H,

d, J = 4.0 Hz, 3-H); MS m/z 231.0255 (M + H) (C$_8$H$_{11}$N$_2$OS$_2$ requires 231.0262).

5-(Benzyloxycarbonylaminomethyl)thiophene-2-methanol (217)
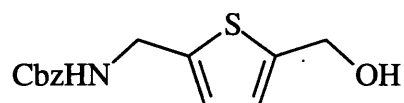
BH$_3$.THF (1.0 M, 1.0 mL, 1.0 mmol) was added to **212** (100 mg, 340 μmol) in dry THF

(2.0 mL) and the mixture was stirred for 18 h. AcOH was added dropwise until no further

bubbling occurred. Evaporation and chromatography (EtOAc / hexane 4:1) afforded **217** (50 mg, 53%) as a pale yellow solid: mp 76-78°C; NMR δ_H 4.50 (2 H, d, J = 5.9 Hz, CH_2N), 4.77 (2 H, s, CH_2OH), 5.13 (2 H, s, $PhCH_2$), 6.84 (2 H, s, 3,4-H_2), 7.36-7.38 (6 H, m, NH + Ph-H_5); MS m/z 278.0856 (M + H) ($C_{14}H_{16}NO_4S$ requires 278.0851); Found C, 60.30; H, 5.61; N, 4.84; $C_{14}H_{15}NO_4S$ requires C, 60.63; H, 5.45; N, 5.05%.

4-Methylthiophene-2-carboxaldehyde (220a) and 3-methylthiophene-2-carbox-aldehyde (220b)

220a   **220b**
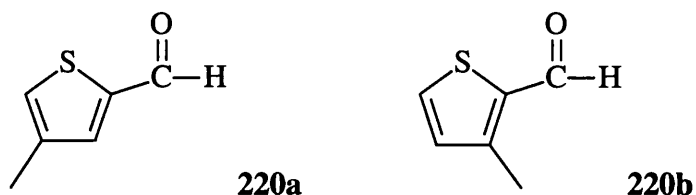
3-Methylthiophene **219** (10.0 g, 102 mmol) was added slowly to butyl lithium (2.0 M, 55 mL, 110 mmol) in dry Et_2O (175 mL) at 0°C and the mixture was stirred for 3 h at 0°C, before being added slowly to N,N-dimethylformamide (10.2 g, 140 mmol) in dry Et_2O (35 mL) at 0°C. The mixture was stirred for 16 h and poured onto ice. The organic layer was washed with H_2O, aq. HCl (1 M), aq. $NaHCO_3$, and with H_2O. Drying, evaporation and distillation gave a mixture of **220a** and **220b** (12.6 g, 61%) as a colourless liquid: NMR δ_H 2.32 (2.3 H, s, Me (235a)), 2.58 (0.7 H, s, Me (235b)), 6.97 (0.22 H, d, J = 5.2 Hz, 4-H (235b)), 7.36 (0.78 H, d, J = 1.3 Hz, 5-H (235a)), 7.58 (0.78 H, d, J = 1.3 Hz, 3-H (235a)), 7.63 (0.22 H, d, J = 5.2 Hz, 5-H (235b)), 9.86 (0.78 H, d, J = 1.3 Hz, CHO (235a)), 10.04 (0.22 H, d, J = 1.3 Hz, CHO (235b)).

4-Methylthiophene-2-carboxylic acid (221a) and 3-methylthiophene-2-carboxylic acid (221b)
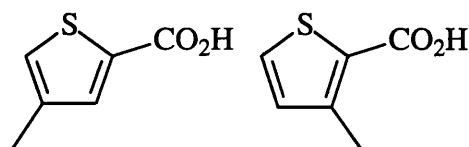
Ag_2O (4.6 g, 20 mmol) was stirred with **220a,b** (2.5 g, 20 mmol) and aq. NaOH (3.2 g, 80 mmol) in H_2O (50 mL) for 16 h. The mixture was filtered, acidified (aq. HCl) and extracted with CH_2Cl_2. Drying, evaporation and recrystallisation (hexane) afforded a mixture of **221a** and **221b** (2.30 g, 82%) as white crystals; mp 118-120°C (lit[229] mp 123-

124°C for **221a**); NMR δ_H 2.30 (2.7 H, s, Me (**221a**)), 2.57 (0.3 H, s, Me (**221b**)), 6.95 (0.1 H, d, J = 4.7 Hz, 4-H (**221b**)), 7.13 (0.9 H, m, 5-H (**221a**)), 7.48 (1 H, d, J = 5.1 Hz, 5-H (**221b**)), 7.69 (0.9 H, d, J = 1.6 Hz, 3-H (**221a**)); MS m/z 143.0169 (M + H) ($C_6H_7O_2S$ requires 143.0167).

Methyl 4-methylthiophene-2-carboxylate (222a) and methyl 3-methylthiophene-2-carboxylate (222b)
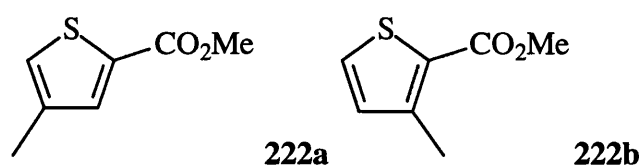
3-Methylthiophene **219** (5.0 g, 51 mmol) was added slowly to butyl lithium (2.0 M in THF, 28 mL, 56 mmol) in dry THF (100 mL) at 0°C and the mixture was stirred for 3 h at 0°C, before being added slowly to methyl chloroformate (6.33 g, 67 mmol) in dry THF (20 mL) at 0°C. The mixture was stirred for 16 h and poured onto ice. The organic layer was washed with H_2O, aq. HCl (1 M), aq. $NaHCO_3$ and with H_2O. Drying, evaporation and distillation (*ca.* 1 torr) afforded a mixture of **222a** and **222b** (5.00 g, 62%) as a colourless oil: NMR δ_H 2.28 (2.4 H, s, Me (237a)), 2.56 (0.6 H, s, Me (237b)), 3.86 (3 H, s, OMe), 6.91 (0.2 H, d, J = 5.1 Hz, 4-H (237b)), 7.13 (0.8 H, m, 5-H (237a)), 7.38 (0.2 H, d, J = 5.1 Hz, 5-H(237b)), 7.60 (1 H, d, J = 1.6 Hz, 3-H (237a)).

Methyl 4-bromomethylthiophene-2-carboxylate (223)
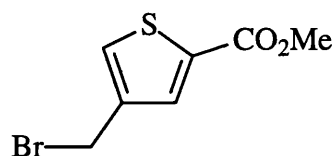
Dibenzoyl peroxide (80 mg, 330 μmol) was boiled under reflux with **222a,b** (2.48 g, 16 mmol) in CCl_4 (40 mL) for 1 h. N-Bromosuccinimide (2.83 g, 16 mmol) was added and the mixture was boiled under reflux for 16 h. During this reflux, additional dibenzoyl peroxide (50 mg, 210 μmol) was added every 10 min for 1 h and then every 30 min (twice). Evaporation and chromatography (hexane / EtOAc 9:1) gave **223** (170 mg, 4.5%) as a pale buff oil; NMR δ_H 3.89 (3 H, Me), 4.46 (2 H, s, CH_2), 7.49 (1 H, d, J = 1.6 Hz, 5-H), 7.80 (1 H, d, J = 1.6 Hz, 3-H).

Methyl 4-(trifluoroacetamidomethyl)thiophene-2-carboxylate (224) and N,N-bis((2-methoxycarbonylthien-4-yl)methyl)trifluoroacetamide (225)
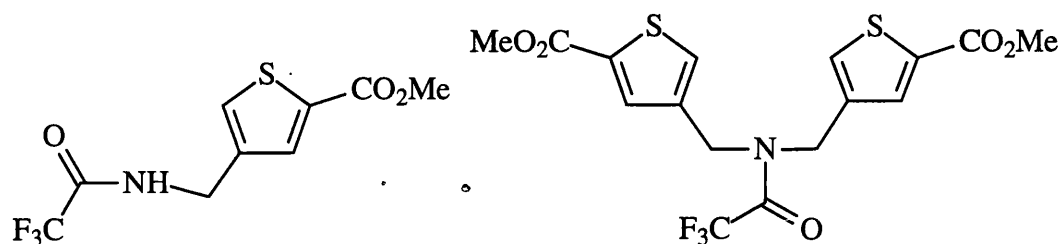
Trifluoroacetamide (570 mg, 5.1 mmol) in dry THF (2.0 mL) was stirred with KOBu^t (570 mg, 5.1 mmol) in dry THF (2.0 mL) for 1 h. Compound **223** (170 mg, 720 μmol) in dry THF (2.0 mL) was added slowly and the mixture was stirred for 15 h. The evaporation residue, in CH_2Cl_2, was washed with H_2O, aq. HCl (1 M) and H_2O. Drying, evaporation and chromatography ($CHCl_3$ / EtOAc 19:1) afforded **225** (10 mg, 3%) as a pale yellow solid: mp 63-65°C; IR (film) v_{max} 1711, 1603, 1541 cm^{-1}; ^1H NMR δ_H 3.89 (3 H, s, Me), 3.90 (3 H, s, Me), 4.50 (2 H, s, CH_2), 4.54 (2 H, s, CH_2), 7.34 (1 H, brs, 5-H), 7.36 (1 H, brs, 5-H), 7.57 (1 H, d, J = 1.6 Hz, 3-H), 7.60 (1 H, d, J = 1.6 Hz, 3-H); NMR δ_F -68.67 (3 F, s, CF_3); MS m/z 422.0340 (M + H) ($C_{16}H_{15}F_3NO_5S_2$ requires 422.0344). Further elution gave **224** (70 mg, 36%) as a pale yellow solid: mp 80-83°C; IR v_{max} 3305 (NH), 1703 ($CF_3C=O$), 1562 (amide) cm^{-1}; NMR δ_H 3.89 (3 H, s, Me), 4.53 (2 H, d, J = 5.8 Hz, CH_2), 6.61 (1 H, br, NH), 7.45 (1 H, m, 5-H), 7.71 (1 H, d, J = 1.7 Hz, 3-H); NMR δ_F -76.2 (3 F, s, CF_3); MS m/z 268.0255 (M + H) ($C_9H_9O_3F_3NS$ requires 268.0246).

4-(Benzyloxycarbonylaminomethyl)thiophene-2-carboxylic acid (227)
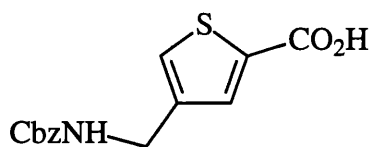
Compound **224** (200 mg, 750 μmol) was boiled under reflux with NaOH (300 mg, 7.5 mmol) in H_2O (3.0 mL) and MeOH (3.0 mL) for 16 h. The MeOH was evaporated. Benzyl chloroformate (380 mg, 2.2 mmol) was added at 0°C and the mixture was stirred vigorously for 4 h, before being washed with EtOAc. The aqueous layer was acidified (aq. HCl) and extracted with EtOAc. Drying, evaporation and chromatography (EtOAc) afforded **227** (180 mg, 82%) as a white solid: mp 149-151°C; NMR ($(CD_3)_2SO$) δ_H 4.08 (2 H, d, J = 5.7 Hz, CH_2N), 5.02 (2 H, s, CH_2O), 7.33-7.36 (5 H, m, Ph-H_5), 7.57 (1 H, m, 5-H), 7.60 (1 H, d, J = 1.2 Hz, 3-H), 7.82 (1 H, t, J = 5.7 Hz, NH); MS m/z 315.0503 (M +

Na) ($^{13}C_1^{12}C_{13}H_{13}NNaO_4S$ requires 315.0496), 314.0462 (M + Na) ($^{12}C_{14}H_{13}NNaO_4S$ requires 314.0463).

Methyl 4-(benzyloxycarbonylaminomethyl)thiophene-2-carboxylate (228)
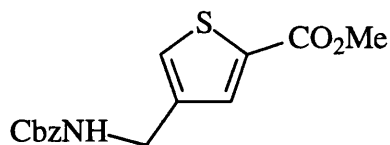
Compound **227** (500 mg, 1.70 mmol) was boiled under reflux with H_2SO_4 (1.00 mL) and MeOH (50 mL) for 2 d. Aq. NaHCO$_3$ was added until no further bubbling occurred. The evaporation residue in CHCl$_3$ was washed with H_2O. Drying and evaporation afforded **228** (430 mg, 82%) as a white solid: mp 64-65°C; NMR δ_H 3.88 (3 H, s, Me), 4.35 (2 H, d, $J =$ 5.9 Hz, CH$_2$N), 5.13 (3 H, m, CH$_2$O + NH), 7.34-7.38 (6 H, m, Ph-H$_5$ +5-H), 7.71 (1 H, br, 3-H); MS m/z 306.0809 (M + H) ($C_{15}H_{16}NO_4S$ requires 306.0800).

Methyl 4-(aminomethyl)thiophene-2-carboxylate hydrobromide (229)
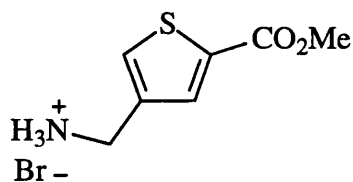
Compound **228** (280 mg, 920 μmol) in AcOH (2.8 mL) was stirred with HBr in AcOH (30%, 2.8 mL) for 20 min. The evaporation residue was washed with Et$_2$O (10 ×) and dried to afford **229** (230 mg, quant.) as a white solid: mp 203-205°C; NMR ((CD$_3$)$_2$SO) δ_H 3.85 (3 H, s, Me), 4.08 (2 H, s, CH$_2$), 7.95 (1 H, d, $J =$ 1.6 Hz, 5-H), 7.97 (1 H, m, 3-H), 8.13 (3 H, br, N$^+$H$_3$); MS m/z 172.0439 (M + H) C$_7$H$_{10}$NO$_2$S requires 172.0432); Found C, 33.20; H, 3.88; N, 5.44; C$_7$H$_9$NO$_2$S.HBr requires C, 33.33; H, 4.00; N, 5.56%.

Methyl 4-(isothiocyanatomethyl)thiophene-2-carboxylate (230)
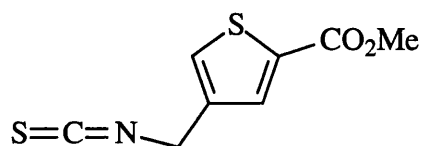
Compound **229** (200 mg, 790 μmol) was stirred with CaCO$_3$ (90 mg, 900 μmol) and thiophosgene (180 mg, 1.6 mmol) in H_2O (2.0 mL) and CHCl$_3$ (10 mL) for 20 h. The solvent

was evaporated from the organic layer. Chromatography (CH_2Cl_2) afforded **230** (104 mg, 62%) as a white solid: mp 69-70°C: IR v_{max} 2115 (NCS), 1711 (C=O) cm^{-1}; NMR δ_H 3.90 (3 H, s, Me), 4.71 (2 H, s, CH_2), 7.48 (1 H, dt, J = 2.0, 0.8 Hz, 5-H), 7.75 (1 H, d, J = 2.0 Hz, 3-H); MS m/z 214 (M + H); Found C, 45.30; H, 3.37; N, 6.66. $C_8H_7NO_2S_2$ requires C, 45.03; H, 3.31; N, 6.57%.

Methyl 4-(thioureidomethyl)thiophene-2-carboxylate (231)
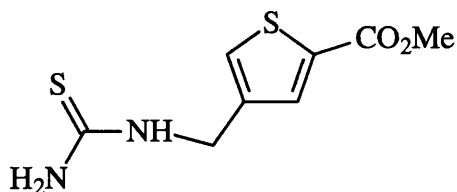
NH_3 was bubbled through **230** (60 mg, 280 µmol) in CH_2Cl_2 (3.0 mL) at 0°C for 20 min. The mixture was stirred for 3 h at 0°C. Evaporation afforded **231** (61 mg, 95%) as a white solid: mp 131-132°C: NMR δ_H 3.87 (3 H, s, Me), 4.64 (2 H, br, CH_2), 5.98 (2 H, br, NH_2), 6.77 (1 H, br, NH), 7.46 (1 H, br, 5-H), 7.72 (1 H, d, J = 1.6 Hz, 3-H); MS m/z 231.0272 (M + H) ($C_8H_{11}N_2O_2S_2$ requires 231.0262).

235

1. Thibodeau, G. A.; Patton, K, T. Louis, S. T. eds. Anatomy and physiology, **1999**, Mosby, London: pp 891-902 (ISBN 0323001920).

2. Tortora, G. J.; Grabowski, S. R. eds. Principles of anatomy and physiology, **2003**, Wiley, New York: pp 1024-1026. (ISBN 0471224723)

3. Guyton, A. C.; Hall, J. E. eds. Textbook of medical physiology, **2000**, Philadelphia, London: Savnders, W. A. pp 916-928. (ISBN 072168677)

4. Underwood, J. C. E.; Britton, R. eds. General and systematic pathology, **2000**, Edinburgh: Churchill Livingstone, pp 526-551. (ISBN 0443062854)

5. MacSween, N. M.; Whaley, K. eds. Muir's textbook of pathology, **1992**, Arnold, London:. pp 1064-1071. (ISBN 0340662336)

6. Stevens, A.; Lowe, J. eds. Pathology, **1995**, Mosby, London:. (ISBN 0397447647)

7. Jani, A. B.; Hellman, S. Early prostate cancer: clinical decision-making. *Lancet* **2003**, *361*, 1045-1049.

8. Frankel, S.; Smith, G. D.; Donovan, J.; Neal, D. Screening for prostate cancer. *Lancet* **2003**, *361*, 1122-1128.

9. Prakash, B. S. Mayo Internal Medicine Board review, Mayo Foundation for Medical Education and Research, Rochester, **1996-97**, p. 629.

10. Grönberg, H. Prostate cancer epidemiology. *Lancet* **2003**, *361*, 859-864.

11. Hayes, R. B.; Liff, J. M.; Pottern, L. M. Prostate cancer risk in US blacks and whites with a family history of cancer. *Int. J. Cancer* **1995**, *60*, 361-364.

12. Gleason, D. F.; Mellinger, G. T.; and the Veterans Administration Cooperative Urological Research Group. Prediction of prognosis for prostatic adenocarcinoma by combined histologic grading and clinical staging. *J. Urol.* **1974**, *111*, 58-64.

13. DeMazo, A. M.; Nelson, W. G.; Isaacs, W. B.; Epstein, J. I. Pathological and molecular aspects of prostate cancer. *Lancet* **2003**, *361*, 955-963.

14. Khan, H.; Khan, F.; Yusuf, S. Prostate cancer screening. *McMaster. Univ. Med. J. (MUMJ)*. **2003**, *1*, 20-26.

15. Oesterling, J. E. Prostate-specific antigen: a critical assessment of the most useful tumour marker for adenocarcinoma of the prostate. *J. Urol.* **1991**, *145*, 907-923.

16. Watt, K. W. K.; Lee, P.; M'Timkulu, T.; Chan, W.; Loor, R. Human prostate-specific antigen: Structural and functional similarity with serine proteases. *Proc. Natl. Acad. Sci. USA* **1986**, *83*, 3166-3170.

17. Papatsoris, A. G.; Papavassiliou, A. G. Prostate cancer: horizons in the development of novel anti-cancer strategies. *Current Medicinal Chemistry – Anti-Cancer Agents.* **2001**, *47-70*.

18. Schild, S. E.; Buskirk, S. J.; Wong, W. W.; Halyard, M. Y.; Swanson, S. K.; Novicki, D. E.; Ferrigni, R. G. The use of radiotherapy for patients with isolated elevation of serum prostate specific antigen following radical prostatectomy. *J. Urol.* **1996**, *156*, 1725-1729.

19. Catalona, W. J.; Carvalhal, G. F.; Mager, D. E.; Smith, D. S. Potency, continence and complication rates in 1870 consecutive radical retropubic prostatectomies. *J. Urol.* **1999**, *162*, 433-438.

20. Weldon, V. E.; Tavel, F. R.; Neuwirth, H. Continence, potency and morbidity after radical perineal prostatectomy. *J. Urol.* **1997**, *158*, 1470-1475.

21. Walsh, P. C.; Mostwin, J. L. Radical prostatectomy and cystoprostatectomy with preservation of potency: results using a new nerve-sparing technique. *Br. J. Urol.* **1984**, *156*, 694-697.

22. Pilepich, M. V.; Asbell, S. O.; Krall, J. M.; Baerwald, W. H.; Sause, W. T.; Rubin, P.; Emami, B. N.; Pidcock, G. M. Correlation of radiotherapeutic parameters and treatment related morbidity: analysis of RTOG Study 77-06. *Int. J. Radiat. Oncol. Biol. Phys.* **1987**, *13*, 1007-1012.

23. Locke, J.; Ellis, W.; Wallner, K.; Cavanagh, W.; Blasko. J. Risk factors for acute urinary retention requiring temporary intermittent catheterization after prostate brachytherapy: a prospective study. *Int. J. Radiat. Oncol. Biol. Phys.* **2002**, *52*, 712-719

24. Newling, D. W. W. The use of adriamycin and its derivatives in the treatment of prostatic cancer. *Cancer Chemother. Pharmacol.* **1992**, *30*, S90-S94.

25. Odrazka, K.; Vanasek, J.; Vaculikova, M.; Stejskal, J.; Filip, S. The role of chemotherapy in prostate cancer. *Neoplasma* **2000**, *47*, 197-203.

26. Logothetis, C. J. A therapeutically relevant framework for the classification of human prostate cancer - Introduction. *Semin. Oncol.* **1999**, *26*, 369-374.

27. Chodak, G. W.; Vogelzang, N. J.; Caplan, R. Independent prognostic factors in patients with metastatic (stage-D2) prostate cancer. *J. Am. Med. Assoc.* **1991**, *265*, 618-621.

28. Zlotta, A. R.; Schulman, C. Neoadjuvant and adjuvant hormone therapy for prostate cancer. *World J. Urol.* **2000**, *18*, 179–182.

29. Cal, C.; Uslu, R.; Gunaydin, G.; Ozyurt, C.; Omay, S.B. Doxazosin: a new cytotoxic agent for prostate cancer? *BJU International* **2000**, *85*, 672-675.

30. MacNeal, J. E. New morphologic findings relevent to the origin and evolution of carcinoma of the prostate and B.P.H. *UICC technical reports series* **1979**, *48*, 24-37.

31. Isaacs, J. T. New principles in the management of metastatic prostate cancer. In: Das Prostatakarzinom zwischen Hormontherapie and Zytostase. *Medical Trends*, **1986**, Solingen, 5027.

32. Huggins, C.; Hodges, C. V. Studies on prostate cancer. 1. The effect of castration, of estrogen and of androgen injection on serum phosphatases in metastatic carcinoma·of the prostate. *Cancer Res.***1941**, *1*, 293-297.

33. Gilman, A.; Phillips, F. S. The biological actions and therapeutic applications of the β-chloroethyl amines and sulfides. *Science* **1946**, *103*, 409-415.

34. Remers, W. A. Wilson and Gisvold`s textbook of organic medicinal and pharmaceutical chemistry, eds. Delgado, J. N.; Remers, W. A, Philadelphia, **1998**, pp 343-401.

35. Creasey, W. A. Cancer, an introduction. New York; Oxford: Oxford University Press, **1981**, p 195. (ISBN 0195029526)

36. Alberts, B.; Bray, D.; Lewis, J.; Raff, M.; Roberts, K.; Watson, J. eds. Molecular biology of the cell. New York; London: Garland, p 260. (ISBN 0815316208)

37. Berettoni, M.; Cipollone, A.; Olivieri, L.; Palomba, D.; Arcamone, F.; Maggi, C. A.; Animati, F. Synthesis of 14-fluorodoxorubicin. *Tetrahedron Lett.* **2002**, *43*, 2867-2871.

38. Torti, F. M.; Bristow, M. R.; Howes, A. E.; Aston, D.; Stockdale, F. E.; Carter, S. K.; Kohler, M.; Brawn, B. W.; Billingham, M. E. Reduced cardiotoxicity of doxorubicin delivered on a weekly schedule. Assessment by endomyocardial biopsy. *Ann. Intern. Med.* **1983**, *99*, 745-749.

39. Binaschi, M.; Capranico, G.; Bo, L. D.; Zunino, F. Relationship between lethal effects and topoisomerase II-mediated double–stranded DNA breaks produced by anthracyclines with different sequence specificity. *Mol. Pharmacol.* **1997**, *51*, 1053-1059.

40. Capranico, G.; Butelli, E.; Zunino, F. Change of the sequence specificity of daunorubicin-stimulated topoisomerase II DNA cleavage by epimerization of the amino group of the sugar moiety. *Cancer Res.* **1995**, *55*, 312-317.

41. Douglas, S. J.; Davies, S. S.; Illum, L. Nanoparticles in drug delivery. *CRC Crit. Rev. Ther. Drug Carrier Sys.* **1987**, *3*, 233-261.

42. Mhaka, A.; Denmeade, S. R.; Yao, W.; Isaacs, J, T.; Khan, I.; Khan, S. R. A 5-fluorodeoxyuridine prodrug as targeted therapy for prostate cancer. *Bioorg. Med. Chem. Lett.* **2002**, *12*, 2459-2461.

43. Seymour, L.W. Passive tumour targeting of soluble macromolecules and drug conjugates. *CRC Crit. Rev. Ther. Drug Carrier Sys.* **1992**, *9*, 135-187.

44. Davis, S. S.; Illum, L.; McVie, J. G.; Thomlinson, E. eds. The reticuloendothelial system and blood clearance, in microspheres and drug therapy, **1984**, Bradfield, J. W. B; Elsevier/North Holland, Amsterdam, p 25.

45. Alving, C. R. Delivery of liposome-encapsulated drugs to macrophages. *Pharm. Ther.* **1983**, *22*, 407-423.

46. Russell, G. F. J. Starch microspheres as delivery systems. *Pharm. Int.* **1983**, *4*, 260-262.

47. Illum, L.; Thomas, N.; Davis, S. S. The effect of a selected suppression of the reticuloendothelial system on the distribution of model carrier particles. *J. Pharm. Sci.* **1986**, *75*, 16-22.

48. Denny, W. A. Prodrugs for gene-directed enzyme prodrug therapy. *Biomed. Biotechnol.* **2003**, *1*, 48-70.

49. Connors, T. A. Prodrugs in cancer chemotherapy. *Xenobiotica* **1986**, *16*, 975-988.

50. Rooseboom, M.; Commandeur, J. M.; Vermeulen, N. E. Enzyme-catalyzed activation of anticancer prodrugs. *Pharmacol. Rev.* **2004**, *56*, 53-102.

51. Begleiter, A. Clinical applications of quinone-containing alkylating agents. *Front Biosci.* **2000**, *5*, E153-171.

52. Dubowchik, G. M.; Walker, M. A. Receptor-mediated and enzyme-dependent targeting of cytotoxic anticancer drugs. *Pharmacol Ther.* **1999**, *83*, 67-123.

53. Partridge, S. E.; Parsons, C.A.; Luo, C.; Green, A.; Olive, P. L. A pilot study comparing intratumoral oxygenation using the comet assay following 2.5% and 5% carbogen and 100% oxygen. *Int. J. Radiat. Oncol. Biol. Phys. Int.* **2001**, *49*, 575-580.

54. Naughton, D. P.; Ferrer, S.; Threadgill, M. D. Drug targeting using bioreductive delivery systems. *Proc. Indian Natl. Sci. Acad. (PINSA)* **2002**, *4*, 371-378.

55. Hay, M. P.; Wilson, W. R.; Denny, W. A. Design, synthesis and evaluation of imidazolylmethyl carbamate prodrugs of alkylating agents. *Tetrahedron* **2000**, *56*, 645-657.

56. Tercel, M.; Lee, A. E.; Hogg, A.; Anderson, R. F.; Lee, H. H.; Siim, B. G.; Denny, W. A.; Wilson, W. R. Hypoxia-selective antitumour agents. 16. Nitroarylmethyl quaternary salts as bioreductive prodrugs of the alkylating agent mechlorethamine. *J. Med. Chem.* **2001**, *44*, 3511-3522.

57. Jaffar, M.; Naylor, M. A.; Robertson, N.; Stratford, I. J. Targeting hypoxia with a new generation of indolequinones. *Anti-Cancer Drug Des*, **1998**, *13*, 593-609.

58. Ferrer, S.; Naughton, D. P.; Threadgill, M. D. Labelled compounds of interest as antitumour agents – VIII. Synthesis of ^{2}H-isotopomers of pentamethylmelamine and of a potential prodrug thereof. *J. Labelled Compd. Radiopharm.* **2002**, *45*, 479-484.

59. Upeslacis, J. Antibody-drug conjugates for cancer therapy. *J. Pharm. Ed.* **1992**, *56*, 464-467.

60. Jiménez, C.; Tramontano, A. Synthesis of a new hapten for generating catalytic antibodies that activate doxorubicin prodrugs. *Tetrahedron Lett.* **2002**, *42*, 7819-7822.

61. Senter, P. D.; Wallace, P. M.; Svensson, H. P.; Kerr, D. E.; Hellstrom, I.; Hellstrom, K. E. Activation of prodrugs by antibody-enzyme conjugates. *Adv. Exp. Med. Biol.* **1991**, *303*, 97-105.

62. Niculescu-Duvaz, I.; Spooner, R.; Marais, R.; Springer, C. J. Gene-directed enzyme prodrug therapy. *Bioconj. Chem.* **1998**, 9, 4-22.

63. Niculescu-Duvaz, D.; Niculescu-Duvaz, I.; Friedlos, F.; Martin, J.; Spooner, R.; Davies, L.; Marais, R.; Springer, C. J. Self-immolative nitrogen mustard prodrugs for suicide gene therapy. *J. Med. Chem.* **1998**, *41*, 5297-5309.

64. Huber, B. E.; Austin, V. C.; Good, V. C.; Knick, V. C.; Tibbels, S.; Richards, C. A. In vivo antitumour activity of 5-fluorocytosine on human colorectal carcinoma cells genetically modified to express cytosine deaminase. *Cancer Res.* **1993**, *53*, 4619-4626.

65. Huber, B. E.; Austin, E. A.; Richards, C. A.; Davis, S. T.; Good, S. S. Metabolism of 5-fluorocytidine to 5-fluorouracil in human colorectal tumor cells transducted with the cytosine deaminase gene: Significant antitumour effects when only a small percentage of tumour cells express cytosine deaminase. *Proc. Natl. Acad. Sci. USA.* **1994**, *91*, 8302-8306

66. Liu, S. C.; Minton, N. P.; Giaccia, A. J.; Brown, J. M. Anticancer efficacy of systematically delivered anaerobic bacteria as gene therapy vectors targeting tumour hypoxia/necrosis. *Gene Ther.* **2002**, *9*, 291-296.

67. Philip, L. C.; Chakravarty, P. K.; Katzenellenbogen, J. A. A novel connecter linkage applicable in prodrug design. *J. Med. Chem.* **1981**, *24*, 479-480.

68. Denmeade, S. R.; Nagy, A.; Gao, J.; Lilja, H.; Schally, A. V.; Issacs, J. T. Enzymatic activation of a doxorubicin-peptide prodrug by prostate-specific antigen. *Cancer Res.* **1998**, *58*, 2537-2540.

69. Dubowchik, G. M.; Firestone, R, A. Cathepsin B-sensitive dipeptide prodrugs. 1. A model study of structural requirements for efficient release of doxorubicin. *Bioorg. Med. Chem. Lett.* **1998**, *41*, 3341-3346.

70. Brady, S. F.; Pawluczyk, J. M.; Lumma, P. K.; Feng, D.; Wai, J. M.; Jones, R.; Jones, D. D.; Wong, B. K.; Stein, C. M.; Lin, J. H.; Oliff, A.; Freidinger, R. M.; Garsky, V. M. Design and synthesis of a pro-drug of vinblastine targeted at treatment of prostate cancer with enhanced efficacy and reduced systemic toxicity. *J. Med. Chem.* **2002**, 45, 4706-4715.

71. Kálal, J.; Drobnik, J.; Kopeček, J.; Exner, J. Synthetic polymer in chemotherapy: general problems, in polymeric drugs, eds. Donaruma, L. G.; Vogl, O, Academic Press, New York, **1978**, 131.

72. Sezaki, H.; Hashida, M. Macromolecule-drug conjugates in targeted cancer chemotherapy. *CRC Crit. Rev. Ther. Drug Carrier Sys.* **1984**, *1*, 1-38.

73. Kopeček, J.; Duncan, R. Targetable polymeric prodrugs. *J. Cont. Rel.* **1987**, *6*, 315-327.

74. Maeda, H.; Matsumura, Y. Tumoritropic and lymphotropic principles of macromolecular drugs. *CRC Crit. Rev. Ther. Drug Carrier Sys.* **1989**, *6*, 193-201.

75. Dvorak, H. F.; Nagy, J. A.; Dvorak, J. T.; Dvorak, A. M. Identification and characterization of the blood vessels of solid tumours that are leaky to circulating macromolecules. *Am. J. Pathol.* **1988**, *133*, 95-109.

76. Dvorak, H. F.; Nagy, J. A.; Dvorak, A. M. Structure of solid tumours and their vasculature - implication for therapy with monoclonal antibodies. *Cancer Cells − Mon. Rev.* **1991**, *3*, 77-85.

77. Mathews, S. E.; Pouton, C. W.; Threadgill, M. D. Macromolecular systems for chemotherapy and magnetic resonance imaging. *Adv. Drug Deliv. Rev.* **1996**, *18*, 219-267.

78. Maeda, H. SMANCS and polymer-conjugated macromolecular drugs: advantages in cancer chemotherapy. *Adv. Drug Deliv. Rev.* **1991**, *6*, 181-202.

79. Kopeček, J. The potential of water-soluble polymeric carriers in targeted and site-specific drug delivery. *J. Cont. Rel.* **1990**, *11*, 279-290.

80. Sezaki, H.; Hashida, M. eds. Macromolecules as drug delivery systems, in directed drug delivery, Humana Press, Clifton N. J, **1985**, p.189.(ISBN 089603089)

81. Matsumoto, S.; Arase, Y.; Takakura, Y.; Hashida, M.; Sezaki, H. Plasma disposition and in vivo and in vitro antitumour activities of mitomycin C-dextran conjugate in relation to the mode of action. *Chem. Pharm. Bull.* **1985**, *33*, 2941-2947.

82. Ouchi, T.; Fujino, A.; Tanaka, K.; Banba, Y. Synthesis and antitumour activity of conjugates of poly(α-malic acid) and 5-fluorouracil bound via ester, amide or carbamoyl bonds. *J. Cont. Rel.* **1990**, *12*, 143-153.

83. Ouchi, T.; Hagihara, Y.; Takahashi, K.; Takano, Y.; Igarashi, I. Synthesis and anti-tumour activity of poly(ethyleneglycol)s linked to 5-fluorouracil *via* urethane or urea bonds. *Drug Design Discovery* **1992,** *9*, 93-105.

84. Bundgaard, H. The double prodrug concept and its application. *Adv. Drug Del. Rev.* **1989,** *3*, 39-65.

85. Kingsburry, W. D.; Boehm, J. C.; Mehta, R. J.; Grapel, S, F.; Gilvarg, C. H. A novel peptide delivery system involving peptidase activated prodrugs as antimicrobial agents. Synthesis and biological activity of peptidyl derivatives of 5-fluorouracil. *J. Med. Chem.* **1984,** *27*, 1447-1451.

86. Nichifor, M.; Schacht, E. H.; Seymour, L. W. Polymeric prodrugs of 5-fluorouracil. *J. Cont. Rel.* **1997,** *48*, 165-178.

87. Bernstein, A.; Hurwitz, E.; Maron, M.; Arnon, R.; Sela, M.; Wilchek, M. Higher antitumour efficacy of daunomycin when linked to dextran: *in vivo* and *in vitro* studies. *J. Natl. Cancer Inst.* **1978,** *60*, 379-384.

88. Trouet, A.; Deprez-De Campeneere, D.; DeDuve, C. Chemotherapy through lysosomes with a DNA-daunorubicin complex. *Nature New Biol.* **1972,** *239*, 110-112.

89. Deprez-De Campeneere, D.; Baurain, R.; Huybrechts, M.; Trouet, A. Comparative study in mice of the toxicity, pharmacology and therapeutic activity of daunorubicin-DNA and doxorubicin-DNA complexes. *Cancer Chemother. Pharmacol.* **1979**, *2*, 25-30.

90. Deprez-De Campeneere, D.; Trouet, A. DNA-anthracycline complexes. I. Toxicity in mice and chemotherapeutic activity against L1210 leukaemia of daunorubicin-DNA and doxorubicin-DNA. *Eur. J. Cancer* **1980,** *16*, 981-986.

91. Coombs, G. S.; Bergstrom, R. C.; Pellequer, J. L.; Baker, S. I.; Navre, M.; Smith, M. M.; Tainer, J. A.; Madison, E. L.; Corey, D. R. Substrate specificity of prostate-specific antigen (PSA). *Chem. & Biol.* **1998**, *5*, 475-488.

92. Seymour, L. W.; Ulbrich, K.; Steyger, P. S.; Brereton, M.; Subr, V.; Strohalm, J.; Duncan, R. Tumour tropism and anticancer efficacy of polymer-based doxorubicin prodrugs in the treatment of subcutaneous murine B16F10 melanoma. *Br. J. Cancer* **1994**, *70*, 636-641.

93. Seymour, L. W.; Duncan, R.; Strohalm, J.; Kopeček, J. Effect of molecular weight (MW) of N-(2-hydroxypropyl)methacrylamide copolymers on body distributions and rate of excretion after subcutaneous, intraperitoneal and intravenous administration to rats. *J. Biomed. Mater. Res.* **1987**, *21*, 1341-1358.

94. Bruce, A. W.; Mahan, D. G.; Sullivan, L. D.; Goldenberg, L. The significance of prostatic acid phosphatase in adenocarcinoma of the prostate. *J. Urol.* **1981**, *125*, 357-360.

95. Vihko, P.; Lukkarinen, O.; Konturri, M.; Vihko, R. Effectiveness of radioimmunoassay of human prostate-specific acid phosphatase in the diagnosis and follow-up of therapy on prostatic carcinoma. *Cancer Res.* **1981**, *41*, 1180-1183.

96. Lee, S.; Kim, H.; Yu, R.; Lee, K.; Gardner, T. A.; Jung, C.; Jeng, M.; Yeung, F.; Cheng, L.; Kao, C. Novel prostate–specific promoter derived from PSA and PSMA enhancers. *Mol. Ther.* **2002**, *6*, 415-421.

97. Su, S. L.; Huang, I. P.; Fair, W. R.; Powell, C. T.; Heston, W. D. Alternatively spliced variants of prostate-specific membrane antigen RNA-ratio of expression as a potential measurement of progression. *Cancer Res.* **1995**, *55*, 1441-1443.

98. Pinto, J. T.; Suffoletto, B. P.; Berzin, T. M.; Qiao, C. H.; Lin, S.; Tong, W. P.; May, F.; Mukherjee, B.; Heston, W. D. Prostate-specific membrane antigen: A novel folate hydrolase in human prostatic carcinoma cells. *Clin. Cancer Res.* **1996**, *2*, 1445-1451.

99. Andra, J.; Berninghausen, O.; Wulfken, J.; Leippe, M. Shortened amoebapore analogs with enhanced antibacterial and cytolytic activity. *FEBS Lett.* **1996**, *385*, 96-100.

100. Warren, P.; Li, L.; Song, W.; Holle, E.; Wei, Y.; Wagner, T.; Yu, X. *In vitro* targeted killing of prostate tumor cells by a synthetic amoebapore helix 3 peptide modified

with two gamma-linked glutamate residues at the COOH terminus. *Cancer Res.* **2001**, *61*, 6783-6787.

101. Chang, S. S.; O'Keefe, D. S.; Bacich, D. J.; Reuter, V. E.; Heston, W. D.; Gaudin, P. B. Prostate-specific membrane antigen is produced in tumor-associated neovasculature. *Clin. Cancer Res.* **1999**, *5*, 2674-2681.

102. Wang, M. C.; Valenzuela, L. A.; Murohy, G. P.; Chu, T. M. Purification of a human prostate specific antigen. *Invest. Urol.* **1979**, *17*, 159-163.

103. Hara, M.; Inorre, T.; Fukuyama, T. Some physico-chemical characteristics of gamma-seminoprotein, an antigenic component specific for human seminal plasma. *Jap. J. Legal Med.* **1971**, *25*, 322.

104. Li, T. S.; Beling, C. G. Isolation and characterization of two specific antigens of human seminal plasma. *Fertil. Steril.* **1973**, *24*, 134-144.

105. Sensabaugh, G. F. Isolation and characterization of a semen specific protein from human seminal plasma: a potential new marker for semen identification, *J. Forensic Sci.* **1978**, *23*, 106-115.

106. Graves, ·H. C. B.; Sensabaugh, G. F.; Blake, R. T. Postcoital detection of male-specific semen protein. Application to the investigation of rape. *New Engl. J. Med.* **1985**, *312*, 338-343.

107. Wang, M. C.; Valenzuela, L. A.; Murphy, G. P.; Chu, T. M. A simplified purification procedure for human prostate specific antigen. *Oncology.* **1982**, *39*, 1-5.

108. Papsidero, L. D.; Wang, M. C.; Valenzuela, L. A.; Murphy, G. P.; Chu, T. M. A prostate antigen in sera of prostate cancer patients. *Cancer Res.* **1980**, 40, 2428-2432.

109. Ast, G. Drug-targeting strategies for prostate cancer. *Curr. Pharm. Des.* **2003**, *9*, 455-923.

110. Sella, A.; Kilbourn, R.; Amato, R.; Bui, C.; Zukiwski, A. A.; Ellerhorst, J.; Logothetis, C. J. Phase II study of ketoconazole combined with weekly doxorubicin in patients with androgen-independent prostate cancer. *J. Clin. Oncol.* **1994**, *12*, 683-688.

111. Denmeade, S. R.; Sokoll, L. J.; Chan, D. W.; Khan, S. R.; Issacs, J. T. Concentration of enzymatically active prostate-specific antigen (PSA) in the extracellular fluid of

primary human prostate cancers and human prostate cancer xenograft models. *The Prostate* **2001**, *48*, 1-6.

112. Otto. A.; Bar, J.; Birkenmerier, G. J. Prostate-specific antigen forms complexes with human alpha 2-macroglobulin and binds to the alpha 2-macroglobulin receptor LDL receptor-related protein. *J. Urol.* **1998**, *159*, 297-303.

113. Garsky, V. M.; Lumma, P. K.; Feng, D. M.; Wai, J.; Ramjit, H. G.; Sardana, M. K.; Oliff, A.; Jones, R. E.; Jones, D. D.; Freidinger, R. M. The synthesis of a prodrug of doxorubicin designed to provide reduced systemic toxicity and greater target efficacy. *J. Med. Chem.* **2001**, *44*, 4216-4224.

114. Denmeade, S. R.; Lou, W.; Lövgren, J.; Malm, J.; Lilja, H.; Isaacs, J. T. Specific and efficient peptide substrates for assaying the proteolytic activity of prostate-specific antigen. *Cancer Res.* **1997**, *57*, 4924-4930.

115. De Jong, J.; Klein, I.; Bast, A.; van der Vijgh, W. Analysis and pharmacokinetics of N-L-leucyldoxorubicin and metabolities in tissue of tumour-bearing BALB/c mice. *Cancer Chemother. Pharmacol.* **1992**, *31*, 156-160.

116. Thastrup, O.; Cullen, P. J.; Drøbak, B. K.; Hanley, M. R.; Dawson, A. P. Thapsigargin , a tumour promoter, discharges intracellular Ca^{2+} stores by specific inhibition of the endoplasmic reticulum Ca^{2+}-ATPase. *Proc. Natl. Acad. Sci. USA.* **1990**, *87*, 2466-2470.

117. Furuya, Y.; Berges, S. R.; Lundmo, P.; Isaacs, J. T. Proliferation independent activation of programmed cell death as a novel therapy for prostate cancer, eds. Mihich, E.; Schimmke, R. T, Plenum Press, New York: **1994**, pp 137-156.

118. Denmeade, S. R.; Jakobsen, C. M.; Janssen, S.; Khan, S. R.; Garrett, E. S.; Lilja, H.; Brogger Christensen, S. B.; Isaacs, J. T. Prostate-specific antigen-activated thapsigargin prodrug as targeted therapy for prostate cancer. *J. Natl. Cancer Inst.* **2003**, *95*, 990-1000.

119. Jakobsen, C. M.; Denmeade, S. R.; Isaacs, J. T.; Gady, A.; Olsen, C. E.; Brogger Christensen, S. Design, synthesis, and pharmacological evaluation of thapsigargin analogues for targeting apoptosis to prostatic cancer cells. *J. Med. Chem.* **2001**, *44*, 4696-4703.

120. Shan, D. X.; Nicolaou, M. G.; Borchardt, R. T.; Wang, B. H. Prodrug strategies based on intramolecular cyclisation reactions. *J. Pharm. Sci.* **1997**, *86*, 765-767.

121. Capasso, S.; Vergara, A.; Mazzarella, L. Mechanism of 2,5-dioxopiperazine formation. *J. Am. Chem. Soc.* **1998**, *120*, 1990-1995.

122. Grathwohl, C.; Wüthrich, K. The X-Pro peptide bond as an NMR probe for the conformation studies of flexible linear peptides. *Biopolymers* **1976**, *15*, 2025-2041.

123. Lewis, N. J.; Inloes, R. L.; Hes, J.; Matthews, R. H.; Milo, G. Synthetic sulfur-containing amino acids. 1. Inhibition of transport systems in S37 ascites tumor cells. *J. Med. Chem.* **1978**, *21*, 1070-1073.

124. Merrifield, R. B. Solid phase peptide synthesis. 1. The synthesis of tetrapeptide. *J. Am. Chem. Soc.* **1963**, *85*, 2149-2154.

125. Yamashiro, D.; Blake, J.; Li, C. H. The use of trifluoroethanol for improved coupling in solid-phase peptide synthesis. *Tetrahedron Lett.* **1976**, *18*, 1469-1472.

126. Lloyd, D. H.; Petrie, G. M.; Noble, R. L.; Tam, J. P. eds. In peptides: Proc. Am. Pept. Sym, **1990**, Rivier, J. E.; Marshall, G. R; Escom: Leiden,; pp 909-910.

127. Mutter, M.; Oppliger, H.; Zier, A. Solubilizing protecting groups in peptide-synthesis effect of side chain attached poly(ethylene glycol) derivatives upon beta-sheet formation of model peptides. *Makromol. Chem. Rapid Commun.* **1992**, *13*, 151-157.

128. Dugave, C.; Demange, L. Cis-trans isomeration of organic molecules and biomolecules: implications and applications. *Chem. Rev.* **2003**, *103*, 2475-2532.

129. Dumy, P.; Keller, M.; Ryan, D. E.; Rohwedder, B.; Wöhr, T.; Mutter, M. Pseudo-prolines as a molecular hinge: reversible induction of *cis* amide bonds into peptide backbones. *J. Am. Chem. Soc.* **1997**, *119*, 918-925.

130. An, S. S.; Lester, C. C.; Peng, J.; Li, Y.; Rothwarf, D. M.; Welker, E.; Thannhauser, T. W.; Zhang, L. S.; Tam, J. P.; Scheraga, H. A. Retention of the cis proline conformation in tripeptide fragments of bovine pancreatic ribonuclease A containing a non-natural proline analogue, 5,5-dimethylproline. *J. Am. Chem. Soc.* **1999**, *121*, 11558-11566.

131. Gallardy, R. E.; Alger, J. R.; Liakopoulos-Kyriakides, M. S-*Cis* and S-*trans* isomerism in acylproline analogs. Models for conformationally locked proline peptides. *Int. J. Pept. Protein Res.* **1982**, *19*, 123-132.

132. Wöhr, T.; Wahl, F.; Nefzi, A.; Rohwedder, B.; Sato, T.; Sun, X.; Mutter, M. Pseudo-prolines as a solubilizing, structure-disrupting protection technique in peptide synthesis. *J. Am. Chem. Soc.* **1996**, *118*, 9218-9227.

133. Wöhr, T.; Mutter, M. Pseudo-prolines in peptide synthesis: direct insertion of serine and threonine derived oxazolidines in dipeptides. *Tetrahedron Lett.* **1995**, *36*, 3847-3848.

134. Woodward, R.; Heusler, K.; Gosteli, J.; Naegeli, P.; Oppolzer, W.; Ramage, R.; Ranganathan, S.; Vorbruggen, H. The total synthesis of cephalosporin C. *J. Am. Chem. Soc.* **1966**, *88*, 852-853.

135. Kemp, D. S.; Carey, R. I. Boc-L-Dmt-OH as a fully N,S-Blocked cysteine derivative for peptide synthesis by prior thiol capture. Facile conversion of N-terminal Boc-L-Dmt-Peptides to H-Cys(Scm)-peptides. *J. Org. Chem.* **1989**, *54*, 3640-3646.

136. Carpino, L. A.; Sadat-Aalaee, D.; Chao, H. G.; DeSelms, R. H. ((9-Fluorenylmethyl)oxy)carbonyl (FMOC) amino acid fluorides. Convenient new peptide coupling reagent applicable to the FMOC / *tert*-butyl strategy for solution and solid-phase syntheses. *J. Am. Chem. Soc.* **1990**, *112*, 9651-9652.

137. Carpino, L. A.; Mansour, M. E.; Sadat-Aalaee, D. *J. Org. Chem.* **1991**, *56*, 2611-2614.

138. Olah, G. A.; Nohma, M.; Kerekes, I. Synthetic methods and reactions; IV. Fluorination of carboxylic acids with cyanuric fluoride. *Synthesis* **1973**, 9, 487-488.

139. Ohmoto, K.; Yamamoto, T.; Okuma, M.; Horiuchi, T.; Imanishi, H.; Odagaki, Y. Kawabata, K.; Sekioka, T.; Hirota, Y.; Matsuoka, S. Development of orally active nonpeptidic inhibitors of human neutropil elastase. *J. Med. Chem.* **2001**, *44*, 1268-1285.

140. White, J. M.; Tunoori, A. R.; Turunen, B. J.; Georg, G. I. [Bis(2-methoxyethyl)amino]sulphur trifluoride, the deoxo-fluoro reagent: application toward one-flask transformations of carboxylic acids to amides. *J. Org. Chem.* **2004**, *69*, 2573-2576.

141. Kisfaludy, L.; Schön, I. Preparation and applications of pentafluorophenyl esters of 9-fluorenylmethyloxycarbonyl amino-acids for peptide synthesis. *Synthesis* **1983**, 325-327.

142. Kisfaludy, L. 9-Fluorenylmethyl pentafluorophenyl carbonate as a useful reagent for the preparation of N-9-fluorenylmethyloxycarbonylamino acids and their pentafluorophenyl esters. *Synthesis* **1986**, 303-305.

143. Kisfaludy, L.; Löw, M.; Nyéki, O.; Szirtes, T.; Schön, I. Die Verwendung von Pentafluorphenylestern bei Peptid Synthesen. *Liebigs Ann. Chem.* **1973**, 1421-1429.

144. Gisin, B. F.; Merrifield, R. B. Carboxyl-catalyzed intramolecular aminolysis. A side reaction in solid-phase peptide sunthesis. *J. Am. Chem. Soc.* **1971**, *94*, 3102-3085.

145. Stewart, D. E.; Sakar, A.; Wampler, J. E. Occurrence and role of cis peptide bonds in protein structures. *J. Mol. Biol.* **1990**, *214*, 253-260.

146. Detar, D. F.; Luthra, N. P. Quantitative evaluation of steric effects in S_N2 ring closure reactions. *J. Am. Chem. Soc.* **1979**, *102*, 4505-4512.

147. Bruice, T. C.; Bradbury, W. C. The *gem* Effect. II. The Influence of 3-Mono- and 3,3-Disubstitution on the Rates of Solvolysis of Mono-*p*-bromophenyl Glutarate. *J. Am. Chem. Soc.* **1965**, *87*, 4846-4855.

148. Szardenings, A. K.; Burkoth, T. S.; Lu, H. H.; Tien, D. W.; Campbell, D. A. A simple procedure for the solid phase synthesis of diketopiperazine and diketomorpholine derivatives. *Tetrahedron Lett.* **1997**, *53*, 6573-6593.

149. Degeilh, R.; Marsh, R. E. A refinement of the crystal structure of diketopiperazine (2,5-piperazinedione). *Acta Cryst.* **1959**, *12*, 1007

150. Sletten, E. Conformation of cyclic dipeptides. The crystal and molecular structures of *cyclo*-D-alanyl-L-alanyl and *cyclo*-L-alanyl-L-alanyl (3,6-dimethylpiperazine-2,5-dione). *J. Am. Chem. Soc.* **1970**, *92*, 172-177.

151. Karle, I. L. Crystal structure and conformation of the cyclic dipeptide *cyclo*-L-prolyl-L-leucyl. *J. Am. Chem. Soc.* **1972**, *94*, 81-84.

152. Mazza, F.; Lucente, G.; Pinnen,. F.; Zanotti, G. Cyclic dipeptides containing praline. Structure and conformation of *cyclo*(-L-Phe-L-Pro-), $C_{14}H_{16}N_2O_2$. *Acta Cryst. C* **1984**, *40*, 19741976.

153. Maes, C. M.; Potgieter, M.; Steyn, P. S. N.M.R assignments, conformation and absolute configuration of ditryptophenaline and model dioxopiperazines. *J. Chem. Soc., Perkin Trans. 1* **1986**, 861-866.

154. Zervas, L.; Photaki, I.; Ghelis, N. On cysteine and cystine peptides. II S-acylcysteines in peptide synthesis. *J. Org. Chem.* **1963**, *85*, 1337-1341.

155. Menger, F. M.; Caran, K, L. Anatomy of a gel. Amino acid derivatives that rigidify water at submillimolar concentrations. *J. Am. Chem. Soc.* **2000**, *122*, 11679-11691.

156. Zervas, L.; Benoiton, L.; Weiss, E.; Winitz, M.; Greenstein, J. P. Preparation and disulfide interchange reactions of unsymmetrical open-chain derivatives of cystine. *J. Am. Chem. Soc.* **1959**, *81*, 1729-1733.

157. Martin, T. A.; Cacsey, D. H.; Sheffner, L.; Wheeler, A. G.; Corrigan, J. R. Amides of N-acylcysteines as mucolytic agents. *J. Med. Chem.* **1967**, *10*, 1172-1176.

158. Harpp, D. N.; Gleason, J. G. Organic sulphur chemistry. X. Selective desulfurization of disulfide. Scope and mechanism. *Org. Sulfur Chem.* **1970**, *15*, 2437-2445.

159. Threadgill, M. D.; Gledhill, A.P. Synthesis of peptides containing *S*-(*N*-alkylcarbamoyl)cysteine residues, metabolites of N-alkylformamides in rodents and in humans. *J. Org. Chem.* **1989**, *54*, 2940-2949.

160. Affleck, J. G.; Dougherty, G. J. The preparation and relative reactivities of many-membered cyclic disulfides. *J. Org. Chem.* **1950**, *15*, 865-868.

161. Carpino, L. A.; Lonescu, D.; El-Faham, A.; Beyermann, M.; Henklein, P.; Hanay, C.; Wenschuh, H.; Bienert, M. Complex polyfluoride additives in Fmoc-amino acid fluoride coupling processes. Enhanced reactivity and avoidance of stereomutation. *Org. Lett.* **2003**, *5*, 975-977.

162. Webb, R. G.; Haskell, M. W.; Stammer, C, H. A nuclear magnetic resonance method for distinguishing α-amino acids from β and γ isomers. *J. Org. Chem.* **1969**, *34*, 576-580.

163. Sheh, L.; Lin, H.; Jeng, K, G.; Chen, C. Studies of the synthesis, immunology, and cytotoxicity of a cyclic octapeptide corresponding to TNF-α-(59-66). *J. Med. Chem.* **1993**, *36*, 4302-4307.

164. Boger, D. L.; Ichikawa, S.; Tse, W. C.; Hedrick, M. P.; Jin, Q. Total syntheses of thiocoraline and BE-22179 and assessment of their DNA binding and biological properties. *J. Am. Chem. Soc.* **2001,** *123,* 561-568.

165. Dragovich, P. S.; Webber, S. E.; Babine, R. E.; Fuhrman, S. A.; Patick, A. K.; Matthews, D. A.; Reich, S. H.; Marakovits, J. T.; Prins, T. J.; Zhou, R.; Tikhe, J.; Littlefield, E. S.; Bleckman, T. M.; Wallace, M. B.; Little, T. L.; Ford, C. E.; Meador, J. W.; Ferre, R. A.; Brown, E. L.; Binford, S. L.; Delisle, D. M.; Worland, S. T. Structure–based design, synthesis, and biological evaluation of irreversible human rhinovirus 3C protease inhibitors. 2. Peptide structure-activity studies. *J. Med. Chem.* **1998,** *41,* 2819-2834.

166. Gaudron, S.; Adeline, M.; Potier, P.; Thierry, J. NAcSDKP analogues resistant to angiotension-converting enzyme. *J. Med. Chem.* **1997,** *40,* 3963-3968.

167. Iguchi, S.; Hirano, K.; Okamoto, H.; Okamoto, Y.; Okada, Y. Amino acids and peptides. XLIV. Synthesis of stereoisomeric pentapeptides of thiol proteinase inhibitor. *Chem. Pharm. Bull.* **1996,** *44,* 1599-1602.

168. Josien, H.; Solange, L.; Brunissen, A.; Saffroy, M.; Torrens, Y.; Beaujouan, J.; Glowinski, J.; Chassaing, G. Design and synthesis of side-chain conformationally restricted phenylalanines and their use for structure-activity studies on tachykinin NK-1 receptor. *J. Med. Chem.* **1994,** *37,* 1586-1601.

169. Kim, S.; Lee, J. I.; Kim, Y. C. A simple and mild esterification method for carboxylic acids using mixed carboxylic-carbonic anhydrides. *J. Org. Chem.* **1985,** *50,* 560-565.

170. Gagnon, P.; Huang, X.; Therrien, E.; Keillor, J. W. Peptide coupling of unprotected amino acids through in situ p-nitrophenyl ester formation. *Tetrahedron Lett.* **2002,** *43,* 7717-7719.

171. Dubowchik, G. M.; Mosure, K.; Knipe, J. O.; Firestone, R. A. Cathepsin B-sensitive dipeptide prodrugs. 2. Models of anticancer drugs paclitaxel (Taxol®), mitomycin C and doxorubicin. *Bioorg. Med. Chem. Lett.* **1998,** *41,* 3347-3352.

172. Szirtes, T.; Kisfaludy, L.; Pálosi, É.; Szporny, L. Synthesis of thyrotropin-releasing hormone analogues. 1. Complete dissociation of central nervous system effects from thyrotropin-releasing activity. *J. Med. Chem.* **1984,** *27,* 741-745.

173. Narita, M.; Ogura, T.; Sato, K.; Honda, S. Design of the synthetic route for peptides and proteins based on the solubility prediction method. 1. Synthesis and solubility properties of human proinsulin C-peptide fragments. *Bull. Chem. Soc. Jpn.* **1986**, *59*, 2433-2438.

174. Molina, M. T.; Valle, C.; Escribano, A. M.; Ezquerra, J.; Pedregal, C. Regioselective ring opening of chiral N-Boc protected pyroglutamate and pyroaminoadipate ethyl esters with heteronucleophiles. *Tetrahedron.* **1993**, *49*, 3801-3808.

175. Ohta, T.; Hosoi, A.; Kimura, T.; Nozoe, S. Direct chain elongation of N-carbamoylpyroglutamate - an efficient synthesis of (-)-pyrrolidine-2,5-dicarboxylic acid. *Chem. Lett.* **1987**, *10*, 2091-2094.

176. Ezquerra, J.; de Mendoza, J.; Pedregal, C.; Ramírez, C. Regioselective nucleophilic attack on N-Boc-pyroglutamate ethyl-ester. *Tetrahedron Lett.* **1992**, *33*, 5589-5590.

177. Schoenfelder, A.; Mann, A. Convenient preparation of dissymmetrical diesters of N-Boc glutamic-acid. *Synth. Comm.* **1990**, *20*, 2585-2588.

178. Bernardi, F.; Garavelli, M.; Scatizzi, M.; Tomasini, C.; Trigari, V.; Crisma, M.; Formaggio, F.; Peggion, C.; Toniolo, C. Pseudopeptide foldamers: the homo-oligomers of pyroglutamic acid. *Chem. Eur. J.* **2002**, *8*, 2516-2524.

179. Betsbrugge, J. V.; Nest, W. V. D.; Verheyden, P.; Tourwé, D. New amino acids derived from *L*-pyroglutamic acid: synthesis of *trans*-4-benzyl-*cis*-5-phenyl-*L*-proline, *L*-α-(2-benzyl-3-phenylpropyl)-glycine and *L*-α-(3-phenylpropyl)-glycine. *Tetrahedron* **1998**, *54*, 1753-1761.

180. Gayo, L. M.; Suto, M. J. Use of pentafluorophenyl esters for one-pot protection/activation of amino and thiol carboxylic acids. *Tetrahedron Lett.* **1996**, *37*, 4915-4918.

181. Green, M.; Berman, J. Preparation of pentafluorophenyl esters of Fmoc protected amino-acids with pentafluorophenyl trifluoroactetate. *Tetrahedron Lett.* **1990**, *31*, 5851-5852.

182. Gatto, B.; Zagotto, G.; Sissi, C.; Cinzia, C.; Uriarte, E.; Palù, G.; Capranico, G.; Palumbo, M. Peptidyl anthraquinones as potential antineoplastic drugs: synthesis, DNA binding, redox cycling, and biological activity. *J. Med. Chem.* **1996**, *39*, 3114-3122.

183. Salvadori, S.; Marastoni, M.; Balboni, G.; Borea, P. A.; Morari, M.; Tomatis, R. Synthesis and structure-activity relationships of deltorphin analogues. *J. Med. Chem.* **1991**, *34*, 1656-1661.

184. Ainscough, E. W.; Brodie, A. M. Nitric oxide – some old and new prespectives. *J. Chem. Educ.* **1995**, *72*, 686-692.

185. Liu, Z. Q.; Wildhirt, S. M.; Zhou, H. H. Specificity of inducible nitric oxide synthase inhibitors: prospects for their clinical therapy. *Acta Pharmacologica Sinica.* **1999**, *20*, 1052-1056.

186. Griffin, R. J.; Makepeace, C. M.; Hur, W. J.; Song, C. W. Radiosensitization of hypoxic tumor cells in vitro by nitric oxide. *Int. J. Radiat. Oncol. Biol. Phys.* **1996**, *36*, 377-383.

187. Pfeiffer, S.; Mayer,B.; Hemmens, B. Nitric oxide: Chemical puzzles posed by a biological messenger. *Angew. Chem. Int. Ed. Engl.* **1999**. *38*, 1714-1731.

188. Uzbay, I. T.; Oglesby, M. W. Nitric oxide and substance dependence. *Neurosci. Biobehavioral Rev.* **2001**, *25*, 43-52.

189. Collins, J. L.; Shearer, B.G.; Oplinger, J. A.; Lee, S.; Garvey, E. P.; Salter, M.; Duffy, C.; Burnette, T. C.; Furfine, E. S. N-Phenylamidines as selective inhibitors of human neuronal nitric oxide synthase: structure-activity studies and demonstration of in vivo activity. *J. Med. Chem.* **1998**, *41*, 2858-2871.

190. Beaton, H.; Hamley, P.; Nicholls, D. J.; Tinker, A. C.; Wallace, A. V. 3,4-Dihydro-1-isoquinolinamines: a novel class of nitric oxide synthase inhibitors with a range of isoform selectivity and potency. *Bioorg. Med. Chem. Lett.* **2001**, *11*, 1023-1026.

191. Sase, K.; Michel, T. Expression and regulation of endothelial nitric oxide synthase. *Trends Cardiovasc. Med.* **1997**, *7*, 28-37.

192. Connor, J. R.; Manning, P. T.; Settle, S. L.; Moore, W. M.; Jerome, G. M.; Webber, R. K.; Tjoeng, F. S.; Currie, M.G. Suppression of adjuvant-induced arthritis by selective inhibition of inducible nitric oxide synthase. *Eur. J. Pharmacol.* **1995**, *273*, 15-24.

193. Babu, B.R.; Griffith, O.W. Design of isoform-selective inhibitors of nitric oxide synthase. *Curr. Opin. Chem. Biol.* **1998**, *2*, 491-500.

194. Garvey, E. P.; Oplinger, J. A.; Tanoury, G. J.; Sherman, P. A.; Fowler, M.; Marshall, S.; Harmon, M. F.; Paith, J. E.; Furfine, E. S. Potent and selective inhibition of human nitric oxide synthases. Inhibition by non-amino acid isothioureas. *J. Biol. Chem.* **1994**, *269*, 26669-26676.

195. Griffith, O. W.; Steuhr, D. J.; Nitric oxide synthases: properties and catalytic mechanism. *Ann. Rev. Physiol.* **1995**, *57*, 707-736.

196. Reif, D. W.; Mccarthy, D. J.; Cregan, E.; Macdonald, J. E. Discovery and development of neuronal nitric oxide synthase inhibitors. *Free Radic. Biol. Med.* **2000**, *28*, 1470-1477.

197. Wink, D. A.; Vodovotz, Y.; Cook, J. A.; Krishna, M. C.; Kim, S.; Coffin, D.; Degraff, W.; Deluca, A. M.; Liebmann, J.; Mitchell, J. B. The role of nitric oxide chemistry in cancer treatment. *Biochemistry* **1998**, *63*, 802-809.

198. Garvey, E. P.; Oplinger, J. A.; Furfine, E. S.; Kiff, R. J.; Laszlo, F.; Whittle, B. J. R.; Knowles, R. G. 1400W Is a slow, tight binding, and highly selective inhibitor of inducible nitricoxide synthase in vitro and in vivo. *J. Biol. Chem.* **1997**, *272*, 4959-4963.

199. Hallinan, E. A.; Tsymbalov, S.; Finnegan, P. M.; Moore, W. M.; Jerome. G. M.; Currie, M.G.; Pitzele, B.S. Acetamidine lysine derivative, N-(5(S)-amino-6,7-dihydroxyheptyl)ethanimidamide dihydrochloride: a highly selective inhibitor of human inducible nitric oxide synthase. *J. Med. Chem.* **1998**, *41*, 775-777

200. Lee, Y.; Marletta, M. A.; Martasek, P.; Roman, L. J.; Masters, B. S. S.; Silverman, R. B. Conformationally-restricted arginine analogues as alternative substrates and inhibitors of nitric oxide synthases. *Bioorg. Med. Chem.* **1999**, *7*, 1097-1104.

201. Webber, R. K.; Metz, S.; Moore, W. M.; Connor, J. R.; Currie, M. G.; Fok, K. F.; Hagan, T. J.; Hansen, D. W.; Jerome, G. M.; Manning, P. T.; pitzele, B. S.; Toth, M. V.; Trivedi, M.; Tjeong, F. S. Substituted 2-iminopiperidines as inhibitors of human nitric oxide synthase isoforms. *J. Med. Chem.* **1998**, *41*, 96-101.

202. Ulhaq, S.; Chinje, E. C.; Naylor, M. A.; Jaffar, M.; Stratford, I. J.; Threadgill, M. D. Heterocyclic Analogues of L-citrulline as inhibitors of the isoforms of nitric oxide Synthase (NOS) and identification of N^{δ}(4,5-Dihydrothiazol-2-yl)ornithine as a potent inhibitor. *Bioorg. Med. Chem.* **1999**, *7*, 1787-1796.

203. Jordan, B. F.; Misson, P.; Demeure, R.; Baudelet, C.; Beghein, N.; Gallez, B. Changes in tumor oxygenation/perfusion induced by the NO donor, isosorbide dinitrate, in comparison with carbogen: monitoring by EPR and MRI. *Int. J. Radiat. Oncol. Biol. Phys.* **2000**, *48*, 565-570.

204. Ulhaq, S.; Chinje, E. C.; Naylor, M. A.; Jaffar, M.; Stratford, I. J.; Threadgill, M. D. S-2-amino-5-azolylpentanoic acids related to L-ornithine as inhibitors of the isoforms of nitric oxide synthase (NOS). *Bioorg. Med. Chem.* **1998**, *6*, 2139-2149.

205. Damen, E. W. P.; Nevalainen, T. J.; van den Bergh, T. J. M.; Groot, F. M. H.; Scheeren, H. W. Synthesis of novel paclitaxel prodrugs designed for bioreductive activation in hypoxic tumour tissue. *Bioorg Med Chem.* **2002**, *10*, 71-77.

206. Goodyer, C. L. M.; Chinje, E. C.; Jaffar, M.; Straford, I. J.; Threadgill, M. D. Syhthesis of N-benzyl-and N-phenyl-2-amino4,5-dihydrothiazoles and thioureas and evaluation as modulators of the isoforms of nitric oxide synthase. *Bioorg. Med. Chem.* **2003**, *11*, 4189-4206.

207. Oussaid, B.; Najem, L.; Garrigues, B. Synthèse de nouveaux derivés du thiophene. *Phosphorus, Sulfur, and Silicon* **1992**, *66*, 13-20.

208. Tominaga, Y.; Castle, R. N.; Lee, M. L. Synthesis of benzo[4,5]phenaleno[1,9-bc]thiophene and Benzo[4,5]phenaleno[9,1-bc]thiophene. *J. Heterocyclic Chem.* **1982**, *19*, 1125-1130.

209. Brown, H. C.; Wetherill, R. B.; Subba Rao, B. C. Selective reduction with diborane, an acidic-type reducing agent. *J. Org. Chem.* **1957**, *22*, 1135-1136.

210. Garrigues, B. Synthèse de derivés du thiophene substitutes en position 2 et 5. *Phosphorus, Sulfur, and Silicon* **1990**, *53*, 75-79.

211. Mitsunobu, O. The use of diethyl azodicarboxylate and triphenylphosphine in synthesis and transformation of natural products. *Synthesis* **1981**, 1-28.

212. Malet, C.; Hindsgaul, O. Versatile functionalization of carbohydrate hydroxyl groups through their O-cyanomethyl ethers. *J. Org. Chem.* **1996**, *61*, 4649-4654.

213. Shinkwin, A. E.; Whish, W. J. D.; Threadgill, M. D. Synthesis of thiophenecarboxamides, thieno[3,4-*c*]pyridin-4(5H)-ones and thieno[3,4-

d]pyrimidin-4(3H)-ones and preliminary evaluation as inhibitors of poly(ADP-ribose)polymerase(PARP). *Bioorg. Med. Chem.* **1999**, *7*, 297-308.

214. Curtin, M. L.; Davidsen, S. K.; Heyman, H. R.; Garland, R. B.; Sheppard, G. S.; Florjancic, A. S.; Xu, L.; Carrera, G. M.; Steinman, D. H.; Trautmann, J. A.; Albert, D. H.; Magoc, T. J.; Tapang, P.; Rhein, D. A.; Conway, R. G.; Luo, G.; Denissen, J. F.; Marsh, K. C.; Morgan, D.-W.; Summers, J. B. Discovery and evaluation of a series of 3-acylindole imidazopyridine platelet-activating factor antagonists. *J. Med. Chem.* **1998**, *41*, 74-95.

215. Harland, P. A.; Hodge, P. Synthesis of primary amines via alkylation of the sodium salt of trifluroacetamide: an alternative to the Gabriel synthesis. *Synthesis* **1984**, 941-943.

216. Ben-Ishai, D.; Berger, A. Cleavage of N-carbobenzoxy groups by dry hydrogen bromide and hydrogen chloride. *J. Org. Chem.* **1952**, *15*, 1564-1570.

217. Detty, M. R.; Hays, D. S. Studies toward alkylthiophene-2-carboxaldehydes. Reduction of 3-alkenylthiophenes with triethylsilane/trifluoroacetic acid. Regioselectivity in formylation reactions of 3-alkylthiophenes. *Heterocycles* **1995**, *40*, 925-937.

218. Dittmer, K.; Martin, R. P.; Herz, W.; Cristol, S. J. The effect of benzoyl peroxide on the bromination of methylthiophenes by N-bromosuccinimide. *J. Am. Chem. Soc.* **1949**, *71*, 1201-1204.

219. Goodyer, C, L. M.; Chinje, E. C.; Jaffar, M. Stratford, I. J.; Threadgill, M. D. Time-dependence and preliminary SAR studies in inhibition of nitric oxide synthase isoforms by homologues of thiocitrulline. *Bioorg. Med. Chem. Lett.* **2003**, *13*, 3679-3680.

220. Beaton, H.; Boughton-Smith, N. B.; Hamley, P.; Ghelani, A.; Nicholls, D. J.; Tinker, A. C.; Wallace, A. V. Thienopyridines: nitric oxide Synthase inhibitors with potent in vivo activity. *Bioorg Med Chem Lett.* **2001**, *11*, 1027-1030.

221. Ogden, J. E.; Moore, P. K. Inhibition of nitric oxide Synthase-potential for a novel class of therapeutic agent?. *Trends Biotechnol.* **1995**, *13*, 70-78.

222. Fry, E. M. Syntheses of cystine. *J. Org. Chem.* **1950**, *15*, 438-444.

223. Curtius. Hydrazid der α und β-dimethylaminopropiosäure, dimethylaminobernsteinsäure und dimethylanthranilsäure. *J. Prakt. Chem.* **1917**, *95*, 340-349.

224. Nartta, M.; Ogura, T.; Sato, K.; Honda, S. Design of the synthetic route for peptides and proteins based on the solubility prediction method. 1. Synthesis and solubility properties of human proinsulin C-peptide fragments. *Bull. Chem. Soc. Jpn*, **1986**, *59*, 2433-2438.

225. Mizutani, M.; Sanemitsu, Y.; Tamaru, Y.; Yoshida, Z. Palladium-catalyzed polyhetero-claisen rearrangement of 2-(allythio)pyrimidin-4(3*H*)-ones. *J. Org. Chem.* **1985**, *50*, 764-768.

226. Griffing, B. M.; Salisbury, L. F. 2,5-bis(bromomethyl)-thiophene and some of its derivatives. *J. Am. Chem. Soc.* **1948**, *70*, 3416-3419.

227. Oussaid, B.; Fayet, J. P.; Pelletier, G.; Garrigues, B. Conformational study of thiophenic. *Bull. Soc. Chim. Belg.* **1992**, *11*, 969-976.

228. Bock, H.; Roth, B. Radical ions 49. redox reactions of some thiophene derivatives. *Phosphorus sulphur* **1983**, *14*, 211-224.

229. Grose, H. G.; Campaigne, E. E. Substituted thenoic acids. *J. Am. Chem. Soc.* **1949**, *71*, 3258-3226.

X-ray crystallography data for compound (**99**)

Identification code	h03mt2
Empirical formula	$C_{18} H_{28} N_4 O_4 S_2$
Formula weight	428.56
Temperature	150(2) K
Wavelength	0.71073 Å
Crystal system	Orthorhombic
Space group	$P2_1 2_1 2_1$
Unit cell dimensions	a = 6.1600(1)Å α = 90°
	b = 6.5280(1)Å β = 90°
	c = 25.9050(5)Å γ = 90°
Volume	1041.70(3) Å^3
Z	2
Density (calculated)	1.366 Mg/m^3
Absorption coefficient	0.287 mm^{-1}
F(000)	456
Crystal size	0.40 x 0.20 x 0.10 mm
Theta range for data collection	4.06 to 27.86°
Index ranges	-8<=h<=8; -8<=k<=8; -34<=l<=34
Reflections collected	15756
Independent reflections	2475 [R(int) = 0.0470]
Reflections observed (>2σ)	2180
Data Completeness	0.995
Absorption correction	None
Refinement method	Full-matrix least-squares on F^2
Data / restraints / parameters	2475 / 1 / 136
Goodness-of-fit on F^2	1.037
Final R indices [I>2σ(I)]	R^1 = 0.0298 wR$_2$ = 0.0697
R indices (all data)	R^1 = 0.0386 wR$_2$ = 0.0730
Absolute structure parameter	0.02(8)
Largest diff. peak and hole	0.192 and -0.219 eÅ^{-3}

Table A   *Crystal data and structure refinement for (99)*

Atom	x	y	z	U(eq)
S(1)	19880(1)	2692(1)	955(1)	35(1)
O(1)	14950(2)	7933(2)	906(1)	34(1)
O(2)	21026(2)	7010(2)	2314(1)	24(1)
N(1)	17551(2)	5845(2)	1243(1)	22(1)
N(2)	17848(2)	8451(2)	2072(1)	22(1)
C(1)	20840(3)	4194(3)	1494(1)	33(1)
C(2)	18808(2)	5215(2)	1698(1)	21(1)
C(3)	19330(2)	6993(2)	2055(1)	19(1)
C(4)	15752(2)	8259(2)	1808(1)	22(1)
C(5)	16054(2)	7355(2)	1269(1)	23(1)
C(6)	18110(3)	4797(3)	747(1)	26(1)
C(7)	14612(3)	10305(2)	1787(1)	32(1)
C(8)	16140(3)	3858(3)	480(1)	37(1)
C(9)	19314(3)	6294(3)	398(1)	38(1)

Table B *Atomic coordinates (x 10⁴) and equivalent isotropic displacement*

parameters (Å² x 10³) for (99).

S(1)-C(1)	1.8054(16)	S(1)-C(6)	1.8360(16)
O(1)-C(5)	1.2209(17)	O(2)-C(3)	1.2423(17)
N(1)-C(5)	1.3518(18)	N(1)-C(2)	1.4682(18)
N(1)-C(6)	1.4963(19)	N(2)-C(3)	1.3194(18)
N(2)-C(4)	1.4658(17)	C(1)-C(2)	1.513(2)
C(2)-C(3)	1.519(2)	C(4)-C(7)	1.510(2)
C(4)-C(5)	1.527(2)	C(6)-C(9)	1.524(2)
C(6)-C(8)	1.525(2)		
C(1)-S(1)-C(6)	90.90(7)	C(5)-N(1)-C(2)	121.58(12)
C(5)-N(1)-C(6)	122.23(12)	C(2)-N(1)-C(6)	116.12(11)
C(3)-N(2)-C(4)	122.18(12)	C(2)-C(1)-S(1)	103.74(11)
N(1)-C(2)-C(1)	106.26(12)	N(1)-C(2)-C(3)	112.72(12)
C(1)-C(2)-C(3)	111.94(12)	O(2)-C(3)-N(2)	123.89(13)
O(2)-C(3)-C(2)	120.96(12)	N(2)-C(3)-C(2)	115.14(11)
N(2)-C(4)-C(7)	110.53(12)	N(2)-C(4)-C(5)	110.57(11)
C(7)-C(4)-C(5)	111.43(12)	O(1)-C(5)-N(1)	124.52(13)
O(1)-C(5)-C(4)	121.17(13)	N(1)-C(5)-C(4)	114.25(12)
N(1)-C(6)-C(9)	109.19(13)	N(1)-C(6)-C(8)	112.97(13)
C(9)-C(6)-C(8)	112.10(14)	N(1)-C(6)-S(1)	103.05(10)
C(9)-C(6)-S(1)	111.43(11)	C(8)-C(6)-S(1)	107.77(12)

Table C *Bond lengths [Å] and angles [°] for (99).*

Atom	U11	U22	U33	U23	U13	U12
S(1)	42(1)	34(1)	28(1)	-11(1)	-5(1)	12(1)
O(1)	35(1)	44(1)	23(1)	-1(1)	-11(1)	12(1)
O(2)	21(1)	27(1)	23(1)	0(1)	-6(1)	0(1)
N(1)	23(1)	27(1)	15(1)	-1(1)	-3(1)	5(1)
N(2)	22(1)	24(1)	20(1)	-4(1)	-4(1)	2(1)
C(1)	33(1)	38(1)	28(1)	-11(1)	-9(1)	15(1)
C(2)	23(1)	22(1)	18(1)	1(1)	-3(1)	2(1)
C(3)	20(1)	22(1)	15(1)	2(1)	1(1)	0(1)
C(4)	18(1)	25(1)	22(1)	-1(1)	-3(1)	2(1)
C(5)	20(1)	27(1)	21(1)	0(1)	-2(1)	0(1)
C(6)	28(1)	32(1)	19(1)	-3(1)	0(1)	5(1)
C(7)	30(1)	32(1)	34(1)	-4(1)	-6(1)	11(1)
C(8)	40(1)	44(1)	28(1)	-11(1)	-8(1)	-1(1)
C(9)	43(1)	47(1)	24(1)	1(1)	8(1)	0(1)

Table D   Anisotropic displacement parameters ($\mathring{A}^2$ x 10^3) for **(99)**.

Atom	x	y	z	U(eq)
H(1A)	21509	3309	1761	39
H(1B)	21917	5225	1380	39
H(2)	17946	4179	1895	25
H(4)	14826	7296	2012	26
H(7A)	14357	10801	2139	48
H(7B)	13220	10152	1608	48
H(7C)	15520	11291	1601	48
H(8A)	15349	2993	725	56
H(8B)	16622	3026	187	56
H(8C)	15183	4953	356	56
H(9A)	18395	7491	331	57
H(9B)	19664	5620	70	57
H(9C)	20659	6733	567	57
H(2A)	18100(30)	9490(20)	2281(6)	34(5)

Table E   Hydrogen coordinates (x 10^4) and isotropic displacement parameters ($\mathring{A}^2$ x 10^3) for **(99)**.

X ray crystallography data for (**100**).

Identification code	c:\backup\helix\h03mt1\maxus\h03mt1
Empirical formula	C11 H18 N2 O2 S
Formula weight	242.33
Temperature	150(2) K
Wavelength	0.71073 Å
Crystal system	Triclinic
Space group	P1
Unit cell dimensions	$a = 5.7440(2)$Å $\alpha = 91.399(1)^\circ$
	$b = 9.7410(3)$Å $\beta = 94.980(1)^\circ$
	$c = 11.0190(4)$Å $\gamma = 98.341(2)^\circ$
Volume	607.29(4) Å^3
Z	2
Density (calculated)	1.325 Mg/m^3
Absorption coefficient	0.255 mm^{-1}
F(000)	260
Crystal size	0.15 x 0.10 x 0.10 mm
Theta range for data collection	3.60 to 27.45°
Index ranges	-7<=h<=7; -12<=k<=12; -14<=l<=14
Reflections collected	9382
Independent reflections	5031 [R(int) = 0.0391]
Reflections observed (>2σ)	4185
Data Completeness	0.995
Absorption correction	None
Refinement method	Full-matrix least-squares on F^2
Data / restraints / parameters	5031 / 5 / 307
Goodness-of-fit on F^2	1.040
Final R indices [I>2σ(I)]	R^1 = 0.0364 wR$_2$ = 0.0760
R indices (all data)	R^1 = 0.0513 wR$_2$ = 0.0818
Absolute structure parameter	0.04(5)
Largest diff. peak and hole	0.253 and -0.242 eÅ^{-3}

Table A   *Crystal data and structure refinement for (100).*

261

Atom	x	y	z	U(eq)
S(1)	-9021(1)	277(1)	1115(1)	41(1)
S(2)	7979(1)	8935(1)	3652(1)	44(1)
O(1)	-5675(3)	2800(2)	-1902(1)	33(1)
O(2)	-2545(3)	3226(2)	2675(1)	38(1)
O(3)	3262(2)	7082(2)	6512(1)	32(1)
O(4)	1924(2)	5777(2)	1723(1)	32(1)
N(1)	-6397(3)	2211(2)	30(2)	24(1)
N(2)	-2802(3)	4267(2)	852(2)	26(1)
N(3)	4474(3)	7449(2)	4619(2)	25(1)
N(4)	1301(3)	5194(2)	3657(2)	28(1)
C(1)	-6584(4)	1304(2)	2027(2)	40(1)
C(2)	-6079(4)	2628(2)	1333(2)	27(1)
C(3)	-3621(4)	3395(2)	1687(2)	27(1)
C(4)	-4282(3)	4493(2)	-258(2)	22(1)
C(5)	-5490(3)	3088(2)	-811(2)	24(1)
C(6)	-7800(3)	820(2)	-318(2)	25(1)
C(7)	-2893(3)	5391(2)	-1146(2)	26(1)
C(8)	-2186(4)	6874(2)	-621(2)	35(1)
C(9)	-753(4)	4796(2)	-1524(2)	34(1)
C(10)	-6224(4)	-162(2)	-743(3)	43(1)
C(11)	-9875(4)	926(2)	-1239(2)	35(1)
C(12)	6219(4)	7524(3)	2745(2)	38(1)
C(13)	3874(3)	7331(2)	3302(2)	27(1)
C(14)	2282(3)	6019(2)	2845(2)	26(1)
C(15)	1557(3)	5417(2)	4975(2)	25(1)
C(16)	3138(3)	6746(2)	5431(2)	25(1)
C(17)	6241(4)	8673(2)	4999(2)	27(1)
C(18)	2479(3)	4190(2)	5623(2)	24(1)
C(19)	5015(4)	4075(2)	5375(2)	34(1)
C(20)	869(4)	2825(2)	5317(2)	34(1)
C(21)	5057(4)	9940(2)	5230(2)	37(1)
C(22)	7926(4)	8414(3)	6087(2)	36(1)

Table B   *Atomic coordinates (x 10^4) and equivalent isotropic displacement parameters (Å^2 x 10^3) for (100).*

S(1)-C(1)	1.809(2)	S(1)-C(6)	1.841(2)
S(2)-C(12)	1.806(2)	S(2)-C(17)	1.862(2)
O(1)-C(5)	1.220(2)	O(2)-C(3)	1.231(3)
O(3)-C(16)	1.221(2)	O(4)-C(14)	1.246(3)
N(1)-C(5)	1.361(2)	N(1)-C(2)	1.471(3)
N(1)-C(6)	1.496(3)	N(2)-C(3)	1.336(3)
N(2)-C(4)	1.467(3)	N(3)-C(16)	1.362(3)
N(3)-C(13)	1.460(3)	N(3)-C(17)	1.476(3)
N(4)-C(14)	1.325(3)	N(4)-C(15)	1.455(3)
C(1)-C(2)	1.520(3)	C(2)-C(3)	1.512(3)
C(4)-C(5)	1.528(3)	C(4)-C(7)	1.528(3)
C(6)-C(10)	1.501(3)	C(6)-C(11)	1.513(3)
C(7)-C(9)	1.518(3)	C(7)-C(8)	1.529(3)
C(12)-C(13)	1.517(3)	C(13)-C(14)	1.507(3)
C(15)-C(16)	1.517(3)	C(15)-C(18)	1.542(3)
C(17)-C(21)	1.519(3)	C(17)-C(22)	1.524(3)
C(18)-C(20)	1.518(3)	C(18)-C(19)	1.525(3)
C(1)-S(1)-C(6)	92.23(9)	C(12)-S(2)-C(17)	94.65(10)
C(5)-N(1)-C(2)	120.37(17)	C(5)-N(1)-C(6)	122.32(18)
C(2)-N(1)-C(6)	117.28(15)	C(3)-N(2)-C(4)	121.13(17)
C(16)-N(3)-C(13)	123.40(16)	C(16)-N(3)-C(17)	121.71(17)
C(13)-N(3)-C(17)	112.77(16)	C(14)-N(4)-C(15)	126.99(19)
C(2)-C(1)-S(1)	104.30(15)	N(1)-C(2)-C(3)	111.25(16)
N(1)-C(2)-C(1)	106.46(18)	C(3)-C(2)-C(1)	112.11(18)
O(2)-C(3)-N(2)	124.70(19)	O(2)-C(3)-C(2)	121.33(18)
N(2)-C(3)-C(2)	113.96(18)	N(2)-C(4)-C(5)	109.06(15)
N(2)-C(4)-C(7)	111.94(15)	C(5)-C(4)-C(7)	113.85(17)
O(1)-C(5)-N(1)	123.56(19)	O(1)-C(5)-C(4)	123.13(17)
N(1)-C(5)-C(4)	113.28(18)	N(1)-C(6)-C(10)	110.46(16)
N(1)-C(6)-C(11)	111.90(17)	C(10)-C(6)-C(11)	112.6(2)
N(1)-C(6)-S(1)	102.78(14)	C(10)-C(6)-S(1)	111.58(15)
C(11)-C(6)-S(1)	107.05(14)	C(9)-C(7)-C(8)	110.92(18)
C(9)-C(7)-C(4)	113.38(17)	C(8)-C(7)-C(4)	110.52(17)
C(13)-C(12)-S(2)	104.01(16)	N(3)-C(13)-C(14)	115.18(17)
N(3)-C(13)-C(12)	105.50(17)	C(14)-C(13)-C(12)	113.04(18)
O(4)-C(14)-N(4)	123.3(2)	O(4)-C(14)-C(13)	118.41(19)
N(4)-C(14)-C(13)	118.27(19)	N(4)-C(15)-C(16)	114.60(16)
N(4)-C(15)-C(18)	111.65(17)	C(16)-C(15)-C(18)	108.37(16)
O(3)-C(16)-N(3)	123.51(18)	O(3)-C(16)-C(15)	118.77(17)
N(3)-C(16)-C(15)	117.55(17)	N(3)-C(17)-C(21)	111.07(17)
N(3)-C(17)-C(22)	113.04(18)	C(21)-C(17)-C(22)	111.47(19)
N(3)-C(17)-S(2)	103.06(14)	C(21)-C(17)-S(2)	109.87(15)
C(22)-C(17)-S(2)	107.93(15)	C(20)-C(18)-C(19)	110.95(18)
C(20)-C(18)-C(15)	112.25(17)	C(19)-C(18)-C(15)	112.18(16)

Table C   *Bond lengths [Å] and angles [°] for (100).*

Atom	U11	U22	U33	U23	U13	U12
S(1)	46(1)	38(1)	31(1)	4(1)	5(1)	-17(1)
S(2)	36(1)	54(1)	37(1)	-10(1)	12(1)	-17(1)
O(1)	41(1)	34(1)	19(1)	1(1)	1(1)	-9(1)
O(2)	47(1)	37(1)	23(1)	5(1)	-9(1)	-13(1)
O(3)	36(1)	34(1)	25(1)	-5(1)	3(1)	-1(1)
O(4)	36(1)	35(1)	24(1)	-1(1)	-5(1)	0(1)
N(1)	26(1)	22(1)	21(1)	1(1)	0(1)	-6(1)
N(2)	27(1)	25(1)	22(1)	2(1)	-5(1)	-6(1)
N(3)	24(1)	24(1)	23(1)	-3(1)	-1(1)	-3(1)
N(4)	30(1)	24(1)	25(1)	1(1)	-7(1)	-5(1)
C(1)	50(2)	39(2)	24(1)	5(1)	-1(1)	-14(1)
C(2)	30(1)	27(1)	20(1)	0(1)	1(1)	-3(1)
C(3)	34(1)	24(1)	23(1)	-4(1)	1(1)	-1(1)
C(4)	23(1)	20(1)	22(1)	1(1)	2(1)	1(1)
C(5)	21(1)	25(1)	24(1)	3(1)	0(1)	2(1)
C(6)	24(1)	22(1)	27(1)	-1(1)	3(1)	-4(1)
C(7)	26(1)	23(1)	26(1)	4(1)	-4(1)	-3(1)
C(8)	46(1)	22(1)	34(1)	4(1)	3(1)	-4(1)
C(9)	32(1)	38(1)	32(1)	3(1)	7(1)	-1(1)
C(10)	37(1)	30(1)	60(2)	-8(1)	5(1)	1(1)
C(11)	33(1)	32(1)	37(1)	2(1)	-6(1)	-7(1)
C(12)	32(1)	45(2)	32(1)	-8(1)	3(1)	-9(1)
C(13)	28(1)	26(1)	24(1)	0(1)	0(1)	1(1)
C(14)	22(1)	26(1)	28(1)	0(1)	-2(1)	3(1)
C(15)	23(1)	27(1)	23(1)	-2(1)	-1(1)	1(1)
C(16)	21(1)	28(1)	24(1)	0(1)	0(1)	3(1)
C(17)	27(1)	27(1)	25(1)	-4(1)	4(1)	-5(1)
C(18)	21(1)	27(1)	22(1)	0(1)	2(1)	4(1)
C(19)	27(1)	39(1)	38(1)	6(1)	7(1)	9(1)
C(20)	31(1)	29(1)	43(1)	6(1)	4(1)	4(1)
C(21)	38(1)	27(1)	46(2)	-1(1)	7(1)	3(1)
C(22)	30(1)	36(1)	40(2)	-7(1)	-6(1)	0(1)

Table D   *Anisotropic displacement parameters ($\mathring{A}^2$ x 10^3) for (100).*

Atom	x	y	z	U(eq)
H(1A)	-7029	1510	2853	48
H(1B)	-5187	814	2102	48
H(2)	-7261	3250	1507	32
H(4)	-5552	5011	-6	26
H(7)	-3976	5436	-1900	31
H(8A)	-1089	6872	112	52
H(8B)	-3600	7247	-408	52
H(8C)	-1418	7455	-1228	52
H(9A)	300	4676	-798	51
H(9B)	93	5433	-2068	51
H(9C)	-1269	3894	-1951	51
H(10A)	-5547	180	-1484	64

H(10B)	-7148	-1084	-916	64
H(10C)	-4948	-222	-104	64
H(11A)	-9295	1195	-2022	53
H(11B)	-10780	1626	-948	53
H(11C)	-10893	24	-1342	53
H(12A)	6009	7767	1879	45
H(12B)	6964	6669	2799	45
H(13)	3043	8132	3066	32
H(15)	-51	5471	5237	30
H(18)	2485	4381	6520	28
H(19A)	5574	3336	5857	51
H(19B)	6027	4958	5601	51
H(19C)	5073	3856	4506	51
H(20A)	832	2596	4444	51
H(20B)	-730	2909	5523	51
H(20C)	1468	2087	5786	51
H(21A)	3920	10046	4535	55
H(21B)	6257	10769	5332	55
H(21C)	4232	9821	5970	55
H(22A)	7095	8385	6828	55
H(22B)	9271	9164	6176	55
H(22C)	8495	7526	5956	55
H(2A)	-1510(30)	4820(20)	1030(20)	28(6)
H(4A)	210(30)	4540(20)	3323(19)	26(6)

Table E *Hydrogen coordinates (x 10^4) and isotropic displacement parameters ($Å^2$ x 10^3) for (100).*